Coupled Trajectory and Economic Analysis of Asteroid Resources

Merel Vergaaij

Submitted in fulfilment of the requirements for the
Degree of Doctor of Philosophy

James Watt School of Engineering
College of Science and Engineering
University of Glasgow

October 2022

Coupled Trajectory and Economic Analysis of Asteroid Resources
Submitted in fulfilment of the requirements for the Degree of Doctor of Philosophy
James Watt School of Engineering
College of Science and Engineering
University of Glasgow

Supervisors
Professor Colin R. McInnes
James Watt School of Engineering, University of Glasgow
Glasgow, United Kingdom

Dr. Matteo Ceriotti
James Watt School of Engineering, University of Glasgow
Glasgow, United Kingdom

Examiners
Dr. Davide Amato
Faculty of Engineering, Department of Aeronautics, Imperial College London
London, United Kingdom

Dr. Patrick Harkness
James Watt School of Engineering, University of Glasgow
Glasgow, United Kingdom

ABSTRACT

To reduce the cost of space missions, asteroid resources have gained significant attention. By using resources from asteroids, water for example, expensive launches from Earth can be minimised. Water obtained from asteroids holds great potential, not just for human life support, but split in its constituents it forms a highly effective propellant: liquid oxygen and liquid hydrogen. This means that asteroid resources can be used as building blocks for a sustainable in-space infrastructure to aid with interplanetary exploration. Several commercial companies have expressed interest in pursuing asteroid mining. This fuels the need for cost estimations and economic models for asteroid mining, as both public and private ventures need to be convinced of the profitability of asteroid mining before investing in expensive space missions. To investigate the profitability of asteroid mining missions, this thesis has integrated economic modelling and trajectory optimisation at an appropriate level of detail and accuracy for each. Due to the coupling of the economic model and trajectory optimisation, trajectories can be designed for cost objectives rather than the more traditional minimum time and minimum propellant objectives. A parametric model has been developed, which can be used to investigate different mining missions, focused on but not limited to asteroid mining. Using this economic model and mission analysis, applied to a range of different missions with varying customer and mining locations, allows for an impartial comparison of the different missions. Potentially profitable value chains can be identified, influential parameters in the model can be found (e.g., certain cost estimates), or trade-offs between variations in mission architectures can be carried out.

Using the model, a trade-off between chemical propulsion and solar sailing to transport asteroid resources has shown that while solar sails have the great advantage that they do not require any propellant, long mission durations have a significant impact on the Net Present Value and Internal Rate of Return, causing these missions to be not competitive with missions utilising chemical propulsion to transport asteroid resources to Earth orbit (e.g., geostationary orbit).

A key finding is the importance of accurate specific launch costs in economic models for asteroid mining. Where other economic models often include specific launch costs in the order of 10,000 $/kg, commercial launch providers are driving down these costs by orders of magnitude by decreasing launch costs and increasing payload capacity. It is shown that this significantly impacts the profitability of asteroid mining, which can only sell resources at a price that is competitive with launching the same resources from the Earth. Assuming high specific launch costs therefore results in overestimating the profitability of asteroid mining.

Another essential conclusion is that for any in-space propellant customer beyond low-Earth orbit, off-Earth mining (e.g., on asteroids, the Moon or Mars) can bring down the cost, mass and risk of future human and robotic space missions. While asteroid mining cannot compete financially with resources mined and processed on the same surface as customers (e.g., on the Moon or Mars), asteroids

are likely to financially compete with other sources for customers in geostationary orbit, Sun-Earth or Sun-Mars Lagrange points, in orbit around or near the Moon or Mars, or in the main asteroid belt.

Finally, it is shown that in a thriving space propellant economy with in-space propellant depots, near-Earth asteroids will be the first asteroids to run out of volatiles, due to their attractive orbits and small size. While asteroid resources are not expected to run out for a long time, this is mainly due to the wealth of resources in main-belt asteroids, which are expensive to mine, especially to supply a depot near Earth. These findings indicate the need for an international regulatory organisation allocating asteroid resources, either to preserve resources for future generations, or to reserve resources for use near Earth.

TABLE OF CONTENTS

LIST OF TABLES

LIST OF FIGURES

ACKNOWLEDGEMENTS

First of all, I am extremely grateful to my PhD supervisors Colin McInnes and Matteo Ceriotti. Your knowledge and experience have encouraged me to come to the University of Glasgow for this research and I am glad I did. You have given me limitless advice and took the time to read all of the many iterations of papers and chapters. You have been endlessly patient, supportive and understanding during all the ups and downs of the last three and a half years. Any PhD student would be lucky with such an exceptional supervisory team.

I would like to thank the external examiner Davide Amato from Imperial College London, internal examiner Patrick Harkness and the convener Andrea Cammarano for the very pleasant viva and the good discussions that we had. Thank you for making the thesis better and for giving me a happy memory while wrapping up my time at the University of Glasgow.

Reaching the end of this PhD required more than just academic support and I therefore have many people to thank. I extend sincere thanks to the SET group and all its members, for being a sounding board and source of inspiration, both online and offline. In particular I would like to thank Iain and Giulia for giving me advice on academic and personal topics, Enric for the bread conversations, and Bonar for helping me out when I needed it the most. I would also like to thank my friends, wherever in the world they may live, for supporting me and keeping me sane throughout the PhD. I am thankful for all the new friends I made while living in the wonderful city of Glasgow.

My gratitude extends to the College of Science and Engineering for the funding opportunity to undertake my studies at the University of Glasgow. Additionally, I would like to express gratitude to the Royal Aeronautical Society and Women in Aerospace - Europe for supporting me financially to attend conferences. Zonta International has given me a lot of confidence and the power to push through by awarding me the Amelia Earhart Fellowship, for which I am very grateful.

Lastly, my family deserves endless gratitude. My father, for being a fantastic role model in the field of technology and engineering. My mother, for her words of encouragement and cheering on. Both of them, for letting me do whatever it was I decided I needed or wanted to do at any time and being proud of my decisions. My sister, for tolerating never-ending rambling about niche topics outside her field of expertise. My grandparents, aunts, uncle, cousin and the Hogervorst family for their unwavering confidence in me. But most of all, Frank, for being so ridiculous and amazing to decide to move to Glasgow with me and go on this adventure, your boundless patience, support, faith in me and encouragement. This thesis is written as a testament to your unconditional love and encouragement.

DECLARATION

I herewith declare that, except where explicit reference is made to the contribution of others, that this dissertation is the result of my own work and has not been submitted for any other degree at the University of Glasgow or any other institution.

Printed name: Merel Vergaaij
Date: October 1st, 2022

NOMENCLATURE

UNITS

All units of measurement throughout this thesis conform to the *Système Internationale*, with deviations from this rule noted where appropriate. The symbol $ refers to US dollars.

SYMBOLS

The following symbols are used throughout this thesis. All scalar quantities are represented by non-bold italic symbols. All vectors are represented by bold italic symbols. Iterators such as i, j, or k are used where necessary, without interfering with the symbols below.

a	semi-major axis, AU
b	learning curve slope
c	specific cost, $/kg
$\mathbf{c}$	constraint vector
$c_{\Delta\text{mass}}$	specific cost of increase in resource mass, $/kg
C	cost, $
CF_t	cash flow during time period t, $
d	diameter, m
e	eccentricity
E	eccentric anomaly, rad
g_0	standard gravity, 9.81 m/s^2
$\mathbf{g}$	path constraints
G	gravitational constant, km^3/s^2
$h_{\max}$	maximum excavation depth, m
H	magnitude
i	inclination, deg or rad
I	discount rate, %
I_{sp}	specific impulse, s
J	objective, multiple units possible
k	number of clusters in k-means algorithm
L	Lagrangian objective function, multiple units possible
m	mass, kg
M	mean anomaly, rad
n	number
$\hat{\mathbf{n}}$	normal unit vector

t	time, s
p	price of resources, $
p'	price of resources as purchased from terrestrial sources, $
p_v	albedo
$\mathbf{p}$	static parameter vector
P	probability
q	perihelion distance, AU
Q	aphelion distance, AU
d	diameter, m
r	radius, m
$\mathbf{r}$	position vector, m
$\hat{\mathbf{r}}, \hat{\boldsymbol{\theta}}, \hat{\boldsymbol{\phi}}$	unit vectors defining axes of frame (B)
R	revenue, $
$\mathbf{u}$	control vector
v_∞	hyperbolic excess velocity, m/s
VI	value of investment, $
x, y, z	Cartesian coordinate, m
$\mathbf{x}$	state vector
$\mathbf{X}$	decision vector
α	cone angle, rad
α^*	cone angle which maximises force in transverse direction of sail, rad
β	lightness number
δ	clock angle, rad
ΔV	change in velocity, m/s
ϵ	structural mass coefficient,
θ	true anomaly, rad
κ	throughput rate, kg/day/kg of MPE
λ	mass fraction
$\lambda_\mathrm{volatile}$	recovery ratio of volatiles, %
μ	gravitational parameter, $\mathrm{km}^3/(\mathrm{s}^2\mathrm{kg})$
ρ	density, $\mathrm{kg/m}^3$
σ	standard deviation
ϕ	heliocentric transfer angle, rad
$\mathbf{\Phi}$	Bolza objective function, multiple units possible
ω	argument of periapsis, rad
$\mathbf{\Omega}$	right ascension of the ascending node, rad
Υ	vernal equinox (reference direction)

Subscripts

$\square_0$	initial
$\square_\mathrm{avg}$	average
$\square_\mathrm{bag}$	storage bag
$\square_\mathrm{cargo}$	cargo spacecraft

$\square_{\text{container}}$	resource container attached to solar sail
$\square_{\text{C}}$	C-type (asteroid spectral type)
$\square_{\text{demand}}$	volatile demand
$\square_{\text{dep}}$	departure
$\square_{\text{dev}}$	development
$\square_{\text{end}}$	end of Lambert arc
$\square_{\text{entry}}$	atmospheric entry phase
$\square_{\text{eq}}$	equality constraints
$\square_{\text{esc}}$	escape
$\square_{\text{f}}$	final
$\square_{\text{GEO}}$	geostationary orbit
$\square_{\text{ineq}}$	inequality constraints
$\square_{\text{ks}}$	kickstage
$\square_{\text{ks,dry}}$	dry kickstage spacecraft
$\square_{\text{ks,prop}}$	propellant used in kickstage
$\square_{\text{ks,transport}}$	transported using kickstage
$\square_{\text{lower}}$	lower boundary
$\square_{\text{l}}$	launch
$\square_{\text{l,orbit}}$	launch to a specific orbit
$\square_{\text{LEO}}$	low-Earth orbit
$\square_{\text{LG}}$	Lunar Gateway
$\square_{\text{main}}$	maintenance
$\square_{\text{man}}$	manufacturing
$\square_{\text{max}}$	maximum
$\square_{\text{min}}$	minimum
$\square_{\text{mining}}$	mining phase
$\square_{\text{mis}}$	mission
$\square_{\text{mpe}}$	mining and processing equipment
$\square_{\text{Moon}}$	Moon
$\square_{\text{MBC}}$	Mars Base Camp
$\square_{\text{MR}}$	mixture ratio
$\square_{\text{p}}$	perigee
$\square_{\text{prop}}$	propellant
$\square_{\text{op}}$	operations
$\square_{\text{r}}$	resources
$\square_{\text{r,available}}$	available resources
$\square_{\text{r,mined}}$	mined resources
$\square_{\text{r,sold}}$	sold resources
$\square_{\text{r,transportable}}$	transportable resources
$\square_{\text{r,vented}}$	resources after venting
$\square_{\text{s}}$	success
$\square_{\text{sails}}$	fleet of solar sails
$\square_{\text{scaled}}$	scaled value
$\square_{\text{spiral}}$	solar-sail spiral around planet

$\square_{\text{start}}$	start of Lambert arc
$\square_{\text{stay}}$	stay at mining location
$\square_{\text{s/c,dry}}$	dry spacecraft
$\square_{\text{s/c,wet}}$	wet spacecraft
$\square_{\text{total}}$	total
$\square_{\text{transfer}}$	transfer
$\square_{\text{trips}}$	trips
$\square_{\text{upper}}$	upper boundary
$\square_{\text{weighted}}$	weighted value

Superscripts

$\square^{(A)}$	in body-fixed reference frame
$\square^{(B)}$	in inertial two-body frame
$\square^{O}$	outbound
$\square^{I}$	inbound

Operators and other notation

$\hat{\square}$	unit vector
$\dot{\square}$	first derivative with respect to time
$\ddot{\square}$	second derivative with respect to time
$\square'$	corrected
$\lceil\square\rceil$	ceiling rounding
$\Delta\square$	difference

ABBREVIATIONS

ASTEROIDS	American Space Technology for Exploring Resource Opportunities in Deep Space
AU	Astronomical Unit
CER	Cost Estimating Relationship
CNSA	China National Space Administration
DART	Double Asteroid Redirection Test
DDT&E	Design, Development, Test and Evaluation
EM-L_1	Earth-Moon Lagrange Point 1
ENPV	Expectation value of Net Present Value
ESA	European Space Agency
ESRIC	European Space Resource Innovation Centre
FY	Fiscal Year
GEO	Geostationary Orbit
GER	Global Exploration Roadmap
GDP	Gross Domestic Product
ISRU	In-Situ Resource Utilisation
ISS	International Space Station
IRR	Internal Rate of Return

JAXA	Japan Aerospace Exploration Agency
JPL	Jet Propulsion laboratory
LEO	Low-Earth Orbit
LG	Lunar Gateway
LH_2	Liquid Hydrogen, $H_{2\ (l)}$
LLO	Low-Lunar Orbit
LMO	Low-Martian Orbit
LOX	Liquid Oxygen, $O_{2\ (l)}$
MBA	Main-Belt Asteroid
MBC	Mars Base Camp
MCA	Mars-Crossing Asteroid
MOXIE	Mars Oxygen In-Situ Resource Utilization Experiment
MPE	Mining and Processing Equipment
MPBR	Mass PayBack Ratio
NASA	National Aeronautics and Space Administration
NEA	Near-Earth Asteroid
NEAR	Near-Earth Asteroid Rendezvous
NEO	Near-Earth Object
NLP	Non-Linear Programming
NPV	Net Present Value
PGM	Platinum-Group Metal
PPP	Public-Private Partnership
OSIRIS-REx	Origins, Spectral Interpretation, Resource Identification, Security, Regolith Explorer
RAV	Replacement Asset Value
REM	Rare-Earth Metal
R&D	Research and Development
ROI	Return on Investment
SBDB	Small-Body Database
SE-L_1	Sun-Earth Lagrange point 1
SE-L_2	Sun-Earth Lagrange point 2
SLOC	Source Lines of Code
SLS	Space Launch System
SM-L_1	Sun-Mars Lagrange point 1
SMASS-II	Small Main-belt Asteroid Spectroscopic Survey, Phase II
SSTO	Single Stage To Orbit
SRU	Space Resource Utilisation
TPBVP	Two-Point Boundary Value Problem
TRL	Technology Readiness Level
WBS	Work Breakdown Structure

Chapter 1

INTRODUCTION

I have announced this star as a comet, but since it is not accompanied by any nebulosity and, further, since its movement is so slow and rather uniform, it has occurred to me several times that it might be something better than a comet.

Giuseppe Piazzi, after the discovery of 1 Ceres in 1801

Space missions have traditionally been expensive. Escaping Earth's deep gravity well comes with a high energy requirement and therefore high cost. Asteroid mining poses as a solution to this costly problem, to significantly reduce the costs associated with space missions by using resources from asteroids, particularly water, thereby reducing the need for expensive launches from the Earth's surface. Asteroid mining not only holds the potential to enhance space exploration, but also life on Earth [1].

For many years, science-fiction writers, space scientists and engineers have hypothesised about the potential advantages of asteroid mining [2]. However, due to technical, financial, and political challenges, commercial asteroid mining seemed to remain a distant fantasy [3]. Nonetheless, the last few years have shown that asteroid mining is moving from a conceptual stage into a development stage. Earth-based observations and studies, combined with a number of missions to asteroids, have demonstrated that asteroids indeed contain vast quantities of valuable resources [3, 4]. While Lunar mining receives an increased amount of attention for near-term exploration [5], this thesis focuses on exploiting asteroids, a number of which are more accessible than the Moon in terms of ΔV [3].

Space resources are incredibly varied. Examples of resources are solar power, minerals, metals, gases, rare-Earth elements and materials for space manufacturing, such as construction metals or regolith. Yet, it is ordinary water that holds the greatest potential in the near term. Besides being necessary for life support of humans in space, when split in its constituents it forms a highly efficient rocket propellant: liquid oxygen (LOX) and liquid hydrogen (LH_2). Research has shown that water is abundant in the inner solar system, including on asteroids [6]. The first goal of space resource utilisation (SRU) is to greatly reduce the cost, reduce the risk and improve the flexibility of space missions, for example by manufacture propellant in-situ. Later, it could be possible to return valuable resources or energy back to Earth, or even to build towards a self-sustaining space society [1].

The resources on asteroids are needed. Easily-accessible key natural resources, upon which the

development of many technologies are dependent, are in limited supply. Although humanity will not run out of easily-accessible critical raw materials for decades or even centuries to come, a point is reached where we can identify the limits of these resources [3]. Furthermore, ambitious crewed interplanetary missions are planned [5, 7], as well as macro-scale structures in Earth orbit [8, 9], for which large quantities of space-based resources are required. Confronted with this, resources from space are becoming increasingly attractive and feasible options, particularly those from near-Earth space [3]. Mining of natural resources from extraterrestrial sources, could provide a solution to the limited supplies of easily-accessible key natural resources on Earth and as building blocks for interplanetary exploration [2, 5].

Asteroids are chosen as the primary objective for an increasing number of space exploration missions. The next few years there are already four missions planned for launch: National Aeronautics and Space Administration's (NASA) NEA Scout (2022) [10] and Psyche (2023) [11] missions, the Japan Aerospace Exploration Agency's (JAXA) DESTINY+ mission (2024) [65] and the China National Space Administration's (CNSA) Zhenghe mission (2025) [12]. Previous missions to asteroids, such as Hayabusa [13], Hayabusa2 [14], Dawn [15], and OSIRIS-REx [16] have made significant contributions to the collective body of knowledge on asteroids, how to explore them and even how to return resources from asteroids. Future missions will contribute to this by demonstrating the ability to go to increasingly small asteroids, to return increasingly larger amounts of resources, and build on the knowledge regarding asteroid composition and properties of asteroids with different classifications.

It is not just the scientific community that is attracted to asteroids. Where space missions were traditionally driven solely by government agencies, this is now being complemented by commercial enterprises. SRU can be the catalyst for a growing space economy [17], with enterprises processing resources and delivering products to customers at a range of locations in space or on Earth. The past decade has seen a number of commercial companies pursuing asteroid mining [18], of which Planetary Resources Inc. and Deep Space Industries are arguably the most well-publicised, founded in 2010 and 2012, respectively [19]. While both of these companies were acquired by other companies following financial issues, a range of companies have been founded since [20]. These companies share a vision for a sustainable in-space economy, some by providing asteroid-derived propellant to in-space customers, but others by returning technology metals to Earth, such as platinum-group metals (PGMs) and rare-Earth metals (REMs) [20].

In recent years, many architectures for asteroid mining missions have been conceptualised and investigated, a number of which including economic models. The need for cost estimations and economic models is fuelled by the interest of commercial companies in asteroid mining, which need to be convinced of profitability before investing in this exciting yet expensive opportunity.

1.1 AIMS AND OBJECTIVES

Commercial companies are interested in asteroid mining due to its perceived profitability. To research the economic viability of asteroid mining, a number of economic models have been created and analysed. These models span a myriad of types and locations of asteroids and customer locations, are conceptualised for different timescales and levels of technology, and have a large number of necessary assumptions. Therefore, comparing these models is a hard task. Furthermore, incorporating trajectory optimisation to investigate missions to asteroids is paramount, to perform calculations with accurate total velocity change (ΔV), transfer times and phasing.

This thesis aims to present a parametric model in which trajectory optimisation and economic

modelling are coupled. Using this parametric model, different mining missions can be compared, focusing on but not limited to asteroids. Using the same economic model and mission analysis, applied to a range of different mission architectures, allows for an unbiased comparison. Because of the many parameters involved in the economic model and mission analysis, a balance in the level of approximation used is essential. This results in a moderately low-fidelity parametric approach that can be applied to many different combinations of resource and customer locations. The results can be used to identify potential value chains to focus further research using high-fidelity models. One of the advantages of parametric models is that it is straightforward to test the sensitivity to one or more of the inputs. In this way, it can be determined which parameters are in need of further investigation because of their influence on profitability. Trade-offs relating to inputs to the model can be performed, for example; the asteroid orbit, customer location, propulsion method or cost estimations.

Following related work on the economic modelling of asteroid mining, the parametric model developed in this thesis can be used to maximise the Net Present Value (NPV) of a mission [21–28], or minimise the specific cost of delivered resources [29–31]. The model focuses exclusively on the mining and processing of volatiles, not PGMs or other high value-to-mass resources, for which the reasons are given in Section 2.3.1.

1.1.1 Research Questions

To provide a key contribution to the body of knowledge on the economic modelling of asteroid mining missions, the following Research Questions will be addressed in this thesis:

1. How can economic modelling and trajectory optimisation be integrated to produce economically viable missions?

2. Can the propellantless nature of solar sailing be leveraged to transport low value-to-mass asteroid resources to GEO in a more economical way than chemical propulsion?

3. What happens to the profitability of selling asteroid volatiles when specific launch costs from Earth (in $/kg) decrease?

4. In which customer locations can asteroid volatiles compete financially with volatiles obtained from the Earth, Moon, and Mars?

5. What happens to the affordability of asteroid volatiles after the lowest cost resources have been used up?

6. Is reusing spacecraft for successive asteroid mining missions for propellant more profitable than single-use spacecraft?

1.1.2 Modelling Time Frame and Scope

This thesis addresses a time frame which is beyond the current economics and operations of the space industry. It addresses a time frame when there is a continuous demand for asteroid resources, when technology has matured to bring down costs of space hardware, and when specific technologies are available for resource mining and processing. Irrespective of when this might happen or how it might be accomplished, there is a general awareness that it will be necessary to use in-situ resources to establish a sustainable space economy [5, 17, 18]. Estimations for when this will occur vary, and early

historical projections regarding asteroid mining being feasible have long passed. Recent estimates by organisations presenting information in the public domain suggest that this could only be 10-20 years into the future [32, 33].

Asteroid mining will be a disruptive innovation, an innovation that creates a new market and eventually disrupts the existing market, displacing established firms, practices and technologies. Again, despite numerous technical, financial, and political challenges, the last few years have shown that asteroid mining is moving from a conceptual stage into a development stage, with a number of related companies emerging, aiming at commercial asteroid mining [18, 32, 33].

In order for asteroid mining to become a reality, a number of technologies have to be developed to a high Technology Readiness Level (TRL). While sample-return missions to asteroids, such as Hayabusa (1 and 2) and OSIRIS-REx have demonstrated a number of these technologies, the sample mass is still very small [14, 16]. Investments have to be made to expand current knowledge on mining and space technologies, to further the understanding of asteroid compositions and to develop the key systems that are needed for processing of asteroid resources, transport and storage, and to carry out these tasks autonomously [34]. These challenges and others are discussed in detail in Section 2.3.3, and many have to be overcome before the first commercial asteroid mining mission can be considered. Nevertheless, this thesis focuses on commercial missions, and will therefore assume that these technologies have been developed. Determining the costs related to technology development from a low to a high TRL is considered outside the scope of this thesis. However, development costs to design the specific required spacecraft using these high-TRL technologies will be considered.

1.2 PUBLISHED WORK

This PhD thesis combines material from three journal publications by the author [35–37], co-authored with the author's PhD supervisors: Prof. Colin McInnes and Dr. Matteo Ceriotti. Two of these papers have been previously presented at a conference [38, 39] and subsequently selected for publication. The thesis outline below will explain which papers relate to which chapter.

Journal papers

- **Vergaaij, M.**, McInnes, C.R., and Ceriotti, M. (2019). *"Influence of launcher cost and payload capacity on asteroid mining profitability"*, Journal of the British Interplanetary Society, Vol. 72, No. 12, pp. 435–444
- **Vergaaij, M.**, McInnes, C.R., and Ceriotti, M. (2021). *"Economic assessment of high-thrust and solar-sail propulsion for near-Earth asteroid mining"*, Advances in Space Research, Vol. 67, No. 9, pp. 3045–3058. doi:10.1016/j.asr.2020.06.012
- **Vergaaij, M.**, McInnes, C.R., and Ceriotti, M. (2021). *"Comparison of material sources and customer locations for commercial space resource utilization"*, Acta Astronautica, Vol. 184, pp. 23–34. doi:10.1016/j.actaastro.2021.03.010

Conference papers

- **Vergaaij, M.**, McInnes, C.R., and Ceriotti, M., *"Economic assessment of high-thrust and solar-sail propulsion for near-Earth asteroid mining"*, 5$^{\text{th}}$ International Symposium on Solar Sailing, 2019, Aachen, Germany

- **Vergaaij, M.**, McInnes, C.R., and Ceriotti, M., *"Influence of launcher cost and payload capacity on asteroid mining profitability"*, 17th Reinventing Space Conference, 2019, Belfast, United Kingdom

1.3 THESIS OUTLINE

This thesis is divided into nine chapters. Following the introduction, the next two chapters (Chapters 2 and 3) will set out an introduction to asteroid resources and a technical introduction to the methods employed, respectively. Next, the baseline methodology for the thesis is discussed, to ensure consistency of approach among the chapters in this thesis. The following four chapters (Chapters 5-8) constitute the main body of work of this thesis, the first three of which are based on published works. The thesis is concluded in a final chapter with the conclusion, limitations of the work, and recommendations for future work made.

- **Chapter 2** provides an overview of asteroid resources. This overview includes information on asteroid composition and properties, categories, and missions to asteroids. Also, background information on SRU is given, setting out its advantages, its history (mainly focused on the past decade), and its future prospects. Finally, background information on asteroid mining is presented covering potential future markets, necessary equipment and technologies, and most importantly, the challenges asteroid mining faces.

- **Chapter 3** sets out the background information for the specific technical work to be undertaken. This includes an overview of cost estimation techniques, economic models, dynamical models, and trajectory optimisation techniques.

- **Chapter 4** describes the baseline mission and methodology, based on work published in Refs. [35–37]. This baseline links together the subsequent chapters in one cohesive thesis. First, the baseline mission architecture is discussed, followed by the adopted parametric economic model, including cost estimations for inputs to this model. Next, the mass budget based on the baseline architecture is discussed, which will provide input to the economic model. A framework for how trajectories are to be calculated and optimised is defined, which provides input to the mass budget and therefore the economic model. This chapter addresses Research Question 1.

- **Chapter 5** employs the baseline mission and methodology to investigate the region of orbital element space where a target asteroid can prove to be profitable. This analysis is carried out for both chemical propulsion and solar sails, and covers the work published in Ref. [36]. This Chapter addresses Research Question 2 and 6.

- **Chapter 6** investigates the impact of launch vehicle cost and payload capacity on the profitability of asteroid mining missions. Case studies based on the SpaceX Starship system and Arianespace Ariane V ES launch vehicles, as well as general results are presented. This Chapter is based on the work published in Ref. [35] and addresses Research Question 3 and 6.

- **Chapter 7** investigates a number of combinations of mining locations and customer locations, to assess which value chains would merit further investigation. This Chapter is based on the work published in Ref. [37] and addresses Research Question 4.

- **Chapter 8** investigates a year-by-year simulation of a growing space economy relying on asteroid resources. The resources that can be retrieved most affordably are used at any point in time, which gives insights into the changing costs for asteroid mining as these affordable resources have been used up. This Chapter addresses Research Question 5 and 6.
- **Chapter 9** concludes this thesis with a brief summary of the baseline mission and answers to the Research Questions. Limitations of this thesis are discussed, and recommendations for future work are given based on the findings in this thesis and their limitations.

CHAPTER 2

BACKGROUND TO ASTEROID RESOURCES

This Chapter will describe background information relevant to asteroid resources. First, asteroids are discussed in some detail. Next, the background of SRU is described, and finally, several aspects of asteroid mining are highlighted.

2.1 ASTEROIDS

Asteroids are minor planets orbiting the Sun, thought to be the shattered remnants of planetesimals. Millions of asteroids exist, primarily residing in the main belt between Mars and Jupiter, but a set of asteroids orbit the Sun at distances closer to the Earth's orbit [40]. The distribution, formation, composition and evolution of asteroids are absolutely fundamental to our understanding of how the formation of planets occurred and, eventually, why life exists on Earth [41]. Since asteroids are remnants from the formation of our Solar System they contain many key resources in quantities and concentrations much higher than can be found on or near the surface of the Earth [42].

Each day, new asteroids are discovered and catalogued. Since the first discovery of an asteroid, in 1801, it took 48 years to discover the 10^{th} asteroid, 19 years for the 100^{th}, 53 years for the $1{,}000^{\text{th}}$, 68 years for the $10{,}000^{\text{th}}$, 16 years for the $100{,}000^{\text{th}}$ and only 15 years for the $1{,}000{,}000^{\text{th}}$ asteroid.[1] This is visualised in Fig. 2.1 from Ref. [15].

The combined mass of asteroids in the asteroid belt, where most of the asteroids are located, is only approximately 0.5% of the mass of the Earth, or 4% of the mass of our Moon [40]. Why are we so curious about asteroids, given that they only comprise such a small portion of our solar system? Because asteroids matter, now more than ever before. Asteroids matter not only to scientists, but to explorers, companies and the long-term future of humanity [15]. This Section will present a review of different categories of asteroids, as well as an overview of past, present and future missions to asteroids.

2.1.1 CATEGORIES OF ASTEROIDS

Whenever large sets of objects are studied, there is a natural desire to group them into categories with similar characteristics. This is also the case for asteroids, which have been catalogued in the Jet Propulsion Laboratory (JPL) Small-Body Database (SBDB).[2] This database includes orbital elements

[1] `https://ssd.jpl.nasa.gov/sbdb_query.cgi`, accessed on August 20^{th}, 2020.

[2] **Please note that throughout this thesis, the JPL database obtained on August 20^{th}, 2020 is used to ensure consistency.**

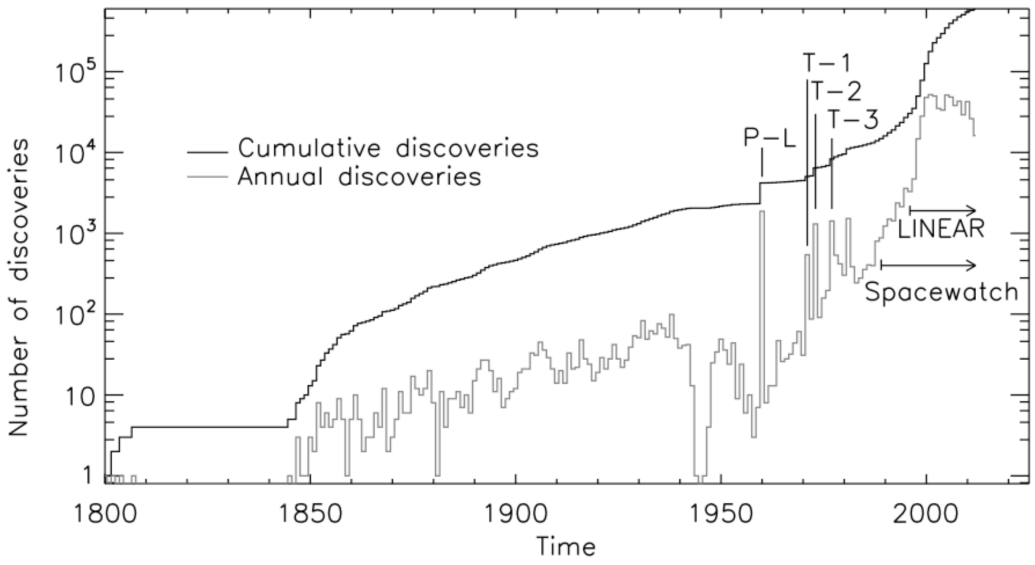

Figure 2.1: Yearly discovery rate and cumulative number of discovered asteroids, reproduced with permission from Ref. [15].

and physical parameters, where known, of asteroids and comets. Both numbered and unnumbered asteroids are catalogued in the database, where numbered asteroids have a more accurate orbit determination and are also catalogued by the Minor Planet Center. Two types of categorising are discussed in this Section, first, based on their orbital elements, and second, based on their estimated composition.

Asteroids are traditionally divided into groups based on the following orbital elements: semi-major axis (a), perihelion distance (q) and aphelion distance (Q). Those closest to Earth orbit are termed Near-Earth Asteroids (NEAs) and by definition have perihelia $q \leq 1.3$ Astronomical Unit (AU) and aphelia $Q \geq 0.983$ AU [40]. This means that they are not necessarily always near the Earth, but they do have the potential to approach the Earth relatively closely. Therefore, they are accessible from the Earth, but they could also pose a danger to Earth. A number of NEAs posing as a potential threat to the Earth have been classified as "potentially-hazardous asteroids". These asteroids have a minimum orbit intersection distance (the minimum distance between all points of two confocal elliptical orbits) with the Earth of 0.05 AU or less and an absolute magnitude of 22.0 or higher.[3]

Other groups are Mars-Crossing Asteroids (MCAs) and Main-Belt Asteroids (MBAs). MCAs are not as strictly defined as the NEAs, but in general, objects with $a > 1.3$ AU and $1.3 \leq q < 1.665$ AU are denoted as MCAs [15]. By that definition, MBAs have $q > 1.665$ AU. In addition, in the JPL SBDB, the maximum values for a and q for MBAs are $a_{\max} = 4.59$ AU and $q_{\max} = 4.21$ AU.

NEAs have been further divided into four categories based on the semi-major axis, perihelia and aphelia of their orbits, and are named after a prominent asteroid within that category: Apollo (Earth-crossing), Amor (outside Earth's orbit), Aten (Earth-crossing), and Atira (within Earth's orbit). The definition of these categories are given in Table 2.1, along with the number of asteroids in each group. The division between the different orbital elements of the groups (NEAs, MCAs and MBAs) is visualised in Fig. 2.2. Based on all NEAs, MCAs and MBAs in the JPL SBDB, a relative distribution of these groups is visualised in Fig. 2.3. It can be seen that the number of MBAs far exceeds the number of MCAs and NEAs combined.

Other groups of asteroids, not directly relevant to this thesis due to their orbital elements, are Trojan asteroids, Centaurs and Trans-Neptunian asteroids. These asteroids reside in orbits with a

[3] `https://cneos.jpl.nasa.gov/about/neo_groups.html`, accessed on August 2nd, 2021.

Table 2.1: NEA groups.[4]

Group	Definition	Number	Percentage of all NEAs
Atira	$a < 1.0$ AU and $Q < 0.983$ AU	23	0.1
Aten	$a < 1.0$ AU and $Q > 0.983$ AU	1,778	4.6
Apollo	$a > 1.0$ AU and $q < 1.017$ AU	12,952	55.2
Amor	$a > 1.0$ AU and $1.017 < q < 1.3$ AU	8,731	37.2

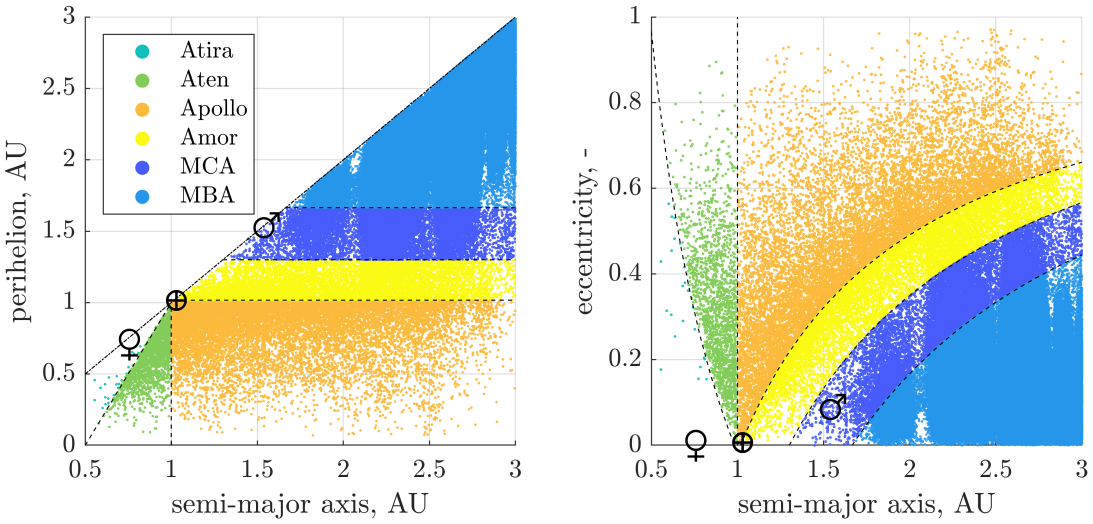

Figure 2.2: Orbital distribution of asteroid groups.

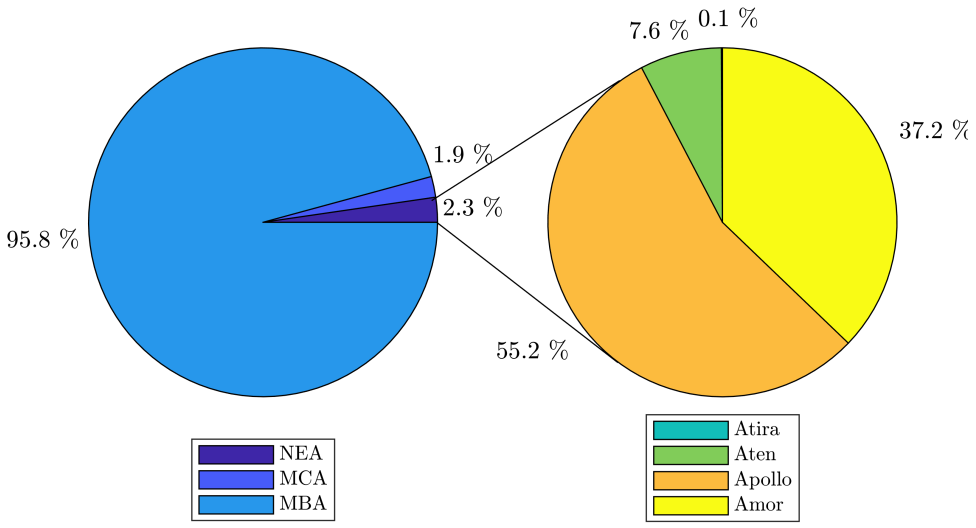

Figure 2.3: Distribution of asteroids over groups, based on orbital elements.

semi-major axis larger than 4.6 AU. Due to their orbits, transfers from Earth are costly in terms of ΔV and time. This is not to say that they are unsuitable for utilising their resources, but that in the short term, asteroids closer by are more easily explored.

It is frequently stated that ∼10% of NEAs are more accessible than the Moon [3, 22, 43], however, these claims date back to estimations by Lewis in 1993 [44]. Sonter [21] recalculated this in 1997 as ∼6%, but even then, only 430 NEAs were discovered [21], only a fraction of all NEAs discovered today. In 2013, this number was recalculated and it was reported that approximately 17% of the NEA population is easier to reach than a soft landing on the Moon [42]. Rather than using these average statements, it would be better if trajectories to the considered asteroids are optimised.

Another taxonomy system is used for asteroids, besides their orbital elements, which distinguishes between spectral types based on the asteroid's emission spectrum, colour and sometimes albedo. The most recent and complete classification is the "Small Main-belt Asteroid Spectroscopic Survey, Phase II" (SMASS-II), based on a survey of 1,447 asteroids [45]. In the SMASS-II taxonomy, three major types are defined: S-, C-, and X-type complexes. These types adhere to the more classical definitions of S-, C- and X-type asteroids [45]. These classical groups have the following characteristics:

- C-type (carbonaceous), water-bearing, with high contents of opaque, carbonaceous material, besides rocks and (hydrated) minerals [22]. Thought to contain ∼10% water in the form of hydrated minerals [46].
- S-type (silicaceous), anhydrous and rocky, mainly consisting of silicates, sulphides, and metals [22].
- X-type, a collection of several types with similar spectral properties, but probably divergent compositions. This mysterious class of objects has ambiguous taxonomic and mineralogical interpretations. This group includes the E-, M-, P- and X-types of the Tholen system [47] and Xe-, Xc-, Xk-, and X-types of the SMASS-II system [45]. These asteroids were initially indistinguishable based on visible-wavelength spectral properties, which is why they are grouped together. Many sub-classes of this type cannot directly be related to meteorites found on Earth, which complicates drawing conclusions about their compositions. Some X-type asteroids could be core remnants of shattered planetesimals: M-types (metallic) are often singled out when discussing asteroid mining due to their composition [48].

Table 2.2 presents data obtained from the JPL SBDB, with all asteroids with a known SMASS-II type. Where possible, types have been grouped together (i.e. all X-subtypes). Two observations can be made from Table 2.2, first, that only a very small subset of asteroids have a known type. Second, a great deal of the presented asteroids are categorised as S-types. However, the discovery and characterisation of higher-albedo objects, such as S-type asteroids, is favoured by strong selection effects. After applying bias-correction factors to the observed NEA population, there are relatively equal proportions of C- and S-type objects, for any given size. The main belt however, is dominated by C-type asteroids by as much as 5:1 [49].

To estimate the mass of an asteroid, to gauge the total value of resource mass, its volume has to be estimated first, which is estimated from its brightness at a known distance and the illumination angle, resulting in an absolute magnitude H [50]. In combination with the asteroid's albedo p_{v}, the asteroid diameter can be approximated by [51]:

$$d \approx 1329 \text{ km} \times \frac{10^{-H/5}}{\sqrt{p_{\mathrm{v}}}} \tag{2.1}$$

Table 2.2: Asteroid types per group, data obtained from JPL SBDB.[5]

Group	A	B	C	D	K	L	O	Q	R	S	T	U	V	X	Total
MBA	**12**	**56**	**328**	**8**	**31**	**44**	**1**	**-**	**4**	**491**	**12**	**1**	**35**	**233**	**1256**
Inner belt	2	-	-	-	-	-	-	-	-	3	-	1	-	5	11
Main belt	9	55	320	6	31	43	1	-	4	487	10	-	35	211	1212
Outer belt	1	1	8	2	-	1	-	-	-	1	2	-	-	17	33
MCA	**4**	**4**	**8**	**-**	**-**	**3**	**-**	**2**	**-**	**63**	**1**	**-**	**-**	**7**	**92**
NEA	**1**	**6**	**18**	**4**	**7**	**8**	**6**	**18**	**1**	**174**	**5**	**3**	**14**	**48**	**313**
Amor	1	-	7	2	4	2	1	1	1	78	3	1	4	22	127
Apollo	-	5	11	2	2	6	4	14	-	83	2	2	9	19	159
Aten	-	1	-	-	1	-	1	3	-	13	-	-	1	7	27
Total	**17**	**66**	**354**	**12**	**38**	**55**	**7**	**20**	**5**	**728**	**18**	**4**	**49**	**288**	**1661**

The diameter, in combination with a density ρ, results in an estimate for the asteroid's mass. Unfortunately, many uncertainties arise when estimating these parameters for an asteroid with an unknown spectral type. Carry [52] outlines the great uncertainties surrounding asteroid densities, as well as the large range of possible average densities per type (ranging from 960 to 9,560 kg/m^3). In the rare case that the spectral type has been determined for an asteroid, Elvis and Esty [50] calculate that the mass of an asteroid is uncertain by a factor of ∼6, contrary to a factor of ∼30 for asteroids with an unknown spectral type.

2.1.2 Past, Present, and Future Missions to Asteroids

Asteroids have generated significant worldwide interest as a result of three decades of asteroid exploration. This Section addresses the missions that have been and will be launched to asteroids.

Figure 2.4 shows a graphic timeline of the missions to asteroids, including which asteroids were visited and what the mission objective was or will be. Due to the long and varying transfer times, as well as the different mission objectives (e.g., flyby or rendezvous), the missions are sorted by their launch date.

On the 29$^{\text{th}}$ of October, 1991, we obtained a close-up image of an asteroid for the first time, thanks to NASA's Galileo spacecraft, launched in 1989. En route to the Jupiter system, on its first pass through the asteroid belt, the spacecraft flew by the asteroid Gaspra [53]. On its second pass through the asteroid belt almost a year later, Galileo discovered a tiny moon orbiting around asteroid Ida, the first-known moon of an asteroid [54].

The first mission to orbit an asteroid was launched in 1996: NASA's Near-Earth Asteroid Rendezvous (NEAR) Shoemaker mission. In February 2000, the spacecraft made history by entering orbit around the asteroid Eros, a large NEA of the Amor group. The spacecraft spent approximately one year in orbit around Eros, allowing for the first long-term study of an asteroid at close range, including measurements on its mass, geology and composition. On its way to Eros, the spacecraft took the first reconnaissance images of a C-type asteroid, the MBA named Mathilde [55].

Around the turn of the century, the well-known NASA and European Space Agency (ESA) Cassini Huygens probe, NASA Deep Space 1 probe, and NASA Stardust probe each performed fly-bys of different asteroids, imaging the asteroids with varying image resolutions and therefore varying scientific return. Interest in asteroids was growing and asteroids were regularly chosen as (secondary) science

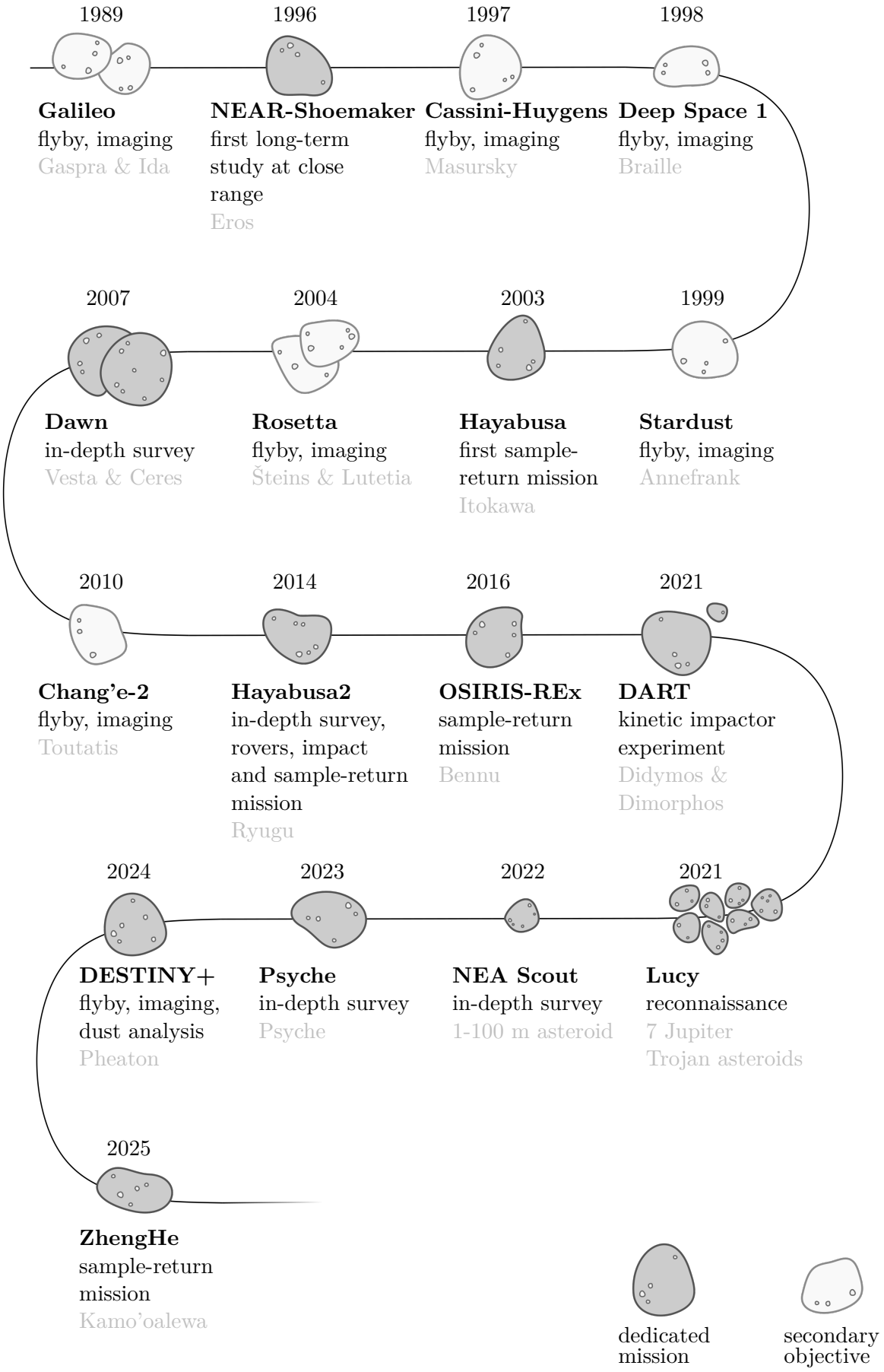

Figure 2.4: Timeline of missions to asteroids.

targets [56–58]. Other missions in which asteroids were selected as a secondary objective, are the ESA cornerstone Horizon 2000 mission Rosetta and the Chang'e-2 by the CNSA, which was the fourth national space agency to explore an asteroid.

The first asteroid sample-return mission was launched in 2003 by JAXA. The Hayabusa project was primarily a technology demonstration project for sample-return missions to asteroids and comets. Hayabusa rendezvoused with NEA Itokawa, an Apollo asteroid of the S-type, in September 2005. The spacecraft experienced many unfortunate events, such as experiencing the largest solar flare that has ever been recorded, only shortly after launch. Many subsequent issues were related to the solar flare, such as loss of communication, damaged fuel line, degradation of the solar cells and engine issues. Nevertheless, upon arrival at the asteroid, data was accumulated on its shape, mass, topography and composition. A sample taken from the asteroid was returned to the Earth and retrieved in June 2010. Because of the issues that the spacecraft encountered during the mission, the sample mass from Itokawa was quite small, only a few thousands of small grains, much less than the planned $\sim$1 g. As a technology demonstration mission, despite the numerous issues during the mission, it was very successful. Many lessons were learned about the technologies required for sample-return missions, which can be seen as the first step for asteroid mining missions, and that sample-return missions are extremely difficult [13, 59].

As part of NASA's Discovery Program, the Dawn spacecraft visited the largest two objects in the main asteroid belt: Ceres and Vesta, which together constitute an estimated 9% of the total mass of the asteroid belt. Dawn entered orbit around Vesta in July 2011 and after a 14-month long survey, moved on to Ceres, around which it entered orbit in March 2015. Doing this, Dawn was the first spacecraft to orbit two extra-terrestrial bodies, demonstrating the feasibility of multi-body exploration. The mission was extended for as long as was possible before it depleted the on-board propellant supply, after which it was placed in a stable orbit around Ceres. Many interesting findings resulted from the mission, including a detailed description of the gravitational field and high-resolution maps of the asteroid surfaces and their features [15].

Just over a decade after Hayabusa, following the initial successes of that mission, Hayabusa2 was launched in 2014 on a journey to NEA Ryugu. The spacecraft carried multiple instruments to observe the asteroid, four small rovers, an impactor and a sample return capsule [60]. In 2018, the first rover exploration of an asteroid was carried out. Two samples have been obtained, both through a touch-and-go operation. The first sample from the surface of the asteroid and the second from sub-surface material. Both samples, in total 5.4 g (far exceeding the original target of 0.1 g), have safely been returned to Earth in December 2020 [14]. Research using the samples is currently ongoing and will further our understanding of asteroid resources. After delivery of the sample capsule, the spacecraft had 30 kg of propellant remaining, allowing for a mission extension. This mission extension, which is still underway at the time of writing, consists of a high-speed fly-by of asteroid 2001 CC21 (possibly an L-type Apollo asteroid) and a rendezvous with asteroid 1998 KY26 (possibly a C-type Apollo asteroid) [61].

The OSIRIS-REx (Origins, Spectral Interpretation, Resource Identification, Security, Regolith Explorer) mission was launched in 2016. Its primary goal is to obtain 60 g of samples (dust, soil and rock) from Bennu, chosen because of its orbit, carbon-rich surface, and because it is a potentially hazardous asteroid, making its study particularly relevant for asteroid deflection. OSIRIS-REx scanned and measured the surface of Bennu for over a year, providing detailed information about its shape, distribution of boulders, craters, slopes and other surface features. Using this information, the sample

site was determined. Collecting the sample was successful, but the sampler head was jammed open by larger rocks, allowing part of the sample to escape. Fortunately, NASA was able to close the sample container and 400 g to 1 kg of sample was retained, much more than the goal of 60 g. The samples will be returned to Earth in September 2023 [16]. The analyses of the returned sample will provide an insight into the composition of this carbon-rich asteroid, which can help in the selection of targets for the first asteroid mining missions.

NASA's Lucy mission was launched in October 2021. Lucy will be the first reconnaissance of the Jupiter Trojan asteroids, the last group of stable asteroids of the solar system to be visited by a spacecraft. Lucy will be able to perform flybys of 7 asteroids, divided over Lagrangian points L_4 and L_5, covering all known taxonomic types. The Trojan asteroids provide a fossil record of planet formation and the mission will provide many insights into planetary origins, sources of volatiles and organics on the terrestrial planets (Mercury, Venus, Earth, and Mars) and the evolution of the planetary system [62].

In November 2021, the Double Asteroid Redirection Test (DART) was launched. It targeted the double asteroid Didymos to perform a kinetic impactor experiment on its moonlet Dimorphos. The spacecraft intentionally creashed into Dimorphos with over ∼6 km/s to alter the binary orbit period, to be measured by Earth-based observatories. This mission has been the first demonstration of a kinetic impactor, an important step for planetary protection to mitigate an asteroid impact threat [63]. Four years after this impact, the Hera mission proposed by ESA will contribute to the DART mission by performing measurements to understand the effect of the DART impact on Dimorphos, during what will be the first rendezvous with a binary asteroid. Dimorphos is only 160 m in diameter and until the DART mission, no other asteroid of such a small size has been visited during a mission [64].

The NEA Scout mission is planned for launch in 2022: a 6U CubeSat equipped with a solar sail. Due to the delays of the maiden Space Launch System (SLS) flight, Artemis 1, the target asteroid is not yet fixed, but will be in the 1 to 100 m range. The current planned target is NEA 1991 VG, which is only thought to be 5 to 12 m in diameter. Asteroids of this size have not yet been visited by spacecraft, so this mission will provide valuable insights into the characteristics of these smaller asteroids [10]. Most NEAs, which are the most accessible group of asteroids and therefore suitable for asteroid mining, are in this size group. The lessons learned by the NEA Scout mission are therefore valuable for the first asteroid mining missions.

A NASA mission due for launch in 2023, Psyche, will visit the asteroid bearing the same name. It will be the first time that a small body not made of rock and ice, but metal is explored. The asteroid is thought to have an effective diameter of 226 km and could be the only exposed metal core in the solar system. The mission will allow for an investigation of a building block of planet formation, the iron cores. Earth's own iron core is too deep to be seen or measured, but investigating Psyche will yield valuable insights into the formation of planets. The surface material will be investigated, as well as the topography and magnetism [11].

JAXA is planning on launching a spacecraft to perform a flyby with the comet-asteroid transition body Phaethon in 2024: DESTINY+. It has the smallest perihelion of the named asteroids and is believed to be the parent body for the Geminids meteor shower in December. Both the Deep Impact and OSIRIS-REx missions considered Phaethon as a target of interest [65].

A mission planned for launch in 2025 is ZhengHe, a mission from the CNSA. ZhengHe is planning on visiting the nearest of Earth's quasi-satellites, Kamo'oalewa, to collect a sample and return this to

(a) Mosaic of two Galileo clear-filter images of Gaspra, taken from about 5,300 km, 10 minutes before closest approach.[6]

(b) Image captured during the OSIRIS-REx touch-and-go sample collection event of Bennu, just before touchdown.[7]

Figure 2.5: Images obtained during the first and most recent asteroid missions (1991 and 2020).

Earth. After returning the sample, planned to be 200-1000g, ZhengHe will transfer to a comet in the main belt, to determine if main-belt comets are a viable source of water [12].

This Section has shown that over the last few decades, there have been many "firsts": first close-up image of an asteroid in 1991, first orbit around an asteroid in 2000, first sample return mission to an asteroid launched in 2003, first moving, robotic observation of an asteroid in 2018 and hopefully the first time a man-made object purposely changed the orbit of an asteroid after launch of the DART mission in 2021. Technology has advanced since the first close-up image, as shown in Fig. 2.5, showing the first picture obtained by Galileo in 1991 and a recent image obtained by OSIRIS-REx in 2020. Our knowledge of asteroids has increased significantly over the past decades, due to asteroid missions: their compositions, shapes, masses, densities, topologies, and much more. The technology to carry out these missions has also greatly improved over time, allowing the spacecraft to orbit and get closer to asteroids, investigate increasingly smaller asteroids, take high-resolution images and other measurements, and even touch asteroids to take a sample. Asteroids have always fascinated scientists, but the sheer number of missions launched in recent years, and to be launched in the next few years, shows that the scientific community is eager to learn more about these small solar system bodies.

2.2 SPACE RESOURCE UTILISATION

The cost, mass and risk of human and robotic activities beyond Earth can be significantly reduced through SRU [66, 67]. SRU is the strategy of using natural resources from the Moon, Mars and other bodies for use in situ or elsewhere in the solar system, which can replace material that would otherwise be brought from Earth [68]. The most widely-used form of SRU is using solar panels to transform sunlight into usable power, a technique used on the International Space Station (ISS), in plans for the Lunar Gateway and on most satellites. As (human) space exploration evolves towards longer journeys into the solar system, missions will become more reliant on SRU, as resupply missions

[6] `https://nssdc.gsfc.nasa.gov/imgcat/html/object_page/gal_p40449.html`, public domain, not copyrighted, accessed on August 26, 2021.

[7] `https://www.nasa.gov/feature/goddard/2020/osiris-rex-tags-surface-of-asteroid-bennu`, public domain, not copyrighted, accessed on August 26, 2021.

will become increasingly more expensive. Mission capabilities can and will multiply when missions are more independent of Earth and space resources are transformed into usable products [18].

When resources are used at or near the place of extraction, the practice is called In-Situ Resource Utilisation (ISRU), or "living off the land" [67].

2.2.1 Advantages of Space Resource Utilisation

There are clearly many advantages to SRU. Benefits achieved through the inclusion of SRU in space missions are in different areas: mass reduction, cost reduction, risk reduction, improved mission flexibility and other capabilities enabled for missions [1]. In addition, using space resources presents opportunities on Earth. The remainder of this Section will first give an overview of potential materials to utilise, followed by a description of the benefits achieved in the different identified areas.

Potential Materials

Potential materials to utilise are different depending on location, the Moon, Mars or on asteroids, but can include water, solar wind implanted volatiles, metals and minerals, abundant solar energy, atmospheric constituents and regolith (a layer of rocks and fine-grained particles) [1].

A key resource can be found on the Moon, Mars and most of the asteroids: water. Uses are, for example, O_2 and H_2O for life support and LOX and LH_2 for propellant. ESA foresees the primary use case for space resources in the foreseeable future to be propellant. Life support consumables are a secondary use case, which alone do not justify the investments needed [32]. On the Moon, water is thought to be concentrated in the permanently-shadowed craters at the poles, but the rest of the Moon is generally considered an anhydrous body and highly depleted in water and volatiles [69]. In recent years, Lunar exploration has shown that there may be a number of possibly exploitable water reservoirs on the Lunar surface [70]. Lunar regolith is thought to consist of 1.5% water in weight [71]. Forming water from hydrogen and oxygen is not straightforward on the Moon, where hydrogen is only available as volatiles implanted by the solar wind, in concentrations of 10 to 120 ppm [71]. On Mars, there are three possible sources of water: as vapour in the atmosphere in small quantities ($\sim$30 ppm, too low for practical harvesting for SRU [72]), as water ice and in hydrated minerals. Current estimates are that there is sufficient water on Mars for a 34 m deep global ocean, most of it in water ice inventories which increase in abundance and shallowness with increasing latitude. Much of the ice is contained in the polar ice caps. High concentrations of hydrated minerals and clays have been revealed by observing the Martian surface. Large parts of the crust are consistent with basaltic rocks, but there are a number of sites where measurements suggest the identification of hydrated minerals with a high water content [72]. General surface regolith on Mars is thought to contain about 1.3% water by weight [71, 73]. Hydrogen is a relatively scarce resource on Mars, so combining hydrogen and oxygen to form water is not preferred [71]. On asteroids, the water content depends on the type of the asteroid. As explained in Section 2.1.1, multiple different types of asteroid are known. C-type asteroids are thought to contain $\sim$10% water in the form of hydrated minerals [46]. It has been shown that this water in asteroids can be easily accessed [74].

Oxygen is another resource that is researched extensively, because it is a vital element of life-support systems. While water can be split into hydrogen and oxygen, oxygen can also be recovered from different sources. Oxygen can be extracted from metal oxides and silicate minerals which are available on the Moon, Mars and many asteroids (depending on their type) [71, 75]. Typical Lunar

regolith contains about 40% oxygen by weight [69, 71], as does Martian regolith [76] and some types of asteroids [26]. On Mars, oxygen can also be extracted from CO_2 in the atmosphere [72].

Metals can be divided in two types: low-value and high-value metals. Low-value metals, such as iron, nickel and cobalt can be used for building structures in space. High-value metals, such as PGMs and gold, can be used in space or on Earth. PGMs are the six noble, precious metallic elements: platinum, palladium, rhodium, ruthenium, iridium and osmium [3].

PGMs tend to occur in the same mineral deposits, both here on Earth and in space. PGMs were abundant during the formation of the Solar System, but are highly depleted in the Earth's crust. The environment just after the formation of the Solar System allowed larger bodies, like Earth, to differentiate gravitationally. This meant that heavier elements, such as iron, nickel and PGMs, were pulled to the core of the Earth. As a result, in the best mines on Earth, concentrations of 4 to 6 parts per billion (ppb) are found. Since many asteroids are believed to be made up from primitive core material, they are rich in PGMs, with concentrations of 30-60 ppb hypothesised in many asteroids, potentially even upwards of 1000 ppb based on meteorite studies [3, 77]. This means that platinum content is up to three orders of magnitude higher than for typical deposits on Earth [26]. The Moon may contain trace elements of PGMs too, but not nearly in the quantities found on asteroids, because the PGMs found on the Moon are deposited by impacted asteroids and comets [69].

Low-value metals are found in abundance in the Lunar regolith, such as iron (14-17 % by weight of regolith in Lunar mares) and aluminium. Aluminium is available on the Lunar highlands in concentrations much higher than in asteroids [69]. The type of asteroid influences the quantity of metals found on them. Based on meteorite samples, M-type asteroids can contain ∼88% iron and ∼10% nickel. For C-type asteroids, this can still be ∼11% free iron and ∼1.4% free nickel and even more in metal oxides [3]. On Mars, the typical regolith contains ∼15% iron [76].

Semiconductor material is found on the Moon, Mars and asteroids, in varying quantities and types. Semiconductors include elements such as phosphorus, gallium, germanium, arsenic, selenium, indium, antimony and tellurium [3]. They can be used in the production of solar panels. Silicon, is abundant in rocks on the Moon and Mars [69, 76].

Helium-3 has received significant attention due to its use in nuclear fusion, even though the first reactor is still decades away at best [78]. Helium-3 is very rare on the Earth, but the solar wind has deposited helium-3 on the Moon, mainly in sunlit areas. Helium-3 is available in concentration of about 4 ppb by mass, so large quantities of regolith would have to be processed [69].

Regolith, available on the Moon, Mars and asteroids, can also be used for various purposes. In its unprocessed form, it can be used for shielding of human habitats. Processed, it can be used to construct habitats, for example through sintering, 3D printing or by converting into concrete [69]. These habitats do not have to withstand launch loads and experience less gravity than on Earth, meaning that they do not have to be as strong. Regolith can also be used as soil for agriculture [79].

Mass Reduction

Using local resources is a way of decoupling space activities from the Earth, by negating the need for expensive launches from the Earth's surface [18]. In-situ production of mission critical consumables significantly reduces the required mass to be delivered to an extraterrestrial surface [1]. Figure 2.6 shows the gravity well of the Earth, the Moon and a fictional Ceres-like asteroid. The fictional asteroid has the mass and diameter of Ceres (the most massive known asteroid in the main belt), but is placed at a distance of 8×10^5 km from the centre of the Earth, just over twice the Earth-Moon distance.

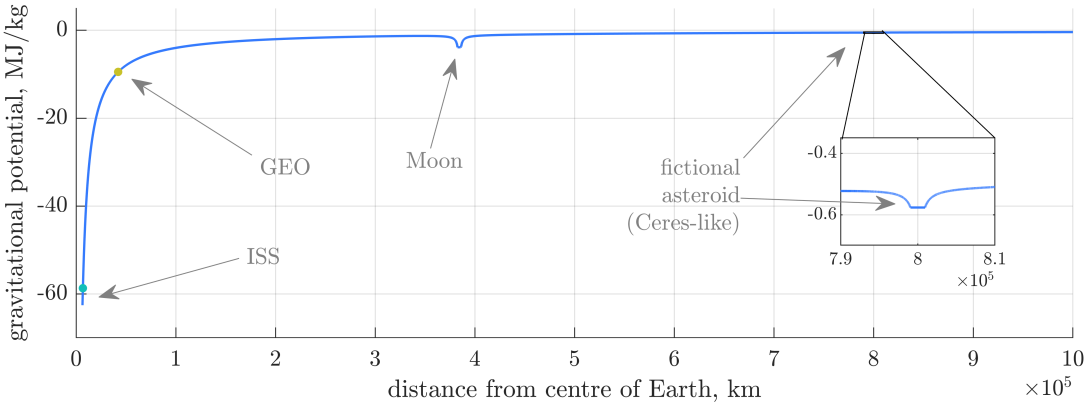

Figure 2.6: Gravitational potential showing the gravity well at the Earth, Moon and a fictional asteroid.

This figure shows how expensive it is to lift material from the deep gravity well of the Earth, in terms of energy. Whereas the gravity well of the Moon is not as deep, it is not insignificant. The gravity well of the (fictional) asteroid however, is almost negligible. The asteroid is modelled after the most massive MBA, but still has an escape velocity of only 0.51 km/s, less than 5% of the Earth's escape velocity. For a smaller asteroid, for example, on Bennu (the destination of the OSIRIS-REx mission) this escape velocity is only $\sim$ 0.2 m/s.[8] Given the exponential relationship in the rocket equation, these differences mean major savings in propellant required when lifting resources from the Moon or an asteroid instead of the Earth.

By not having to transport propellant for both the outbound and return segments of a mission, the total mass that has to be lifted from Earth's deep gravity well can be reduced, or the payload capability can be increased. Launch mass requirements can be decreased significantly, for example, for a Lunar outpost, up to 90% of the required launch mass can be saved [80]. Returning from Mars can be impractical and expensive without SRU, due to the ΔV requirement for launch from Mars and the interplanetary transfer [81].

Using SRU to construct and shield habitats also greatly reduces the mass that has to be launched from Earth. Shielding for habitats, for example for radiation, micrometeoroid or even protection from nuclear power plants, can be created from raw or processed in-situ materials. Construction of the infrastructure necessary for a sustained human presence would benefit from SRU, which could negate the need for logistics supply from Earth.

Cost Reduction

Importantly, a reduction in launch mass leads to a reduction in launch costs. Smaller launch vehicles can be used, and/or less launches are required, both of which reduce the total cost of a mission. Especially the elimination of a re-supply spacecraft and launch has a significant impact on the total cost of a mission [1].

The use of SRU may also provide a means for commercial entities to earn revenue through space exploration by delivering resources [25, 82–84]. This means that, even if SRU technology is not included in the mission, it could still be possible to use resources produced in space, by purchasing these from another company. Again, this can allow for significant savings in terms of launch mass and

[8] `https://ssd.jpl.nasa.gov/tools/sbdb_lookup.html#/?sstr=bennu`, accessed on April 19th, 2022.

therefore in cost. Examples of this are propellant depots with extraterrestrial propellant in space, as proposed by Orbit Fab [85, 86], solar panels manufactured in space, as proposed by Maana Electric,[9] or 3D printing of metal structures, as proposed by SpaceFab.[10] Competition between these companies could stimulate research to minimise the costs of the processed resources to be sold, at further benefit to the customer [42].

Risk Reduction

Through the application of SRU, risk can be reduced by providing a back-up and in-situ capability for human life support, such that mission capabilities and flexibility can be increased [67].

For a mission to be a success, many events must all be executed successfully. Each separate event adds to the total risk of a mission, thereby, reducing the number of events lowers the risk. Through the inclusion of SRU in a mission, a reduction in the number of separate launches could be possible, or could enable a direct return to Earth without rendezvous, which could mean fewer events, leading to a lower overall mission risk [1].

A lower mission risk can also be realised when SRU is used for maintenance and repair. Despite extensive checks before a mission, failures happen. This means that replacement parts have to be available, so a larger mass has to be launched from Earth. Through the application of SRU to produce replacement parts, not only the costs would be (much) lower, it also decreases the risk of the mission because parts necessary for repair can be produced, when necessary. Safety margins can be increased by reducing reliance on Earth delivered hardware [1]. Currently, shielding for radiation for astronauts follows the principle "as safe as reasonably achievable", balancing an acceptable risk with the mass of the shielding material. Using SRU this shifted balance would mean much greater protection to astronauts [1].

Mission Flexibility and Enabled Capabilities

If it is possible to refuel during a mission, a wealth of opportunities open up. Missions can be extended beyond their usual mission duration, for example by using the additional propellant for station-keeping or for exploring new targets (i.e. in multiple-asteroid missions). For missions to larger bodies (e.g. the Moon), hoppers can be used for long-range surface mobility using in-situ propellant, eliminating the need for multiple launches from the Earth. When SRU capabilities are introduced into missions, they can significantly impact the delivered and returned payload mass of missions. Furthermore, high-energy missions are enabled through intermediate refuelling, for example to the outer solar system [1].

Flexibility for human missions is also significantly impacted through the inclusion of SRU for life-support, especially for long duration missions. When consumables can be obtained from nearby sources, rather than Earth, they allow for a reduction in cost, mass and risk of the mission, in turn allowing for missions that were previously infeasible or impractical due to constraints in cost, mass, risk, and energy [32].

[9] `https://www.maanaelectric.com/`, accessed on August 18, 2021.

[10] `https://www.spacefab.us/future-of-spacefab.html`, accessed on August 18$^{\text{th}}$, 2021.

Benefits on Earth

Space resources are not only of use in space, but also present opportunities on Earth. While it is unlikely that transporting water or low value-to-mass metals back to Earth will be economically viable, there are certainly resources that are in increasingly short supply on Earth, such as PGMs. Our technology development, especially related to renewable energy, is endangered because it relies on these critical metals [25]. Limited platinum reserves and high platinum production costs may slow or even halt fuel cell adoption [3]. Although it is unlikely we will ever completely run out of so-called technology metals, the cost of rare Earth elements rises each year as the mining costs for poorer ores rise. Importing these metals obtained through SRU would have future benefits on Earth [25]. Mining for PGMs on Earth is harmful and exploitative and has a very large energy demand, so moving this practice into space comes with a range of benefits [87, 88]. For each kilogram of PGM that is produced, 40 tonnes of CO_2-equivalent are emitted into the atmosphere [89].

Another benefit of SRU is the opportunities for commercial entities to generate a revenue. It is estimated that the SRU industry will generate a market revenue of 73 to 170 billion euros over the 2018-2045 period, supported by a total of 845,000–1,800,000 full-time employee years. Customers of space resources are expected to gain efficiency in the form of cost savings of 54–135 billion euros in the same 2018–2045 period (accounting for propellant, water for life support and construction resources) [33]. ESA estimates that spill-overs in terms of technology and knowledge will be in the order of 2.5 billion euros over 50 years, which could even be considered a conservative estimate [32].

The inspirational aspect of the SRU challenge can be a driver of innovation for many industries [32]. Technology developed for SRU can also be valuable on Earth. As an example, Maana Electric aims to produce solar panels on the Moon, but to raise funds to do so, is currently using this technology to produce solar panels on Earth from sand.[11] Technologies developed for SRU have implications on the Sustainable Development Goals and increasing resource scarcity. Sectors with innovation of relevance to Earth include chemical processing, mining, metallurgy, and oil and gas [32].

2.2.2 A Brief History of Space Resource Utilisation

SRU is not a recent innovation, but has a long heritage which is aligned with political motives to explore and to advance human exploration and presence in space. The inception of SRU may be traced and attributed to the author A.C. Clarke, who suggested in the 1950s that using Lunar resources to produce propellant would facilitate future space exploration [18, 90]. Since shortly after the inception of NASA in 1958, research has been undertaken related to SRU on the Moon and Mars, and later asteroids. Different US administrations have changed the focus of SRU many times, shifting between Lunar and Martian resources. A lack of long-term commitment has resulted in short-lived periods of increased funding [18].

During the past decade, SRU has gained momentum. SRU research and development (R&D) is no longer a US-only initiative, but a truly global one. There have been a number of developments, ranging from the establishment of private companies with ambitious SRU plans, government efforts for legal frameworks, to the first successful demonstration of SRU to produce oxygen on another planet. The remainder of this Section will summarise these exciting developments, not necessarily in chronological order, but grouped per theme.

Since 2010, there has been an ever-growing list of companies pursuing SRU. Some focus only on

[11] `https://www.maanaelectric.com/`, accessed on August 25th, 2021.

Lunar SRU, but there are also a number of companies focusing on (only) asteroid mining. An overview of companies pursuing SRU is given in Table 2.3.

In addition to the companies listed in Table 2.3, in 2016, Elon Musk presented his vision for the SpaceX Mars architecture [96], with the ultimate goal of making humans a multi-planetary species [81]. Musk states that he thinks it is challenging to become multi-planetary on the Moon, because it is much smaller than an planet, does not have an atmosphere, and is not as resource-rich as Mars. His vision includes SRU for creating propellant for ascent from the Martian surface, from CO_2 from the atmosphere and water-ice in the soil, together creating methane (CH_4) and oxygen (O_2) [81].

Legislation surrounding SRU has been debated for a long time. In 2014, the American Space Technology for Exploring Resource Opportunities in Deep Space Act (ASTEROIDS Act) was introduced to the House Committee on Science, Space, and Technology in the US. This bill was not introduced in a way that it could become actual legislation, but it once again brought discussions of private property rights in outer space to the forefront. It was aimed to direct US agencies to facilitate commercial exploration and utilisation of asteroid resources, to meet national needs and providing property rights to private commercial entities. With that, American legislators have, perhaps incidentally, undermined the core principles of Article II of the Outer Space Treaty: *"Outer space, including the Moon and other celestial bodies, is not subject to national appropriation by claim of sovereignty, by means of use or occupation, or by any other means."* Space law experts have been arguing about the inherent ambiguity of Article II and how it leaves the contents open for negotiation [97, 98].

In 2015, the Commercial Space Launch Competitiveness Act was established in the US. Title IV of the Act, "Space Resource Exploration and Utilization", was an updated version of the ASTEROIDS Act. It was appended to a larger bill that contained a number of updates to US Space Law not associated with extraterrestrial resources, which likely made the controversial legislation easier to pass [97].

In 2016, Luxembourg launched the SpaceResources.lu initiative and announced that it has set aside 200 million euros in order to advance its goal to "support and promote the development of a sustainable commercial industry for space resource utilization" [33, 99]. Following this, in 2017, Luxembourg adopted a legal framework to ensure that "private operators can be confident about their rights on resources they extract in space". As the first European nation to offer a legal framework for SRU, Luxembourg aims to be the European hub for SRU [100]. Luxembourg's lenient legal regime ([101]) is intended to give registered companies right to claim extracted resources as private property and provide favourable compensation and liability rules [101].

ESA and SpaceResources.lu have jointly established the European Space Resource Innovation Centre (ESRIC), an "internationally recognised centre of expertise for scientific, technical, business and economic aspects related to the use of space resources for human and robotic exploration, as well as for a future in-space economy."[18] ESRIC's activities are based on four pillars: space resources R&D, support for economic activities, knowledge management and community management. This follows a trend of public-private partnerships (PPPs) in the space economy [102].

Another party to show interest in asteroid mining is the financial sector, which acts as a catalyser for

[12] `https://ispace-inc.com/aboutus/`, accessed on August 18th, 2021.
[13] `https://asteroidminingcorporation.co.uk/our-vision`, accessed on August 18th, 2021.
[14] `https://www.spacefab.us/future-of-spacefab.html`, accessed on August 18th, 2021.
[15] `https://www.maanaelectric.com/`, accessed on August 18th, 2021.
[16] `https://spaceindustries.com.au/about/`, accessed on August 18th, 2021.
[17] `https://karmanplus.com/#mission`, accessed on January 26th, 2022.
[18] `esric.lu`, accessed on August 5th, 2021.

Table 2.3: Overview of companies founded to pursue SRU.

Years	Name	Country	Notes
2010 – present	Moon Express	US	The company has a long-term goal of mining the Moon for rare-Earth metals and helium-3. In 2016 it became the first private company in history to receive permission for operations beyond low-Earth orbit (LEO) by the US government [91, 92].
2010 – present	iSpace Inc.	Japan, US, Luxembourg	The company aims to construct a sustainable Earth and Moon ecosystem using SRU, in particular water on the Moon.[12]
2012 – 2018	Planetary Resources Inc.	US	The company's vision: "Planetary Resources is bringing the natural resources of space within humanity's economic sphere of influence, propelling our future into the twenty-first century and beyond. Water from asteroids will fuel the in-space economy, and rare metals will increase Earth's GDP." The first targets for the company would be water-containing asteroids, as they viewed water the most valuable resource in space [19, 42].
2013 – 2019	Deep Space Industries	US, Luxembourg	The company intended to develop a fleet of small spacecraft to survey small NEAs, followed by the development of robotic spacecraft to mine valuable asteroids [19].
2015 – present	TransAstra Corporation	US	TransAstra's vision is to create the space infrastructure necessary for SRU on the Moon, Mars and asteroids, for which it has been able to attract significant NASA funding [93].
2016 – present	OffWorld	US, South Africa, Luxembourg	The company envisions human expansion beyond Earth, enabled by robots. These robots are intended to mine, manufacture and build on the Moon, asteroids and Mars [94].
2016 – present	Asteroid Mining Corporation	UK	The company, as evident by its name, has the ultimate goal to mine asteroids.[13]
2016 – present	SpaceFab	US	The company's ultimate goal is to make humankind a spacefaring civilisation. They plan on building an infrastructure using space resources, specifically from metallic asteroids.[14]
2018 – present	Maana Electric	The Netherlands, Luxembourg	The company is developing techniques to create solar panels using low-cost in-situ resources (e.g. sand) on Earth and in space.[15]
2018 – present	Space Industries	Australia	The company aims to mine helium-3 on the Moon and in their pursuits to do so, have developed technology to produce water on the Moon and Mars.[16]
2018 – present	Orbit Fab	US	The company envisions providing fuel to satellites, eventually from extraterrestrial sources [85].
2020 – present	Interplanetary Enterprises	US	The company has the ultimate goal to mine asteroids for growing economic productivity in space [95].
2021 – present	Karman+	Global (HQ in The Netherlands)	The company aspires to mine NEAs to provide abundant, sustainable water and mineral resources for the space economy.[17]

investments and generating coalitions with entrepreneurs. In 2017, a Goldman Sachs report states that asteroid mining is a realistic activity that, due to rapidly decreasing infrastructure costs, could become profitable [101, 103]. In 2018, the new Global Exploration Roadmap (GER) was published, which recognises the growing private sector interest in space exploration and expanding human presence throughout our Solar System, enabled by SRU [5].

In 2018, a workshop by ESA for ISRU confirmed European interest in SRU [104, 105]. The workshop led to the ESA Space Resources Strategy in Ref. [32].

In 2020, the Mars 2020 rover was launched, which included an experiment called Mars Oxygen In-Situ Resource Utilization Experiment (MOXIE). MOXIE's objective was to prepare for future human exploration by demonstrating SRU in the form of creating O_2 from CO_2. On April 20$^{\text{th}}$, 2021, the 60$^{\text{th}}$ Martian day of the Mars 2020 mission after landing, MOXIE successfully demonstrated converting carbon dioxide into oxygen, by producing 5.37 g of oxygen from the Martian atmosphere. By doing so, it was the first instrument to produce oxygen on another world and the first technology of its kind to enable future human missions to "live off the land" [106, 107]. With that, CO_2 electrolysis in space has reached TRL 7, albeit at a very small scale [72].

2.2.3 The Future for Space Resource Utilisation

As the previous Section shows, where space exploration missions were driven solely by government agencies, this is now being complemented by commercial enterprises. SRU can stimulate the growing space economy [17], with enterprises processing resources and delivering products to customers at a range of locations.

Ongoing projects from the previous Section, which have yet to show results, include the SpaceX propellant manufacturing on Mars, as well as companies working on topics as diverse as in-space infrastructure, construction, mining on the Moon and asteroids. After two early asteroid mining companies went out of business due to financial issues (Deep Space Industries and Planetary Resources), other companies are also focussing on alternative revenue streams to fund their R&D for SRU, significantly increasing their chances of success.

NASA is making long-term investments to advance SRU technology, with particular focus on regolith-based volatile extraction and processing, regolith-based manufacturing and construction, and Mars atmosphere-based SRU.[19] ESA released a document with priorities and outcomes by 2030, including maturing technologies critical to the production of oxygen from regolith to TRL 6, end-to-end demonstration of production of water and oxygen on the Moon, and plans for technology demonstrations for SRU in an international context. These projects will contribute to a sustained and sustainable human presence on the Moon by 2040 [32]. The GER includes several projects to advance SRU on the Moon and Mars, with asteroids as a secondary goal. Private sector initiatives and PPP opportunities are identified as a necessary component of making human space exploration sustainable, opening up new markets and allowing for economic expansion. Many of these partnerships and initiatives are already underway and will influence future architectures and mission approaches. International cooperation will enable challenging missions and increase their probability of success. In order for private sector efforts to succeed, the certainty of long-term governmental commitment is needed, as are continued opportunities to introduce ideas into government thinking and supportive national business environments [5, 32].

[19] `https://www.nasa.gov/isru/overview`, accessed on August 26$^{\text{th}}$, 2021.

Space law is in need of modernisation, to create an international regulatory scheme for exploitation. The Moon Treaty, not ratified by any spacefaring nation, stipulates the need for such a scheme, as soon as such exploitation is about to become feasible. No major treaty on space law has been developed in the last four decades, so nations can and should legislate SRU on a national level until international consensus is reached [84].

2.2.4 Commercial Interest in Asteroids

There are three incentives for exploration and understanding the minor planets of the solar system; enhancing scientific knowledge, mitigating impact hazard and utilising resources. Strong synergies exist between these three incentives. Before impact mitigation or resource utilisation, it is necessary to know more about asteroids, both in general and specific asteroids of interest. In return, the wealth locked in asteroids could be leveraged to offset the expenses incurred during exploration of the ever-increasing number of catalogued asteroids in the solar system [4].

Figure 2.7 shows the number of publications for two search queries using the Scopus search engine,[20] first for `asteroid` and second for `asteroid AND mining`. It shows that interest in asteroids themselves has been climbing steadily for the past decades, but also that interest in asteroid mining specifically has grown significantly in the last 10 years. A growth in scientific publications on a wide array of technical and legal aspects of asteroid mining can be interpreted as a sign that the space industry's next frontier is undergoing preparatory work [108].

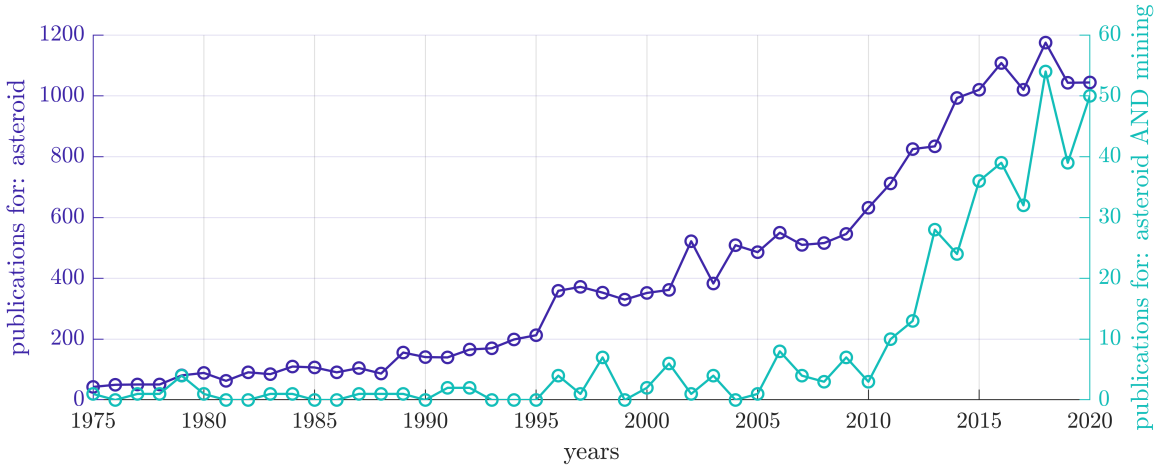

Figure 2.7: Number of publications related to asteroids and asteroid mining, from the Scopus search engine.

While government agencies appear to mainly focus on Lunar and Martian SRU in the short term, asteroid mining is discussed in all the major roadmaps and strategy documents: in the GER, ESA's space resources strategy, NASA's Technology Roadmaps and in the SpaceResource.lu SRU study document [5, 32, 33, 109]. Resources which are not found (in significant quantities) on the Moon, but are to be found on asteroids, are carbon and PGMs, for example. In addition, water reservoirs on the Moon are a finite resource. Most volatile-rich NEAs are undifferentiated and have well-constrained mineralogies. This means that information on properties of a region of the object is sufficient to determine the properties of the bulk of the asteroid. Therefore, they do not need the same prospecting that is necessary for mining on the Earth, Moon and Mars [110]. For these reasons, investigating asteroids for SRU is imperative to complement Lunar and Martian SRU.

[20] www.scopus.com

These reasons have also caught the attention of several companies, as discussed in Section 2.2.2. PGM mining on asteroids is expected to be very lucrative. For example, one platinum-rich asteroid with a diameter of 500 m contains about 174 times the yearly worldwide output of platinum and 1.5 times the total reserve of PGMs [42]. M-type bodies are thought to contain the highest concentrations of PGMs, but S-class asteroids could possibly be a better source of platinum than metallic M-class asteroids. Even though S-class asteroids have a lower concentration of PGM, they are much more abundant than M-type asteroids [111]. Also, laboratory research suggests that metals tend to 'float' to the surface of asteroids due to cooling and outgassing [3]. This suggests easier extraction of the PGMs on NEAs, which orbit relatively close to the Sun, in addition to the fact that higher grade ores already imply easier extraction.

For use of space resources off the surface of the Moon and Mars, launching from the surface requires using a significant portion of mined water to be processed into propellant. In contrast, escape from asteroids requires very small ΔVs, retaining a much larger portion of the mined resources used as propellant. Starting from Earth, a subset of NEAs can be accessed for a smaller ΔV than going to the Lunar surface, making them the most easily accessible objects in the solar system [110]. Return to Earth is even easier [3, 110]. NEAs are nearly ideally located to serve as a source of propellant for cislunar and trans-Mars transportation networks [110]. For in-space use near Mars, MCAs and MBAs could be used, a portion of which have small ΔVs to near-Mars space.

While asteroid mining is by no means a low-cost endeavour, Earth-based mining can be very expensive too. Exploration costs for new mines may run into the tens of millions of dollars over several years, and the costs of building a major new mine may be anywhere from $200 million to $1 billion [3, 24]. For terrestrial mining, statistically only one project out of several hundred investigated in a desktop study may survive and become a paying mine. For asteroids, where the resource expected to be most profitable in the near-term is water, a high proportion of them could prove to be profitable, since many asteroids are thought to be water-bearing [112].

2.3 ASTEROID MINING

The underlying behaviour regarding resources is often based on taking what is available and parsing it out in increasingly smaller pieces. Scarcity of resources is considered to justify increasing prices and restricting availability. Each society has rules for the allocation of scarce resources, ranging from water to rare metals and minerals. Asteroid mining offers the possibility to *add* resources available on Earth or in strategic locations in space, rather than re-allocating current resources [34].

Where Section 2.2.4 has already shown that there are very good reasons to mine asteroids, this Section presents a more elaborate discussion on future Earth-based and space-based markets, equipment and technologies required for asteroid mining and the challenges that asteroid mining faces today.

Asteroid mining lives at the intersection of mining and space technology. While asteroid mining is still in its infancy stage, many of the proven methods of terrestrial mining and space missions can be applied [42].

2.3.1 Future Markets

Accessing the resources on NEAs offers to completely change commercial and governmental space exploration [113]. As shown in Section 2.1.1 and Section 2.2.1, asteroids contain a wealth of resources, ranging from volatiles to semiconductors and (rare) metals. This Section will relate all these resources

to potential future markets.

First, a compiled list of the resources for which Ross [22] predicts a future market for a number of resources, confirmed by many other researchers [3, 23, 25, 114]:

- **Volatiles**: life support (H_2O, N_2, O_2), propellant (H_2, O_2, CH_4, CH_3OH), agriculture (CO_2, NH_4OH, NH_3), oxidiser (H_2O_2), refrigerant (SO_2), and metallurgy (CO, H_2S, $Ni(CO)_4$, $Fe(CO)_5$, H_2SO_4, SO_3)
- **Semi-conductors**: used in electronic devices (silicon, aluminium, phosphorus, gallium, germanium, arsenic, cadmium, copper, selenium, indium, antimony, tellurium)
- **Construction metals**: sheets and beams (iron, nickel, cobalt), shielding (gravel, regolith)
- **Precious metals:** gold, REMs (lanthanides) and PGMs

From the list above, it can be seen that future markets for asteroid mining businesses can broadly be divided into two categories: Earth-based and space-based markets, both of which have very different needs, benefits and challenges. These will be described in the next two Sections, for the Earth- and space-based markets, relatively.

Earth-Based Future Markets

Earth-based markets are mainly focused on the last element in the list above: precious metals. Only resources with a high value-to-mass ratio are interesting for return to Earth, due to the high cost involved with asteroid mining [115]. As discussed in Section 2.2.1, these resources are in increasingly short supply on Earth from increasingly poorer ores, causing prices to rise, and are critical for key technology development. Compared to other precious metals, PGMs have a high technological importance. They are valuable due to their resistance to corrosion and oxidation, have high melting points, electrical conductivity and catalytic activity. PGMs have wide industrial applications, such as in the chemical, electronic, electrical, automotive and glass industries. The consumption and use of PGMs have expanded dramatically over the last 75 years. Demand for PGMs has constantly exceeded supply, resulting in large price increases [88]. Logic dictates that as the cost for Earth-based mining increases, asteroid mining will become competitive with Earth-based mining at some point in the future [25].

Estimated market values for PGM-rich asteroids range from $24 billion for a 1 km diameter NEA (also rich in semiconductors) [116] to a more recent estimation of $1.2 billion for a 100 m NEA [117]. Kargel [116] estimates that one 1-km M-type asteroid with a fair PGM-content would contain twice the PGM already harvested on Earth combined with the economically-viable PGM in the Earth's crust. Note that prices for valuable resources can fluctuate significantly when large quantities are injected into the market [23].

Despite their name, REMs are relatively abundant in the Earth's crust. It is due to their low local concentrations that they are often difficult to extract economically [88].

Besides precious metals, there is another near-term market for customers based on Earth: scientific samples. For a cost that is far lower than sending dedicated scientific missions to asteroids, a rich stream of scentific data and even surface samples from asteroids can be delivered to Earth from commercial missions [3].

To finance initial mission costs, there is a need for near-term markets. At the start of the space mining era, the best candidates are those for which an actual market exists today. Without a viable

infrastructure in place for space-based markets, Earth-based markets could generate the revenue for early space-mining businesses [3].

Space-Based Future Markets

While Earth-based markets could be targeted during first generation space mining due to the initial lack of infrastructure in space, the most profitable markets are space-based. These markets revolve around volatiles, semiconductors and construction metals, used as listed above. However, markets are based on need, not just the existence of the product. Potential space-based markets for NEA resources may be worth hundreds of billions within twenty years [3], but lack the infrastructure in space and demonstrable demand to be viable today.

In a contrasting forecast, the study summary of SpaceResources.lu [33] expects the value chain for propellant to be the most viable business case and near-term opportunity. In the near-term the authors foresee Lunar water to be used, because of the high confidence in demand and availability of water on the Moon. Asteroidal water is expected to follow this in the near-to-medium term. Only in the long term ($>$ 20 years), do they expect PGMs to be a viable market, due to the technical challenges of extracting elements from asteroids, while remaining competitive with market prices on Earth [33].

Reference [24] compares the asteroid mining market to the terrestrial mining market. The authors outline that in space, many products already have been identified, but the markets are either non-existent or government-dependent. For example, habitats, metals, concrete, water, air, and helium-3, have no real demand yet in the space environment, except as government-sponsored activities. It becomes very difficult to calculate the actual value of space-based resources under these circumstances [24]. Governments, unlike industries, do not have to compete and show a profit [2].

Irrespective of the opinion about when the space-based market for volatiles will be profitable, it is widely considered to become the most valuable market [3, 29, 32, 33]. Volatiles are some of the easiest products to extract and there is a huge potential for future in-space markets. Markets include water for space stations, or propellant as feedstock for orbital propellant depots to service a wide range of spacecraft [3]. Another use for water in space is for metal mining on asteroids [118].

Significant investments are required to establish the infrastructure required for the distribution of volatiles, semiconductors and metals. Nonetheless, once an infrastructure is in place, a feedback loop will foster more human activity in space: early materials are likely to support space-based operations that will, in turn, be able to more cost-effectively acquire and process additional materials [3]. Such an infrastructure could be used to manufacture ambitious and visionary large-scale space projects, such as solar collectors [9], Mars-transfers [43], space hotels for space tourism [22], or space stations [22].

Semiconductors can be utilised for production of photovoltaic arrays in orbit, as well as other electronic applications [3, 114], which can provide an in-situ supply of photovoltaics for large solar power satellites for terrestrial energy delivery.

In addition, there is interest in space-based production of high-value pharmaceuticals, semiconductors, ultra-pure crystals for many applications, and in general the production of any product requiring large-scale material purity [21]. Asteroid resources can be used to build the required infrastructure, as well as provide the raw material for these processes.

Focus of This Thesis

This thesis will focus on a subset of the resources noted in the previous Sections. Most related research focuses on either water (or water-based resources or other volatiles) or on PGMs, as these have been identified as very promising markets, albeit at different timescales.

The processing of regolith to extract water is at TRL 4 and has been demonstrated in vacuum, while metal extraction from regolith or de-alloying technologies are still at TRL 1. A TRL of 1 makes it extremely difficult to determine how much research is still needed and when (or even if) a technology can be developed [31, 119, 120]. For this reason, the scope of this thesis is limited to mining volatiles, such as water. The remainder of this literature review will therefore not go in detail about other resources.

The Scottish economist and philosopher Adam Smith once famously stated that "Nothing is more useful than water: but it will purchase scarce any thing; scarce any thing can be had in exchange for it" [121]. Published in 1776, it is unlikely that Adam Smith could have fathomed how valuable water is in space, and how much companies will be willing to trade for it.

2.3.2 Equipment and Technologies for Asteroid Mining

There are a number of steps before water(-based) products are stored in a depot or delivered to a customer. This Section aims to address these different steps: prospecting, excavating, processing, storing and transporting [119, 120]. These are the steps specific to the mining elements of the mission and are performed on top of the more general steps in space missions, such as the launch, transfers, rendezvous, landing and take-off. The necessary equipment and technologies are discussed in this Section. However, note that in-depth technology reviews are out of the scope of this thesis, which addresses economic models and trajectory optimisation of asteroid mining and not the supporting technologies.

Prospecting

Before mining activities can commence, a suitable asteroid and location on the asteroid have to be found. Because asteroid mining missions are a costly endeavour, investors are likely to insist on prospecting missions to determine which asteroid is the most promising target for mining [29].

Prospecting asteroids can generally be split into three separate phases: discovery, remote characterisation, and local characterisation of promising candidates. Each of these phases becomes more demanding, so it must be carried out for a smaller and smaller set of asteroids [122].

The first two phases can be performed using ground-based radar and telescopes and space-based telescopes [123]. Remote characterisation can be split in two categories: spectroscopic and photometric, where the former determines the surface mineral content and the latter the rotation rate and shape. These initial characteristics aid in the selection of asteroids to be prospected in-situ during the next phase [122]. Spectroscopic data can give indications on the mineral compositions of the surface of the asteroid, indicating whether an asteroid is carbonaceous, stony or metallic. What it cannot indicate though, is the resource richness. Meteorites have shown that resource richness spans a wide range [124].

More detailed information about the asteroid can only be determined through proximity measurements. Using gravitational models, density maps and other information, the composition of the asteroid below the surface can be estimated. However, for more accurate estimations, samples need to

be taken. Traditionally this would be undertaken using one lander with a comprehensive set of sensors and technologies, but miniaturisation trends allow for a team of small and redundant spacecraft which together compile a detailed model of the asteroid [120]. Prospecting multiple asteroids in one mission, for example using propellantless solar sails [125], can be used to limit prospecting costs.

Mining and Processing

For mining the asteroid, multiple different options exist, such as in-situ excavation and extraction, excavation and delivery to an extraction plant, or even capturing the entire asteroid which can then be delivered to an extraction plant [119]. Not every option is suited for each asteroid, smaller asteroids could be moved to Earth capture, but even these smaller asteroids require very large quantities of propellant for such a transfer. For large asteroids, this is practically infeasible altogether.

The mining method depends on the material being sought (e.g., unprocessed regolith, solid metal, or volatiles) and the surface material. If the surface material is loose regolith, a scraper, winch, or bucket system will suffice [120, 126]. These technologies for mining are more conventional and involve drilling, digging and beneficiation [29]. For water ice, vaporisation can be used [126]. Another option altogether is to envelop an asteroid in a bag and use concentrated solar power to spall the surface of the asteroid to release water, which would then be captured in the bag [93]. Because these operations are performed in microgravity, anchoring to the asteroid is important and depends on the type of material on the surface and just below.

Processing the material again depends on the material being mined. Some materials might need to undergo grinding or milling to reduce the particle size, other materials might require separation or sorting for particle size. For the processing of water, separating gases from solids and condensing vapours are necessary [126]. If not pure water but LOX and LH_2 are required, processing using electrolysis is required [29]. A widely-used way to incorporate mining and processing in a technological-economic model is through a throughput rate, which relates the mass of the mining and processing equipment (MPE) to the mined mass per unit of time [21, 23, 126, 127].

Storing and Transporting

Storing water in space can be as simple as filling up a large storage bag (or bladder), where it can be stored as liquid water or as ice [126]. Storage in tanks or pressure cylinders is also possible, so it can easily be heated and sublimated [119]. In both cases the effect of sloshing on the centre of mass should be taken into account.

Water obtained during mining and processing is then electrolysed into LOX and LH_2, which can be used for propellant in chemical rockets, but are volatile and difficult to contain due to the extremely low temperatures required. However, Lockheed Martin and NASA believe that high-thrust chemical propulsion (and in particular LOX/LH_2) is necessary to provide sufficient thrust to launch from the surface of the Moon or to descend to the Martian surface [29, 128]. To minimise the issues concerning cryogenic storage, the resource can be stored as water and later be electrolysed into propellant [120], for example at a depot at the Earth-Moon L_1 Lagrangian point. Such a depot, or orbital refuelling station, can store water, propellant and other (raw) resources, similar to a terrestrial petrol station [120].

Before transporting resources, the tailings (waste material left after extracting target resources from ore) are discarded on the asteroid, minimising the mass that has to be transported [126]. Using Earth-sourced propellant to transport the mined resources defeats the purpose of asteroid mining, as

the whole point is to deliver large quantities of propellant at a cost less than launching them from Earth [126]. Therefore, concepts for asteroid mining missions often - if not always - use the propellant produced [22, 25, 126, 129, 130] or propellantless solar sails [23, 131]. Propulsion systems utilising water(-based) propellant or no propellant at all include:

- Chemical LOX/LH_2 propulsion, I_{sp} of 446 s. Widely used, but cryogenic temperatures are challenging to maintain for extended periods of time [132].
- Solar-thermal steam propulsion, I_{sp} of 190–320 s. Uses liquid water heated using solar energy, does not require very pure water which means simplified mining and processing [133].
- Nuclear-thermal propulsion, up to I_{sp} of 900 s using hydrogen as both the reactor coolant and propellant [134].
- Water electrolysis high-thrust propulsion, with I_{sp} potentially up to 400–450 s [135, 136]. Uses liquid water, still under development for large spacecraft [137].
- Water electrolysis low-thrust propulsion, with I_{sp} potentially upwards of 4000 s, using the electrolysis products: hydrogen and oxygen gas. Still under development [138]
- Solar sails [139] or magnetic sails [140], which use solar radiation pressure or the solar wind for spacecraft thrust, respectively. Both are propellantless, but mission durations are often very long and the generated thrust is not sufficient to successfully take-off and land on larger bodies.

2.3.3 Challenges for Asteroid Mining

However promising the future markets and possibilities appear, there are many challenges that need to be overcome in order to establish a thriving, sustainable and profitable asteroid resource market. First and foremost because, as Ryan and Kutschera succinctly put it [34]:

> *"... nothing involving space is ever truly routine, at least not yet."*

Besides the learning curve for any new space activity, there are a host of challenges more specific to asteroid mining that need to be overcome. A number of these challenges have been introduced in the previous Sections. These challenges can be grouped into the following topics:

- **Time- and distance-related issues**
  The flight time from Earth to Mars is expressed in months with even the best propulsion systems currently imagined. The majority of asteroids are found in the main belt, with orbits outside Mars', meaning that economical transfers to MBAs could well take years with present-day technology. This poses as a problem for asteroid mining missions, on several different aspects. This means that human missions are extremely challenging, which is exacerbated by infrequent launch windows [34]. Whereas the Moon is in constant close proximity to the Earth, asteroids, especially those with orbits similar to Earth's, suffer from long synodic periods with respect to the Earth's orbit. This could mean that there is a long time to wait for a favourable orbital configuration to transfer to Earth or another asteroid [22].

  For operations at the asteroid, the choice has to be made between robotic and human missions, both of which have their own advantages and drawbacks. A combination of the two is also possible, which introduces new issues again [34]. Humans have not ventured past LEO for almost

50 years, with the Moon as the most distant location humans have ever reached. While a number of asteroids are more accessible in terms of ΔV [3], launch windows are infrequent and return to Earth could not be readily possible in case of emergency. Missions that decide to include human involvement in space, will see their costs increase significantly, as human presence in space is very costly. It is therefore highly probable that ventures will include significant robotic, possibly even autonomous equipment [34].

The communication delays with Mars are between 7 and 20 minutes, depending on the relative orbital position of the Earth and Mars, and communication with spacecraft near asteroids will suffer from similar delays, complicating remote troubleshooting. Operational self-sufficiency is therefore paramount. Multiple relay stations for communication might also be required, when the orbital configuration causes an obstructed line-of-sight [34].

- **Automated technologies and engineering challenges**
  Robotic operations must be highly autonomous. This in itself adds many challenges to the mission. For example, mining equipment will need to be adapted to work without constant human intervention, whereas terrestrial equipment requires regular installation of new drill bits [29]. It is likely that the entire infrastructure to deliver resources to its final destination will be automated [120].

  Another range of engineering challenges are introduced by the microgravity environment. Whereas rovers, drilling mechanisms and other large-scale systems have been designed for use on the Earth, Moon and Mars, performing these operations in microgravity needs to be researched and issues addressed appropriately [120].

  Current spacecraft are of a relatively modest size, compared to what is likely necessary for asteroid mining. Large and efficient propulsion systems have to be designed [34], which should be able to accommodate large payloads, or possibly also high-performance solar sails [113]. MPE comes with a high power requirement, some of which may have to continue during eclipse [120].

  These engineering challenges bring another challenge with them: the risk for such novel technologies is high, which means that investors require a very high Return on Investment (ROI) to offset these risks. In combination with long payback periods due to interplanetary travel, this translates to significant financial challenges [24]. Asteroid mining missions will have to depend on well-performing precursor missions to mature the required technologies [141]. The expertise to solve all these engineering challenges does not completely exist in the space industry. Partnerships with non-space industries are therefore fundamental to success and advancing the asteroid mining sector [32].

- **Financial barriers**
  For asteroid mining, the near-term hurdles are mainly financial. Lead times are too long for investors to develop the technology necessary for a successful mission. Historically, governments have stepped in to bring down the risk for entrepreneurs by investing in new technologies [95]. ESA envisions the public sector to be the primary source of financing for SRU activities, by integrating space resources into mission architectures of the future. They foresee that there is insufficient rationale for comparable or greater investment by the private sector. Until this is no longer the case, ESA expects the public sector to be the primary source of SRU activity financing, for at least the next decade and possibly beyond that [32].

Operational and organisational risks are high, because of the uncertainties currently associated with asteroid mining, the inherent risks of space missions and the many novel technologies required. These high risks are generally associated with expectations of higher ROI [34].

Most of the practical problems which asteroid mining faces have clear an unambiguous solutions. The majority of technical problems, with just a few exceptions, centre on cost rather than practicality. The time-frame until successful and profitable asteroid mining ventures are possible is therefore dictated by how much money is invested in research [34]. Many interesting business opportunities are deferred until the need develops, at which point businesses will need to catch up. For something as complex as asteroid mining, consistent efforts are needed for it to become profitable. However, finding investors for such a forward-looking endeavour is not an easy task [34].

Another issue related to finances is unknown profits and near-term demand. Sales are generated by two requirements: the existence of a product and a market for the product. While many asteroid products are identified, markets are currently non-existent or government-dependent [24]. A business can only be profitable if there is a need for its product, if there is a market. The market for in-space water is currently non-existent. An accurate estimation of the future total addressable market, pricing strategy, let alone a forecast of the profitability of such a business therefore is not possible. In the case of asteroid mining, companies will not only have to create a business, they might also have to create the customers [142].

Another challenge to note is the current lack of infrastructure in space to distribute processed material. Setting up such an infrastructure requires enormous up-front costs and effort [25, 43, 143]. Initial asteroid mining ventures would not be able to benefit from such infrastructure, creating an even more challenging environment to start a commercially viable enterprise.

- **Property rights and legal issues**
  As noted in Section 2.2.2, another key issue is property rights and ownership issues of asteroids, which are currently not addressed in any binding internationally-agreed legal document [97, 144]. Selling property, including asteroid property, requires ownership. Without property rights, asteroid miners are not able to sell. Current extraterrestrial law suggest that ownership by private entities in space is not possible. Companies pursuing asteroid mining are likely to run into major legal hurdles until private rights in space are clarified [34].

  It is however expected that, at some point, activities to exploit asteroid resources will have a substantial foundation in international law. This will be similar to how orbital slots in geostationary orbit (GEO) are recognised as property in space, or how satellites can be bought or sold. For material extracted from the Moon it has been established that parts of another celestial body can indeed be subject to ownership once removed from that body [34]. Whether legal issues will be resolved on a national or international level is yet unclear, but it is unlikely that all nations will agree to an international agreement, as shown by the Moon Treaty [97].

  Another challenge concerns which countries can actually participate in asteroid mining. Higher-income nations are much more likely to be technologically and economically capable to participate. Asteroid mining may therefore reinforce or widen the income gap between countries [145]. Activities to exploit asteroid resources could easily end up mirroring the increasing conflicts and disagreements over resources on Earth [34]. The process of selecting the participating companies may have unforeseen political and economic consequences [24].

Concern over use of nuclear power is another political risk, which effectively precludes nuclear propulsion and power generation, even though it is the ideal long-term solution for power generation [3].

- **Unknown asteroid properties and environment**
  As described in Section 2.3.2, locating an asteroid that turns out to be profitable is a complicated task. This is due the limited information available for most asteroids.

  Once an asteroid is discovered, all that is known is its orbit and absolute magnitude. Through Eq. (2.1), the diameter of the asteroid can be calculated based on its magnitude, if the albedo is known. As noted in Section 2.1.1, when the spectral type of an asteroid is unknown, the mass of an asteroid is uncertain to a factor of ∼30. Not knowing the mass of an asteroid directly translates to not knowing how much money can be made when exploiting that asteroid.

  Additional uncertainties are introduced by not knowing the spectral type, which is the case for many asteroids. The spectral type can not only provide clues about the albedo and density, but also about the surface material, whether the surface is loose or solid, rock or metal. This important information and more can only be determined accurately after an in-situ survey. In order to know more about the sub-surface material, probes and drills are necessary, resulting in an even more costly mission [117]. Equipment necessary to mine the material is, unsurprisingly, dependent on the type of material. Without any knowledge about the material of which the asteroid is made, a spacecraft might arrive with the wrong equipment. This underlines once more the need for proper prospecting of an asteroid before the mining mission commences [126]. Although significant research has been undertaken to characterise NEAs to determine their composition [45], there are still many unknowns. And even if the properties of an asteroid are known, very flexible systems capable of operating under many different potential environmental conditions must be developed [3].

The challenges described above will not be solved soon. Estimates about when asteroid mining becomes a realistic alternative to Earth-launched resources vary significantly. In 1988, Ref. [146] envisaged missions to asteroids around the turn of the millennium, resulting in a flourishing space renaissance by 2010. In 1997, Ref. [21] projected that by 2010, the in-orbit market would "easily" exceed 1000 tonnes per year. Written in 2005, Ref. [3] projected a $100 billion market for volatiles within 15 years. As another example, in 2012, Planetary Resources announced their goal to put an orbiting propellant depot supplying LOX and LH_2 split from asteroidal water in space by 2020. Instead, in 2020 the company had to auction off all assets after continuous delays and failures to secure funding.

Recent estimates for timelines for SRU are given by various public organisations. ESA predicts that by the late 2020s an end-to-end demonstrator will prove the feasibility of producing water or oxygen from Lunar resources, followed by a pilot plant integrated in a mission in the early 2030s. Specific timelines for asteroid mining are not given by ESA [32]. SpaceResources.lu also foresees Lunar mining for water in the short term, by 2028. Asteroid mining for water is foreseen in the medium term, by 2033-2038, followed by asteroid mining for metals/PGMs in the long term [33]. Whether or not these timelines will materialise, only time can tell. Differences in time estimates are determined by how soon activities for infrastructure development are undertaken and how much investment is accumulated. Smaller investments lengthen the time needed for developments and push timelines further into the future [34]. This means that while solving certain engineering challenges, visionary thinking is required. This requires multi-disciplinary concurrent engineering with uncertainties [3].

Despite all these challenges and issues, it is arguably not a question of *whether* space resources will be exploited, but *when* they will be exploited. Without a doubt, new problems, challenges and issues will be encountered, which were not even considered initially. This is normal for new opportunities and new enterprises [34]. Ending with one more, very relevant quote from Ref. [34]:

> *"What should not surprise anyone is how poorly the predictions of the future will prove to be."*

CHAPTER 3

TECHNICAL BACKGROUND

This Chapter will lay out the necessary models and inputs to formulate the parametric model of asteroid resources used throughout this thesis. The technical background for this can be divided into economic models and trajectory models.

3.1 ECONOMIC MODELLING

Sonter [21] expresses the need for a general method to quantitatively compare and rank a very large number of alternative architectures for asteroid mining, including combinations of resources, destinations, trajectories, engineering solutions, and mission scenarios.

Economic modelling for commercial space missions combines the challenges arising from the space environment and the complexity of finance, operations and marketing. Similarly, lack of practical experience with asteroid mining introduces challenges when estimating cost and sales for these space ventures [147].

Money management is driven by two simple ideas: more money is better than less, and money now is better than money later. Investors require short payback periods, especially for high risk ventures, since this limits their exposure to risk [24]. The NPV, which takes the time-value of money into account, has been widely adopted as the current best metric to assess the economic viability of asteroid mining mission concepts [3, 21–28, 148, 149]. The NPV will be used extensively in Chapters 5 and 6.

This Section first sets out figures of merit that can be used during economic modelling, including the NPV. This is followed by a review of potentially suitable cost estimation methods. The section concludes with a review of existing economic models for asteroid mining architectures.

3.1.1 FIGURES OF MERIT

This Section will briefly introduce a number of figures of merit that can be used to indicate the financial viability of a business venture, including commercial space missions. These figures of merit will be adapted for use in the parametric model of asteroid resources in Section 4.2.2.

Mass Payback Ratio

Traditionally, the mass payback ratio (MPBR) was used to quantify the fitness of an asteroid mining venture: the ratio of the total units of mass returned for each unit of mass originally launched [2]:

$$MPBR = \frac{\text{mass returned}}{\text{mass launched}} \tag{3.1}$$

MPBRs can increase depending on departure and arrival orbits, or by reusing the same spacecraft for multiple trips. Examples for the MPBR are given in Ref. [2]: the MPBR can be 3:1 for one round trip mission from LEO to a NEA, or using the same system for five of these round trips 15:1, or up to 100:1 for five round trips from a highly-elliptical Earth orbit to a NEA. Although high MPBR may seem more beneficial, this does not consider the duration of the mission or the upfront investments. In addition, the MPBR does not take into account development costs, a difference in the value between the mass launched and mass returned, nor does it take into account the time-value of money [22, 27].

Net Present Value

The NPV was first proposed as a figure of merit to assess the profitability of asteroid mining ventures in Ref. [27]. The NPV takes into account the forgone interest that invested funds could have been earning: the longer the wait for income, the less present worth it has, and the more heavily discounted it must be [22]. An NPV analysis uses costs and revenues over time and calculates the present value of the entire project, summed over all N years the project runs [150]:

$$NPV = \sum_{t=0}^{N} \frac{CF_t}{(1+I)^t} \tag{3.2}$$

where CF_t is the net cash flow (cash inflow - cash outflow) during a single period t, and I the discount rate or return that could be earned by investing in alternative investments. In the case of just one upfront investment and one moment of revenue being earned, the equation for NPV reduces to:

$$NPV = \frac{R}{(1+I)^{t_{\text{total}}}} - C_0 \tag{3.3}$$

in which R is the revenue, t_{total} is the total time in years, and C_0 is the incurred cost at the start of the process. For an asteroid mining mission with only a single round-trip, Eq. (3.3) can be rewritten as:

$$NPV = \frac{R_{\text{mis}}}{(1+I)^{t_{\text{mis}}}} - C_0 \tag{3.4}$$

with the subscript $\square_{\text{mis}}$ denoting the mission. For these missions, all costs are expended upfront and the revenue is earned at the end of the mission only.

Central to the NPV calculation is the decision for the discount rate that is applied. For very high discount rates, future cash flows are heavily discounted and therefore worth much less, causing the NPV to asymptotically approach the initial cash flow. Discussion exists about which discount rate is appropriate for decision making. While some maintain that long-term government bond rates are most appropriate, others maintain that the discount rate should be no lower than the typical rate of return achieved by alternative investments in the private sector. In the case of the former, a rate of 10% is often applied [150]. This rate is also adopted in Refs. [22, 23] for economic modelling of asteroid mining ventures.

The implications of incorporating the time-value of money are that asteroid mining missions taking longer than ∼3 years will require very good MPBRs, in order for the NPV to be positive [22], while it also puts an upper limit on the allowable project lifetime [3]. For investors, preferred pay-back times for their investments are three to five years, and anything over ten years is considered unattractive [24, 126, 151].

A decision strategy in investments is to focus on maximising NPV. When the NPV is used in decision making, the following should be done [150]:

- $NPV > 0$, the investment will add value to the company, so the project should be accepted;
- $NPV < 0$, the investment will make the company lose value, so the project should be rejected;
- $NPV = 0$, the investment will not make the company gain or lose value, so the decision to accept or reject the project should be based on other criteria, such as a improving the strategic position in the market or other factors that are not explicitly included in the NPV calculation.

EXPECTATION VALUE OF NPV

Another useful figure of merit is the expectation value of NPV (ENPV), its most likely value, weighted by the probability of each outcome (P) which is calculated as [21]:

$$ENPV = (NPV)_{\text{weighted}} = P_1 \cdot NPV_1 + P_2 \cdot NPV_2 + \cdots + P_n \cdot NPV_n \tag{3.5}$$

in which

$$\sum_{i=0}^{n} P_i = 1 \tag{3.6}$$

For example, the ENPV can be used to introduce the probability of mission success in the decision-making process, with P_s the probability of success of the mission [28]:

$$ENPV = P_\text{s}\left(\frac{R_\text{mis}}{(1+I)^{t_\text{mis}}} - C_0\right) + (1-P_\text{s})\,(-C_0) = P_\text{s}\left(\frac{R_\text{mis}}{(1+I)^{t_\text{mis}}}\right) - C_0 \tag{3.7}$$

which is often used in the decision-making process for terrestrial mining ventures [152].

INTERNAL RATE OF RETURN

The internal rate of return (IRR) is the discount rate for which $NPV = 0$. To this extent, Eq. 3.4 can be rewritten as follows [26]:

$$NPV \quad = \tfrac{R_\text{mis}}{(1+I)^{t_\text{mis}}} - C_0 = 0 \tag{3.8a}$$

$$\rightarrow I \quad = \left(\tfrac{R_\text{mis}}{C_0}\right)^{\frac{1}{t_\text{mis}}} - 1 \tag{3.8b}$$

as shown in Fig. 3.1.

Due to the perceived high risks associated with asteroid mining, some suggest an IRR of 30% is necessary in order to offset these risks [3, 22, 153].

RETURN ON INVESTMENT

One last metric for commercial viability is the ROI. The ROI measures the gain or loss generated on an investment, compared to the investment itself. Even though it does not incorporate the time-value

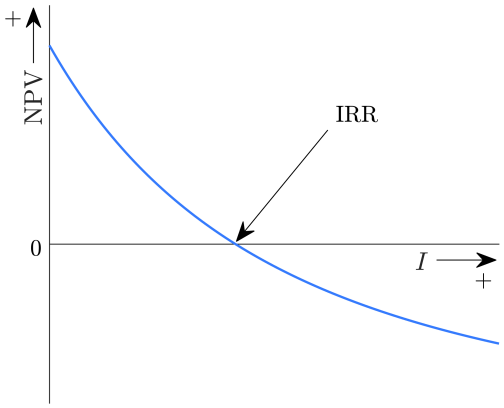

Figure 3.1: Net Present Value and the Internal Rate of Return.

of money, ROI can still be used to compare different missions. The ROI is calculated as [154]:

$$ROI = \frac{VI_{\mathrm{f}} - VI_0}{COI} \tag{3.9}$$

in which VI is the value of investment, with $\square_{\mathrm{f}}$ denoting final and $\square_0$ denoting initial. COI is the cost of investment, which is here equal to VI_0, therefore Eq. (3.9) reduces to:

$$ROI = \frac{VI_{\mathrm{f}}}{VI_0} - 1 \tag{3.10}$$

Typical values for the ROI as a function of risk are shown in Table 3.1, in which the risk for an asteroid mining venture could be classified as "risky" or even "wildcatting" [24].

Table 3.1: Typical expected return on investment as a function of risk [24].

Project risk	**ROI**	**Notes**
Low	$< 15\%$	Small projects
Moderate to high	$20 - 50\%$	Industrial projects, large projects, mature industries
Risky	$50 - 200\%$	Novel products/ventures
Wildcatting	$> 200\%$	A very novel product, area and/or customer

3.1.2 Cost Estimation Techniques

During early phases of space mission planning, cost estimation has to be performed, but can be challenging. In an economic model, such as the model discussed in this thesis, inputs have to be estimated for the cost elements included in the model. This can be done using one of many ways.

Reference [155] identifies three main methods forming the backbone of tools applied for cost estimation within the space sector: bottom-up, analogy and parametric approaches. Expert judgement can be included as another approach, and although there does not appear to be a clear consensus on whether this is appropriate, its use is widespread [155]. Prince [156], a highly-esteemed NASA cost estimator, is a strong advocate for a process-based approach, which has therefore been added to this overview. These methods can be used to estimate different cost contributions, such as the costs of hardware or yearly operations, for example.

- **Parametric** cost models relate independent, quantifiable characteristics (e.g., mass, power, complexity, TRL) of a system to an estimated cost, in the form of cost estimating relationships (CERs), which are based on historical data [157]. Parametric cost estimation is used prolifically and is often the foundation of key models used during early-phase space mission design, when only basic requirements are available and detailed system and sub-system models are not yet established. CERs relate cost to physical, technical and performance parameters which are known to strongly correlate with the cost of a mission. While it is assumed that CERs are the most effective way to estimate costs in early phases, actually formulating the CERs requires significant time and effort to collect data, normalise this data, adjust for consistency and calculate the relationships. Sufficient, accurate, and representative cost data has to be acquired at a sufficient level of detail. Often, obtaining data is challenging due to contractual and administrative complexity [155]. Several tools based on CERs have been developed, but availability of these tools varies, as some are restricted to government use or are paid commercial tools, which provide limited to no insight into the CERs on which they are based [158]. CERs are only as robust, reliable, and credible as their underlying database of projects.

- **Analogy-based** models rely on closely related space missions and apply an adjustment factor, usually based on complexity [159]. Judgement is required regarding the similarity of projects and the adjustments that have to be made for differences. These differences can be wide-ranging; examples are complexity, project size, technology or team experience. Identifying a suitable analogue for a mission can be challenging, especially with lack of technical, program or cost data of either the to-be-designed mission or historical missions. Once such an analogue is found, the comparison is then often based on one single data point. Cost estimations are subject to experience, knowledge and judgement of the cost estimator, but will be based on factual historical data [155].

- **Bottom-up** models are a summation of many (detailed) estimates at low levels of the work breakdown structure (WBS) [155, 159]. This very specific analytical approach can be applied for cost estimation of a mission when all parameters at the system and sub-system level are known and clearly defined. Low-level cost estimations are usually directly undertaken by engineers working on these systems. It is an extremely resource-intensive approach with significant associated costs, especially in the case of changes to specifications, requirements and design, which are very common in the early stages of space mission design [155].

- **Expert judgement** estimations are just that: estimations done by experts who have been in the field for many years. Estimations are subjective at best, but this is a commonly applied methodology and is consistently and extensively used in the generation of cost estimates. The approach can be used throughout all project phases and can be beneficial when historical data is scarce or even unavailable. Expert judgement suffers from inconsistencies among experts and is prone to knowledge or experience bias. Other cost estimation methods have been designed with expert judgement at its core, most notably analogy-based models [155].

- **Process-based** cost models, sometimes called activity costing, translate space hardware system characteristics into a set of discrete activities required to produce space hardware, which can be directly linked to costs associated with these activities. Currently there is a lack of data at the process/activity level, because of the novelty of the approach, but the potential benefits are

promising enough that more effort should be focused on this type of cost estimation. Expert opinions will have to feed into these models, to determine the proper inputs and responses of any process-based model [156, 157].

Of course some of the above techniques can be strategically combined into a hybrid estimation technique. Nevertheless, all modelling efforts, independent of the method, have to deal with limited data sets and the effect of rapidly changing technologies [157, 160]. Some argue that in very early stages of space mission design, only parametric modelling and analogous modelling are possible [159]. In turn, Prince [156] critiques parametric approaches because they "predict the past better than the future" and that they rely on "small, imperfectly understood data sets", resulting in a situation where the credibility of the estimate can be questioned, especially in the case when only one analogous data point is available.

Besides expert judgement, all cost estimation listed above require (detailed) information about the space system, for example mass, power, complexity, TRL or a complete WBS. This level of detail is simply not available during concept development and early development studies [157], especially in the case of "first-of-a-kind" or "state-of-the-art" missions [159]. In addition, even if there was historical data analogous to a proposed asteroid mining mission (i.e., very large space structures, interplanetary cargo systems, high-performance solar sails, mining equipment, and/or highly-autonomous robots), historical data often suffers from a temporal, cultural, and technological gap due to a time delay, causing wildly inaccurate estimations. Parametric models are not well-suited to accommodate process improvements in space hardware design, development, build and test [156]. Also, extrapolating results beyond the limits of the data points should by definition be discouraged [159].

It is likely that conventional cost estimation technologies would not be able to accurately estimate the development and operations costs for commercial ventures. The development cost of SpaceX's Falcon and Dragon projects have recently been studied, suggesting that traditional cost estimation techniques as used for NASA projects would have resulted in over-estimating the costs for these commercial projects by up to four times [31]. Technically, all methods listed above could produce an estimation for the hardware cost for a commercial asteroid mining mission, but since the inputs for the models will be doubtful at best, the results will be uncertain.

Because of the complexity of accurately predicting the cost for spacecraft hardware, a specific cost based on mass is often employed, merely because it is the simplest to apply. Also, while mass might not be a cost driver, it is generally a cost predictor: bigger spacecraft cost more [156]. In Ref. [23] the specific cost for manufacturing space hardware ranges between 10,000 and 1,000,000 $/kg. Reference [3] suggests a value between 50,000 and 75,000 $/kg for a state-of-the-art program, based on a study of several small missions, but it is not clear whether this is development, manufacturing or total specific costs for spacecraft hardware. Other studies, such as those described in Ref. [31] have a quite different approach: due to the lack of specific cost information for analogous missions, it assumes a fixed cost for spacecraft development. It can be concluded that a consensus has not been reached, and that other strategies for estimating development and manufacturing costs for asteroid resource missions will have to be explored, especially for the costing of commercial ventures.

Learning Curve Effect

Regardless of the cost estimation method to be used, one key element can be taken into account for manufacturing cost: the learning curve effect. This well-known phenomenon is characterised

by a significant reduction in manufacturing costs as additional units are built. This decrease in marginal manufacturing cost is most noticeable during the first units, but eventually decays to a negligible change. The marginal manufacturing cost per unit, C_{man} after n units can be calculated using [23, 30, 161]:

$$C_{\text{man}} = C_{\text{man}_0} \times n^{\frac{\log(b)}{\log(2)}} \tag{3.11}$$

in which C_{man_0} is the theoretical first unit cost and b is the learning curve slope. For aerospace engineering, this slope can be estimated at 0.85 [23, 30, 162] or more conservatively at 0.90 [161, 162]. Figure 3.2 shows what this means for the cost of subsequent units, using $C_{\text{man}_0} = \$1000$ and $b = 0.9$.

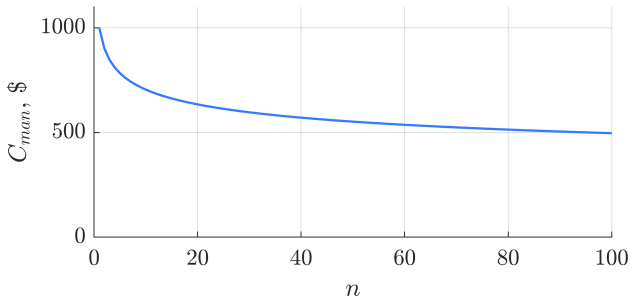

Figure 3.2: Learning curve effect.

Selling Price

The price for which the resources are sold is dependent on the type of material to be sold (low value-to-mass or high value-to-mass) and where this material will be sold. If the material is to be sold in orbit, the price has to be competitive with the cost if the same material is launched from Earth. Kargel [116] assumed that resources will be sold for a value p per kg:

$$p = p' + c_{\text{l,orbit}} \tag{3.12}$$

where p' is the cost of these materials purchased from terrestrial sources and $c_{\text{l,orbit}}$ is the launch cost per kg to the required orbit. Since it is generally the case that these materials will be of low value-to-mass, such as volatiles, p' can often be neglected compared to $c_{l,orbit}$.

For high value-to-mass resources such as PGMs sold on terrestrial markets, terrestrial prices will have to be adopted [3, 22, 24, 25, 115]. The supply and demand effect of injecting large quantities of platinum into the terrestrial market have been investigated, using price elasticity and substitution [23]. Especially with expected increased shortages of terrestrial PGMs, this will have to be taken into account to ensure a proper analysis.

3.1.3 Existing Economic Models for Asteroid Mining Architectures

In recent years, many architectures for asteroid mining missions have been conceptualised and investigated, some of which include an economic model. This section will compare and analyse these architectures and their economic models. Summaries for a number of notable economic models are given in Appendix A.

Resources to be extracted in these missions are either low value-to-mass resources (e.g., water possibly split into LOX/LH_2, or other volatiles) [28–31, 93, 110, 126], high value-to-mass resources

such as PGMs [3, 127, 130] or both [22, 23, 25, 26, 163–166]. The proposed architectures are varied, not just differing in the type of resource to be extracted.

While most architectures extract usable resources at the asteroid and subsequently transport these resources to a customer [3, 22, 23, 25, 28–31, 93, 110, 126, 127, 166], a number of these missions aim to return a complete asteroid to an orbit more accessible from the Earth, for example, to enable (human) missions to the asteroids in cislunar space [26, 114, 163–165, 167]. The latter type of mission could prove to be easier to execute, or to be valuable training for astronauts, but are unlikely to be profitable due to the additional costs related to transporting the slag (stony waste material) from its original orbit [31]. Not coincidentally, out of these papers describing architectures to return a complete asteroid, only Refs. [26, 164] include a (partial) cost estimation, the others (Refs. [114, 163, 165, 167]) do not. For the architectures only transporting the extracted resources, a far greater number of cost estimations and economic models exists; Refs. [3, 22, 23, 25, 28–31, 93, 126, 127] all include (detailed) cost estimations and economic models.

In addition to the work on economic models and cost estimations for asteroid mining missions noted above (Refs. [3, 22, 23, 25, 26, 28–31, 93, 126, 127, 164]), the economics related to the use of SRU on various other planetary bodies has been investigated [17, 24, 168–170]. These combined works address specific mission architectures with a sometimes impressive level of detail, as well as an array of economic models. In general, economic models for (asteroid) mining are varied, each employing different cost estimation techniques and business models, some even including costs and revenues of space hotels. Common elements among these analyses are:

- The NPV is a valuable tool to assess the feasibility of a mission or architecture [3, 21–28, 148, 149].
- Asteroid mining missions in the near term are likely only feasible when including in-situ water as propellant for the cargo/transport spacecraft [22, 25, 93, 126].
- Agreement that ‘traditional’ cost estimation, based on heritage data, is likely to overestimate incurred costs by commercial parties [25, 31, 93].
- Cost components have to be calculated for (at least) development, production (manufacturing), launch and operation [3, 23, 25, 30, 31, 93, 126].
- Learning curve effect to estimate the cost subsequent units of spacecraft [23, 26, 30, 166].
- *If* the spacecraft is designed in some detail, its mass, power and TRL can be used to estimate costs using CERs [30, 93], however, this is often not the case.
- Upfront financing is required, as infrastructure has to be operational for a number of years before turning profitable [23, 25, 30, 93].
- Spacecraft may have to be used for multiple missions in order to turn a profit [23, 30, 164], but this could lead to undesirable long waiting times for a ROI, and can lead to issues with phasing requirements due to synodic periods [126].
- The price of the resources sold in space are often based on being competitive with Earth-launched resources [25, 30, 116, 126, 126].
- Demand models are uncertain, especially for the mid-to far term, but the results often heavily depend on the projected demand [23, 29, 30, 93].

Where an appropriate selection of cost models, methods and tools is already a difficult task for space engineering [155], on top of that, there are many different assumptions involved in economic assessments, as well as different decisions for mission architectures. A number of models are created with an emphasis on the mining methods (Refs. [126, 170]), others with an emphasis on spacecraft design (Refs. [25, 31, 93]), again another with an emphasis on logistics (Ref. [28]). The multidisciplinary nature of this challenge, in which all disciplines are important, unfortunately implies that these analysis often fall short on some aspects of the analysis. In the opinion of the author of this thesis, it is often trajectory design that is compromised on and which needs addressing.

Trajectories are often incorporated in analyses using generic and optimistic inputs, such as a low ΔV or mission duration, independent of the target asteroid and neglecting the long synodic period of these near-Earth objects. Examples can be found in Ref. [23], which in an otherwise effective parametric model, incorporates a pre-determined bootstrapping factor of 99, meaning that the spacecraft (in this case solar or electric sails) will carry 99 times its own weight in payload, yet the sail is expected to complete a mission in less than 10 years. In addition, Ref. [23] does not address the orbit of any target asteroid, nor the actual trajectory, but expects regular round trips to these asteroids to be feasible. Another example is Ref. [30], which bypasses calculating trajectories by assuming a transfer time of 160 days following Ref. [171] (which uses $I_{\text{sp}} = 314$ s), using a water electrolysis thruster from Ref. [172] (cited at $I_{\text{sp}_{\text{avg}}} = 258$ s) to asteroids within 0.03 AU. The system proposed in Ref. [30] can deliver maximum $\Delta V = 473$ m/s, but asteroids within 0.03 AU have long synodic periods – a minimum of 23 years, which should be taken into account when multiple one-year round trips within 10 years are envisioned. This shows that incorporating trajectories to asteroids is key during the design of a profitable asteroid mining mission.

3.2 TRAJECTORY OPTIMISATION

Chemical, high-thrust propulsion is often used in research regarding asteroid mining [3, 25, 126]. These missions are generally faster than missions employing low-thrust propulsion, which is important when taking the time-value of money into account [126]. However, these propulsion systems require vast amounts of propellant. This propellant either has to be launched from Earth, which is costly, or mined from the asteroid, resulting in less saleable mass. To mitigate this, solar sailing has also been identified as a promising propulsion method for asteroid mining missions, due to its propellantless nature [23, 131].

Whichever method of propulsion is selected, the missions need to be optimised. Trajectory optimisation can be summarised as determining a trajectory subject to specified initial and terminal conditions, which minimises some parameter of importance, to carry out the required mission. The parameter of importance can for example relate to minimum propellant usage or equivalently maximum payload capacity, minimum transfer time, maximum observation time for scientific activities, or economic objectives, as is the case in this thesis.

Generally, the optimisation problem is complicated, because of one (or more) of the following reasons: (1) the dynamical system is non-linear, (2) the initial and terminal conditions might not be known, (3) time-dependent forces are involved, and (4) the basic structure for the optimal trajectory might be unknown [173]. For high-thrust spacecraft, the duration of the burn is very short in relation to the total mission duration, such that it is reasonable to model the burn as instantaneous. Using low-thrust propulsion instead of high-thrust propulsion increases the complexity of trajectory optimisation further, as the thrust is now continuous. Trajectory arcs are not simply coast arcs and the control

has a continuous time history that has to be determined by seeking the solution to an optimal control problem [174]. For example, in the case of an interplanetary transfer using solar sailing or solar-electric propulsion, the fact that the distance to the Sun changes has an influence on the trajectory as well [175].

Analytical solutions to the low-thrust optimisation problem can only be obtained for very specific missions and therefore numerical optimisation is the main focus of research in this area. Also, the vast majority of the literature on trajectory optimisation is focused on numerical optimisation [173].

To this extent, this Section will focus on numerical trajectory optimisation for chemical propulsion, using impulsive burns, and for solar sailing. Dynamical models are introduced in Section 3.2.1, followed by a discussion of Lambert arcs and trajectory optimisation methods. The optimisation methods and techniques presented in here are by no means exhaustive, but merely provide an insight into the endless possibilities.

3.2.1 Dynamical Models

In this thesis, the two-body problem is used to model orbit transfers. The two-body problem is governed by [176]:

$$\ddot{\mathbf{r}} = -\frac{\mu}{r^3}\hat{\mathbf{r}} \tag{3.13}$$

The variable $\mathbf{r}$ represents the position vector of the spacecraft with respect to the central body. The gravitational parameter μ is defined as:

$$\mu \coloneqq G(m_1 + m_2) \tag{3.14}$$

in which m_1 and m_2 are the mass of the main body (central) and orbiting body (spacecraft), respectively. The gravitational parameter $\mu = 1.3271244 \times 10^{11}$ km^3/s^2 for the Sun-centred two-body problem, and $\mu = 3.985071 \times 10^5$ km^3/s^2 for the Earth-centred two-body problem [132]. See Fig. 3.3a for a graphical representation of the two-body model.

(a) Two-body problem centred at the larger central body.

(b) Cone and clock angle definitions for a solar sail.

Figure 3.3: Reference frame schematics.

SOLAR-SAIL TWO-BODY PROBLEM

To model solar-sail trajectories, the dynamical model is again the two-body problem, but complemented with ideal solar-sail acceleration [139]:

$$\ddot{\mathbf{r}} = -\frac{\mu}{r^3}\hat{\mathbf{r}} + \beta\frac{\mu}{r^2}\left(\hat{\mathbf{r}}\cdot\hat{\mathbf{n}}\right)^2\hat{\mathbf{n}} \tag{3.15}$$

in which β is the sail lightness number and $\hat{\mathbf{n}}$ is the sail normal unit vector. The dimensionless solar-sail lightness number is the ratio of solar pressure acceleration with respect to the local solar gravitational acceleration, which both have an inverse square variation with the Sun-sail distance, meaning that the lightness number is independent of the Sun-sail distance. The sail normal vector is a unit vector directed normal to the sail surface, defined in the radial-transverse-normal frame in terms of the cone angle, α, and the clock angle, δ, as shown in Fig. 3.3b. As can be seen in Fig. 3.3b, the cone angle is the angle between the incoming solar radiation and the sail normal, and the clock angle fixes the sail normal in three-dimensional space, as the angle between the projection of $\hat{\mathbf{n}}$ on the plane perpendicular to the sunlight direction $(\hat{\boldsymbol{\theta}}, \hat{\boldsymbol{\phi}})$ and a reference direction. In the Radial-Transverse-Normal body-fixed reference frame (A), the sail normal vector is defined as:

$$\hat{\mathbf{n}}^{(A)} = \begin{bmatrix} \cos(\alpha) \\ \sin(\alpha)\cos(\delta) \\ \sin(\alpha)\sin(\delta) \end{bmatrix} \tag{3.16}$$

The reference frame transformation from the body-fixed reference frame to the inertial two-body frame (B) is performed by [139]:

$$\hat{\mathbf{n}}^{(B)} = \begin{bmatrix} \hat{\mathbf{r}} & \hat{\boldsymbol{\theta}} & \hat{\boldsymbol{\phi}} \end{bmatrix}\hat{\mathbf{n}}^{(A)} \tag{3.17}$$

where

$$\hat{\boldsymbol{\theta}} := \frac{\hat{\mathbf{z}}\times\hat{\mathbf{r}}}{|\hat{\mathbf{z}}\times\hat{\mathbf{r}}|} \tag{3.18}$$

$$\hat{\boldsymbol{\phi}} := \hat{\mathbf{r}}\times\hat{\boldsymbol{\theta}} \tag{3.19}$$

for the sake of simplicity, the superscript $\square^{(B)}$ will be dropped and all future references to $\hat{\mathbf{n}}$ will be in the two-body reference frame.

ORBITAL ELEMENTS

To uniquely define a specific orbit in space, orbital elements are used. The most widely used set of orbital elements are the Keplerian orbital elements: the semi-major axis a, eccentricity e, inclination i, argument of periapsis ω, right ascension of the ascending node Ω and the true anomaly θ. These orbital elements are illustrated in Fig. 3.4. The ecliptic is often used as a reference plane, and the vernal equinox (Υ) is often used as a reference direction, as is the case in the JPL SBDB used to obtain ephemerides in this thesis.[1]

The set of orbital elements is fundamentally different from a set of rectangular or spherical coordinates, because only the last coordinate (θ) changes continuously over time as a body moves along

[1] `https://ssd.jpl.nasa.gov/planets/eph_export.html`, accessed on April 19th, 2022.

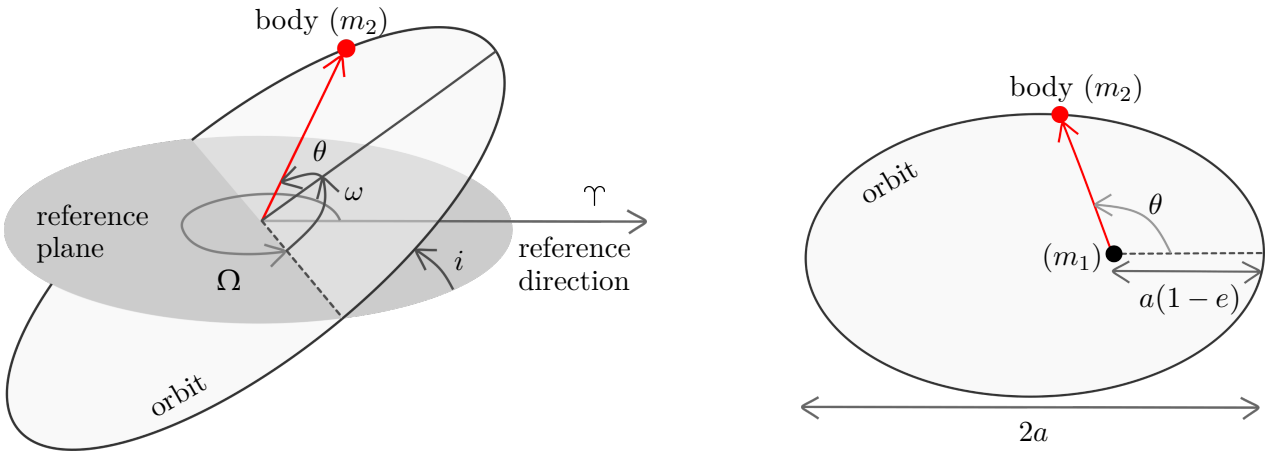

(A) THREE DIMENSIONAL REPRESENTATION. (B) VIEW IN ORBITAL PLANE.

FIGURE 3.4: DEFINITION OF KEPLERIAN ORBITAL ELEMENTS.

its orbit, while the first five orbital elements remain constant in the absence of perturbations. Instead of the true anomaly, the eccentric anomaly E or mean anomaly M can be used to define the position along the orbit. Other options for orbital element sets are equinoctial orbital elements, modified equinoctial orbital elements, or Delauney variables. The choice for the set of orbital elements depends on the problem, possible singularities that need to be avoided, or the specific trajectory optimisation method that is selected [173].

3.2.2 LAMBERT PROBLEM

Most economic analyses of asteroid mining missions do not include trajectory optimisation, but (sometimes even implicitly) employ simple phase-free Hohmann transfers to estimate the total ΔV and mission duration [21, 22]. While this is useful as a first estimate to compare different asteroid target orbits, the ΔVs for these transfers are independent of time, thereby neglecting important aspects such as the launch window, mining duration, and the timing of departure/arrival at target orbits. One well-known method to incorporate time-dependency is through the Lambert problem.

Lambert's problem is an orbital boundary value problem, which states that [177]:

> *"The transfer time of a body moving between two points on a conic trajectory is a function only of the sum of distances of the two points from the origin of force, the linear distance between the points, and the semi-major axis of the conic."*

This is visualised in Fig. 3.5a, with c the chord (or linear distance) between two points, $\mathbf{r}_1$ the position vector at t_1, $\mathbf{r}_2$ the position vector at t_2, F the focal point of the transfer orbit, and ϕ the heliocentric transfer angle [177]. Lambert's problem is therefore a boundary value problem for the ballistic two-body problem, governed by Eq. (3.13). Two different times t_1 and t_2 and two position vectors $\mathbf{r}_1$ and $\mathbf{r}_2$ are given. The solution of the Lambert problem is the arc of trajectory $\mathbf{r}(t)$ satisfying Eq. 3.13, for which:

$$\mathbf{r}(t_1) = \mathbf{r}_1 \tag{3.20}$$

$$\mathbf{r}(t_2) = \mathbf{r}_2 \tag{3.21}$$

The solution to Lambert's theorem is a Lambert arc. Multiple different versions of this arc can be calculated, differing in the number of full revolutions and energy level. Figure 3.5b shows a possible

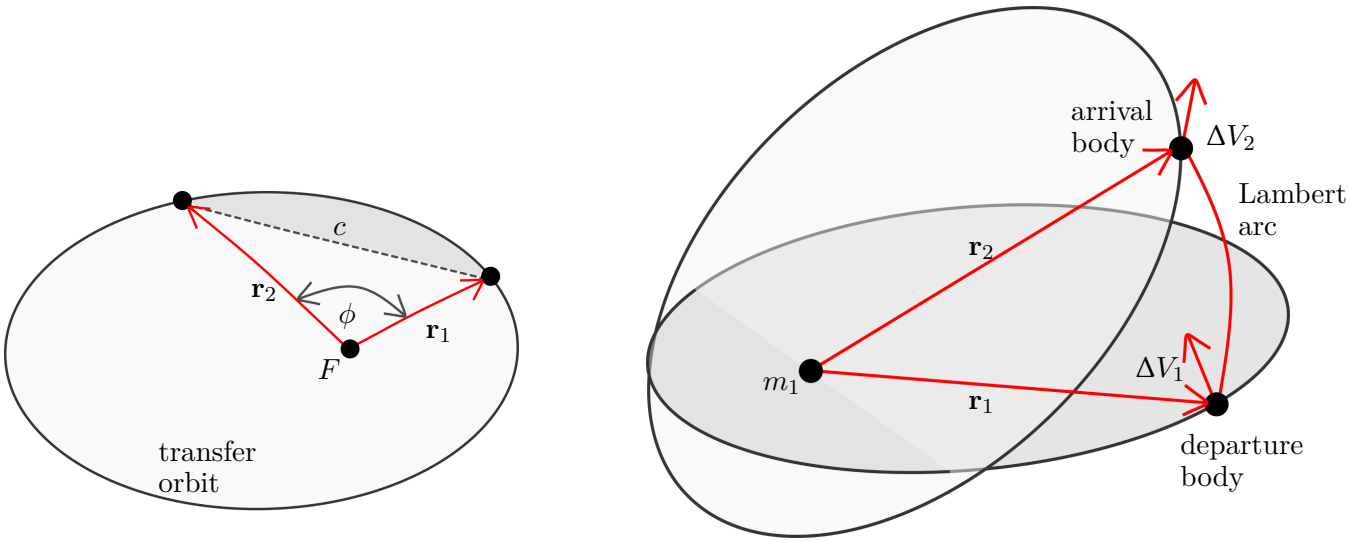

(a) Geometry of Lambert's Theorem.

(b) Geometry of Lambert arc between two bodies.

Figure 3.5: Schematics for Lambert Problem.

Lambert arc. An impulse ΔV_1 has to be applied in order to depart on the transfer arc, followed by another impulse ΔV_2 at the terminal point of the transfer arc, to match the velocity of the arrival body in its orbit. Lancaster and Blanchard [178] presented a solution to the Lambert Problem in which each iteration requires only one inverse function to be calculated. This procedure was built upon in Ref. [179] by Gooding, which only requires three iterations and achieves a high precision up to 13 significant digits. The resulting procedure is considered extremely efficient, highly accurate and to have a low computational cost [180]. Gooding's approach is widely considered the most accurate and fast approach to solve Lambert's Problem, and it has been used as the basis of many slightly different Lambert solvers for the next few decades [180].

Izzo [180] recently revisited the Lambert problem, building upon the work by Lancaster and Blanchard (Ref. [178]), and most notably changes the initial guess used to feed to the algorithm. The resulting Lambert solver requires on average only two iterations for single-revolution cases and three for multiple-revolution cases. The procedure is simple to implement, provides a significant reduction in the solver complexity, is highly accurate when compared to the state-of-the-art algorithm by Gooding, and provides a solution in a shorter time than Gooding's algorithm [180]. Out of existing Lambert solvers, it is considered to have the best ratio of speed, robustness and accuracy [181].

Where a Lambert solver produces the Lambert arc between two points for a given transfer time and number of evolutions, the arc is, in general, not optimal. The position of a body, such as an asteroid or the Earth, is directly related to time. An optimisation strategy can be used to find the optimal departure and arrival time, to minimise the total ΔV needed for the transfer shown in Fig. 3.5b: $\Delta V = \Delta V_1 + \Delta V_2$ [173]. Options for these optimisation strategies are presented in the next Section.

3.2.3 OPTIMISATION PROBLEM DEFINITION

The goal of trajectory optimisation is to minimise an objective J, which can be written in the Bolza form as [182]:

$$\min_{\mathbf{u}(t) \in U} \quad J = \Phi(\mathbf{x}(t_f), t_f) + \int_{t_0}^{t_f} L(\mathbf{x}(t), \mathbf{u}(t), \mathbf{p}, t) dt, \tag{3.22}$$

where $\mathbf{x}$ is the state vector, $\mathbf{u}$ the control vector, $\mathbf{p}$ the vector of static parameters (independent of time) and t the time. The control vector depends on the spacecraft and can for example be the thrust direction and magnitude.

A Bolza objective function includes an end-cost term (Φ) and general function of the instantaneous state, control and time, integrated over time along the trajectory, known as the Lagrangian (L). An objective function with $\Phi = 0$ is known as a Lagrange problem, and one with $L = 0$ is a so-called Mayer problem. Naturally, when the goal is to maximise rather than minimise, the objective function is multiplied by -1.

The trajectories are subject to a system of non-linear differential equations, such as those described in Section 3.2.1, generically:

$$\dot{\mathbf{x}} = f(\mathbf{x}, \mathbf{u}, t) \tag{3.23}$$

States, controls, and static parameters can be subject to bounds, such that:

$$\mathbf{x}_{\text{lower}} \leq \mathbf{x} \leq \mathbf{x}_{\text{upper}} \tag{3.24}$$

$$\mathbf{u}_{\text{lower}} \leq \mathbf{u} \leq \mathbf{u}_{\text{upper}} \tag{3.25}$$

$$\mathbf{p}_{\text{lower}} \leq \mathbf{p} \leq \mathbf{p}_{\text{upper}} \tag{3.26}$$

with subscript $\square_{\text{lower}}$ denoting the lower bound and subscript $\square_{\text{upper}}$ denoting the upper bound. The solution must also satisfy any path constraints $\mathbf{g}$:

$$\mathbf{g}_{\text{lower}} \leq \mathbf{g}\left[\mathbf{x}(t), \mathbf{u}(t), \mathbf{p}, t\right] \leq \mathbf{g}_{\text{upper}} \tag{3.27}$$

and any (in)-equality constraints:

$$\mathbf{c}_{\text{eq}}\left[\mathbf{x}(t), \mathbf{u}(t), \mathbf{p}, t\right] = 0 \tag{3.28}$$

$$\mathbf{c}_{\text{ineq}}\left[\mathbf{x}(t), \mathbf{u}(t), \mathbf{p}, t\right] \leq 0 \tag{3.29}$$

More specifically, in this thesis, the objective for the optimisation is not as traditional as minimum time or minimum propellant, which is the focus of many optimisation strategies in the field of trajectory optimisation. Instead, the entire mission is optimised for an economic objective, which can include an implicit trade-off of propellant usage and time. A mission with a high propellant mass requirement is undesirable, but so is a mission with a long duration. The optimisation method should therefore not only focus on one of these issues. The optimisation method should be capable of selecting the optimal:

- departure and arrival times, which fix the position of the departure and arrival body
- mining duration (linked to arrival and departure time at the asteroid)
- static parameters related to the spacecraft (e.g. mass of mining equipment)

while constraining the problem with:

- physical limits of the spacecraft (e.g. minimum structural coefficient, enforce payload capacity)
- bounds on times
- bounds on static parameters
- dynamics of the system

3.2.4 Optimisation Methods

As noted in the introduction of Section 3.2, high-thrust trajectories can be modelled using instantaneous burns, while low-thrust trajectories are modelled using a continuous time history for the controls. This means that the methods to optimise these trajectories differ and they will therefore be treated separately.

High-Thrust Trajectory Optimisation

For high-thrust missions, the optimisation reduces to a problem with a number of discrete parameters that need to be determined. Only a small number of parameters, for transfer time and a number of static parameters, will suffice to completely describe the solution [173]. The optimisation can go beyond just trajectory optimisation, but combine system and trajectory optimisation [182].

The problem described in Section 3.2.3 is non-linear and non-convex, i.e. can have multiple local minima. Therefore, a global optimisation strategy should be used, in order to find the global minimum. Local optimisation strategies will locate a minimum close to the initial guess, but might miss out on a different minimum in a different basin.

Global optimisation strategies used for the optimisation of Lambert arcs include a grid search [183, 184], Monte-Carlo sampling [185], or heuristic methods. Heuristic methods can search very large search spaces and methods used for Lambert arc optimisation include swarm-based approaches (e.g. particle swarm optimisation [186–188]), differential evolution [189–191], or genetic algorithms [192–196], where the latter is the most popular version [173, 192].

These methods are relatively simple to implement, with a varying degree of computational cost. The most promising and often-applied methods are particle swarm optimisation or a genetic algorithm, especially when it is undesirable to overly constrain the search space a-priori. These are capable of exploring large search spaces at a moderate computational cost. Like other heuristic methods, these methods are more likely to locate global minima than other conventional optimisers [173]. For problems that are sensitive to the optimisation parameters, genetic algorithms are very suitable [197].

Genetic algorithms have recently become a popular global optimisation method for (preliminary) trajectory optimisation [173, 193]. The algorithm is based on the mechanics of natural selection and natural genetics, mimicking Darwin's principle of survival of the fittest. The process starts with a random initial population, based on the bounds on the parameters. For each new iteration ("generation"), the population is created through crossover and mutation. Crossover means that the new generation uses information of the fittest part of the previous population, combining these into the new candidate solutions ("genes" or "individuals"). Fitter candidate solutions in the previous iteration ("parents") have a higher chance of being selected to produce the next population, which will produce better new candidate solutions ("offspring" or "child") to have a better chance at surviving. As happens in natural genetics, mutation is applied with a given probability to a candidate solution

to maintain diversity and prevent premature convergence. To perform the crossover and mutation, not just the method has to be selected, but also parameters such as the mutation rate [198]. Genetic algorithms have been used successfully for the optimisation of Lambert transfers [192–196] and show great accuracy and efficiency in finding a near-optimal solution.

Solar-Sail Trajectory Optimisation

Finding optimal low-thrust trajectories requires the solution to an optimal control problem. Direct optimisation methods to find the solution to this optimal control problem describe the continuous optimal control problem as a parameter optimisation problem. Non-linear constraint equations are generated, which must be satisfied by the discrete representations of the state and control time histories. This means that the problem is converted into a non-linear programming (NLP) problem [173]. Parametrisation of the problem means that the freedom of the control is limited compared to a continuous control history, but this effect is negligible for most cases and very good results can be obtained [182].

Finding solutions to optimal control problems generally requires a two-stage procedure: first find an initial guess and then locally optimise this initial guess. To obtain an initial guess, various methods can be employed, which can be dependent on the problem. While modern NLP solvers are rather robust, a reasonable initial guess still has to be provided, especially for large systems. Reasonable initial guesses are those that satisfy the system's equations of motion, satisfy initial and terminal constraints, and/or satisfy the bounds of the parameters. Initial guess methods can be generated through many different methods, such as using a grid search or genetic algorithm, a shape-based method, or may also be derived using in-depth knowledge of the dynamical model (e.g. using invariant manifolds) [173].

Subsequent optimisation of these initial guess trajectories can be done through, for example, multiple shooting, direct collocation or pseudospectral methods. The solution obtained by these methods may correspond to a local minimum of the optimisation problem, so that multiple initial guesses may be required to obtain the global minimum [173]. These optimisation methods are often presented as software packages, such as for PSOPT (a pseudo-spectral optimiser, used for solar-sail trajectory optimisation in Refs. [39, 175, 199]) or GPOPS-II (a general-purpose optimal control solver, used for solar-sail trajectory optimisation in Refs. [200, 201]). Internally, these optimisers employ general optimal control solvers like IPOPT or SNOPT [202, 203].

The traditional two-stage strategy for finding optimal low-thrust trajectories, despite producing accurate solutions, can be complex and computationally expensive. For each trajectory, a new initial guess has to be produced, which then has to be optimised in a dedicated solver, which needs fine-tuning to obtain a suitable solution. As this thesis aims to explore many different missions to many different asteroids, as part of a multi-disciplinary approach involving more than just the trajectory optimisation, producing very high-quality optimal trajectories is considered out of the scope of this thesis. Considering the computational cost and fidelity of the proposed parametric model, this thesis focuses on finding approximate trajectories for solar sails, more akin to an initial guess.

If a limited number of parameters can be obtained, the global optimisation methods discussed for high-thrust trajectory optimisation can be applied to find approximate near-optimal trajectories. If the number of parameters is too large, the search space quickly grows, especially for methods such as the grid search and Monte Carlo Simulation. Heuristic methods, such as genetic algorithms or particle swarm optimisation, are better suited to explore larger search spaces [182]. Ref. [204] investigates the effect of using piece-wise constant control laws for solar-sail trajectories. Compared with $n = \infty$

segments (i.e. a continuous control history), using $n = 4$ only introduces a relatively small penalty on the optimal time of flight, of $2.40 - 3.96\%$.

Another method would be to employ artificial neural networks to approximate the solar-sail trajectories. Artificial neural networks have been applied in many fields, ranging from speech recognition, cancer diagnosis, finance and also trajectory optimisation [205, 206]. If such a network is trained using a large set of parametrised optimal trajectories, an optimal trajectory for a new set of input values (i.e. the position of both bodies at a certain time) can be found quickly [207].

Creating the training data is a laborious undertaking, which is why it is very useful if a trained network can be used. Most of these trained networks are not open source. An example of a trained network for solar-sail trajectories is presented in Ref. [208], where the network is trained using a shape-based method to produce minimum time trajectories. One major drawback of using readily-trained networks is that users are limited by decisions made by the creators of those networks. In the case of Ref. [208], this means that trajectories are limited to ± 5 deg inclination change, because it assumes co-planar orbits.

Chapter 4

BASELINE MISSION

To ensure consistency among the Chapters in this thesis, a baseline mission scenario is introduced. Unless noted otherwise, the mission description and calculations, as well as the optimisation methods discussed here are used for the remainder of the thesis.

The goal of this thesis is to investigate various issues related to the profitability of asteroid mining. In order to do so, one must look wider than just asteroid mining, but also compare it to Lunar and Martian mining. To this extent, the baseline mission should also be applicable to mining on the Lunar and Martian surface, and preferably also to a wide range of customer locations. As noted in Section 3.1.3, comparison of different economic assessments existing in the literature is complicated, due to the myriad of different architectures, assumptions and cost inputs.

A parametric approach is presented in this thesis. Using the same economic model, applied to a range of different mission architectures, allows for an unbiased comparison. Because of the many parameters involved in the economic model and mission analysis, a balance in the level of approximation used is essential. This results in a moderately low-fidelity parametric approach that can be applied to many different combinations of resource and customer locations. This parametric approach is based on an economic model coupled with trajectory optimisation, used to optimise an economic objective (e.g. the specific cost or NPV) for delivering propellant (LOX and LH_2) as a product to customers.

The structure of this Chapter is as follows. First, the mission architecture for the baseline mission using chemical propulsion will be discussed in detail, from launch to delivery of resources. Next, the economic model is defined, including figures of merit that can be optimised. This is followed by the mass budget calculations needed to feed into the economic model. A generic method for calculating and optimising trajectories is discussed last.

4.1 MISSION ARCHITECTURE

A baseline mission architecture, which uses chemical propulsion, is presented in Fig. 4.1 and includes the following elements:

- The mission starts with a launch to LEO using SpaceX's Starship, a fully reusable launch system. The system consists of a first stage, Super Heavy, and a second stage, Starship. This commercial system has been selected due to its very low projected launch costs and high payload capacity. For the launch, a circular orbit with an altitude of 185 km is assumed based on previous SpaceX

launches [209]. The maximum payload capacity of the launch vehicle is estimated at 150 tons (i.e. 136 metric tonnes [209]), which is used to size the combined mass of the cargo spacecraft, the MPE required and the propellant needed for the first orbit transfer manoeuvre.

- During the next stage, the cargo spacecraft loaded with the MPE departs from LEO to transfer to the material source location (e.g. asteroid, Moon or Mars). For all material sources except the Moon, this will include a hyperbolic escape trajectory. The hyperbolic excess velocity will be used to perform the first impulsive burn of the outbound transfer. The second burn of the outbound transfer will be performed at the material source location, which depending on the material source location, can include a hyperbolic capture trajectory.
- After arrival at the material source location, the MPE is installed and mining and processing water into propellant can start, producing LOX and LH_2. The duration of the mining phase is equal to the stay time at the material source location, minus a 14 day window. This time window can be used to perform analyses to determine the landing site, land on the material source, install the MPE and, at the end of the mining phase, use some time to disconnect from the MPE. During the mining phase, resources can be stored in the cargo spacecraft as they become available.
- When the mining phase has completed, the cargo spacecraft transfers to the location of the resource customer. During this transfer, the cargo spacecraft utilises part of the mined and processed payload as propellant. If necessary, depending on the mining and customer location, the inbound transfer will include a hyperbolic escape and/or capture trajectory, where the hyperbolic excess velocity is again sized appropriately to match the impulse needed for the transfer.
- At the final destination, the customer location, the remaining propellant will be sold to the customer.

Based on the specific scenario, i.e. a given combination of material source and customer location, this architecture can be adapted. For example, for landing on Mars, the mission will have to deal with atmospheric entry. Also, if a solar sail is used in the mission, the baseline mission will have to be adapted to accommodate this: the solar sail will provide continuous thrust rather than the impulsive burns discussed above, and escaping the Earth's gravity well with a solar sail can require a long duration, meaning that other options should be explored. Any changes to the baseline mission will be stated clearly in the Chapter in which it is used.

4.2 ECONOMIC MODEL

A baseline economic model is explained in this Section, which includes the calculation for the total cost and all the separate cost contributions. A calculation for the NPV is given too, but note that this is not used in all upcoming Chapters.

For the cost of the baseline mission, the following cost contributions are taken into account, following Section 3.1.3:

- Launch cost
- Development cost for the spacecraft (cargo spacecraft and MPE)
- Manufacturing cost for the spacecraft (cargo spacecraft and MPE)

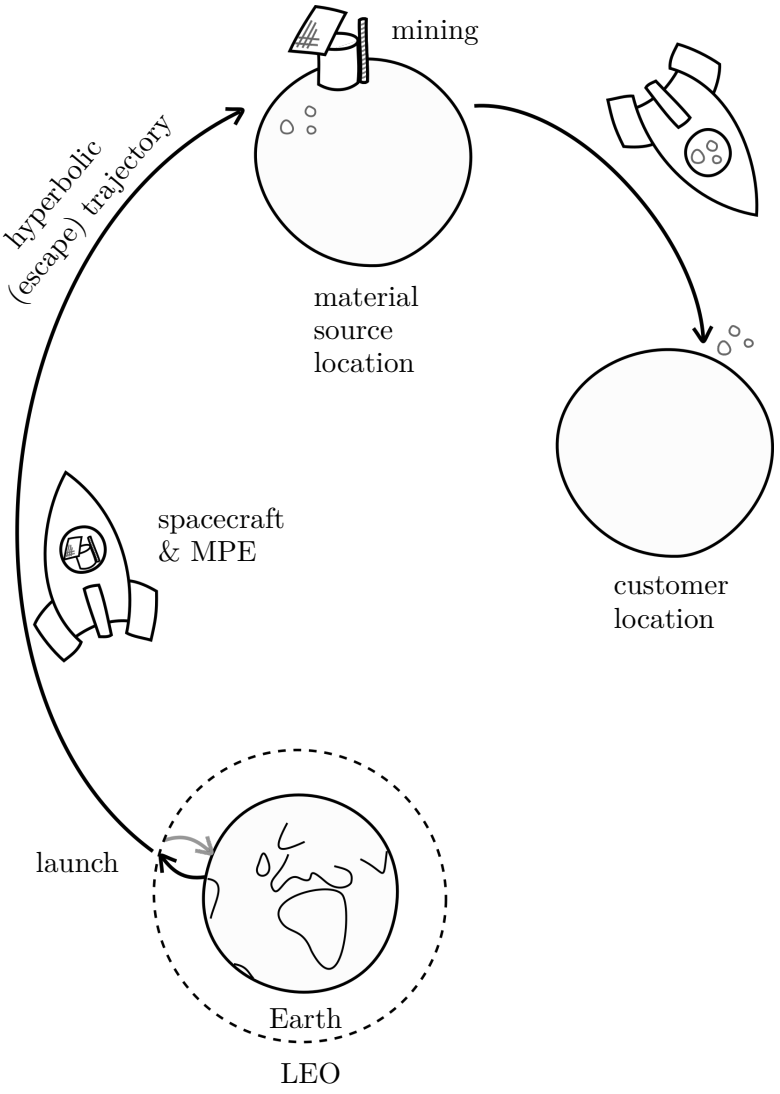

Figure 4.1: Baseline mission architecture.

- Operational cost
- Propellant cost (for the outbound transfer, but not for the launch to LEO, that is included in the launch cost)

To compute the total cost, C, specific costs c for the elements are multiplied by the total mass or time for that element:

$$C = C_{\mathrm{l}} + (c_{\mathrm{dev}} + c_{\mathrm{man}})m_{\mathrm{s/c,dry}} + c_{\mathrm{op}}t_{\mathrm{mis}} + c_{\mathrm{prop}}m^{O}_{\mathrm{prop}} \tag{4.1}$$

in which:

- C_{l} is the launch cost;
- c_{dev} is the specific cost for development (per kg);
- c_{man} is the specific cost for manufacturing (per kg);
- $m_{\mathrm{s/c,dry}}$ is the combined dry mass of the cargo spacecraft and MPE (in kg);
- c_{op} is the operation cost (per year);

- t_{mis} the total mission duration (in years);
- c_{prop} is the specific cost for propellant (per kg);
- and m^{O}_{prop} the propellant required for the outbound transfer with the cargo spacecraft (in kg).

The Section below will summarise the methodology for obtaining the separate cost elements, with final data given in Table 4.6.

4.2.1 Cost Estimation

The separate cost contributions in Eq. (4.1) will be treated below in order of occurrence. In addition, the estimation for the resource selling price will be given at the end of the Section. Sensitivity analyses will be carried out in Sections 5.3, 6.4 and 7.3 to investigate a number of the costs estimated in this Section.

Where necessary, all costs are been corrected for inflation to Fiscal Year 2020 (FY2020) using NASA inflation tables [210], as the cost contributions are taken from different sources with costs given in different years. The yearly inflation index is given in Table 4.1. For example, to adjust a cost C given in FY2014 to FY2016, one will need to multiply by (1.015×1.013). More generally:

$$C\ [\text{FY}j] = C\ [\text{FY}i] \cdot \prod_{k=i+1}^{j} (\text{inflation index year } k) \tag{4.2}$$

in which i is the year in which the cost is given, j the year the cost is desired, and k the index of the year for which the inflation index is required.

Table 4.1: NASA inflation indices as determined in 2018 [210].

Year	**Inflation index**
2005	1.038
2006	1.042
2007	1.036
2008	1.029
2009	1.013
2010	1.023
2011	1.020
2012	1.010
2013	1.018
2014	1.021
2015	1.015
2016	1.013
2017	1.022
2018	1.027
2019	1.030
2020	1.030

Launch Cost, C_{l}

The launch costs for the baseline mission are based on the projected cost for the Starship system, which includes the Super Heavy first stage and the Starship second stage. As this is a fully reusable

system, SpaceX projects the costs to be "less than the cost of Falcon 1" [209]. At the time of writing, the Starship system has not become operational yet, so the launch cost are assumed to be equal to the cost of the Falcon 1 vehicle, taken from Ref. [132]: 10.9 M$ in FY2011. Inflated to FY2020$, the launch costs are equal to 13.1 M$.

Development Cost, c_{dev}

As reviewed in Section 3.1.2, conventional methods for determining the costs for hardware are parametric cost models, analogy-based models, bottom-up models, expert judgement or process-based models. These methods all have to deal with limited data sets and the effects of rapidly changing technologies [157]. In addition, these models require detailed information on the spacecraft and mission (e.g., mass, power, TRL, complexity, and/or a WBS). This level of detail is not available during concept development [157], especially in the case of "first of a kind" or "state-of-the-art" missions [159], as is the case in this work. Also, even if historical data analogous to the proposed asteroid mining mission existed, historical data often suffers from a temporal, cultural, and technological gap due to time delay [156], resulting in inaccurate estimations for the estimated cost. Also, it has been concluded in Section 3.1.3 that traditional cost estimation methods, based on heritage data, are likely to overestimate the incurred costs by commercial parties [25, 31, 93]. Therefore, another strategy for estimating the development and manufacturing cost has been explored.

Again, even though mass may not be a cost driver, it is generally a cost predictor [156]. In combination with the specific cost ($/kg), the total cost for a system can be calculated. A method to estimate these specific costs has to be found. Reference [9] discusses the costs for future space solar power plants, a novel far-term ultra-large structure in orbit. Space, aviation and large-scale consumer product costs are compared, and it is concluded that in order for the space solar power structure to be cost-competitive, costs associated with current large-scale consumer products are needed. Whereas costs this low are unforeseeable for space hardware in the near future, costs comparable with current aviation hardware costs, the middle ground discussed in Ref. [9], are more likely. Therefore, in this work, it is assumed that in a mid- to far-term time frame, the specific cost for space systems has decreased to the current specific cost for aviation systems. This is considered a fair assumption, since the current space sector increasingly resembles the history of aviation: growth of the space industry, commercialisation, high production volumes [211] and reusability [209]. As will be shown in Chapter 8, the number of cargo spacecraft needed for a large-scale asteroid mining operation are very high, justifying the comparison with the high production volumes of aircraft.

Reference [161] presents an overview of development and manufacturing cost per unit mass for each part of an aircraft and a fractional weight breakdown for a typical aircraft (in this case, a Boeing 777-200). A weighted average can be computed for the specific cost per kg. The non-recurring development cost investigated in Ref. [161] consists of components for: engineering, manufacturing engineering, tool design, tool fabrication and support. The aircraft is divided into the following components: wings, empennage, fuselage, landing gear, installed engines, systems and payloads. Using Tables 4.2 and 4.3, the weighted average of the specific costs for the Boeing 777-200 can be calculated as 45,024 $/kg, or 75,600 $/kg in FY2020 (note that this includes a transformation from lbs to kg).

Also, in line with assuming aviation specific costs, aviation production volumes are also taken into account. Through May 2019, 2033 Boeing 777s have been ordered.[1] Since these costs are non-recurring, the development cost can be spread evenly over these units, resulting in 37.19 $/kg.

[1] `http://www.boeing.com/commercial/#/orders-deliveries`, accessed May 31st, 2019

Table 4.2: Estimated empty weight breakdown fraction for typical commercial aircraft [161].

Component	Weight fraction
Wings	23%
Empennage	3%
Fuselage	23%
Landing gear	8%
Installed engines	18%
Systems	12.5%
Payloads	12.5%

Table 4.3: Non-recurring specific costs per component in FY2000 in $/lb [161].

Component	Engineering	Manufacturing engineering	Tool design	Tool fabrication	Support
Wings	7,093	1,773	1,862	6,171	833
Empennage	20,862	5,216	5,476	18,150	2,451
Fuselage	12,837	3,209	3,370	11,169	1,508
Landing gear	999	250	262	869	117
Installed engines	3,477	869	913	3,025	408
Systems	13,723	3,431	3,602	11,939	1,612
Payloads	4,305	1,076	1,130	3,746	506

Table 4.4: Recurring specific costs per component in FY2000 in $/lb [161].

Component	Labour	Materials	Other
Wings	609	204	88
Empennage	1,614	484	233
Fuselage	679	190	98
Landing gear	107	98	16
Installed engines	248	91	36
Systems	315	91	46
Payloads	405	100	59
Final assembly	58	4	3

Manufacturing Cost, c_{man}

Similar to the development cost, manufacturing costs are calculated as a weighted average according to data provided by Ref. [161]. First, Table 4.4 is given with the recurring cost components for: labour, materials and other costs (such as quality assurance, recurring engineering and recurring tooling). The components of the aircraft are the same as for the development cost, with one additional cost contribution for the final assembly. The cost displayed for the final assembly is also a specific cost, corresponding to the total empty weight of the aircraft.

The weighted average of the recurring costs for the first unit can then be calculated as 1,712 $/kg in FY2000, or 2,875 $/kg in FY2020.

Following Section 3.1.3, the learning curve effect is also incorporated for manufacturing costs, which is characterised by a significant reduction in costs as additional units are built. The marginal

manufacturing cost per unit, c_{man} after n units can be calculated using [161]:

$$c_{\text{man}} = c_{\text{man}_0} n^{\frac{\log(b)}{\log(2)}} \tag{4.3}$$

in which c_{man_0} is the theoretical first unit cost and b is the learning curve slope. The learning curve slope used here is $b = 0.909$, which is a weighted average of labour (0.85), materials (0.95), and other (0.95) learning curve slopes, as taken from the same source as the specific costs for the Boeing 777-200 [161]. A slope of 0.85 to approximately 0.9 is often quoted in the aerospace industry [23, 212]. Using again the production volume of 2033 units, the manufacturing costs fall to 1,007.72 \$/kg (FY2020).

Operation Cost, c_{op}

For the baseline mission, the annual costs for operations are based on a robotic, low to moderately complex mission [132]. While it can be argued that the mission is more complex than this, the spacecraft will be in hibernation or an autonomous mode for most of the duration of the transfers. Moreover, increased maturity of technology in the mid- to far-term time frame can be considered. The operation costs come from a parametric model described in Ref. [132], for the costs of such a mission in 2011. It is reasonable to assume that by the time the baseline mission will be flown, the costs can be brought down due to automation. Table 4.5 presents the parametric model from Ref. [132], in which SLOC stands for Source Lines Of Code, a metric used in software engineering to measure the size of a computer program, simply by counting the number of lines in the source code. The same model has been used for the economic modelling of asteroid mining missions in Refs. [23] (conservative scenario) and [30], which are discussed in detail in Section 3.1.3 and Appendix A.

The resulting annual operation costs are 5.69 M\$ in FY2010, or 6.98 M\$ inflated to FY2020.

Table 4.5: Parametric model for operations cost [132].

Component	**Assumptions and calculations**	**Annual cost, k\$ FY2010**
Space segment software maintenance	100k SLOC/16k ≈ 6 FTE at \$200k	1,200
Ground segment		
Mission operations	8 engineers at \$200k + 4 technicians at \$150k	2,200
Ground segment software maintenance	25k SLOC/28.2k ≈ 1 FTE at \$200k	200
Ground hardware maintenance	7% of hardware acquisition cost (\$1,400k)	98
Facilities	$1,000\text{m}^2$ at \$1,250 per m^2	1,250
Program management and systems engineering	15% of other operations costs	742
Total annual operations cost		5,690

Propellant Cost, c_{prop}

Costs for propellant are calculated for a LOX/LH_2 engine, using standard prices for aerospace products reported by the Defense Logistics Agency from the US.[2] These propellant costs are only calculated for the propellant stored inside the cargo spacecraft, to be used for the transfer from LEO to the material source. The propellant for the launch to LEO is included in C_1.

With the cost for LOX stated as 143.05 \$/metric tonne (FY2012) and the cost for LH_2 as 3.77 \$/lb (FY2012), the average cost for propellant is found to be 0.95 \$/kg.

[2] `https://www.dla.mil/Energy/Business/StandardPrices.aspx`, accessed May 31st, 2019

Maintenance Cost, c_{main}

In the case that the cargo spacecraft or MPE are reused, maintenance costs are taken into account for any subsequent missions. While this is not used in Chapters 5–7, it is part of the methodology in Chapter 8.

Heritage data for maintenance in space is not readily available, as maintenance in space is limited to the ISS and Hubble telescope. These have been extremely expensive repairs, carried out by astronauts, and are not thought to be representative for the maintenance proposed in this thesis, on a commercial scale.

Instead, consistent with the development and manufacturing costs, the maintenance cost will be based on mass. One way to quantify maintenance cost is in comparison with the replacement asset value (RAV), expressed as a percentage. The RAV is the value needed to replace the production capability of the present assets. To achieve World Class Maintenance standards, annual maintenance costs should be between 1.5–2.5% [213], or up to 9% for a best-practice benchmark [214]. There are no set rules for each industry or company.[3] Spending too little on maintenance could cause early failure, but spending too much on maintenance is wasteful and unnecessary [214].

The cost of recovery and refurbishment of each SpaceX mission is estimated at less than 10% of the initial manufacturing costs.[4] Note that this value is based on a full mission and not per year. In the case of the missions in Chapter 8, the only chapter where the maintenance costs are incorporated, both the mean and median mission duration are 4.4 years. Assuming that the maintenance costs for the SpaceX missions can be used in the economic model for asteroid mining missions, the 10% divided by 4.4 years results in 2.27% per year, consistent with the standards discussed above. Therefore, maintenance costs for the cargo spacecraft are estimated at 10% of manufacturing costs, at 100.71 \$/kg.

For highly-mechanised mining processes, higher maintenance costs are expected than for other industries/sectors [215]. In absence of analogous data for asteroid mining equipment, maintenance costs for the MPE is estimated at double the maintenance costs for the cargo spacecraft, at 20% of manufacturing costs, at 201.42 \$/kg. This would still be below the maximum of the yearly best-practice benchmark of 9% [214].

Resource Selling Price to Customers in Orbit, p

The price for which the resources are sold is dependent on the type of material to be sold (low value-to-mass or high value-to-mass) and where this material will be sold. If the material is to be sold in orbit, the price has to be competitive with the cost if the same material is launched from Earth. Again, Ref. [116] proposes that resources will be sold for a price p per kg:

$$p = p' + c_{\text{l,orbit}}$$

where p' is the cost of these materials purchased from terrestrial sources, in the case of LOX/LH_2 equal to c_{prop}, and $c_{\text{l,orbit}}$ is the launch cost per kg to the target orbit. For the sake of consistency, $c_{\text{l,orbit}}$ is calculated in the same manner as the cost for the missions discussed in this thesis, and therefore includes a launch to LEO (185 km) using a fully loaded Starship system and a kickstage to transport the resources. The kickstage is costed the same as the cargo spacecraft for the baseline

[3] `https://www.upkeep.com/answers/asset-management/budget-for-equipment-maintenance`, accessed on January 31st, 2022.

[4] `https://www.inverse.com/innovation/spacex-elon-musk-falcon-9-economics`, accessed on January 31st, 2022

mission (i.e. using specific development and manufacturing costs). The total mass of the kickstage (m_{ks}) is calculated such that the complete launch capacity of the Starship is utilised. The sizing of the kick stage will be discussed as part of the mass budget in Section 4.3. The total cost for the mission to the destination are then divided by the total mass delivered to the destination by the kickstage ($m_{\text{ks,transport}}$):

$$c_{\text{l,orbit}} = \frac{C_{\text{l}} + (c_{\text{dev}} + c_{\text{man}})m_{\text{ks,dry}} + c_{\text{prop}}m_{\text{ks,prop}}}{m_{\text{ks,transport}}} \tag{4.4}$$

For these very short missions, operation costs are not taken into account, as these are assumed to be part of the launch service.

Table 4.6: Cost element inputs for NPV model.

Cost element	**Value, FY2020 $**	
C_{l}	13.09×10^6	
c_{dev}	37.19	/kg
c_{man}	1007.12	/kg
c_{op}	6.98×10^6	/year
c_{prop}	0.95	/kg
$c_{\text{main}_{\text{cargo}}}$	100.71	/kg
$c_{\text{main}_{\text{mpe}}}$	201.42	/kg
p	dependent on destination	

4.2.2 Figures of Merit

This Section will present the analysis needed to calculate the figures of merit introduced in Section 3.1.1, tailored to the baseline scenario presented.

If a calculation of the NPV is required for this mission, Eq. (3.4) is rewritten using the cost contributions as follows:

$$NPV = \frac{pm_{\text{r,sold}}}{(1+I)^{t_{\text{mis}}}} - (c_{\text{dev}} + c_{\text{man}})\, m_{\text{s/c,dry}} - c_{\text{prop}}m^{O}_{\text{prop}} - C_{\text{l}} - c_{\text{op}}t_{\text{mis}} \tag{4.5}$$

in which p is the resource price ($/kg) to customers, $m_{\text{r,sold}}$ is the total mass sold to customers (kg), $m_{\text{s/c,dry}}$ is the dry mass of the cargo spacecraft (kg) and m^{O}_{prop} is the propellant mass used during the outbound transfer from the parking orbit in LEO (kg). All masses are explained separately later in this Section.

Other figures of merit can also be used, such as the ENPV, IRR, and ROI, as discussed in Section 3.1.1, by substituting $R_{\text{mis}} = pm_{\text{r,sold}}$:

$$ENPV = P_s\frac{pm_{\text{r,sold}}}{(1+I)^{t_{\text{mis}}}} - C \tag{4.6}$$

$$I = \left[\frac{pm_{\text{r,sold}}}{C}\right]^{\frac{1}{t_{\text{mis}}}} - 1 \tag{4.7}$$

$$ROI = \frac{pm_{\text{r,sold}} - C}{C} \tag{4.8}$$

Finally, the specific cost, c (in \$/kg), can be calculated using:

$$c = \frac{C}{m_{\mathrm{r,sold}}} \tag{4.9}$$

The resulting specific cost for a mission can be used to price the resources for customers. It is a useful metric to compare different missions, as it does not just look at which mission is cheaper or can deliver more resources to a customer, but it combines these two metrics. Specific costs for launch vehicles from Earth are frequently quoted to compare launch vehicles [216], as this can be more useful than the absolute cost for one launch, especially in the case of ride shares.

4.3 MASS BUDGET

This Section describes the method for calculating the mass budget of the baseline mission. The mass budget is explained here step by step, with a supporting graphic shown in Fig. 4.2.

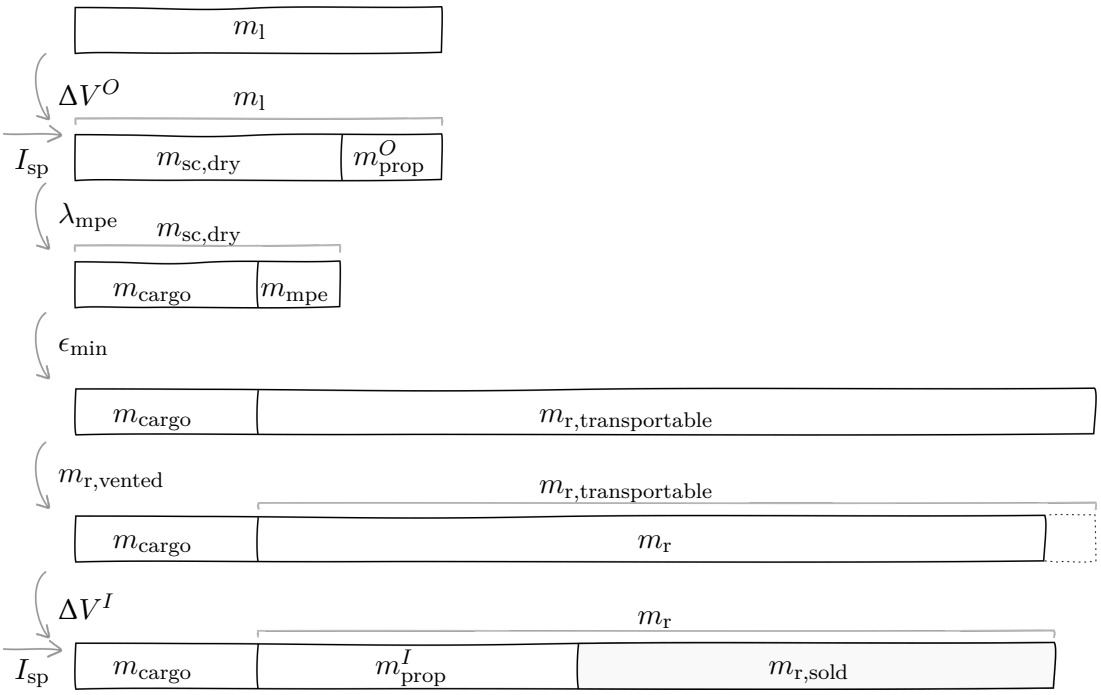

Figure 4.2: Supporting graphic for all masses related to the spacecraft in the mass budget calculation, all variables defined in text.

As described in Section 4.1, all missions start with a Starship system (Super Heavy and Starship combined) utilised at maximum payload capacity. The payload capacity (m_{l}) is divided over the dry mass for the cargo spacecraft loaded with the MPE ($m_{\mathrm{s/c,dry}}$) and the propellant for the outbound transfer manoeuvre (m^O_{prop}):

$$m_{\mathrm{l}} = m_{\mathrm{s/c,dry}} + m^O_{\mathrm{prop}} \tag{4.10}$$

First, the propellant mass requirement m^O_{prop} is calculated as:

$$m^O_{\mathrm{prop}} = m_{\mathrm{l}} \left(1 - e^{-\frac{\Delta V^O}{I_{\mathrm{sp}} g_0}}\right) \tag{4.11}$$

in which ΔV^O is the velocity change required for the outbound transfer from the LEO parking orbit

of the launch vehicle to the material source location and I_{sp} is the specific impulse of the propulsion system. Section 4.4 will detail how ΔV^O is obtained. The propulsion system used throughout this work is assumed to be LOX/LH_2 with $I_{\text{sp}} = 446$ s, to allow the use of in-situ propellant manufactured from water. The total dry mass of the cargo spacecraft loaded with MPE can then be calculated from Eq. (4.10).

Next, the total dry mass of the composite spacecraft, $m_{\text{s/c,dry}}$, is split using a mass fraction, λ_{MPE}, which can be optimised:

$$m_{\text{s/c,dry}} = m_{\text{cargo}} + m_{\text{mpe}} \tag{4.12a}$$

$$m_{\text{MPE}} = m_{\text{s/c,dry}} \lambda_{\text{mpe}} \tag{4.12b}$$

$$m_{\text{cargo}} = m_{\text{s/c,dry}} (1 - \lambda_{\text{mpe}}) \tag{4.12c}$$

where m_{cargo} is the dry mass of the cargo spacecraft and m_{mpe} is the mass of the MPE.

The total quantity of volatiles that is mined and processed at the source, $m_{\text{r,mined}}$, is determined by: m_{mpe}, the duration of the mining phase (t_{mining} in days), and the throughput rate (κ in kg/day/kg of MPE, determined in Section 4.3.2), such that

$$m_{\text{r,mined}} = m_{\text{MPE}} \kappa t_{\text{mining}} \tag{4.13}$$

in which t_{mining} is related to the stay time at the asteroid, Δt_{stay}, following the description of the mission architecture written in Section 4.1:

$$t_{\text{mining}} = \Delta t_{\text{stay}} - 14 \text{ days} \tag{4.14}$$

to account for proximity operations, installing the MPE and the completion of the transport of the resources to the cargo spacecraft at the end of the mining phase.

If the material source is an asteroid, $m_{\text{r,mined}}$ is limited by the available mass on the asteroid: $m_{\text{r,available}}$. It is assumed that the available mass on the Moon or Mars exceeds the cargo capacity of the cargo spacecraft. The total volatile mass available from the target asteroid is approximated using the absolute magnitude of the asteroid (H), the average geometric albedo for C-type asteroids ($p_{\text{v}_\text{C}} = 0.06$ [217]) and the average density of C-type asteroids ($\rho_{\text{C}} = 1,300$ kg/m^3 [217]), along with an expected volatile recovery ratio $\lambda_{\text{volatile}}$ of 10% for asteroidal regolith [21, 46]. It is therefore implicitly assumed that all asteroids for which this baseline mission is calculated are C-type because, as discussed in Section 2.1.1, the type is only known for a very small subset of asteroids, so limiting this thesis to only known C-type asteroids would be ineffective. First, the diameter of the asteroid (assumed spherical) can be approximated using Eq. (2.1), from which the total available volatile mass can be estimated, when taking into account a maximum excavation depth $h_{\max}$, as:

$$m_{\text{r,available}} = \begin{cases} \frac{\pi}{6} d^3 \rho_C \lambda_{\text{volatile}}, & \text{if } d \leq h_{\max} \\ \frac{\pi}{6} \left(d^3 - (d - 2h_{\max})^3 \right) \rho_C \lambda_{\text{volatile}}, & \text{otherwise} \end{cases} \tag{4.15}$$

after which:

$$m'_{\text{r,mined}} = \texttt{min} \left\{ m_{\text{r,mined}}, m_{\text{r,available}} \right\} \tag{4.16}$$

where $m'_{\text{r,mined}}$ is the mined mass corrected for the available mass. Current robotic missions lack the ability to drill more than a few centimetres into a surface, but an excavation depth of 10 metres is

foreseen [218].

One issue not taken into account yet, is the combustion mixture ratio of LOX/LH_2, since the MPE produces LOX/LH_2 in a stoichiometric ratio (i.e. the ratio at which complete combustion takes place, which is the resulting ratio after electrolysis, $\sim 7.9:1$). However, current propulsion systems are designed for a fuel-rich mixture ratio, meaning that there is an excess of oxygen after electrolysis. A mixture ratio of $6.5:1$ is adopted in this work, which is slightly higher than currently used ($6:1$), but still considered very reasonable [219]. The closer the mixture ratio is to the stoichiometric ratio, the smaller the excess of oxygen. In this model, the excess oxygen is vented, which is a common approach [29, 71, 219]:

$$m_{\mathrm{r,vented}} = m'_{\mathrm{r,mined}} \lambda_{\mathrm{MR}} \tag{4.17}$$

in which $m_{\mathrm{r,vented}}$ is the total quantity of volatiles after venting the excess oxygen, and λ_{MR} the fraction left after venting in order to reach a combustion mixture ratio of $6.5:1$, which makes $\lambda_{\mathrm{MR}} = 0.8392$. While the MPE may be able to produce a certain quantity of LOX/LH_2, the total mass that can be transported to the customer (m_{r}) is constrained by the maximum mass that can be transported by the cargo spacecraft ($m_{\mathrm{r,transportable}}$):

$$m_{\mathrm{r}} = \mathtt{min}\left\{m_{\mathrm{r,vented}}, m_{\mathrm{r,transportable}}\right\} \tag{4.18}$$

A minimum structural mass coefficient $\epsilon_{\mathrm{min}} = 0.1$ will be assumed for the cargo vehicle [220], such that the total mass that can be transported using the cargo spacecraft is determined as:

$$m_{\mathrm{r,transportable}} = \frac{1-\epsilon_{\mathrm{min}}}{\epsilon_{\mathrm{min}}} m_{\mathrm{cargo}} \tag{4.19}$$

A supporting graphic visualising the different masses that result in m_{r} is given in Fig. 4.3.

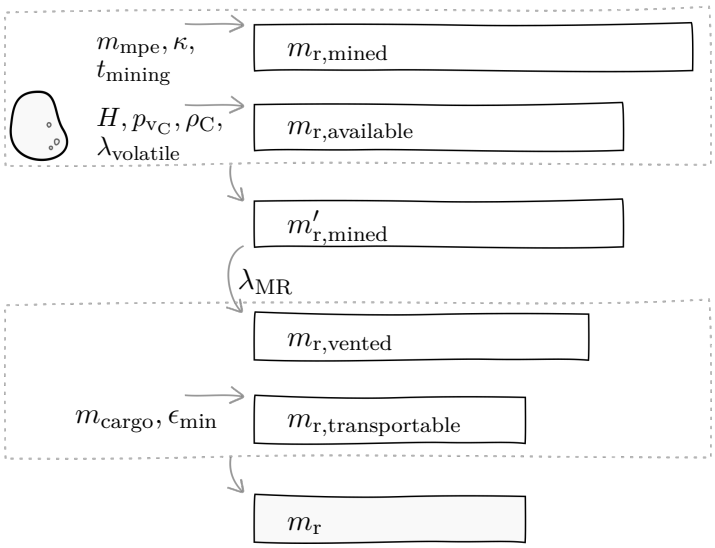

Figure 4.3: Supporting graphic for all masses resulting in m_{R} in mass budget calculations, all variables defined in text.

Finally, because the cargo spacecraft employs ISRU, consuming part of the LOX/LH_2, the quantity of resources that can be sold at the customer destination is:

$$m_{\mathrm{r,sold}} = m_{\mathrm{r}} - m^{I}_{\mathrm{prop}} \tag{4.20}$$

in which m^{I}_{prop} is the required propellant mass for the inbound transfer, i.e. the transfer from the material source location to the customer location. The quantity of propellant required is calculated using:

$$m^{I}_{\mathrm{prop}} = (m_{\mathrm{cargo}} + m_{\mathrm{r}}) \left(1 - e^{-\frac{\Delta V^{I}}{I_{\mathrm{sp}} g_0}}\right) \tag{4.21}$$

where ΔV^{I} is the velocity change required to transfer from the material source to the customer location. Again, Section 4.4 will detail the method for determining ΔV^{I}.

4.3.1 Kickstage

In this thesis, two types of kickstages are foreseen. First, a kickstage transporting propellant directly to a customer, without any off-Earth mining involved. Second, a kickstage transporting another spacecraft, such as the cargo spacecraft. A graphic depicting these two types of kickstages is shown in Fig. 4.4. For both types of kickstages, the propellant mass requirement for the kickstage ($m_{\mathrm{ks,prop}}$), the dry mass of the kickstage ($m_{\mathrm{ks,dry}}$) and the mass that can be transported using the kickstage ($m_{\mathrm{ks,transport}}$) have to be calculated.

First, the propellant mass required for the kickstage can be calculated. The propellant mass $m_{\mathrm{ks,prop}}$ is naturally dependent on the ΔV requirement of the transfer from LEO to the destination (ΔV_{ks}), and calculated similar to Eq. (4.11), substituting $m_{\mathrm{ks,prop}}$ for m^{O}_{prop} and ΔV_{ks} for ΔV^{O}:

$$m_{\mathrm{ks,prop}} = m_{\mathrm{l}} \left(1 - e^{-\frac{\Delta V_{\mathrm{ks}}}{I_{\mathrm{sp}} g_0}}\right) \tag{4.22}$$

For the mass of the kickstage transporting propellant, the minimum structural coefficient ϵ_{min} is used to calculate the dry mass of the kickstage $m_{\mathrm{ks,dry}}$. If the kickstage is transporting liquids, it will be holding both the propellant needed for the transfer ($m_{\mathrm{ks,prop}}$) and the propellant transported as

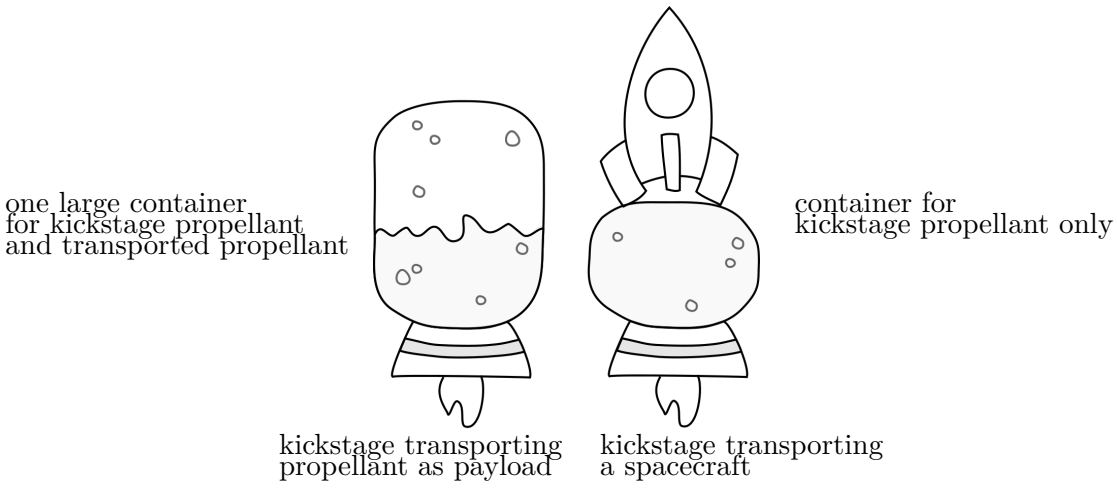

Figure 4.4: Graphic depicting the two types of kickstages.

payload ($m_{\text{ks,transport}}$), thus:

$$m_{\text{ks,dry}} = \epsilon_{\text{min}} m_{\text{l}} \tag{4.23}$$

as the total payload capacity of the launch vehicle is used and any non-structural mass is liquid and needs to be encapsulated using the structural mass.

If the kickstage is transporting another spacecraft, such as the cargo spacecraft, it will only have to hold the propellant needed for the transfer, as the other spacecraft can be mounted on the kickstage and does not need to be enveloped in a container. It is assumed that the mass required for this mounting can be accommodated for by the rather conservative ϵ_{min} employed in this work, so that:

$$m_{\text{ks,dry}} = \frac{\epsilon_{\text{min}}}{1 - \epsilon_{\text{min}}} m_{\text{ks,prop}} \tag{4.24}$$

For both types of kickstages, the mass that can be transported by the kickstage is then equal to:

$$m_{\text{ks,transport}} = m_{\text{l}} - m_{\text{ks,dry}} - m_{\text{ks,prop}} \tag{4.25}$$

4.3.2 Throughput Rate

The throughput rate κ to mine water and process it into LOX and LH_2 is calculated using a relatively conservative ([221]) initial throughput of 200 kg/day per kg of MPE. This includes the equipment necessary for collecting and grinding, separating gases from solids and condensing vapours [126]. In order to calculate the throughput after adding additional equipment required, the total mass for an example system is calculated.

Reference [126] suggests 1500 kg can be allocated for the elements of the equipment responsible for the 200 kg/day per kg of MPE throughput above, which therefore means a mass flow rate of 300,000 kg/day. In addition to this equipment mass, the mass of the power system for mining water and electrolysing the water into LOX/LH_2, along with the mass of the required structure, heat engine and compressors must be added. Reference [126] suggests a structural mass of 300 kg, a compressor mass of 10 kg, a heat engine mass of 100 kg and a power requirement of 200 kW for the above mass flow rate. In the mid- to far-term, solar array performance is envisioned to reach 4 kg/kW [222]. The power requirement for the electrolysis is estimated using the Gibbs free energy of water for dissociation into H_2 and O_2 which is 13.16 MJ/kg [223]. Using the mass flow rate of 300,000 kg/day, the power requirement for electrolysis can be estimated, followed by the required solar array mass. It is assumed that cooling of the gases to liquid is performed by directing flow pipes into the shadow, while providing sufficient heat transfer to cold space [224]. Subsequently, a 10% margin is added to the total system mass to account for uncertainties. The mass flow rate can then be divided by the total mass of the system to obtain the throughput rate including all equipment.

Two factors determine the throughput for different material sources. First, different water content of the regolith at the various material sources, and second, the solar distance:

- *Water content*, affects the amount of water extracted from the same quantity of regolith. The same mass of equipment is required to process the same amount of regolith, but this results in less harvested water. A water content of 10% is assumed in the calculation above, consistent with water-bearing asteroids [112], but this is only 1.3% for typical Martian regolith [71, 73] and 1.5% for typical Lunar regolith [71]. Because less water is harvested, the power requirement for electrolysis decreases too.

- *Solar distance*, influences the solar flux and therefore the performance of the solar panels to power the MPE. This change in performance has an effect on the total solar panel mass required to power the equipment for mining, processing and electrolysis. An approximation for the solar panel performance is based on an inverse-square relationship with the semi-major axis of the material source body.

This calculation results in throughput rates for different material sources as shown in Table 4.7, with two sample asteroids, one close to Earth's orbit and one in the main belt.

Table 4.7: Assumed throughput rate for all material sources.

Material source	**Throughput rate κ, kg/day/kg of MPE**
Lunar surface	1.358
NEA 2000 SG344	1.538
Martian surface	0.602
MBA 2015 AE282	0.365

4.3.3 Example Calculations

This Section briefly sets out some example calculations for the mass budget discussed in Section 4.3, for a mission to an asteroid. Some parameters usually dependent on the material source or determined during optimisation are given, such as ΔV^O, ΔV^I, κ, H, λ_{mpe} and t_{stay}.

Assuming a Starship launch vehicle delivering $m_{\text{l}} = 136,077$ kg to LEO [209], $\Delta V^O = 4$ km/s and $\lambda_{\text{mpe}} = 0.1$, the following can be calculated:

$$\begin{aligned} m^O_{\text{prop}} &= m_{\text{l}} \left(1 - e^{-\frac{\Delta V^O}{I_{\text{sp}} g_0}}\right) = 81,551 \text{ kg} \\ m_{\text{s/c,dry}} &= m_{\text{l}} - m^O_{\text{prop}} = 54,526 \text{ kg} \\ m_{\text{mpe}} &= m_{\text{s/c,dry}} \lambda_{\text{mpe}} = 5,453 \text{ kg} \\ m_{\text{cargo}} &= m_{\text{s/c,dry}} (1 - \lambda_{\text{mpe}}) = 49,073 \text{ kg} \end{aligned}$$

Then, assuming a stay time $t_{\text{stay}} = 60$ days on an asteroid on which the throughput rate $\kappa = 1.538$ kg/day/kg of MPE (equal to κ calculated for NEA 2000 SG344 in Table 4.7):

$$\begin{aligned} t_{\text{mining}} &= t_{\text{stay}} - 14 = 46 \text{ days} \\ m_{\text{r,mined}} &= m_{\text{mpe}} \kappa t_{\text{mining}} = 385,793 \text{ kg} \\ m_{\text{r,vented}} &= m_{\text{r,mined}} \lambda_{\text{MR}} = 323,738 \text{ kg} \end{aligned}$$

which have to be checked against $m_{\text{r,available}}$ and $m_{\text{r,transportable}}$. For the sake of this example, a magnitude $H = 26$ is assumed for the asteroid, and the albedo and density are taken for a C-type

asteroid, so that:

$$\begin{aligned} d &= 1329 \times \frac{10^{-\frac{H}{5}}}{\sqrt{p_{\mathrm{vC}}}} = 34.2 \text{ m} \\ m_{\mathrm{r,available}} &= \frac{\pi}{6} d^3 \rho_{\mathrm{C}} \lambda_{\mathrm{volatile}} = 2,730,801 \text{ kg} \\ m_{\mathrm{r,transportable}} &= \frac{1-\epsilon_{\min}}{\epsilon_{\min}} m_{\mathrm{cargo}} = 441,663 \text{ kg} \end{aligned}$$

This means that $m_{\mathrm{r}} = m_{\mathrm{r,vented}}$ as it passes both tests ($m_{\mathrm{r,mined}} < m_{\mathrm{r,available}}$ and $m_{\mathrm{r,vented}} < m_{\mathrm{r,transportable}}$). Then assuming $\Delta V^I = 2$ km/s, the resource mass that can be sold at the destination can be determined as:

$$\begin{aligned} m^I_{\mathrm{prop}} &= (m_{\mathrm{cargo}} + m_{\mathrm{r}}) \left(1 - e^{-\frac{\Delta V^I}{I_{\mathrm{sp}} g_0}}\right) = 136,819 \text{ kg} \\ m_{\mathrm{r,sold}} &= m_{\mathrm{r}} - m^I_{\mathrm{prop}} = 186,920 \text{ kg} \end{aligned}$$

4.4 TRAJECTORIES

The missing parameters to calculate the masses in the mass budget and the accompanying economic model, are the ΔV requirements for the various transfers. This Section explains how these are calculated and optimised. It aims to explain the process for all combinations of material sources and customer locations discussed in this thesis.

A patched-conic approach is used, connecting a number of segments in relevant two-body systems, using the equations presented in Section 3.2.1. Ephemerides of planetary bodies and asteroids are taken from JPL databases.[5]

Interplanetary segments of the transfers are modelled using Lambert arcs, and transfers between closed planet-centred orbits (e.g. around the Earth, Moon or Mars) are modelled using Hohmann transfers. Transfers to escape or from capture are modelled using hyperbolic trajectories with a ΔV applied at the periapsis. The methodology for calculating ΔV^O and ΔV^I and two examples are given below.

The ΔV and transfer time, t_{t}, for each segment can be determined using one of four ways:

1. A two-burn Hohmann transfer can be used to calculate the ΔV between two closed orbits around the Earth, Moon or Mars. Between circular and elliptical orbits around the same main body, ΔV and t_{transfer} are both calculated using the Hohmann transfer, taking the inclination change into account where necessary.

2. For transfers from a circular or elliptical orbit to escape, or from capture to a circular or elliptical orbit, a single ΔV is applied at the periapsis of the transfer orbit. Hyperbolic escape orbits are designed such that the hyperbolic excess velocity, v_∞, is equal to the ΔV of the next segment of the escape orbit, or the previous segment of the capture orbit. A single ΔV is applied at periapsis of the hyperbolic transfer orbit. The transfer time, t_{transfer}, is estimated as the time from periapsis of the transfer orbit to the sphere of influence of the main body.

3. A Lambert arc is used to calculate interplanetary transfers between bodies (e.g., Earth escape to Mars capture or an asteroid), as well as transfers to Lagrange points. Where applicable, the

[5] `https://ssd.jpl.nasa.gov/tools/sbdb_query.html`, accessed on August 20th, 2020.

ΔV at the start (ΔV_{start}) and end (ΔV_{end}) of the Lambert arc is used to compute the hyperbolic trajectories. The timing, and thereby ΔV requirement of these Lambert arcs is optimised. Based on the summary in the literature review, the Lambert solver used in this paper is designed and written by Dario Izzo (Ref. [180]). It is written in Python, but translated to MATLAB®.

4. Fixed values of ΔV or t_{transfer} for certain segments can be used as listed in Table 4.8. For atmospheric (re)-entry at Earth and Mars, a ballistic trajectory from capture followed by a direct descent (i.e. without first getting into orbit around the planet) is assumed. Parking orbits are assumed at an altitude of 100 km, for both low-Lunar orbit (LLO) and low-Martian orbit (LMO). For transfers to and from the parking orbits at 100 km, the value for t_{transfer} is set to zero, because this duration is negligible compared to the duration of the other segments. Otherwise t_{transfer} is approximated by the time taken to transfer from the edge of the sphere of influence, along the capture trajectory with periapsis at the surface, to the periapsis of that trajectory. SpaceX states that most of the energy is dissipated aerodynamically during atmospheric entry: 99.9% for Earth atmospheric entry and 99% for Mars atmospheric entry [225]. However, supersonic retro-propulsion is necessary to land on Mars [226]. The estimated ΔV given for this propulsive descent is based on the Mars Design Reference Architecture 5.0 [227], which also utilises supersonic retro-propulsion for the descent on Mars.

Table 4.8: Fixed segment ΔV and t_{transfer}.

Segment	**ΔV, km/s**		**t_{transfer}, days**
Earth capture → Earth surface	0	Ref. [227]	7.8
Mars capture → Mars surface	0.595	Ref. [227]	11.7
LLO (100 km) → Lunar surface	1.963	Ref. [228]	0
Lunar surface → LLO (100 km)	1.905	Ref. [228]	0
Mars surface → LMO (100 km)	4.028	Ref. [229]	0

For the hyperbolic trajectories, the ΔV applied at the periapsis of the transfer orbit is calculated using:

$$\Delta V = \sqrt{v_\infty^2 + v_{\text{esc}}^2} - v_{\text{p}} \tag{4.26}$$

in which v_∞ is the hyperbolic excess velocity, set equal to the ΔV of the next or previous segment as discussed above, v_{esc} the local escape velocity at periapsis of the transfer orbit, and v_{p} the orbital velocity in periapsis of the closed orbit after capture or before escape.

Two examples are treated in this Section. The first example is for a mission to an asteroid, delivering resources to GEO. This trajectory is visualised in Fig. 4.5. The ΔVs are calculated as follows:

- Outbound, ΔV^O
  - $\mathbf{\Delta V_1}$: A ΔV at periapsis of a hyperbolic escape trajectory from LEO to Earth escape, with $v_\infty = \Delta V_{\text{start}}$ of the Lambert arc from Earth to the asteroid;
  - $\mathbf{\Delta V_2}$: The ΔV_{end} of the Lambert arc from Earth to the asteroid, on arrival at the asteroid.
- Inbound, ΔV^I
  - $\mathbf{\Delta V_3}$: The ΔV_{start} of the Lambert arc from the asteroid to Earth, on departure from the asteroid;

– $\mathbf{\Delta V_4}$: A ΔV at periapsis of a hyperbola from Earth capture to GEO with $v_\infty = \Delta V_{\text{end}}$ of the asteroid-Earth Lambert arc.

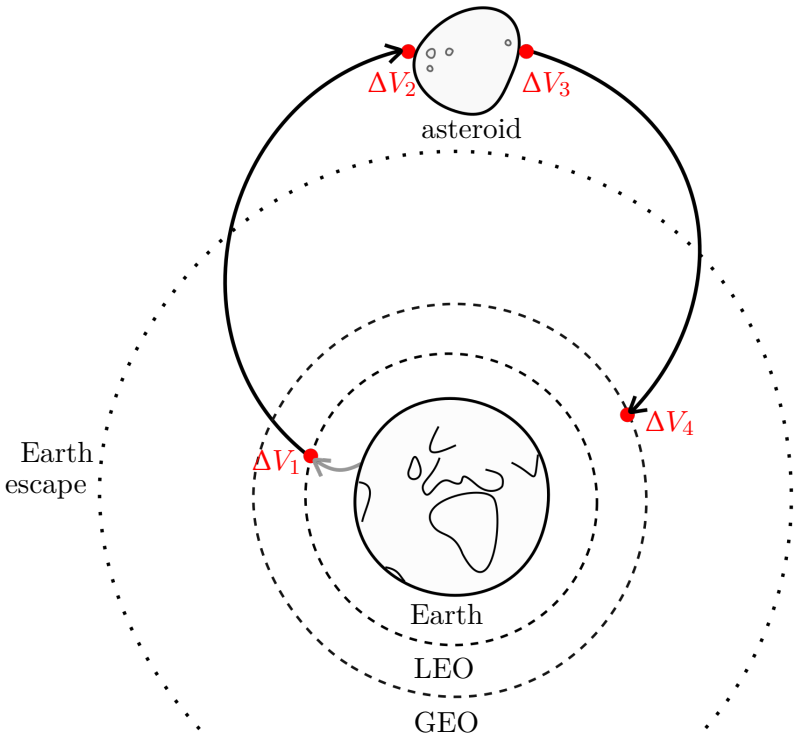

Figure 4.5: Schematic for example trajectory for a mission to an asteroid, with customers at GEO. Red dots showing where the impulsive ΔVs are applied.

The second example is for the scenario where resources are mined on the Lunar surface and transported to the Mars Base Camp, which is in an elliptical Martian orbit with a period of one Martian day (1 sol) and periapsis at 400 km [230]. Figure 4.6 illustrates where the separate impulsive ΔVs are applied. This example utilises all four methods to determine the total ΔV:

- Outbound, ΔV^O
  - $\mathbf{\Delta V_1}$: A ΔV at periapsis of a Hohmann transfer orbit from a LEO parking orbit to Lunar capture;
  - $\mathbf{\Delta V_2}$: A ΔV at periapsis of a hyperbolic trajectory to LLO (100 km), with v_∞ equal to the ΔV at apoapsis of the Hohmann transfer orbit from the LEO parking orbit to Lunar capture;
  - $\mathbf{\Delta V_3}$: Given ΔV for powered descent from LLO to Lunar surface, from Table 4.8.
- Inbound, ΔV^I
  - $\mathbf{\Delta V_4}$: Given ΔV for powered ascent to LLO (100 km);
  - $\mathbf{\Delta V_5}$: A ΔV at periapsis of a hyperbolic trajectory from LLO to Lunar escape, with $v_\infty = v_\text{p} - v_{Moon}$, in which v_{Moon} is the circular velocity of the Moon around the Earth and v_p is the velocity at periapsis of a hyperbola from Lunar escape to Earth escape with $v_\infty = \Delta V_{\text{start}}$ of an Earth-Mars Lambert arc;
  - $\mathbf{\Delta V_6}$: A ΔV at periapsis of a hyperbola from Mars capture to Mars Base Camp with $v_\infty = \Delta V_{\text{end}}$ of the Earth-Mars Lambert arc.

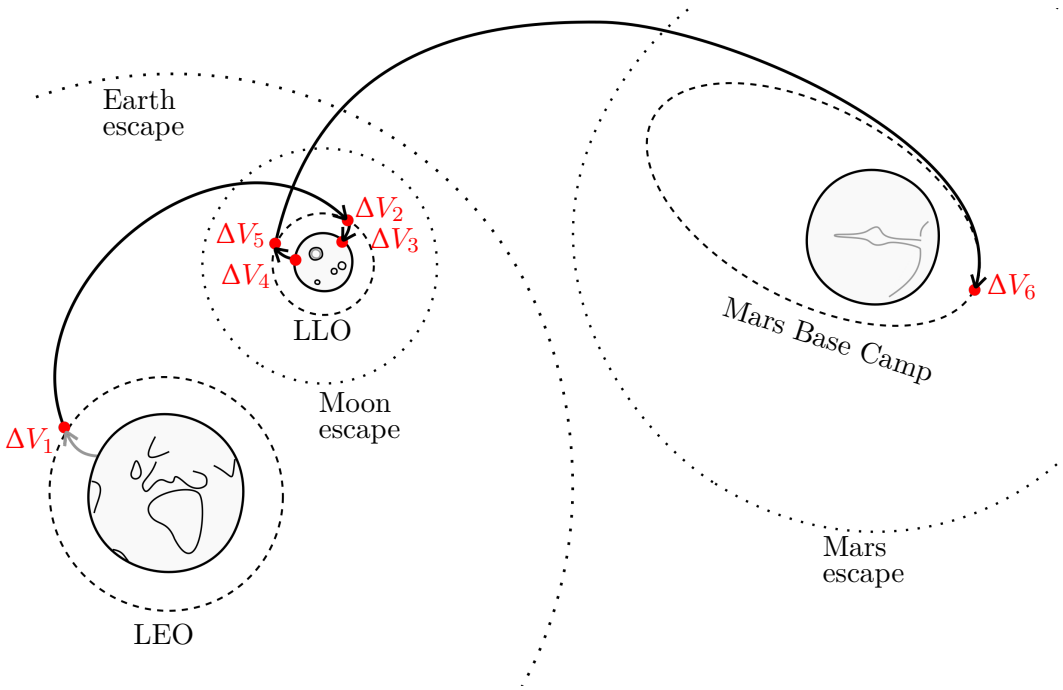

Figure 4.6: Schematic for example trajectory for a mission to the Lunar Surface, with customers at the Mars Base Camp. Red dots showing where the impulsive ΔVs are applied.

In combination with the other information given this Chapter, all variables are available to compute the mass budget, economic model and chosen figure of merit. The transfers described in this Section then have to be optimised for the figure of merit, which will be explained in the next Section.

4.5 TRAJECTORY OPTIMISATION

There are a number of parameters that have to be optimised for each scenario, in order to find the optimal figure of merit, such as the highest NPV or the lowest specific cost.

A genetic algorithm is employed to find a global optimum without the need for an initial guess [39, 192, 193]. The built-in genetic algorithm in MATLAB® is used,[6] using default parameter settings, except for the initial population, which is uniformly randomly spread throughout the whole domain instead of biased towards the lower and upper boundaries, and the constraint tolerance (10^{-6} instead of 10^{-3}). Default parameters used are uniform crossover with a crossover fraction of 0.8, 5% elitist selection, stochastic universal sampling, Gaussian mutation on a population of 200 candidate solutions. Due to the inclusion of non-linear constraints, an augmented Lagrangian genetic algorithm is used by default.

For the baseline chemical mission, as described in detail in this Chapter, the general decision vector for the genetic algorithm is as follows:

$$\mathbf{X} = \begin{bmatrix} \Delta t^O & \Delta t_{\text{stay}} & \Delta t^I & t^O_{\text{dep}} & \lambda_{\text{mpe}} \end{bmatrix} \tag{4.27}$$

in which Δt^O is the transfer time for the outbound Lambert arc, Δt_{stay} the stay time at the asteroid, Δt^I the transfer time for the inbound Lambert arc, t^O_{dep} the departure date for the outbound transfer and λ_{mpe} the mass fraction to divide the spacecraft's dry mass into m_{mpe} and m_{cargo}. Note that rather

[6] `https://uk.mathworks.com/help/gads/ga.html`, accessed on September 11th, 2022.

than absolute dates and times, a combination of one absolute date and three relative durations are used, to aid convergence of the genetic algorithm and remove the need for linear constraints to ensure that the dates are chronological. With these parameters, the entire mission is defined: the timing of the transfers (as dictated by the first four parameters in Eq. (4.27)) defines the transfers, resulting in ΔV^O and ΔV^I, which in combination with the last parameter of Eq. (4.27) fully defines the mass budget for a given target. This mass budget can then be used to calculate the associated cost and figures of merit.

Depending on the scenario, certain decision variables may be superfluous, i.e.:

- Δt^O, Δt_{stay}, and λ_{mpe} are not needed for the scenarios including Earth as the source of material, since those scenarios do not include a mining phase.
- Δt^O and/or Δt^I are not needed for the transfers covered by Hohmann manoeuvres, only for those that include Lambert arcs.
- If all transfers are covered by Hohmann transfers, t^O_{dep} is not necessary either.

Bounds are enforced on the decision variables in Eq. (4.27):

- 30 days $< \Delta t^O <$ 3 years
- 14 days $< \Delta t_{\text{stay}} <$ 3 years, to ensure that $t_{\text{mining}} > 0$, per Eq. (4.14)
- 30 days $< \Delta t^I <$ 3 years
- January 1$^{\text{st}}$, 2035 $< t^O_{\text{dep}} <$ December 31$^{\text{st}}$, 2060. Not only is this at the start of the time-frame when asteroid mining is likely considered feasible (following Section 2.3.3), a time-span of 25 years covers a multitude of synodic periods for most asteroids. Allowing a longer time-span is not necessary and in most cases would slow the optimisation down unnecessarily. Asteroids with a semi-major axis 0.025 AU from Earth have synodic periods of approximately 25 years, any semi-major axis smaller or larger has much shorter synodic periods, e.g. only three years for an asteroid with a semi-major axis of 1.3 AU.
- $0 < \lambda_{\text{mpe}} < 1$

These bounds are wide enough to accommodate all scenarios up to and including the main asteroid belt, thereby eliminating the need for individual fine-tuning of the genetic algorithm for each scenario. The genetic algorithm is initialised by 25 different seeds to increase the chances of finding the global optimum. It should be noted that most seeds result in very similar results, thus showing that the solutions are reliable.

The problem is also subject to a number of non-linear constraints. Non-linear constraints are included to enforce the minimum structural coefficient (ϵ_{min}) during all phases of the mission and that there is at least enough propellant to get to the destination. In case of an atmospheric entry, a mass penalty is applied to the structural mass through an additional structural coefficient, $\Delta\epsilon_{\text{entry}}$ to be applied in the non-linear constraints. Reference [231] states that the structural coefficient for SpaceX's Starship and the Deutsches Zentrum für Luft- und Raumfahrt SpaceLiner 7, both designed to be capable of multiple atmospheric entries, are 9.9% and 15.6%, respectively. The higher estimate for the structural coefficient of the SpaceLiner is linked to the intentionally robust design philosophy

of the concept [231]. Therefore, it is assumed that an additional $\Delta\epsilon_{\text{entry}} = 0.05$ is reasonable on top of $\epsilon_{\text{min}} = 0.1$ already in place. For each transfer, it is checked whether the following holds:

$$\frac{m_{\text{s/c,dry}}}{m_{\text{s/c,wet}}} \geq \epsilon \tag{4.28}$$

where $\epsilon = \epsilon_{min}$ or $\epsilon = \epsilon_{min} + \Delta\epsilon_{\text{entry}}$, depending on whether (re)-entry is part of the scenario.

4.6 SUMMARY OF CHAPTER

This concludes the baseline mission, which includes a baseline mission architecture that can be adjusted based on the desired mining location and customer location, directions for the calculation of any required ΔV, mass budget and accompanying cost. Costs are estimated for launch, development, manufacturing, maintenance, operations and propellant. After choosing the mining and customer location, only five parameters have to be optimised to fully define the mission, including the mass budget and associated costs and revenue. These five parameters determine the timing of the transfer and how much MPE is launched to the mining location.

This approach will be used in the subsequent Chapters to investigate a range of missions and the effect of some decisions and assumptions made in this Chapter.

Chapter 5

COMPARING PROPULSION METHODS FOR RESOURCE TRANSPORT

This Chapter explores the trade-off between solar sail and chemical propulsion by investigating the region of Keplerian orbital elements for which a single asteroid mining mission to GEO could return a profit. This is achieved by calculating the maximum possible NPV for each mission, both for the chemical baseline mission as described in Chapter 4 and for an alternative mission scenario utilising a low-thrust solar sail. GEO has been identified as a market for propellant for in-orbit servicing, e.g. refuelling of GEO satellites for life extension, collecting and removing space debris, removing non-operational GEO satellites, inclination lowering or orbital node rotation [232].

Issues associated with the cost and duration of mining are not considered yet, as the aim of this Chapter is to investigate the relative merits of chemical and solar-sail propulsion for resource transportation, trading off the benefits of solar sailing in reducing propellant mass with the impact on economics due to longer trip times.

Rather than investigating the current family of over 20,000 discovered NEAs, nearly 20,000 discovered MCAs and nearly 1 million discovered MBAs,[1] a more limited number of fictitious asteroids are investigated. This will indicate suitable regions of the parameter space for real target asteroids. The fictitious asteroids are distributed on a grid in the parameter space. To limit the dimensionality of the grid, only semi-major axis (a), eccentricity (e) and inclination (i) are considered as parameters, leaving the remaining Keplerian orbital elements free in the optimisation. The optimisation as described in Chapter 4 will therefore also have to include the argument of periapsis (ω), right ascension of the ascending node (Ω) and initial mean anomaly (M_0). This results in the maximum NPV possible for each given combination of semi-major axis, eccentricity and inclination.

The work is this Chapter is based on the work published in Ref. [36], but due to progressive insights, certain aspects of this work have evolved since that publication. Notable changes with respect to Ref. [36] are the removal of a kickstage to escape, a change in the calculation of the resource price p, and an investigation into the container mass during transportation with the solar sails. The effect of removing the kickstage from the mission is investigated, with results given for both scenarios including and excluding the kickstage.

[1] `https://ssd.jpl.nasa.gov/tools/sbdb_query.html`, accessed on August 20$^{\text{th}}$, 2020.

5.1 METHODOLOGY

The methodology for this Chapter is split into multiple parts, depending on the usage of the propulsion (chemical or solar sail) and kickstage (included or excluded). For a more fair comparison, the methodology is designed to be as similar as possible. However, the different nature of the propulsion methods means that some elements will inevitably differ. An overview of the separate scenarios is given in Table 5.1, details are presented in the next Sections.

Table 5.1: Overview of methodology for comparison. − and + refer to a removal from and addition to the baseline mission, respectively.

	Chemical propulsion	**Solar sail**
No kickstage	Baseline mission – mining phase – intrinsic value of resources	Baseline mission – mining phase – intrinsic value of resources + spiral to escape + solar-sail two-body model
Kickstage	Baseline mission – mining phase – intrinsic value of resources + kickstage to escape	Baseline mission – mining phase – intrinsic value of resources + kickstage to escape + solar-sail two-body model

For each of the scenarios in Table 5.1, the mining phase has been removed, as well as the intrinsic cost of the delivered resources when purchased from terrestrial sources, p'. Note that this last change is minor, as $p' = 0.95$ \$/kg in the baseline mission. However, it means that rather than LOX/LH_2, H_2O can be transported, which has less demands on the resource container, which is necessary for the sail, as will be shown in Sections 5.1.3 and 5.3.2. For the sake of comparison, the same resources will be delivered using the chemical propulsion scenarios. However, note that chemical propulsion will still require a portion of the mined resources to be LOX/LH_2, used for the inbound transfer. For all scenarios discussed here, Eq. (3.12) is therefore altered to:

$$p = c_{\mathrm{l,orbit}} \tag{5.1}$$

which implies that the price charged to the customer is based solely on the launch costs to the customer location, which is the price that has to be competed with.

Note that the calculation of $c_{\mathrm{l,orbit}}$ differs slightly from the method in Ref. [36], where the dry mass for the kickstage is erroneously based on Eq. (4.24) instead of Eq. (4.23), meaning that the dry mass was too low. Using Eq. (4.23) means that the dry mass needed to transport the Earth-launched resources to orbit increases, thereby both increasing the cost for this mission and decreasing the transported resource mass, both of which increase the price of these Earth-launched resources. This means that the resource price that has to be competed with was overly conservative in Ref. [36].

For each of these different mission scenarios, MATLAB®'s built-in genetic algorithm is used for the optimisation, with the following objective:

$$J = -NPV \tag{5.2}$$

The genetic algorithm will optimise, in addition to the timing of the interplanetary transfers, the

three free Keplerian orbital elements (ω, Ω, and M_0) and the resource mass to be transported. M_0 is the mean anomaly of the target asteroid at t_0 (January 1$^{\text{st}}$, 2000, 11:58:55.816, consistent with the JPL Horizons database). Note that in the baseline optimisation problem, the launch date (t^O_{dep}) is used to provide a reference epoch for the transfer, which in combination with the transfer and stay times defines the timing of all transfers. While optimising the timing of the transfers, the free orbital elements of the target asteroid and t^O_{dep} can accomplish the same effect and therefore using both can negatively impact the computational time. The free orbital elements can be chosen to eliminate the effect of a fixed t^O_{dep}, thereby negating the need to include the departure date in the decision vector. The departure date is (arbitrarily) set to January 1$^{\text{st}}$, 2035, at the start of the allowed departure window in Chapter 4.

This means that the decision vector is as follows:

$$\mathbf{X} = \begin{bmatrix} \Delta t^O & \Delta t_{\text{stay}} & \Delta t^I & \lambda_{\text{r}} & \omega & \Omega & M_0 \end{bmatrix} \tag{5.3}$$

where λ_{r} is defined as the ratio of the resource mass and the dry mass of the spacecraft:

$$\lambda_{\text{r}} := \frac{m_{\text{r}}}{m_{\text{s/c,dry}}} \tag{5.4}$$

The boundaries for the transfer and stay time variables are as given in Section 4.5. For the remaining variables, the boundaries are as follows:

- $0 \leq \lambda_{\text{r}} \leq 9$, to comply with the requirement for the minimum structural mass ($\epsilon_{\text{min}} = 0.1$)
- $0 \leq \omega \leq 2\pi$
- $0 \leq \Omega \leq 2\pi$
- $0 \leq M_0 \leq 2\pi$

To find the hyperspace of orbital elements where the NPV can be positive, the total hyperspace of these orbital elements has to be pruned. Based on the results in Ref. [36], the paper on which this Chapter is based, the search space could be sampled to find the approximate edges where the NPV changes from negative to positive. A grid for the fictitious asteroids is then created based on these edges.

5.1.1 Chemical Propulsion, No Kickstage

Out of the four scenarios investigated, this scenario is closest to the baseline mission as discussed in Chapter 4. Changes are limited to the elimination of the mining phase and p'. This means that no equipment has to be delivered to the asteroid and the stay time at the asteroid is unrelated to the mass that can be delivered. The elimination of the mining phase means a change to the equations in the mass budget described in Section 4.3 by Eqs. (4.10) through (4.21).

Equations (4.12a)–(4.12c) are replaced by:

$$m_{\text{cargo}} = m_{\text{s/c,dry}} \tag{5.5}$$

and Eqs. (4.13) through (4.19) are irrelevant. The resource mass to be collected from the asteroid, m_{r}, is determined during the optimisation process using λ_{r}. Since no existing asteroid is used in

the mission, this resource mass is only limited by what the spacecraft can transport, not by what is available on the asteroid.

A graphic depicting this mission scenario is presented in Fig. 5.1a.

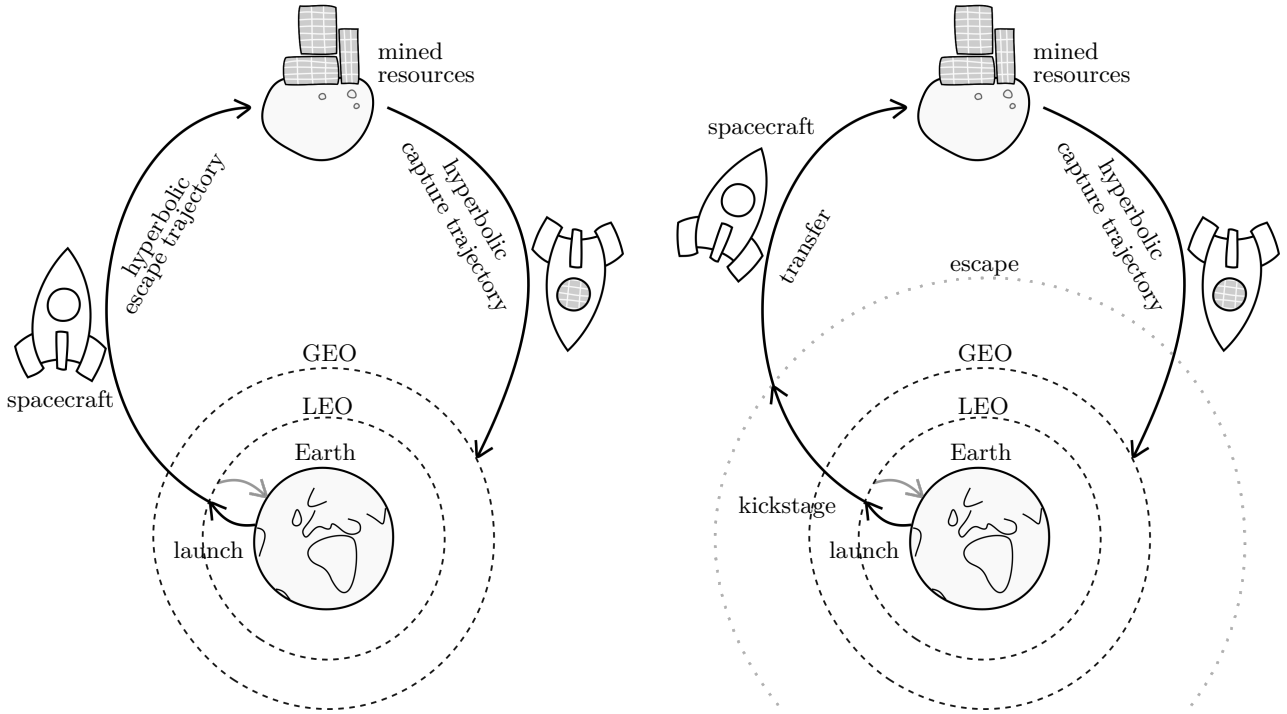

(a) Excluding the kickstage. (b) Including the kickstage.

Figure 5.1: Mission architecture for the missions based on chemical propulsion.

5.1.2 Chemical Propulsion, Kickstage

When a kickstage to escape is included in the mission, Eqs. (4.22), (4.24) and (4.25) are used to size this, repeated here for the sake of completeness:

$$\begin{aligned} m_{\text{ks,prop}} &= m_{\text{l}} \left(1 - e^{-\frac{\Delta V_{\text{ks}}}{I_{\text{sp}} g_0}}\right) \\ m_{\text{ks,dry}} &= \frac{\epsilon_{\text{min}}}{1 - \epsilon_{\text{min}}} m_{\text{ks,prop}} \\ m_{\text{ks,transport}} &= m_{\text{l}} - m_{\text{ks,dry}} - m_{\text{ks,prop}} \end{aligned}$$

after which the remainder of the payload capacity of the launch vehicle ($m_{\text{ks,transport}}$) replaces m_{l} in the scenario without the kickstage, as described in Section 5.1.1. The ΔV requirement for the remainder of the outbound transfer is then based on a transfer from Earth escape, rather than from LEO. The remainder of the mass budget is the same as for the scenario without the kickstage described above.

A graphic depicting this mission scenario is presented in Fig. 5.1b.

5.1.3 Solar Sail, No Kickstage

For this scenario more amendments to the baseline mission are necessary, due to the nature of solar-sail propulsion. First and foremost, the cargo spacecraft is replaced by a fleet of solar sails:

$$m_{\text{sc,dry}} = m_{\text{sails}} \tag{5.6}$$

in which m_{sails} is the total mass of the sails. The performance of each sail is expressed through the lightness number β: the non-dimensional ratio of the solar sail's maximum acceleration with respect to the solar gravity. A lightness number of $\beta_0 = 0.1$ is used for the solar-sail assembly without payload, representative of mid-term solar sails [233]. Since the lightness number is non-dimensional, solar sails can be scaled, allowing for a fleet of solar sails of reasonable size rather than one very large sail with a mass of m_{sails}, without affecting the analysis in any way. It is therefore not necessary to specify the number of sails. It is assumed that the mass of the sail includes the mass for the container for the resources, which can be as little as a properly-sealed bag or bladder [126]. Reference [126] estimates that a materials storage bag for 4,000 tonnes of resource mass will weigh 1.6 tonnes, only 0.04% of the resource mass. This fraction will increase as the resource mass decreases, due to the surface and volume of the storage bag scaling differently, but the mass fraction will remain small for the resource masses considered in this scenario, and can therefore be absorbed in the mass of the solar-sail assembly.

The mass of the material storage bag can be calculated using m_{sails}, λ_{r} and the resource mass and storage bag mass from Ref. [126]. First, the resource mass can be calculated as:

$$m_{\text{r}} = m_{\text{sails}} \lambda_{\text{r}} \tag{5.7}$$

and subsequently the storage bag mass in kg, scaling the storage bag mass from Ref. [126] and noting the scaling of surface area to volume (all masses m in kg):

$$m_{\text{bag}} = 1,600 \text{ kg} \left(\frac{m_{\text{r}}}{4,000,000 \text{ kg}} \right)^{(2/3)} \tag{5.8}$$

Dividing by the sail mass m_{sail}, this results in a fraction of the dry mass dedicated to the storage bag, as shown in Fig. 5.2. Figure 5.2 shows that even when transporting the maximum resource mass (for $\lambda_{\text{r}} = 9$, following the imposed $\epsilon_{\text{min}} = 0.1$), the storage bag is still only a very small fraction of the dry mass of the sail: 0.53%. Because of this, the assumption that the storage bag mass can be included with the dry mass of the sail is valid, and no additional dry mass has to be included in the calculations.

The interplanetary trajectories are governed by the solar-sail augmented two-body problem as defined in Eqs. (3.15) through (3.17). The planet-centric segment of the transfers are modelled using a spiral to or from escape. An analytical approximation is used to determine the time in days required for the spiral from LEO to Earth escape and from Earth capture to GEO [139]:

$$t_{\text{spiral}}(\beta, r) = \frac{2805 \text{ days}}{\beta \sqrt{r}} \tag{5.9}$$

where r is the radius of the Earth-centric orbit, e.g. LEO or GEO. During the outbound transfer, the lightness number is $\beta^O = \beta_0$. Upon collecting the mined resources at the asteroid, the lightness

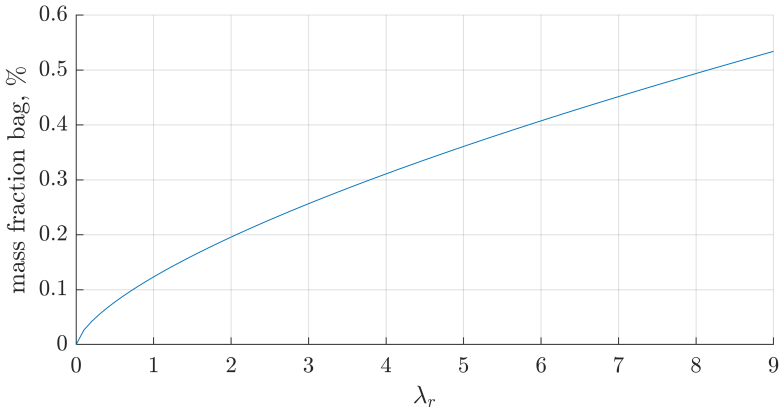

Figure 5.2: Mass fraction of sail dry mass dedicated to the materials storage bag.

number of the sails for the inbound transfer decreases accordingly:

$$\beta^I = \beta_0 \frac{1}{1+\lambda_\mathrm{r}} \tag{5.10}$$

The total mission duration is then calculated using:

$$t_\mathrm{mis} = t_\mathrm{spiral}(\beta^O, r_\mathrm{LEO}) + \Delta t^O + \Delta t_\mathrm{stay} + \Delta t^I + t_\mathrm{spiral}(\beta^I, r_\mathrm{GEO}) \tag{5.11}$$

Due to the foreseen long durations of solar-sail missions, especially for the inbound transfer when the sail is loaded with asteroid resources, the boundaries for Δt^I are changed to 120 days $< \Delta t^I <$ 5 years. However, a maximum mission duration of 10 years is enforced, to ensure that the mission duration does not become excessive, as very long missions are undesirable for investors, as explained in Section 2.3.3. Note that for missions with such long durations, high revenues are needed for the NPV to be positive, because after 10 years with a yearly discount rate I of 10%, revenues are discounted by 159% ($(1+I)^{10} = 1.1^{10} = 2.59$), compared with only 33% for a three-year mission.

The mission architecture is shown in Fig. 5.3a, note the spiral from LEO to escape and the spiral from capture to GEO.

For the missions utilising chemical propulsion, the interplanetary transfers are calculated using Lambert arcs. For the solar-sail missions, a different technique has to be used. Traditionally, optimising solar-sail transfers is done through seeking the solution to an optimal control problem, resulting in a continuous time history for the controls. As discussed in Section 3.2.4, this can be a complex and time-consuming process, starting with an initial guess and then local optimisation of this initial guess. However, considering the high computational effort of finding a suitable initial guess, solving an optimal control problem, and the fine-tuning of the solver that might be necessary for each target asteroid, this is infeasible for the scale of the problem at hand. Therefore, an alternative method is adopted, which has been chosen such that it strikes a balance between accuracy, computational effort and ease of implementation. The optimal time history for the controls is not necessarily required, as the only outcome that needs to be determined is: "can the solar sail transfer from the departure state to the arrival state in the allotted time?"

The method to determine whether a transfer is feasible, is based on the technique used in Ref. [234]. Using this method, an initial state is propagated forwards, and a final state is propagated backwards. Piecewise-constant controls are then optimised to minimise the discontinuity at the junction of the

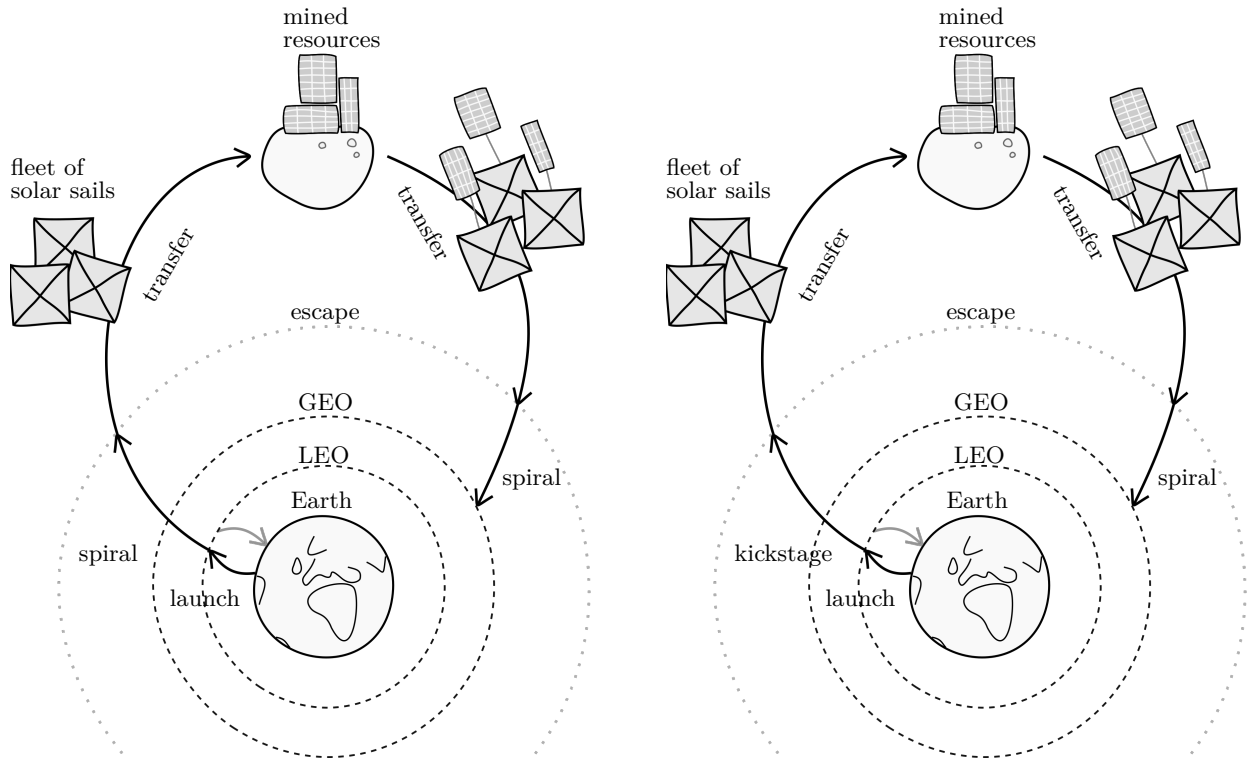

(a) Excluding the kickstage. (b) Including the kickstage.

Figure 5.3: Mission architecture for the missions based on solar sails.

forward and backward phase. The `fmincon` function from MATLAB® is used to determine four sets of constant controls (two to propagate forwards and two to propagate backwards). To increase the probability of `fmincon` converging to a solution, up to four different initial guesses can be used to initialise the optimisation. For all four sets ($i = 1, 2, 3, 4$), these initial guesses are defined as follows:

$$\left[\alpha_i, \delta_i\right] = \left\{ \left[\alpha^*, 0\right], \left[\alpha^*, \tfrac{\pi}{2}\right], \left[\alpha^*, \pi\right], \left[\alpha^*, 3\tfrac{\pi}{2}\right] \right\} \tag{5.12}$$

i.e., for the first initial guess, all four sets of controls are $\left[\alpha^*, 0\right]$, for the second initial guess $\left[\alpha^*, \frac{\pi}{2}\right]$, etc. Furthermore, α^* is the cone angle which maximises the force in the transverse direction of the sail [139]:

$$\tan \alpha^* = \frac{1}{\sqrt{2}} \tag{5.13}$$

The discontinuity in Cartesian coordinates (including both the position and velocity) at the junction of the forward- and backward-phase is calculated in non-dimensional units, where the unit of length is 1 AU, and the unit of time is 1 year. Using these non-dimensional units, a transfer is considered feasible if the norm of the discontinuity is less than 0.025. An optimal control solver is likely to be able to overcome a discontinuity of this magnitude [175, 234, 235]. Also, note that this Chapter provides only an initial investigation into the targets that are potentially profitable. Once a target has been determined, a more high-fidelity approach could be used to optimise trajectories and obtain optimal control histories. Figure 5.4 shows an example of the iterations of `fmincon` to achieve a feasible solution. Figure 5.5 shows the evolution of the discontinuity over the number of iterations, showing that the solver quickly converges to a small discontinuity for the transfer shown in Fig. 5.4.

While this technique does not guarantee that optimal minimum-time transfers are found, the

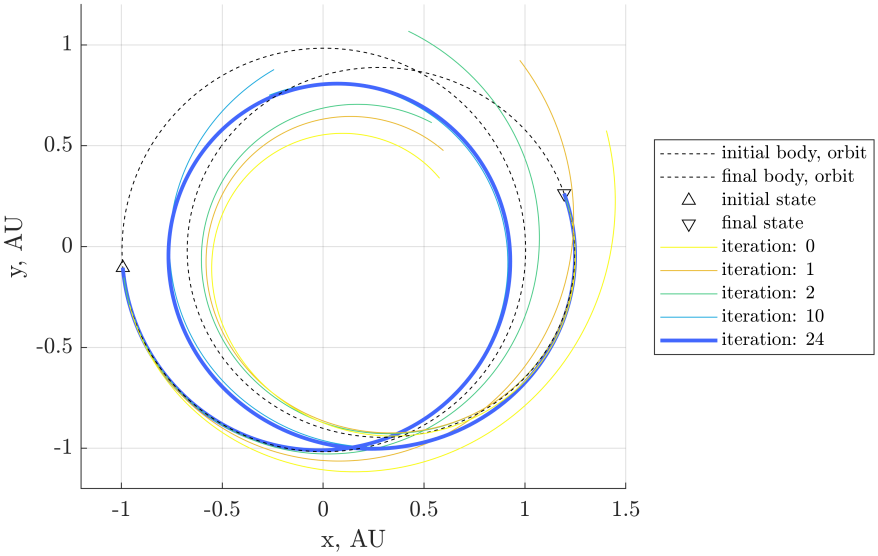

Figure 5.4: Example of the convergence of `fmincon` to a feasible transfer with a non-dimensional discontinuity of 0.020.

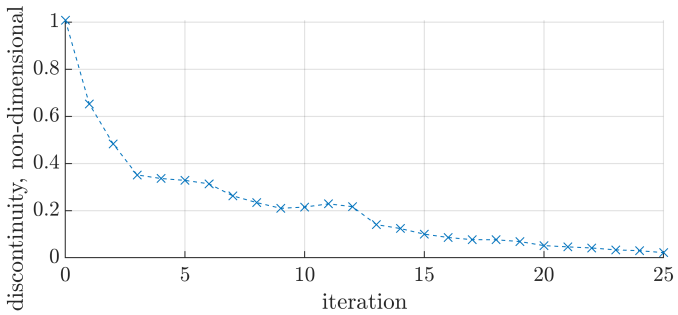

Figure 5.5: Evolution of the discontinuity at the matching time of the forward- and backward phase, for transfer shown in Fig. 5.4.

genetic algorithm, with the decision vector as Eq. (5.3), is used to optimise the timing of the transfers for maximum NPV. Using a piecewise-constant control laws is shown to only cause a minor penalty on the transfer time, up to ∼4% [204]

5.1.4 Solar Sail, Kickstage

This mission scenario which includes a solar sail and a kickstage draws upon the methodologies set out in Sections 5.1.2 and 5.1.3. The mass and payload capacity of the kickstage for this mission is calculated in the same manner as for the chemical mission and replaces the spiral to Earth escape for the solar-sail mission without a kickstage. All other calculations follow those described for the solar-sail mission described above.

The mission architecture is shown in Fig. 5.3b.

5.2 RESULTS

Using the methodology described in Section 5.1, suitable regions of the parameter hyperspace have been determined for the different mission architectures. The results for the chemical propulsion scenarios are given in Section 5.2.1 and the results for the solar-sail scenarios in Section 5.2.2.

Nodes on the grid for semi-major axis, eccentricity and inclination are placed at:

- a: 0.70, 0.85, 1.00, 1.15, 1.30, 1.45 AU
- e: 0.0, 0.1, 0.2, 0.3, 0.4
- i: 0, 2, 4, 6, 8, 10 deg

Additional scenario-specific grid points are added for the separate scenarios to further narrow down the region of orbital elements for potentially profitable target asteroids.

5.2.1 Chemical Propulsion Scenarios

Figure 5.6 shows the maximum NPV for each node on the grid over semi-major axis, eccentricity and inclination, for both the scenario including and excluding the kickstage. The grid nodes which generated a positive NPV are shown as filled green circles, and those resulting in a negative NPV are open orange circles, all with an accompanying label with the realisable NPV. Note that any node labelled with a negative NPV is still accessible, but will not result in the venture making a profit.

As Fig. 5.6 only shows the resulting NPV, an asteroid from the Horizons system has been selected based on the region of potentially profitable targets. The same analysis is performed to show additional insight into a possible mission to NEA 2006 QQ56. Note that in this case the remaining orbital elements are fixed and given by the JPL SBDB and will therefore not be optimised. Instead, the departure date for the outbound transfer is added back in to the optimisation, to conform to the methodology in Chapter 4 and to allow for selecting an optimal timing of the transfers. The parameters resulting from the optimisation for maximum NPV are given in Table 5.2 for both the scenario with and without the kickstage. The results in Table 5.2 are merely given as an illustration of the data for a possible mission with a positive NPV, not to give the maximum NPV possible for all real target NEAs. The actual available volatile mass on the asteroid is taken into account in the analysis using Eqs. (2.1) and (4.15).

For the missions presented in Table 5.2, the IRR and ROI can be calculated according to Eqs. (3.8b) and (3.10), respectively. For the mission including the kickstage, an IRR of 57.1% can be achieved, compared with 85.3% for the mission without the kickstage. To calculate the ROI, the total cost (C_0) is used as the initial value of the investment and the revenue (R_{mis}) as the final value of the investment, thereby neglecting that the spacecraft itself still has a value after delivery. Determining this value is outside the scope of this thesis. For the mission including the kickstage, an ROI of 90.1% can be achieved, compared with 157.9% for the mission without the kickstage, but considering that the spacecraft itself also has a final value, the actual ROI would be higher for both. These ROI and IRR values can be compared against those for the other scenarios in Section 5.2.3.

5.2.2 Solar Sail Scenarios

Similar to the chemical propulsion case, Fig. 5.7 shows the maximum NPV for each node on the grid over semi-major axis, eccentricity and inclination for the solar-sail mission scenarios. In addition, the details of an example mission to NEA 2006 QQ56 are shown in Table 5.3 to gain insight into the relative cost of the different elements of the missions, both with and without the kickstage. Again, the results in Table 5.3 are given as an illustration of the data for a possible mission with a positive NPV, again not to give the maximum NPV possible for all real target asteroids. The actual available resource mass on the asteroid is also taken into account.

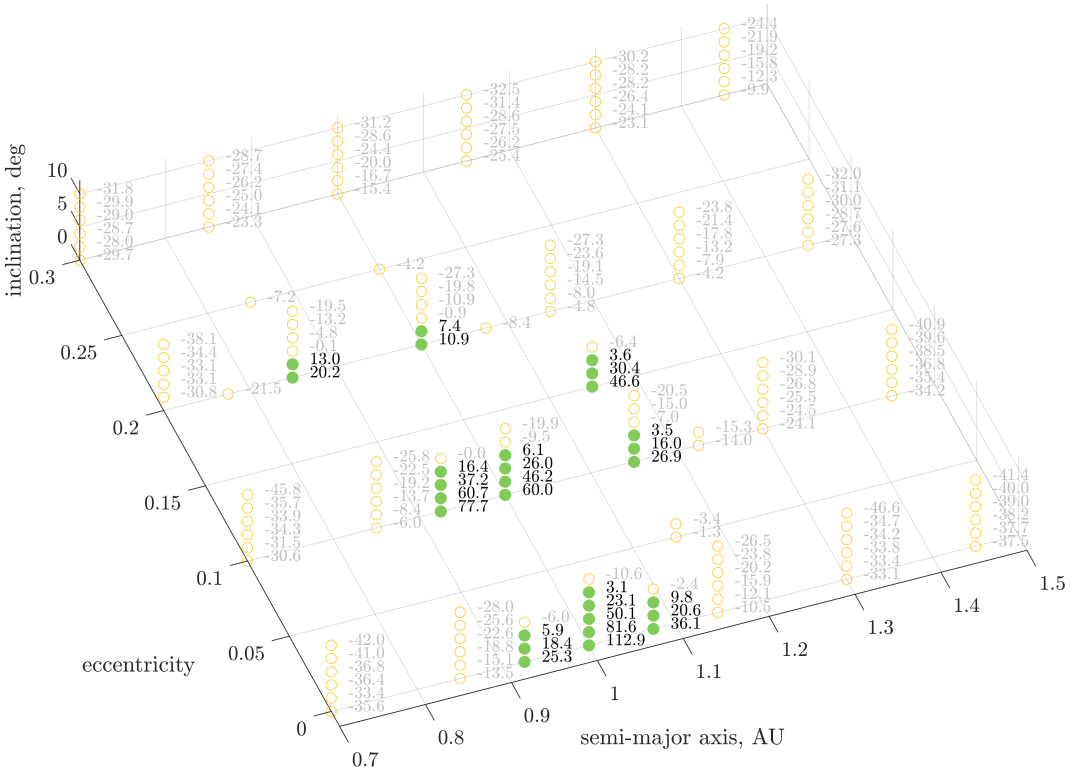

(A) With kickstage.

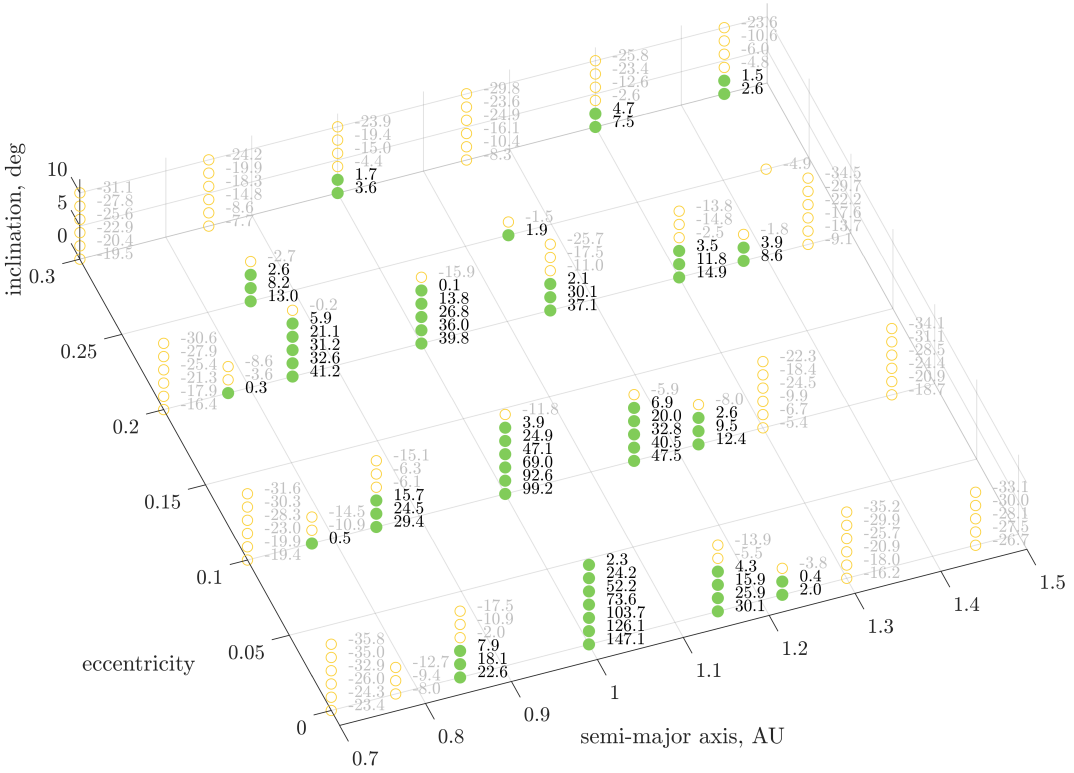

(B) Without kickstage.

Figure 5.6: Maximum possible NPV (FY2020 M$) for each node on the grid for the chemical mission scenarios.

Table 5.2: Example missions to NEA 2006 QQ56 using chemical propulsion.

Parameter	**Unit**	**Kickstage**	**No kickstage**
Semi-major axis	AU	0.9850	0.9850
Eccentricity		0.0456	0.0456
Inclination	deg	2.7981	2.7981
Launch date		15-10-2048	07-03-2047
Duration outbound transfer	days	302	268
Stay time at asteroid	days	14	41
Duration inbound transfer	days	204	251
ΔV^O	km/s	1.9574	3.8954*
ΔV^I	km/s	1.8804	1.7019
m_{l}	tonnes	136.1	136.1
$m_{\mathrm{ks,prop}}$	tonnes	71.0	N/A
$m_{\mathrm{ks,dry}}$	tonnes	8.0	N/A
m^O_{prop}	tonnes	20.6	80.2
$m_{\mathrm{s/c,dry}}$	tonnes	36.5	55.8
m_{r}	tonnes	328.7	502.6
m^I_{prop}	tonnes	127.6	180.0
$m_{\mathrm{r,sold}}$	tonnes	201.1	322.6
Launch cost	$	13,095,922	13,095,922
Development cost kick stage	$	293,553	N/A
Manufacturing cost kick stage	$	7,954,986	N/A
Propellant cost kick stage	$	67,380	N/A
Development cost spacecraft	$	1,358,136	2,076,740
Manufacturing cost spacecraft	$	36,804,091	56,277,485
Propellant cost spacecraft	$	19,551	76,091
Operations cost	$	9,920,025	10,714,714
Total cost	$	69,513,647	82,240,953
Revenue	$	132,178,985	212,063,930
Total mission duration	years	1.422	1.536
NPV	$	45,910,971	100,942,935

* Note that this includes the ΔV to escape.

The available resource mass on the asteroids can be an issue for the solar-sail missions, as these missions are often required to transport more resources than the chemical missions to turn a profit, which might not always be available on the target asteroids. Because no launch vehicle payload capacity has to be used for propellant for the outbound journey, the dry mass of the fleet of solar sails is higher than the chemical mission, meaning that it has a greater payload capacity, which may need to be utilised completely in order to have a profitable mission.

The IRR and ROI for the solar-sail missions are calculated the same as for the chemical missions. The IRR is 18.4% and 21.3% for the scenario with and without the kickstage, respectively. The ROI is 175.0% and 293.1% for the scenario with and without the kickstage, respectively. These ROI and IRR values can be compared against those for the other scenarios in Section 5.2.3.

Table 5.3: Example missions to NEA 2006 QQ56 using solar-sail propulsion.

Parameter	**Unit**	**Kickstage**	**No kickstage**
Semi major axis	AU	0.9850	0.9850
Eccentricity		0.0456	0.0456
Inclination	deg	2.7981	2.7981
Launch date		02-08-2048	30-06-2046
Spiral time to escape	days	N/A	346
Duration outbound transfer	days	164	194
Stay time at asteroid	days	15	16
Duration inbound transfer	days	662	669
Spiral time to GEO	days	1366	1366
β^O		0.1	0.1
β^I		0.01	0.01
m_{l}	tonnes	136.1	136.1
$m_{\mathrm{ks,prop}}$	tonnes	71.0	N/A
$m_{\mathrm{ks,dry}}$	tonnes	8.0	N/A
m_{sails}	tonnes	57.1	136.1
m_{r}	tonnes	514.2	1,224.7
$m_{\mathrm{r,sold}}$	tonnes	514.2	1,224.7
Launch cost	$	13,095,922	13,095,922
Development cost kick stage	$	293,553	N/A
Manufacturing cost kick stage	$	7,954,986	N/A
Propellant cost kick stage	$	67,380	N/A
Development cost spacecraft	$	2,124,741	5,060,273
Manufacturing cost spacecraft	$	57,578,253	137,128,113
Operations cost	$	41,800,471	49,504,914
Total cost	$	122,915,306	204,789,223
Revenue	$	338,033,491	805,050,138
Total mission duration	years	5.992	7.097
NPV	$	68,035,684	204,535,603

5.2.3 Discussion

Suitable real target NEAs can be found in the regions resulting from Figs. 5.6 and 5.7, however, a positive NPV is not guaranteed: the combination of the remaining orbital elements is also important for the trajectory optimisation to real target asteroids. In addition, the cost and effort for mining

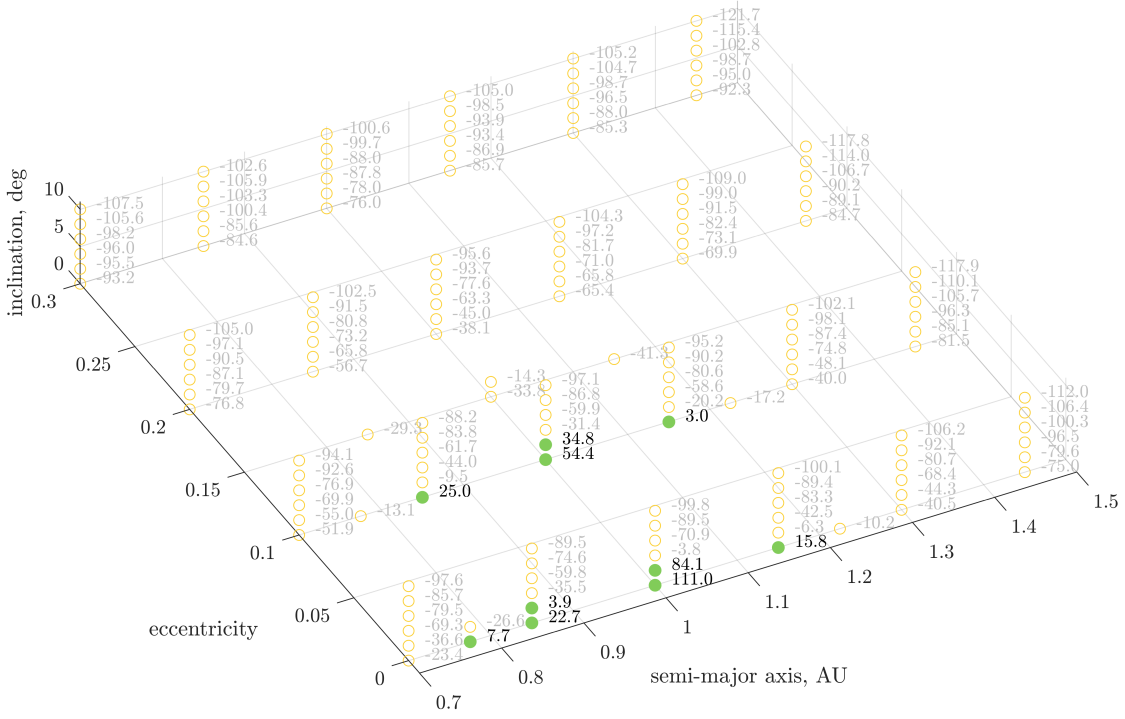

(a) With kickstage.

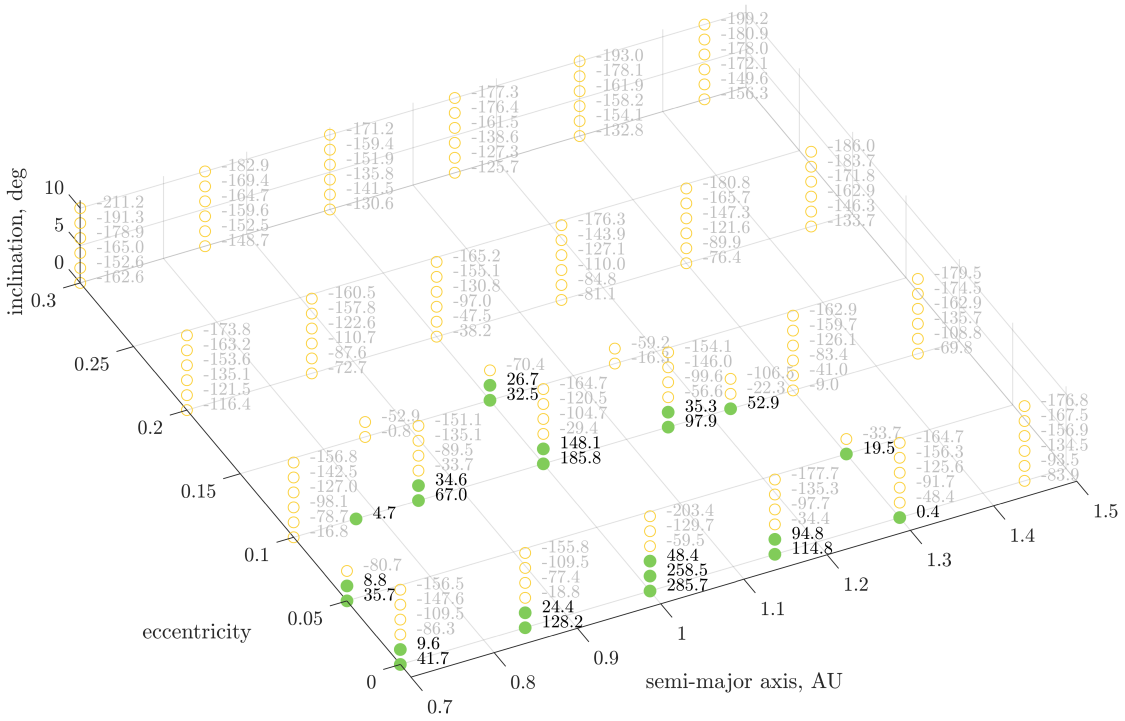

(b) Without kickstage.

Figure 5.7: Maximum possible NPV (FY2020 M$) for each node on the grid for the solar-sail mission scenarios.

the resources has to be taken into account. However, the methodology presented here can be used to prune the search space for future research.

From Fig. 5.6 it is evident that, using chemical propulsion, not only more targets can be profitable *without* a kickstage, but also that a higher NPV can be realised. Due to a larger cargo spacecraft launched to an asteroid, the costs of the mission increases, but this is offset by an increase in revenue due to the larger cargo spacecraft bringing more resources to the customer. For the chemical scenario including a kickstage, suitable targets can be found between: $0.85 \leq a \leq 1.15$ AU, $0 \leq e \leq 0.2$ and $0 \leq i \leq 8$ deg. For the chemical scenario without a kickstage, suitable targets can be found between: $0.775 \leq a \leq 1.45$ AU, $0 \leq e \leq 0.3$ and $0 \leq i \leq 12$ deg. Note that these values are approximate because the grid nodes are discrete and not continuous. As shown in Fig. 5.6, for combinations of a and e further from Earth's orbit, potentially profitable targets can have lower inclinations, as expected. For more elliptical target orbits, the range of semi-major axes is larger than for more circular orbits.

Similarly, Fig. 5.7 shows the region of potentially profitable targets for the solar-sail mission with the kickstage between: $0.775 \leq a \leq 1.15$ AU, $0 \leq e \leq 0.1$ and $0 \leq i \leq 2$ deg. For the solar-sail scenario without the kickstage, this region is between: $0.7 \leq a \leq 1.30$ AU, $0 \leq e \leq 0.15$ and $0 \leq i \leq 4$ deg. Similar to the chemical scenarios, higher inclinations can be reached for combinations of semi-major axis and eccentricity close to the Earth, and for more elliptical orbits, the range of semi-major axes is larger than for circular orbits. Figure 5.7 shows that again, the scenario without a kickstage outperforms the scenario with a kickstage, both in terms of how many asteroids can be reached and in terms of NPV for the same grid point.

Comparing Fig. 5.6 and Fig. 5.7 shows that the chemical scenarios outperform the solar-sail scenarios in most cases. A wider range of orbital elements gives a positive NPV, especially without the use of a kickstage. Target asteroids with orbits farther from Earth can be reached, to higher inclinations. While the results show that more asteroids can be profitable using chemical propulsion, higher profits can be generated for asteroids close to the Earth using the solar-sail no-kickstage scenario. Even though the costs of a solar-sail mission are higher due to the increase in $m_{\text{sc,dry}}$ and increased mission duration, far higher revenues can be generated for asteroids close to the Earth, causing an increase in profitability with respect to the chemical scenarios. Also, the solar-sail scenarios appears to perform better than the chemical scenarios for smaller semi-major axes, which can be explained by the fact that solar sails experience higher accelerations closer to the Sun. Unfortunately, not many asteroids exist in the region where the solar-sail scenarios outperform the chemical scenarios. This means that the chemical scenarios have a more useful region of suitable orbital elements.

The calculated IRR and ROI for the example missions show a difference between the chemical and solar-sail missions too. Because the scenarios without the kickstage can generate significantly more revenue for a more modest increase in total cost, both IRR and ROI is higher for these scenarios, as shown in Table 5.4. Only considering the ROI, the example missions have ROIs consistent with what would be required for very risky projects (following Table 3.1), projects in which the product is very novel and in a new area with a new customer. While the ROI for the solar-sail examples is significantly higher than for the chemical examples, this shows exactly where the ROI metric is lacking: the mission duration is not taken into account. The IRR for the solar-sail missions, which does take the mission duration into account, shows lower values than for the chemical mission, which means that they are less attractive for investors. While the missions have not been optimised specifically for the IRR, it is to be expected that the optimal IRR are close to those calculated in Sections 5.2.1 and 5.2.2, as an optimisation for the NPV also balances the revenue, cost and mission duration.

Table 5.4: IRR and ROI for missions.

	IRR, %	**ROI, %**
Chemical, no kickstage	85.3	157.9
Chemical, kickstage	57.1	90.1
Solar sail, no kickstage	21.3	293.1
Solar sail, kickstage	18.4	175.0

While the results presented here do not include the cost and effort for mining the resources, this can be included by bringing MPE along to the asteroid, following Chapter 4. Part of the launched mass will be dedicated to this equipment rather than the cargo spacecraft/sails, meaning a lower dry mass of the spacecraft itself which causes a decrease in payload capacity on the inbound transfer, causing a decrease in revenue for both the chemical and solar-sail mission. Also, the outbound transfer using the solar sail will take longer due to the increase in mass and corresponding decrease in lightness number. In addition, time has to be spent at the asteroid to mine and process the resources, which influences the total mission duration and therefore the calculation of the discount in the NPV. An equal increase in mission duration for the missions in Tables 5.2 and 5.3 would have a larger absolute effect on the solar-sail missions, because the absolute decrease in discounted revenue is greater, but in relative terms the effect is similar. In general, the NPV will decrease for both missions. Also, in the case of a separate mining mission before the transportation mission, the increase in cost would be equal for both the chemical and solar-sail mission, causing an equal absolute reduction in NPV.

A disadvantage of the chemical propulsion scenario is that it requires a portion of the resources to be LOX/LH_2, enough for m^I_{prop}. The remaining resources can be of any type: water, other volatiles, low-value or high-value metals or even regolith. A constraint for the resources that can be transported using the solar sail is that it can be contained in a simple container and not require special storage. For the chemical propulsion scenarios, it can mean that multiple types of MPE have to be used before the resources can be transported, which can complicate operations at the asteroid and come with increased cost. This can be a disadvantage of using chemical propulsion instead of solar sails.

A major disadvantage of using chemical propulsion is that due to ISRU, a large fraction of the mined volatiles are consumed. While this Chapter assumes an infinitely large quantity of resource material available at the asteroid and costs for mining and processing operations are not considered in the analysis, in reality this is not the case. MPE has to be placed on an asteroid of finite size, and if a large fraction (e.g., 50%) of the processed resources never reach a customer, the MPE has effectively only resulted in *half* the resources being delivered at the customer for the *full* cost. In contrast, solar sails do not consume propellant, and are able to deliver the full payload to the customer, thereby leaving the total "value" of the asteroid and the MPE intact.

Note that in this work it is assumed that all costs are incurred at the start of the mission, which in reality can be considered true for all costs except the operation costs. Costs incurred later would benefit from a higher discount, which is beneficial during the calculation of the NPV, especially for long duration missions, such as the solar-sail missions in Table 5.3.

5.3 SENSITIVITY ANALYSIS

This Section provides four types of sensitivity analyses based on the results obtained in Section 5.2. First, the changes in profitability of changing destinations from GEO to the Lunar Gateway are

investigated. Next, an investigation to include a container for LOX/LH_2 rather than H_2O for the solar-sail scenario. This is followed by an approximation for a multiple round-trip mission. Finally, a range of Monte Carlo simulations is presented to investigate the effect of uncertainties of a number of input values for the model.

5.3.1 Propellant Depot at Lunar Gateway

Another interesting location to sell volatiles is at or near the Lunar Gateway, where spacecraft can refuel before or after interplanetary transfers [5]. Changing the destination varies the propellant mass (m^I_{prop}) or spiral time for the inbound transfer, as well as the resource price (p) because of a change in $c_{\text{l,orbit}}$ in Eq. (5.1). The location of the Lunar Gateway, at a halo orbit in the Earth-Moon system, is approximated as a circular orbit at the Lunar distance from the Earth, r_{Moon}. This requires the following modifications:

- For the chemical scenarios, in Eq. (4.21), ΔV^I has to be calculated differently, following the methodology in Section 4.4, to a closed orbit around the Earth at a distance of r_{Moon}.
- For the solar-sail scenarios, in Eq. (5.11), r_{GEO} is replaced by r_{Moon}, affecting the mission duration.
- For all missions, the calculation of $c_{\text{l,orbit}}$ in Eq. (5.1), the ΔV from LEO to the Lunar Gateway is used as ΔV_{ks} in Eq. (4.22), see Table 5.5.

Table 5.5: Updated resource price for customers in the Lunar Gateway.

Parameter	Unit	GEO	Lunar Gateway
ΔV_{ks} (to determine p)	km/s	3.940	3.968
p	\$/kg	658	663

Tables 5.6 and 5.7 show the optimised results for a single resource-return trip to the asteroid 2006 QQ56, along with the baseline results to GEO for easier comparison. The parameters not shown in these tables are equivalent to those for the mission to GEO (and timing of the transfers are comparable, within two days difference), as shown in Tables 5.2 and 5.3.

Table 5.5 shows that for missions to the Lunar Gateway, the resource price is increased because of a slight increase in ΔV from LEO, causing an increase in $c_{\text{l,orbit}}$ and therefore p. This, in combination with a lower ΔV^I, means that a higher NPV can be realised for the chemical missions, both for the scenario with and without the kickstage. Similarly, for the solar-sail missions, a lower t^I_{spiral} means

Table 5.6: Changed parameters for missions to the Lunar Gateway for chemical propulsion (based on Table 5.2).

		Kickstage		No kickstage	
Parameter	**Unit**	**GEO**	**Lunar Gateway**	**GEO**	**Lunar Gateway**
ΔV^I	km/s	1.9574	1.4599	1.7019	1.2345
m^I_{prop}	tonnes	127.6	100.1	180.0	137.3
$m_{\text{r,sold}}$	tonnes	201.1	217.3	322.6	365.3
Revenue	\$	132,178,985	144,062,298	212,063,930	242,195,285
NPV	\$	45,910,971	65,166,958	100,942,935	126,386,166

Table 5.7: Changed parameters for missions to the Lunar Gateway for solar-sail propulsion (based on Table 5.3).

		Kickstage		No kickstage	
Parameter	**Unit**	**GEO**	**Lunar Gateway**	**GEO**	**Lunar Gateway**
t^I_{spiral}	days	1366	452	1366	452
Total mission duration	years	5.992	3.491	7.097	4.595
Operations cost	$	41,800,471	24,353,510	49,504,914	32,056,509
Total cost	$	122,915,306	105,468,345	204,798,922	187,340,817
Revenue	$	338,033,491	340,933,610	805,050,138	811,956,973
NPV	$	68,035,684	138,964,572	204,535,603	336,638,845

that a higher NPV can be realised, this time mainly because the revenue is discounted less, which has a significant effect due to the long duration of the solar-sail missions.

5.3.2 LOX/LH_2 Container Solar Sail

If the type of resource that is transported needs to be stored in a container that is not just a properly-sealed bag or bladder, as above in Section 5.1.3, it can no longer be assumed that the mass for this container can be absorbed in the solar-sail assembly mass. This Section investigates the effect of adding a heavier container to a solar sail. This container has to be launched from Earth, therefore taking up valuable payload capacity of the launch vehicle, but does not contribute (in any meaningful way at least) to the area of the sail used to propel the spacecraft. This will therefore decrease the outbound β as:

$$\beta^O = \beta_0 \frac{m_{\text{sails}} - m_{\text{container}}}{m_{\text{sails}}} \tag{5.14}$$

where $m_{\text{container}}$ is the mass of the container. The mass of such a container should be based on the mass of the resources, such that:

$$m_{\text{container}} = \lambda_{\text{container}} m_{\text{r}} \tag{5.15}$$

The dry mass dedicated to the solar sails themselves, excluding the container, can then be calculated as:

$$m_{\text{sails}} = \frac{m_{\text{l}}}{1 + \lambda_{\text{container}} \lambda_{\text{r}}} \tag{5.16}$$

and subsequently the dry mass for the container as:

$$m_{\text{container}} = m_{\text{l}} - m_{\text{sails}} \tag{5.17}$$

Note that the total cost for all space hardware (sails and container) has to be included in the calculation for the total cost.

The upper limit for λ_{r} to be used in the optimisation also has to take into account the additional container mass. Following the same requirement for the minimum structural mass:

$$\epsilon_{\text{min}} = \frac{m_{\text{sails}} + m_{\text{container}}}{m_{\text{sails}} + m_{\text{container}} + m_{\text{r}}} = \frac{1 + \lambda_{\text{container}} \lambda_{\text{r}}}{1 + (1 + \lambda_{\text{container}}) \lambda_{\text{r}}} \tag{5.18}$$

The lightness number for the inbound transfer also has to take the added container mass into

account:

$$\beta^I = \beta_0 \frac{1}{1 + (1 + \lambda_{\text{container}} \lambda_{\text{r}})} \tag{5.19}$$

These equations can be incorporated into the methodology described in Section 5.1.3, adapted for an existing asteroid by replacing the free orbital elements with given orbital elements. As a first approximation it is assumed that half of the dry mass in the chemical scenario is dedicated to the containers, with $\epsilon_{\text{min}} = 0.1$, resulting in $\lambda_{\text{container}} = 0.05$. Using $p' = c_{\text{prop}}$, to change the intrinsic value of the resources from H_2O to LOX/LH_2, this results in the mission described in Table 5.8. Note that this mission is to the same asteroid as the results in Table 5.3, meaning that these results can be compared.

The results in Table 5.8 show that due to the increase in container mass, the mission duration increases and the revenue decreases, both resulting in a significant decrease in NPV compared to the result in Table 5.3 for the mission without the kickstage. The increase in mission duration is due to the decrease in β for both the outbound and the inbound transfer, caused by the additional mass of the container. The decrease in revenue is because of a significantly smaller transported m_{r}. Transporting more resources would not only impact the inbound transfer duration, but also the outbound transfer duration. This is because a higher $m_{\text{container}}$ would have to be launched from Earth, taking up valuable space in the launch vehicle which can no longer be used for the solar sail. Increases in transfer duration (including the spiral times) due to a lower β has a profound negative impact on the NPV, through an increased discount on the revenue.

5.3.3 Multiple Round Trips

While this Chapter focuses on single-trip missions, an approximation for a multiple round-trip mission can be calculated. These follow-up round trips are only considered for the missions without the kickstage to escape, as those are unlikely to be available in GEO, after the initial round trip.

The NPV for an extended mission is approximated through:

$$NPV = \frac{R_1 - c_{op} t_{\text{mis}_2}}{(1+I)^{t_{mis_1}}} + \frac{R_2}{(1+I)^{t_{\text{mis}_1} + t_{\text{mis}_2}}} - C \tag{5.20}$$

in which R_1 and R_2 are the revenue for the first and second round trip, respectively, and t_{mis_1} and t_{mis_2} the mission duration of the first and second round trip. In Eq. (5.20), it is assumed that the increase in operation costs for the extended operations are paid at the start of the second round trip. Other costs, such as the launch, development, manufacturing, operations of the first round trip, and initial outbound propellant costs are assumed fixed.

Other modifications are:

- For the chemical mission, ΔV^O for the follow-up round trip is determined using the methodology described in Section 4.4, for a transfer from GEO to the asteroid using a hyperbolic escape trajectory. ΔV_1 and ΔV_2 of the optimised outbound Lambert arc are used to compute the total ΔV^O from GEO to the asteroid.

- For the chemical mission, a fraction of the resources that were to be sold in GEO are now used during the outbound transfer of the second round trip, thereby reducing the revenue of the first round trip.

- For the solar-sail mission, the spiral time for the spiral from GEO to escape, $t^O_{\text{spiral}_2}$, is calculated

Table 5.8: Example mission to NEA 2006 QQ56 using solar-sail propulsion, incorporating a container mass of 5% of the resource mass.

Parameter	**Unit**	**No kickstage**
Semi-major axis	AU	0.9850
Eccentricity		0.0456
Inclination	deg	2.7981
Launch date		04-01-2047
Spiral time to escape	days	507
Duration outbound transfer	days	199
Stay time at asteroid	days	15
Duration inbound transfer	days	701
Spiral time to GEO	days	1466
β^O		0.068
β^I		0.0093
m_l	tonnes	136.1
m_sails	tonnes	93.0
$m_\mathrm{container}$	tonnes	43.1
$m_\mathrm{r} = m_\mathrm{r,sold}$	tonnes	861.9
Launch cost	$	13,095,922
Development cost spacecraft	$	5,060,273
Manufacturing cost spacecraft	$	137,128,113
Operations cost	$	55,073,853
Total cost	$	210,358,162
Revenue	$	566,595,592
Total mission duration	years	7.895
NPV	$	56,618,371

using Eq. (5.9) with $r = r_{\text{GEO}}$ and $\beta = \beta_0$, as the sail will not have any payload on the outbound transfer. This replaces the spiral time from LEO used in the first outbound transfer.

The results of Tables 5.2 and 5.3 are used, no new optimisation is performed. The results for this analysis are shown in Table 5.9 and 5.10, for the chemical and solar-sail missions, respectively. However, it should be noted that this analysis ignores the phasing of the second round trip, which is likely to add a waiting period in GEO before the second round trip commences.

Table 5.9: Extended mission to NEA 2006 QQ56 using chemical propulsion, without a kickstage.

Parameter	**Unit**	**Value**
t_{mis_1}	years	1.536
ΔV_2^O	km/s	2.169
$m^O_{\text{prop}_2}$	tonnes	35.7
m_{r} left to sell 1$^{\text{st}}$ trip	tonnes	286.7
t_{mis_2}	years	1.536
C	\$	82,240,953
$c_{\text{op}} t_{\text{mis}_2}$	\$	10,714,715
R_1	\$	188,490,896
R_2	\$	212,063,930
NPV	\$	202,098,971

Table 5.10: Extended mission to NEA 2006 QQ56 using solar-sail propulsion, without a kickstage.

Parameter		**Value**
t_{mis_1}	years	7.097
$t_{\text{spiral}}(\beta_0, r_{\text{GEO}})$	days	137
t_{mis_2}	years	6.522
C	\$	204,789,223
$c_{\text{op}} t_{\text{mis}_2}$	\$	45,497,604
R_1	\$	805,050,138
R_2	\$	805,050,138
NPV	\$	401,235,078

As shown in Table 5.9, the spacecraft employing chemical propulsion can be used for a second round trip to an asteroid. Even though the revenue of the second round trip is discounted, it can be seen that a higher NPV can be realised: \$202 million instead of \$101 million (note that the exact doubling of the NPV is a coincidence). Similarly, as shown in Table 5.10, a solar sail can be reused for a second round trip to an asteroid. Again, the revenue of the second round trip is heavily discounted, but higher NPV can be realised: \$401 million instead of \$205 million. The long duration of the solar-sail mission means that the additional revenue suffers from a higher discount than is the case for the chemical propulsion mission. However, the revenue of the first round trip is not compromised because a portion of the delivered resources have to be reserved for the second round trip, meaning that the NPV is still nearly doubled, as is the case for the chemical mission. Note that the total mission duration could increase due to phasing before starting the second round trip, but solar sails are more flexible in responding to changes in departure time, so this effect can likely be mostly mitigated.

Note that the asteroid investigated here is relatively close to Earth, for asteroid further away, for which longer mission durations are necessary, the discount would be even more significant. If phasing for the second round trip is taken into account, ΔVs are expected to increase, possibly for both trips, as the synodic period for asteroids this close to Earth are very long. Therefore, the results obtained here are optimistic and can only decrease, not increase, when a higher fidelity analysis is performed.

5.3.4 Monte Carlo Analysis

To investigate the sensitivity of the analysis with respect to the input values for the cost model, a range of Monte Carlo simulations have been performed. Separate simulations have been performed for the development cost (per kg), manufacturing cost (per kg), operation cost (per year), launch cost and discount rate, for both the chemical missions and the solar-sail missions to GEO. Table 5.11 shows the input parameters which have an influence on the resulting NPV and the parameters used to model the uncertainty as a normal probability density function. The standard deviation σ used is arbitrarily chosen as 10% of the mean value. However, this approach should result in a relative metric for the sensitivity of each parameter with respect to the others. Note that the lack of coupling between the parameters means that the results can only be used to compare the sensitivity of the model to these parameters, but do not represent the results of the model in a statistical sense.

Table 5.11: Inputs for Monte Carlo simulation of optimised missions.

Parameter	**Mean value**	**Standard deviation, σ**	
Development cost, c_{dev}	37.19	3.72	\$/kg
Manufacturing cost, c_{man}	1007.12	100.71	\$/kg
Operations cost, c_{op}	6.98×10^6	6.98×10^5	\$/year
Launch cost, C_{l}	13.09×10^6	13.09×10^5	\$
Discount rate, I	10	1	%

The results of the case studies as shown in Tables 5.2 and 5.3 are used as the baseline mission. For each simulation, 2000 scenarios are investigated, each changing only one input while leaving the others as in the baseline. A local optimisation starting from the result in Tables 5.2 or 5.3 is performed using `fmincon`.

The results are shown in Fig. 5.8 using boxplots. The central line of the boxplot indicates the median value, with the bottom and top edges of the box marking Q_1 as the 25^{th} and Q_3 as the 75^{th} percentiles, respectively. The whiskers of the boxplot, the dashed lines, extend to the most extreme results which are not considered outliers, with outliers shown separately in red. An outlier is defined as being greater than $Q_3 + 1.5(Q_3 - Q_1)$ or less than $Q_1 - 1.5(Q_3 - Q_1)$. These figures show that the assumed manufacturing and launch cost have a significant effect on the resulting NPV, for all scenarios. These two cost elements are the largest contributions to the total cost, so this results is as expected. For the solar-sail mission, which has a relatively long duration, the effect of the discount rate and yearly operation costs are more significant than for chemical propulsion, as expected.

It is important to note that a change in the investigated cost elements not only influence the cost of the mission, but they also influence the price of the resources, p, through a change in $c_{\text{l,orbit}}$.

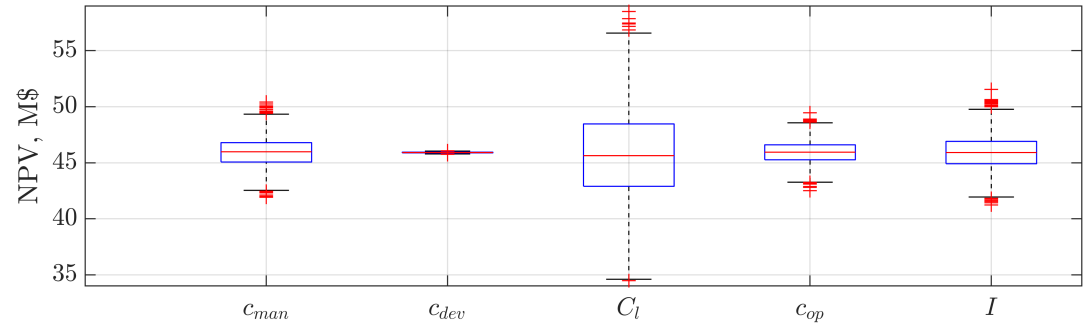

(A) Chemical, with kickstage.

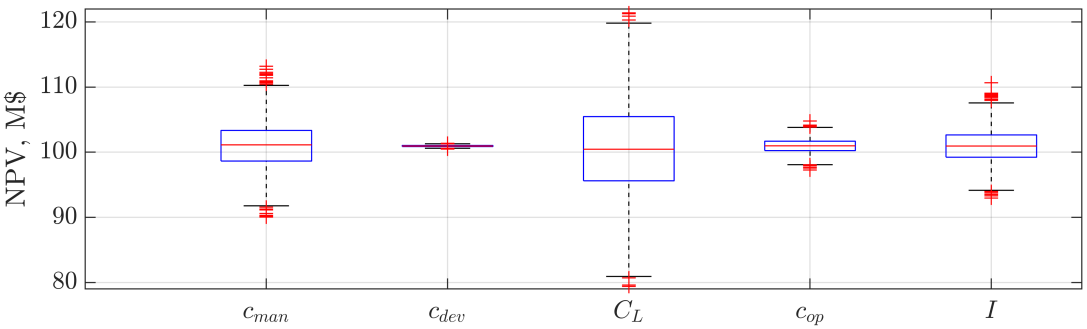

(B) Chemical, without kickstage.

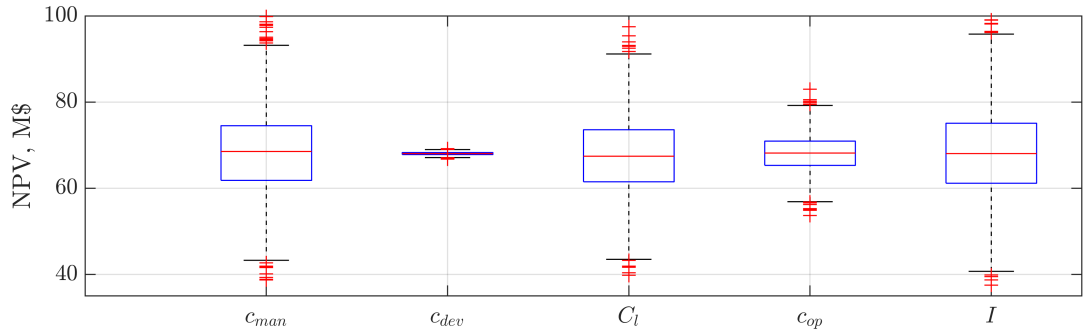

(C) Solar sail, with kickstage.

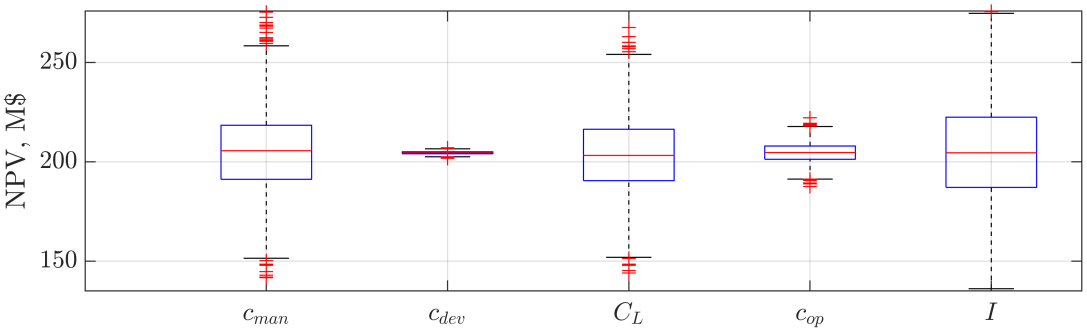

(D) Solar sail, without kickstage.

Figure 5.8: Monte Carlo analysis results for all scenarios.

5.4 KEY FINDINGS

When departing from LEO directly without the use of a kickstage to escape, both the chemical and solar-sail missions can generate a higher NPV than when using a kickstage to escape. Using chemical propulsion, more target asteroids can prove to be profitable, because not many asteroids exist where the solar sail outperforms the chemical scenario within the explored parameter space. While solar sails can return significantly more resources using the same launched mass, resulting in a much higher revenue, the NPV is often lower than when chemical propulsion would be used due to the very long mission durations. Only for customers close to Earth, solar sails can outperform the chemical scenarios in terms of NPV. In addition, the IRR is higher for the chemical scenarios than it is for solar-sail scenarios, again due to long mission durations, which makes the chemical scenarios more attractive for investors. One major drawback of the chemical propulsion scenarios is that part of the recovered resources must be LOX/LH_2 due to ISRU. A large fraction of the resources is used, which can therefore no longer be sold to the customer. Using solar sails, all the recovered resources can reach the customer.

When delivering resources to the Lunar Gateway instead of GEO, higher NPVs can be realised, for all scenarios considered (chemical or solar sail, kickstage or not). Also, including a LOX/LH_2 container in the solar-sail scenario results in a significantly lower NPV due to an increased mission duration and a decrease in revenue. Next, multiple round-trips to an asteroid using the same spacecraft can be beneficial to increase NPV, but any additional revenue is highly discounted due to long mission durations, especially when using a solar sail. Finally, a Monte Carlo analysis shows that the results are sensitive to the launch cost, as this impacts both the cost and revenue, and the long solar-sail missions are relatively sensitive to the imposed discount rate.

Chapter 6

LAUNCH VEHICLE CONSIDERATIONS

For economic modelling, many assumptions must be made concerning a range of elements of the mission. One such element is the launch vehicle, with assumptions on payload capacity and launch cost. While one of the key justifications for the utilisation of asteroid resources is the high costs otherwise incurred if the same resources were to be launched from Earth, the effect of decreasing launch costs and increasing payload capacity is not yet fully understood. With current trends in launch vehicle development, this is an important issue to investigate. Therefore, this Chapter aims to investigate the influence of launch vehicle cost and payload capacity on the economic profitability of asteroid mining missions.

The baseline mission from Chapter 4 is used. This Chapter is based on the work published in Ref. [35], but through progressive insights, certain aspects of the methodology have evolved since that publication. Notable changes with respect to Ref. [35] are the removal of a kickstage to escape, a change to the calculation of the resource price p (as explained in Section 5.1), venting of excess oxygen after mining, and an updated region of potentially profitable asteroids following Chapter 5.

First, a methodology to investigate the impact of launch cost and payload capacity is established. Two case studies are presented and the methodology is subsequently applied to derive general relationships between the launch vehicle characteristics and the profitability of an asteroid mining mission. Several sensitivity analyses are performed: a mission scenario with two round-trips instead of one, selling resources at the Lunar Gateway instead of GEO, investigating the effect of incorporating the probability of mission success, and a set of Monte Carlo simulations to investigate the sensitivity of the results to certain input parameters.

6.1 METHODOLOGY

The baseline mission as introduced in Chapter 4 is employed in this methodology, with a material source at an asteroid and a customer location in GEO. This specific mission scenario is visualised in Fig. 6.1.

In this Chapter, the calculations for the baseline mission will be followed, but including a varying payload capacity (m_l) and a varying launch cost (C_l). Following the mass budget, changing m_l has an effect on all masses in the budget, as these are all based on a fully-utilised payload capacity of the launch vehicle. A change in m_l causes a proportional change in all other masses in the mass budget, up to and including the mass that can be delivered to the customer, $m_\mathrm{r,sold}$. A change in the launch

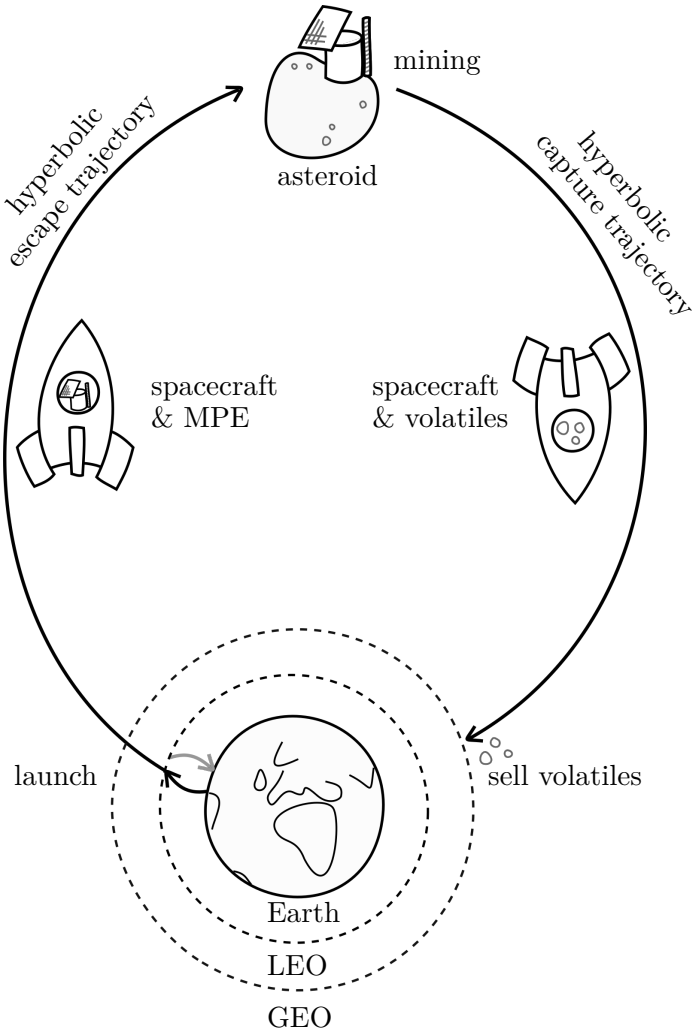

Figure 6.1: Schematic for mission scenario for mining on an asteroid and delivery to customers in GEO.

cost causes a direct change to the total costs.

The launch cost and payload capacity do not only have a direct impact on the total cost of a mission, through Eq. (4.1), but also on the revenue that can be generated, through Eq. (3.12), repeated here for clarity:

$$\begin{aligned} C &= C_\mathrm{l} + (c_\mathrm{dev} + c_\mathrm{man}) m_\mathrm{sc,dry} + c_\mathrm{op} t_\mathrm{mis} + c_\mathrm{prop} m^O_\mathrm{prop} \\ p &= p' + c_\mathrm{l,orbit} \end{aligned}$$

where the launch cost to orbit ($c_\mathrm{l,orbit}$) is calculated through:

$$c_\mathrm{l,orbit} = \frac{C_\mathrm{l} + (c_\mathrm{dev} + c_\mathrm{man}) m_\mathrm{ks,dry} + c_\mathrm{prop} m_\mathrm{ks,prop}}{m_\mathrm{ks,transport}}$$

where the masses in the calculation for $c_\mathrm{l,orbit}$ also depend on the payload capacity, through Eqs. (4.23),

(4.25) and (4.22):

$$\begin{aligned} m_{\text{ks,dry}} &= \epsilon_{\min} m_{\text{l}} \\ m_{\text{ks,prop}} &= m_{\text{l}} \left(1 - e^{-\frac{\Delta V_{\text{ks}}}{I_{\text{sp}} g_0}}\right) \\ m_{\text{ks,transport}} &= m_{\text{l}} - m_{\text{ks,dry}} - m_{\text{ks,prop}} \end{aligned}$$

The equations repeated here show that the payload capacity and launch cost greatly influence both the cost and revenue sides of the asteroid mission, thereby influencing profitability.

6.1.1 Optimisation

The profitability of this scenario is expressed through the NPV. Optimisation of the transfers is therefore aimed at maximising the NPV, with:

$$J = -NPV \tag{6.1}$$

Optimisation is performed precisely as described in Section 4.5. This means that the variables for the timing of the outbound and inbound Lambert arcs (Δt^O, Δt_{stay}, Δt^I, and t^O_{dep}) and mass fraction for MPE (λ_{MPE}) are optimised using a genetic algorithm. Bounds for these variables are given in Section 4.5, as are the non-linear constraints to ensure that the spacecraft does not contain more payload and propellant than it can transport and that sufficient propellant is mined for the inbound transfer.

6.1.2 Target Selection

The range of orbital elements for suitable asteroids is based on the results obtained in Chapter 5. As the mission scenario used here is closest to that for the "chemical, no kickstage" scenario in Chapter 5, these results are used. Note that the time and effort related to mining of the resources are taken into account here, meaning that the boundaries for the region where the NPV can be positive, when taken from Chapter 5, are conservative. Rather than using one 3D cuboid to define the region, as was done in Ref. [35] (the paper on which this Chapter is based), a number of smaller 3D cuboids are used, to ensure a better fit to the region of potential targets found in Chapter 5. The regions extracted from Fig. 5.6b are given in Table 6.1. Note that there is an overlap between these regions, but each asteroid is only investigated once. All asteroids within these ranges are considered, as shown in Figure 6.2. A total of 1,693 asteroids are found within the considered regions.

The absolute magnitude of the specific asteroid is also taken into account, since the recoverable volatile mass can be approximated using the absolute magnitude. The subset of asteroids considered

Table 6.1: Subset of orbital element space where missions can potentially result in a positive NPV, based on Fig. 5.6b.

Region	**a, AU**	**e**	**i, deg**
1	[0.775, 1.225]	[0.00, 0.25]	[0, 4]
2	[0.900, 1.200]	[0.00, 0.20]	[0, 12]
3	[0.800, 1.300]	[0.15, 0.25]	[0, 8]
4	[0.800, 1.450]	[0.20, 0.30]	[0, 4]

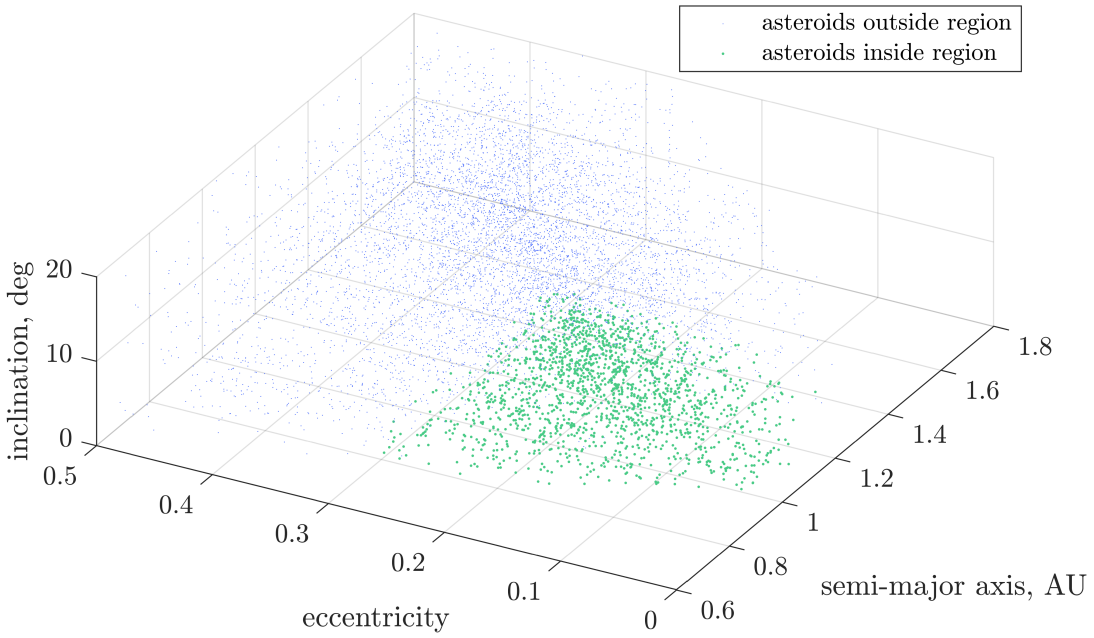

Figure 6.2: Distribution of orbital elements in asteroid subset.

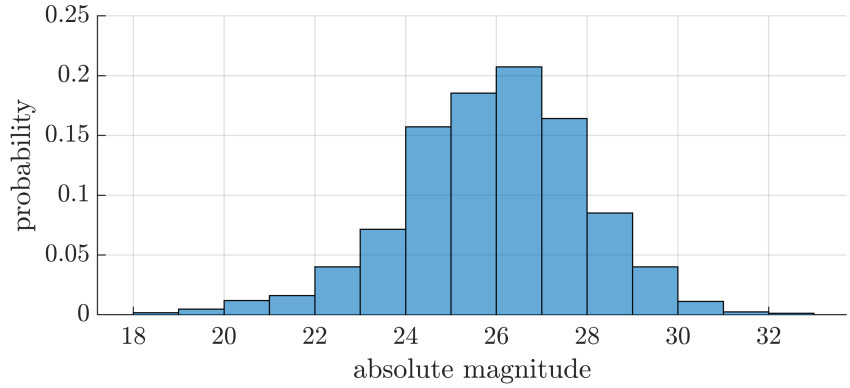

Figure 6.3: Distribution of absolute magnitude of asteroid subset.

are observed with absolute magnitudes ranging from 18.5 to 32.1, with a distribution given in Fig. 6.3. Figure 6.3 shows that the absolute magnitudes of approximately 72% of these asteroids are between 24 and 28, and only 3.7% are 22 or lower. An estimate for the diameter of an asteroid, based on the absolute magnitude, is given in Table 6.2. Using this diameter, an estimate of the available resource mass can be determined using Eq. (4.15) and is given for a suitable range of absolute magnitudes in Table 6.2. Note that a maximum excavation depth of 10 metres is used, following Section 4.3, which means that asteroids with a diameter under 20 metres are processed and depleted entirely. Also, note that it is assumed that all the asteroids considered are C-type asteroids, which affects the estimated density ρ, geometric albedo p_v and expected volatile recovery ratio $\lambda_{\text{volatile}}$.

Table 6.2: Estimated diameter and recoverable volatile mass as a function of absolute magnitude.

Absolute magnitude	**Diameter, m**	$\mathbf{m_{r,available}}$**, kg**	**Processed entirely**
19.0	860	2.950×10^9	N
20.0	543	1.159×10^9	N
21.0	342	4.512×10^8	N
22.0	216	1.734×10^8	N
23.0	136	6.527×10^7	N
24.0	86.0	2.372×10^7	N
25.0	54.3	8.135×10^6	N
26.0	34.2	2.535×10^6	N
27.0	21.6	6.859×10^5	N
28.0	13.6	1.723×10^5	Y
29.0	8.6	4.328×10^4	Y
30.0	5.4	1.087×10^4	Y
31.0	3.4	2.731×10^3	Y
32.0	2.2	6.859×10^2	Y

6.2 CASE STUDIES

To provide specific examples of the mission scenario detailed in Section 6.1, three case studies are now investigated: the SpaceX Starship system, the Arianespace Ariane V ES and a combination of both. The first is chosen as an example for new generation, reusable and less expensive launch vehicles, while the second is an example of traditional high-cost launch vehicles often used in economic models. The third case study investigates the effects of using an expensive launch vehicle when a less expensive launch vehicle is also available.

6.2.1 Starship System (SpaceX)

From all (super-)heavy-lift launch vehicles currently under development, the SpaceX Starship system promises one of the lowest specific launch costs per kg. The Starship system, which includes a Super Heavy first stage and Starship second stage, will have a payload capacity m_l to LEO of 150 tons (136 metric tonnes) with a launch cost potentially lower than the launch cost of the Falcon 1, according to estimates from SpaceX [209]. Therefore, following their estimates, the cost C_l of one fully-reusable Starship system is estimated at 13.1 M$, the FY2020 cost of a Falcon 1 launch [132].

Using these parameters and the methodology described above, the genetic algorithm returns the maximum NPV as given in Table 6.3 for the twenty most profitable asteroids during the launch window 2035-2064. For the most profitable mission, to asteroid 2000 SG344, the details for the mission are provided in Table 6.5. The mission is visualised in Fig. 6.4, including the transfers and stay time at the asteroid.

Table 6.3: Results for case study: Starship system. Best 20 asteroids.

Asteroid	NPV, FY2020 M$	Absolute magnitude	Semi-major axis, AU	Eccentricity	Inclination, deg	Category
2000 SG344	102.2	24.7	0.977	0.0670	0.112	Aten
2017 HU49	83.3	26.5	0.971	0.0551	2.625	Aten
2006 QQ56	82.3	25.9	0.985	0.0456	2.798	Aten
2014 QD364	74.3	27.2	0.986	0.0415	4.009	Aten
2001 GP2	72.2	26.9	1.037	0.0735	1.273	Apollo
2020 PJ6	71.3	25.6	0.965	0.0979	0.813	Aten
2020 FA1	70.8	26.3	1.030	0.0335	3.524	Apollo
2015 KE	70.8	26.2	0.974	0.1243	0.619	Aten
2018 PM28	70.2	25.7	1.027	0.0748	2.276	Apollo
2014 DJ80	70.0	26.3	0.977	0.0670	3.027	Aten
2016 YR	68.7	27.2	1.027	0.0673	3.446	Apollo
2019 TF2	68.5	26.4	1.042	0.0799	2.413	Apollo
2018 TG6	66.0	27.1	1.064	0.0837	0.710	Apollo
2020 KQ7	64.5	26.4	0.969	0.1143	2.110	Aten
2007 VU6	62.8	26.5	0.976	0.0905	1.224	Aten
2014 WA366	61.5	26.9	1.034	0.0715	1.559	Apollo
2003 YN107	61.3	26.5	0.989	0.0139	4.321	Aten
2008 ST	60.0	27.1	0.964	0.1259	1.908	Aten
2015 JD3	60.0	25.5	1.059	0.0079	2.718	Amor
2014 QN266	59.6	26.3	1.053	0.0923	0.488	Apollo

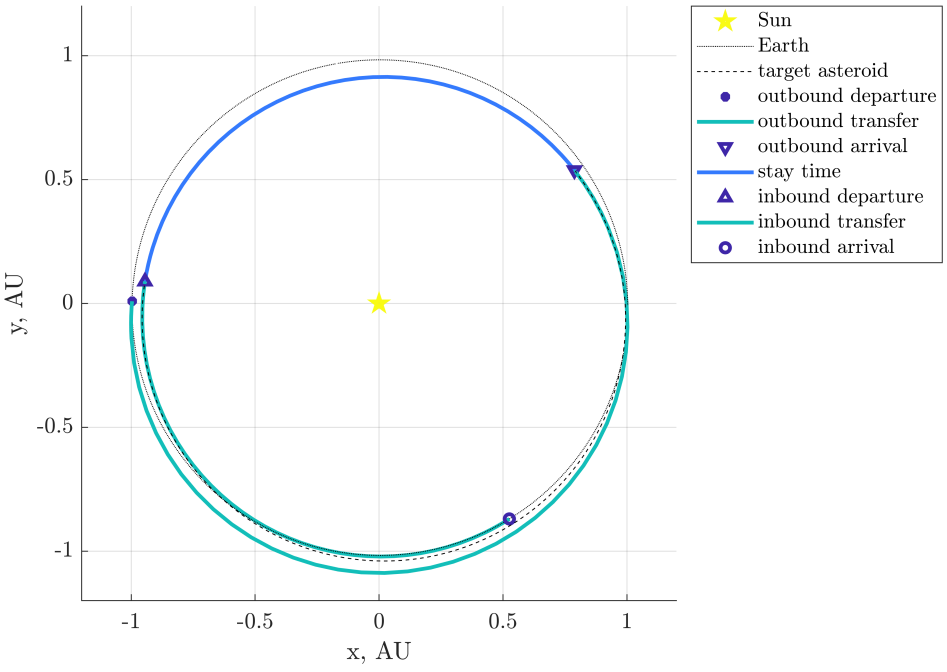

Figure 6.4: Mission profile for most profitable mission to 2000 SG344 using the Starship launch vehicle.

6.2.2 Ariane V ES

The same analysis has been undertaken for an Ariane V ES launch vehicle, which delivers 21,500 kg to LEO at a cost of 194.89 M$ (FY2020) [216]. While this results in a significantly higher specific cost to LEO than the Starship (9,065 vs 96 $/kg), it is still lower than the often quoted 10,000 $/kg,

used for the economic modelling of other asteroid mining ventures [3, 22, 115, 126, 132]. The results of this analysis can be found in Table 6.4. As can be seen, asteroid 2000 SG344, which was the most profitable target for the Starship mission, still provides the highest NPV.[1] The mission details for the most profitable mission to this asteroid are given in the rightmost column of Table 6.5. The reasons for the difference in NPV will be discussed later. Figure 6.5 shows the obtained NPV for the Ariane V ES missions in comparison with the NPV obtained using the Starship, with each data point referring to the same target asteroid.

Table 6.4: Results for case study: Ariane V ES. Best 20 asteroids.

Asteroid	NPV, FY2020 M$	Absolute magnitude	Semi-major axis, AU	Eccentricity	Inclination, deg	Category
2000 SG344	1111.4	24.7	0.977	0.0670	0.112	Aten
2010 JW34	1104.3	28.1	0.981	0.0547	2.259	Aten
2010 VQ98	1070.0	28.2	1.023	0.0271	1.475	Apollo
2011 UD21	1019.5	28.5	0.979	0.3037	1.062	Aten
2006 QQ56	1007.6	25.9	0.985	0.0456	2.798	Aten
2014 QD364	1001.2	27.2	0.986	0.0415	4.009	Aten
2011 UU190	990.2	28.1	1.037	0.0337	0.205	Apollo
2019 PO1	976.1	27.8	1.036	0.0610	1.120	Apollo
2016 YR	965.2	27.2	1.027	0.0673	3.446	Apollo
2017 HU49	959.4	26.5	0.971	0.0551	2.625	Aten
2008 EL68	943.3	27.7	1.039	0.0571	1.039	Apollo
1991 VG	941.0	28.3	1.032	0.0525	1.430	Apollo
2018 VT7	923.5	27.9	0.983	0.0882	2.544	Aten
2012 TF79	891.5	27.4	1.050	0.0382	1.006	Apollo
2015 KE	886.8	26.2	0.974	0.1243	0.619	Aten
2015 XZ378	883.5	27.2	1.015	0.0348	2.718	Aten
2001 GP2	881.6	26.9	1.037	0.0735	1.273	Apollo
2020 PJ6	879.2	25.6	0.965	0.0979	0.813	Aten
2020 FA1	864.3	26.3	1.030	0.0335	3.524	Apollo
2018 PU23	863.1	28.1	0.964	0.0841	0.828	Aten

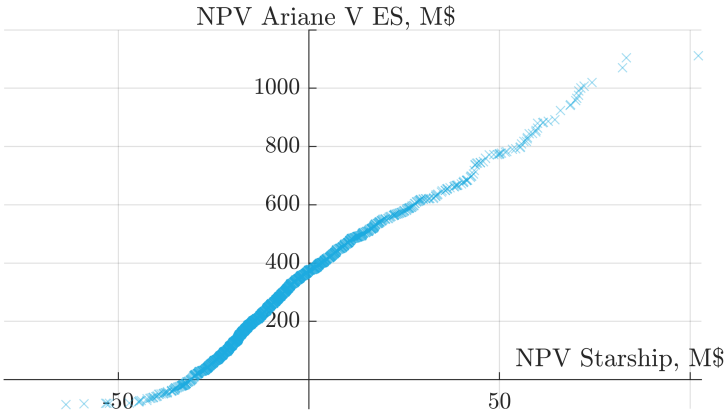

Figure 6.5: Comparison of NPV of Starship and Ariane V ES launch vehicles. Each data point refers to the same target.

[1] Note that the original paper in Ref. [35] finds asteroid 2018 AV2 as the most profitable target. This asteroid, with SPK-ID 3797463, no longer exists in the JPL database obtained on August 20th, 2020.

Table 6.5: Mission details for most profitable mission.

Parameter	**Unit**	**Starship**	**Ariane V ES**
Asteroid		2000 SG344	2000 SG344
Semi-major axis	AU	0.9774	0.9774
Eccentricity		0.0670	0.0670
Inclination	deg	0.1122	0.1122
Launch date		25-03-2055	27-03-2055
Duration outbound transfer	days	240	243
Stay time at asteroid	days	127	121
Duration inbound transfer	days	137	137
ΔV^O	km/s	3.824	3.811
ΔV^I	km/s	1.576	1.577
m_{l}	tonnes	136.1	21.5
m^O_{prop}	tonnes	79.3	12.5
m_{cargo}	tonnes	53.5	8.45
m_{mpe}	tonnes	3.31	0.548
m_{r}	tonnes	481.1	76.0
m^I_{prop}	tonnes	161.7	25.6
$m_{\mathrm{r,sold}}$	tonnes	319.4	50.5
p	\$/kg	658	29,947
Launch cost	\$	13,095,922	194,893,660
Development cost spacecraft	\$	2,110,947	334,490
Manufacturing cost spacecraft	\$	57,204,464	9,064,315
Propellant cost spacecraft	\$	75,218	11,860
Operations cost	\$	9,633,360	9,596,213
Total cost	\$	82,119,913	213,900,537
Revenue	\$	210,233,397	1,510,977,855
Total mission duration	years	1.381	1.376
NPV	\$	102,185,790	1,111,403,709

6.2.3 Both Starship System and Ariane V ES

The baseline mission architecture assumes that the same launch vehicle is used for launching the asteroid mining venture and to calculate the resource price that has to be competed with. This Section explores the effects of using the Ariane V ES launch vehicle for the asteroid mining venture, but instead basing the resource price on the far cheaper Starship system. The asteroids from Table 6.4 are reoptimised using $p = 648$ \$/kg, consistent with the Starship mission. Results are shown Table 6.6, preserving the original order of the asteroids as given in Table 6.4.

Table 6.6: Results for case study: Ariane V ES, with the resource price based on the Starship system. Results from Table 6.4 copied for reference and order of asteroids is preserved.

Asteroid	**NPV with p = 29,947 \$/kg, FY2020 M\$**	**NPV with p = 658 \$/kg, FY2020 M\$**
2000 SG344	1111.4	-184.6
2010 JW34	1104.3	-184.0
2010 VQ98	1070.0	-185.6
2011 UD21	1019.5	-183.3
2006 QQ56	1007.6	-186.1
2014 QD364	1001.2	-186.7
2011 UU190	990.2	-187.4
2019 PO1	976.1	-186.7
2016 YR	965.2	-189.0
2017 HU49	959.4	-184.8
2008 EL68	943.3	-187.4
1991 VG	941.0	-187.1
2018 VT7	923.5	-189.4
2012 TF79	891.5	-189.4
2015 KE	886.8	-188.5
2015 XZ378	883.5	-194.0
2001 GP2	881.6	-188.4
2020 PJ6	879.2	-188.3
2020 FA1	864.3	-189.3
2018 PU23	863.1	-187.2

6.2.4 Discussion of Case Studies

For a given launch vehicle, the difference in profitability of the missions to different target asteroids is due to two aspects: first, the orbital elements of the target asteroid (which determines the mission duration and ΔVs) and second the absolute magnitude (which determines the maximum recoverable volatile mass, $m_{\mathrm{r,available}}$). Because of the large payload capacity of the Starship system (136 metric tonnes) and the resulting capacity of the cargo spacecraft, the effect of the absolute magnitude is much more important for the Starship case study than for the Ariane V ES case study. This is reflected in Table 6.3 and Table 6.4, where the most successful targets for the Starship have in general a lower absolute magnitude than for the Ariane V ES, meaning that the recoverable volatile mass is greater, following Table 6.2.

Both cases show that for the most profitable targets, Aten and Apollo asteroids are favourable. The 20 most profitable asteroids for the Ariane V launch vehicles include the top 9 asteroids of the

Starship launch vehicle: 2000 SG344, 2017 HU49, 2006 QQ56, 2014 QD364, 2001 GP2, 2020 PJ6, 2020 FA1, 2015 KE, and 2016 YR. The other 11 asteroids of the top 20 have a magnitude of 27.2 or higher. As an example, for the Starship mission to asteroid 2000 SG344 from Table 6.5, it can be seen that the payload capacity of the cargo spacecraft is 481 tonnes. The maximum absolute magnitude for which $m_{\text{r,available}}$ is larger than this cargo capacity is 27.25. For other missions, the maximum absolute magnitude for which there is no unused capacity on the cargo spacecraft is dependent on the mass budget of the mission (which follows from the ΔVs required to reach the asteroid and GEO), but this value can serve as a guide for a Starship launch. For asteroids less accessible (i.e. with higher ΔVs), the cargo capacity will be lower, allowing for a slightly higher maximum absolute magnitude, noting that the available mass does not scale linearly (see Table 6.2).

The most obvious difference between the first two case studies is the profitability, as seen in Fig. 6.5. The Ariane V ES case study shows significantly higher NPVs in general. Out of the 1693 asteroids, 475 asteroids resulted in a positive NPV for the Starship launch vehicle, versus 1575 using the Ariane V ES launch vehicle. This large difference is mainly due to the difference in the competitive market price in GEO, p, which is higher when using an Ariane V ES (29,947 \$/kg) than when using the Starship (658 \$/kg). This difference in market price is due to the increased specific launch cost, which is higher for the Ariane V ES due to its smaller payload capacity and higher launch cost. If only Ariane V ES launch vehicles are available, it will be far more expensive to launch resources directly from Earth to GEO and hence asteroid resources will be more competitive, resulting in a greater generated revenue. If both the Ariane V ES and Starship system are available, and the asteroid mining venture launches using the more expensive Ariane V ES launch vehicle, the results in Table 6.6 show that the NPV is negative for all asteroids.

6.3 GENERAL TRENDS

This Section investigates the influence of changing the payload capacity and launch vehicle cost on the profitability of the Starship mission as a basis. The reason for choosing the Starship mission scenario over the Ariane V scenario is that the cost reductions for the Starship are more likely in a mid-to far-term time frame.

First, the effect of a changing m_{l} or C_{l} on the resource price p that can be charged is given in Fig. 6.6, where all parameters except for the dependent variable are as given in the baseline mission from Chapter 4. Figure 6.7 shows the resulting resource price p for combinations of m_{l} and C_{l}, from Eq. (3.12). A number of well-known launch vehicles and their launch cost and payload capacity are included in the graph, with a line connecting their combination of m_{l} and C_{l} with the resulting resource price p. From these figures it can be concluded that, all other things equal, the price of Earth-launched resources increases when either the payload capacity decreases or the launch cost increases. For a lower payload capacity, it means that the fixed costs, i.e. those for the launch and operations, have to be amortised over less sold resources, therefore driving up the resource price p. An increase in launch costs C_{l} naturally leads to higher total costs, which also drive up the cost of Earth-launched resources and therefore the resource price p.

Figure 6.8a shows the influence of changing launch cost on the NPV, total cost, and (discounted) revenue. The mission for which the NPV is calculated is to asteroid 2000 SG344, the same as in Table 6.5. Similarly, Figure 6.8b shows the influence of changing the payload capacity on the NPV. A linear equation has been fitted to the resulting data, for which the coefficients are given in Table 6.7. In addition, Fig. 6.9 shows the combined effect of changing the launch cost and payload capacity on

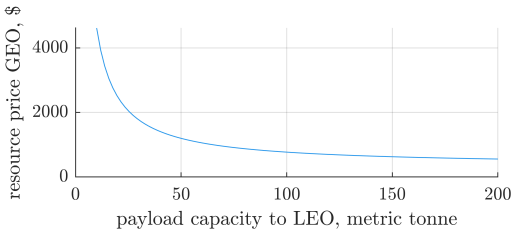

(a) Relationship between payload capacity and resource price in GEO.

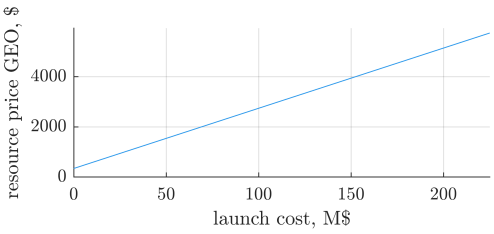

(b) Relationship between launch cost and resource price in GEO.

Figure 6.6: Effect of parameters on resource price p.

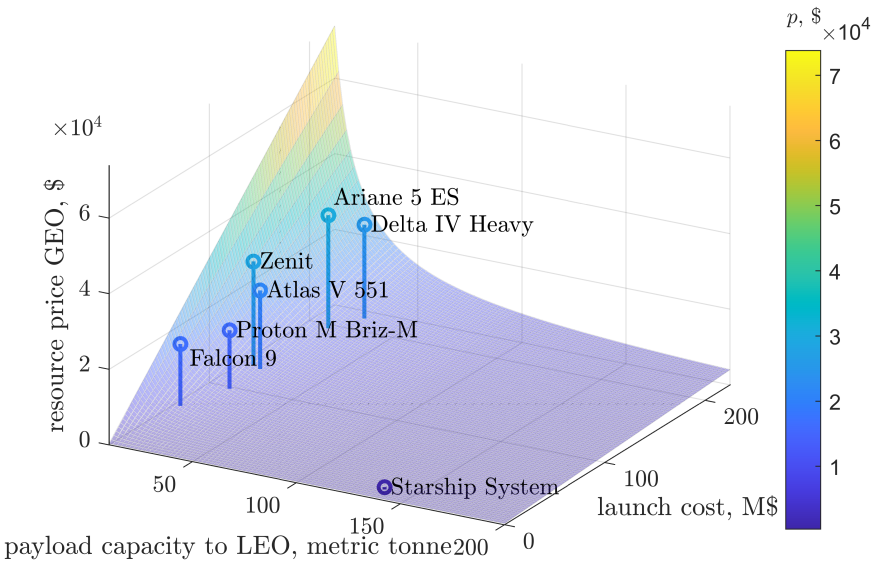

Figure 6.7: Relationship between resource price and combinations of payload capacity and launch cost. The combinations of launch cost and payload capacity of existing launch vehicles are added for reference.

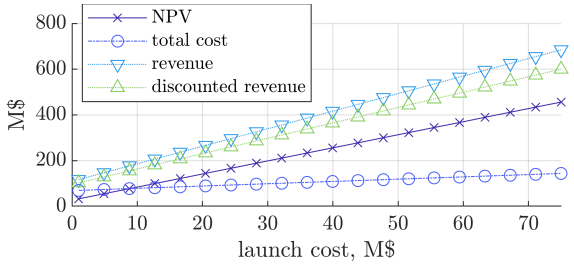

(a) Influence of launch vehicle cost on mission profitability.

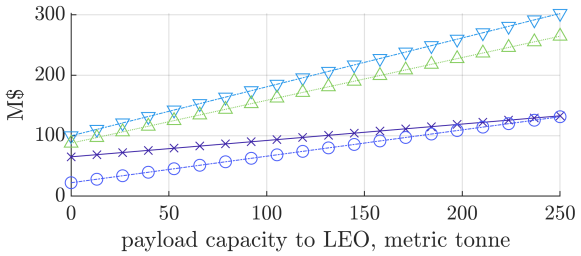

(b) Influence of launch vehicle payload capacity on mission profitability.

Figure 6.8: Effect of parameters on mission profitability (NPV).

the total mission cost, discounted revenue and NPV.

In the original paper in Ref. [35], the relationship between m_l and NPV was negative: for an increase in m_l, the NPV would decrease slightly. While the discounted revenue would increase for an increase in m_l, the total cost would increase *more*. With the updated mission scenario, i.e. the removal of the kickstage and the recalculation of the resource price, this is no longer the case. These updates have resulted in a higher p and a more effective use of the payload capacity, both of which

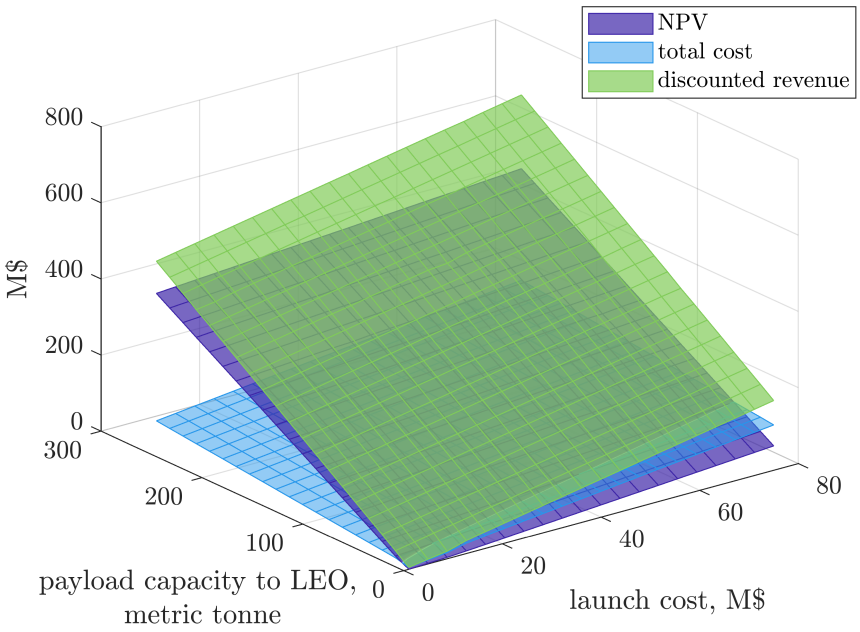

Figure 6.9: Influence of both launch vehicle cost and payload capacity on mission profitability.

Table 6.7: Linear fit to NPV data from Figs. 6.8 and 6.9.

Dependent variable	**Equation (m_l in kg, all others variables in \$)**
Launch cost	$NPV = 5.72C_l + 27.3 \times 10^6$
Payload capacity	$NPV = 270.9m_l + 65.3 \times 10^6$
Launch cost and payload capacity	$NPV = 5.72C_l + 270.3m_l - 9.6 \times 10^6$

are in favour of a higher NPV. For an increase in m_l, the increase in discounted revenue is greater than the increase in cost, therefore resulting in a slightly higher NPV.

With launch costs decreasing and payload capacities increasing, a trend that can be seen over time [216], the resulting NPV can therefore either increase or decrease. Comparing the equations presented in Table 6.7 is not straightforward due to the differences in units (kg and \$). However, within the parameter space investigated, the effect of the launch cost on NPV is stronger than the effect of the payload capacity. Therefore, it can be concluded that, for the trend of decreasing launch costs and increasing payload capacity, the NPV is likely to show a net decrease. It is unlikely that the decrease in NPV (due to a decrease in launch costs) can be completely offset by an increase in NPV (due to an increase in payload capacity). However, this depends on the ratio of decrease in launch cost and increase in payload capacity.

As one last example, the NPV is calculated for a hypothetical spacecraft which costs 10% less than the Starship, while having a 10% higher payload capacity. For the mission to 2000 SG344, a NPV of 98.4 M\$ can be generated, lower than for the Starship (102.2 M\$). Here it can be seen that the increase in NPV due to the higher payload capacity is not sufficient to compensate for the decrease in NPV due to lower launch costs.

6.4 SENSITIVITY ANALYSIS

This Section provides a number of different sensitivity analyses based on the results obtained in Section 6.2. First, a multiple round trip mission is optimised. Next, the change in profitability when delivering resources to the Lunar Gateway instead of GEO is investigated. This is followed by an analysis for the expected value of the NPV: the ENPV. Finally, Monte Carlo simulations are presented to investigate the effect of a number of input values for the model.

6.4.1 Multiple Round Trips

To investigate the profitability of multiple round trips, the Starship case study is extended to add a second round trip. The same mission scenario as the single trip is envisioned until delivery to GEO. Then, after a stay time in GEO (Δt_{GEO}), the cargo spacecraft transfers to an escape trajectory for the second round trip using a portion of the delivered propellant. The same mission strategy can then be used; a Lambert arc to the asteroid, proximity operations at the asteroid and then a Lambert arc to return to GEO. However, the asteroid volatile mass that can be produced ($m_{\text{r,mined}}$) is now no longer dependent on the stay time at the asteroid during this second trip (Δt_{stay_2}), but on the time since the previous departure from the asteroid, since the MPE is left to operate at the target asteroid. Also, as propellant for the second outbound transfer has to be reserved from the delivered resources, the mass that can be sold decreases:

$$m_{\text{r,sold}_1} = m_{\text{r}_1} - m^I_{\text{prop}_1} - m^O_{\text{prop}_2} \tag{6.2}$$

in which the subscripts denote the first and second round trip. This mission scenario means that the decision vector for the genetic algorithm, with again subscripts denoting the round trip where necessary, is extended to:

$$\mathbf{X} = \begin{bmatrix} t^O_{\text{dep}_1} & \Delta t^O_1 & \Delta t_{\text{stay}_1} & \Delta t^I_1 & \Delta t_{\text{stay,GEO}} & \Delta t^O_2 & \Delta t_{\text{stay}_2} & \Delta t^I_2 & \lambda_{\text{MPE}} \end{bmatrix} \tag{6.3}$$

For this mission, the NPV is calculated using Eq. (5.20), repeated for the sake of clarity:

$$NPV = \frac{R_1 - c_{\text{op}} t_{\text{mis}_2}}{(1+I)^{t_{mis_1}}} + \frac{R_2}{(1+I)^{t_{\text{mis}_1} + t_{\text{mis}_2}}} - C$$

in which t_{mis_2} now also includes the waiting time in GEO before the second leg commences.

In this analysis, several assumptions are made. First, the discount for the second trip is based on the total mission duration calculated from the start of the first trip. Second, the operation costs for the second trip are only paid at the start of the second trip.

Results for this optimisation can be found in Table 6.8 to the asteroid for which the most profitable mission using the Starship was found: 2000 SG344. It can be seen that when simultaneously optimising two consecutive trajectories, due to the long synodic period (approximately 28 years), the obtained ΔVs are slightly higher, but still very low. The decrease in sold resources caused by $m^O_{\text{prop}_2}$ causes a significant reduction of the revenue of the first mission. Because the revenue R_1 is not as discounted as R_2, this has a relatively high impact on the NPV. Nonetheless, due to the additional revenue of the second mission and the modest increase in cost (only operational costs), the final NPV after the second mission is still 46.4 M$ higher than for the single-trip mission in Table 6.5. Note that this is a significantly smaller increase than the additional revenue generated compared to the single mission: a total of 317.4 M$ compared to 210.2 M$.

Table 6.8: Mission details for a two-trip mission to asteroid 2000 SG344 using the Starship launcher.

Parameter	**Unit**	**Value**
Asteroid		2000 SG344
Semi-major axis	AU	0.9774
Eccentricity		0.0670
Inclination	deg	0.1122
Launch date		12-05-2054
Duration outbound transfer (1)	days	403
Stay time at asteroid (1), Δt_{stay_1}	days	137
Duration inbound transfer (1)	days	198
Stay time in GEO, $\Delta t_{\text{stay,GEO}}$	days	30
Duration outbound transfer (2)	days	106
Stay time at asteroid (2), Δt_{stay_2}	days	24
Duration inbound transfer (2)	days	106
ΔV_1^O	km/s	3.939
ΔV_1^I	km/s	1.576
ΔV_2^O	km/s	1.667
ΔV_2^I	km/s	1.748
m_{l}	tonnes	136.1
$m_{\text{prop}_1}^O$	tonnes	80.8
m_{cargo}	tonnes	52.3
m_{mpe}	tonnes	2.97
m_{r_1}	tonnes	470.9
$m_{\text{prop}_1}^I$	tonnes	158.3
$m_{\text{prop}_2}^O$	tonnes	128.9
$m_{\text{r,sold}_1}$	tonnes	183.7
m_{r_2}	tonnes	470.9
$m_{\text{prop}_2}^I$	tonnes	172.4
$m_{\text{r,sold}_2}$	tonnes	298.5
p	\$/kg	658
Launch cost	\$	13,095,922
Development cost spacecraft	\$	2,056,186
Manufacturing cost spacecraft	\$	55,720,502
Propellant cost spacecraft	\$	76,615
Operations cost, $c_{op}t_{\text{mis}_1}$	\$	14,110,019
Operations cost, $c_{op}t_{\text{mis}_2}$	\$	9,690,714
Total cost first mission, C	\$	85,059,246
Revenue first mission, R_1	\$	120,905,802
Revenue second mission, R_2	\$	196,507,673
First mission duration, t_{mis_1}	years	2.023
Second mission duration, t_{mis_2}	years	1.389
NPV	\$	148,609,632

6.4.2 Propellant Depot at Lunar Gateway

Similar to the sensitivity analysis presented in Section 5.3.1, the destination is changed to the Lunar Gateway. Relevant parameters are presented in Table 6.9 for both the Starship and Ariane V ES mission to asteroid 2000 SG344 and the Lunar Gateway. The remaining optimised mission details are as shown in Table 6.5, within 1 day difference of phasing, which is considered within the tolerances of the genetic algorithm.

The results in Table 6.9 show that due to the modest increase in p and the decrease in ΔV^I (causing an increase in $m_{\text{r,sold}}$) the NPV for a mission to the Lunar Gateway would be greater than to GEO, for both the Starship and Ariane V mission. The increase in revenue is equal percentage-wise, but due to different cost and revenue ratios, the percentage increase of NPV is bigger for the Starship (38.6%) than it is for the Ariane V ES mission (25.6%).

Table 6.9: Modified parameters for mission to the Lunar Gateway. GEO results from on Table 6.5.

Parameter	**Unit**	**Starship**		**Ariane V ES**	
		GEO	**Lunar Gateway**	**GEO**	**Lunar Gateway**
ΔV_{ks}	km/s	3.940	3.968	3.940	3.968
p	\$/kg	658	664	29,947	30,203
ΔV^I	km/s	1.575	0.866	1.577	0.867
m^I_{prop}	tonnes	161.6	95.9	25.6	15.2
$m_{\text{r,sold}}$	tonnes	319.3	385.0	50.5	60.8
Revenue	\$	210,199,603	255,606,018	1,510,977,855	1,837,189,084
NPV	\$	102,181,163	141,671,140	1,111,403,709	1,395,782,969

6.4.3 Expectation Net Present Value

Following the equation for the expectation NPV (ENPV, Eq. (4.6)), which takes the probability of mission success (P_{s}) into account, it can be calculated what the minimum probability of mission success has to be for a positive NPV. Using the values from Table 6.5, the ENPV is as shown in Fig. 6.10 for both the Starship and Ariane V ES launch vehicles, for both the GEO and Lunar Gateway missions. Figure 6.10 shows the ENPV for a probability of mission success from 0 to 100%.

Results show that when assuming Ariane V ES launch cost and payload capacity, a lower chance of success would be possible to still achieve break-even than when assuming the Starship. Note that in the case of failure of a single mission, this break-even is not reached, but if multiple of the same missions are executed this metric is useful. Also, the results demonstrate that to the Lunar Gateway scenarios, a lower chance of success is possible. Both of these observations are explained by the higher generated revenue in the Ariane V ES and Lunar Gateway missions.

6.4.4 Monte Carlo Simulations

In order to investigate the influence of key parameters used in the optimisation, a range of Monte Carlo simulations is performed. The Monte Carlo simulations are based on the results of the Starship to the asteroid 2000 SG344, which are more conservative than when considering the high specific launch costs of the Ariane V ES. Uncertainties on the input parameters are considered, after which the uncertainty of the resulting NPV can be determined. Table 6.10 shows a range of input parameters which have

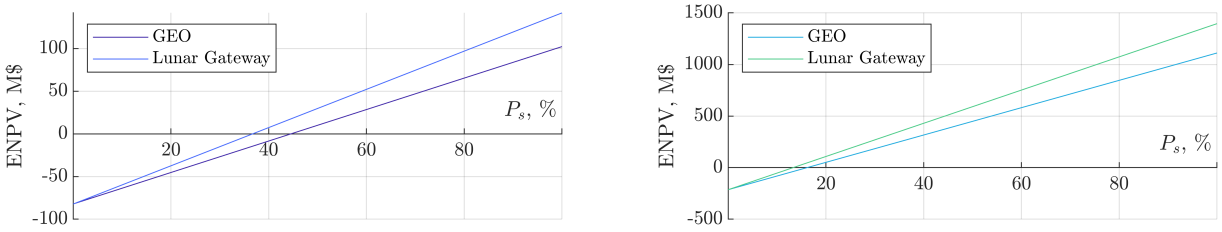

(a) For Starship missions.

(b) For Ariane V ES missions.

Figure 6.10: Expectation Net Present Value for missions to asteroid 2000 SG344. Based on Table 6.5 for GEO and Table 6.9 for the Lunar Gateway.

an influence on the resulting NPV and the parameters used to model the uncertainty as a normal probability density function. The standard deviation σ used is arbitrarily chosen as 10% of the mean value. This should result in a relative metric for the sensitivity of each parameter with respect to the others.

Table 6.10: Inputs for Monte Carlo simulation of optimised missions.

Parameter	**Mean value**	**Standard deviation σ**	
Base throughput rate, κ_{base}	200	20	kg/day/kg of MPE
Discount rate, I	10	1	%
Manufacturing cost, c_{man}	1007.12	100.71	\$/kg
Development cost, c_{dev}	37.19	3.72	\$/kg
Operations cost, c_{op}	6.98×10^6	6.98×10^5	\$/year
Minimum structural coefficient, ϵ_{min}	0.10	0.01	
Albedo, p_{vC}	0.06	0.006	
Density, ρ_{C}	1300	130	kg/m^2
Recovery ratio, $\lambda_{\text{volatile}}$	0.10	0.01	

The simulations are performed for the Starship case study using asteroid 2000 SG344 for all parameters except p_{vC}, ρ_{C}, and $\lambda_{\text{volatile}}$. These parameters influence $m_{\text{r,available}}$ and since this is much larger than $m_{\text{r,mined}}$ for asteroid 2000 SG344, the effect on the NPV would not be visible. Therefore, the mission to asteroid 2016 RD34 is investigated for these three input parameters, for which $m_{\text{r,available}}$ is used completely in the Starship mission optimised for maximum NPV.

For each simulation, 1000 scenarios are optimised and the resulting NPV is displayed using a boxplot in Fig. 6.11. For each boxplot, the central line indicates the median value and the box contains 50% of the results, with the bottom and top edges of the box marking the 25$^{\text{th}}$ and 75$^{\text{th}}$ percentiles, respectively. The dashed lines extend to the most extreme results not considered outliers, with the outliers are plotted individually in red. Rather than performing a computationally expensive global optimisation for each simulation, a local optimisation starting from the result in Table 6.5 is performed using `fmincon`.

From Fig. 6.11 the relative influence of certain parameters on the final NPV can be seen, by comparing the boxplots, in particular the 25% and 75% markings of each box. It can then be deduced that one of the most influential parameters is the minimum structural coefficient. This has to be taken into account in the determination of $m_{\text{r,transportable}}$ and therefore limits m_{r}, as well as while calculating the resource price p because it influences the mass of the kickstage used for Earth-launched resources. A value of $\epsilon_{\text{min}} = 0.1$ has been used in this work, which is considered reasonable for current and

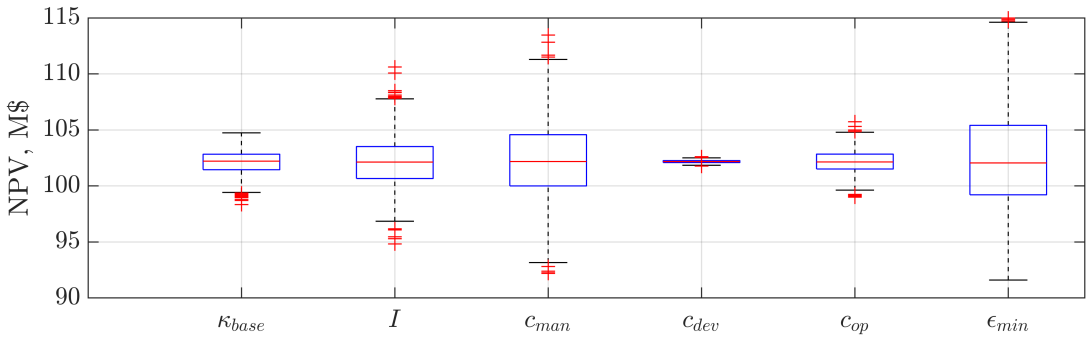

(a) To asteroid 2000 SG344.

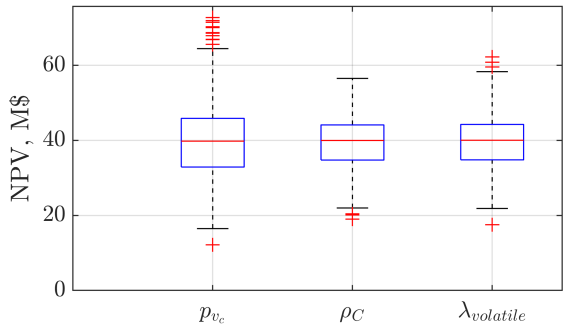

(b) To asteroid 2016 RD34 (with $H = 27.6$), $\sigma = 10\%$ of mean value.

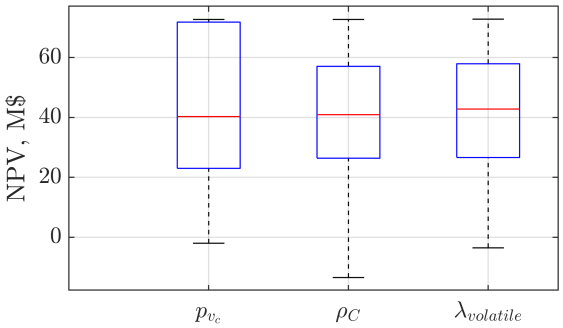

(c) To asteroid 2016 RD34 (with $H = 27.6$), $\sigma = 40\%$ of mean value.

Figure 6.11: Monte Carlo analyses.

near-future technology [220], and slightly lower values could be expected in the future, as shown by the proposed Starship with $\epsilon = 0.099$ including protection for repeated atmospheric entries.

The Monte Carlo analyses on asteroid 2016 RD34 is also carried out for a higher standard deviation, to highlight that at some point the cargo spacecraft is at full capacity. To this extent, a four times higher standard deviation is used and the result is presented in Fig. 6.11c. What stands out in Fig. 6.11c is that no NPV above 72.7 M$ is found, because at that point the cargo spacecraft is at full capacity and the transfers cannot be optimised further to increase this cargo capacity. For all other simulations, the cargo spacecraft would have unused storage capacity left with the optimal transfers and resulting ΔVs. The optimiser then aims to minimise this unused cargo capacity in order to not spend unnecessary funds on the development/manufacturing of such a large cargo spacecraft. This can be done by optimising the transfers to and from the asteroid such that $m_{\text{sc,dry}}$ decreases, possibly to as low as is allowed by ϵ_{min}. In addition, Figs. 6.11b and 6.11c show that a change in albedo has a relatively larger effect on $m_{\text{r,available}}$ than the same relative change of density and recovery ratio.

6.5 KEY FINDINGS

For decreasing launch costs, the NPV that can be achieved also decreases, because the decrease in total cost is more than offset by the decrease in revenue. The revenue is dependent on the launch cost because the resources are sold at a price competitive with launching them from Earth. The market price therefore decreases if the specific launch cost decrease. On the other hand, the results show that for increasing payload capacity, the NPV increases slightly. Depending on the ratio of how much launch costs decrease and payload capacities increase in the future, the net resulting NPV can therefore either increase or decrease, but are more likely to decrease because the launch cost effect is

stronger.

Case studies for the SpaceX Starship system (136 metric tonnes for an assumed cost of 13.1 M$) and the Arianespace Ariane V ES (21.5 metric tonnes for 195 M$) show that for asteroid 2000 SG344, the NPV is 102.2 M$ and 1111.4 M$, respectively. Here it is assumed that the launch vehicle under consideration is the only launch vehicle that can be used for delivering resources to GEO. If the Ariane V ES launch vehicle is used while the less expensive Starship system is available too, the NPV is negative for all asteroids because the resource price has to be competitive with launching the same resources from Earth using the Starship system.

Extending the investigated mission scenario for the Starship case study with a second trip shows that a higher NPV can be generated, although a considerable portion of the returned resources have to be used for the next outbound transfer. Also, it is shown that by selling the resources at the Lunar Gateway instead of GEO, which changes ΔV^I and the market price, a higher NPV can be generated.

The results show that it is very important to take the specific launch costs into account when assessing the profitability of an asteroid mining venture. In some other economic models for asteroid mining, even recent studies [3, 22, 30, 115, 126], the specific launch costs are closer to the results of the Ariane V ES launch vehicle investigated here, thereby overestimating the profitability of asteroid mining.

Chapter 7

IDENTIFYING VALUABLE SUPPLY CHAINS

Comparing the economic aspects of asteroid mining with those of Lunar and Martian mining is important. Compared to asteroid mining, both Lunar and Martian mining have had more research dedicated to them. It is therefore imperative to know what the relative merits of asteroid mining are, to focus further research towards or away from asteroid mining.

This Chapter aims to explore the economic and commercial potential of SRU at a number of customers in various locations, through the parametric approach described in Chapter 4. Using the same economic model, applied to a range of different mission architectures, allows for an unbiased comparison. These results can then be used to identify potential value chains to focus further research. The goal of this Chapter is therefore to identify combinations of material sources and customer locations for which mining, processing and selling LOX/LH_2 has the lowest specific cost.

This Chapter is based on the work published in Ref. [37], with no notable changes besides the sensitivity analyses: regarding aerocapture at Earth and the inclusion of MCAs. Reference [236] offers an extension to the work originally published in Ref. [37], focused on one specific scenario addressed in this work. Where relevant, the conclusions of Ref. [236] are addressed.

7.1 METHODOLOGY

The methodology of this Chapter is as described in Chapter 4, including the calculations for the total cost, mass budget and trajectories. The objective for the optimisation will be the specific cost, c, repeated here:

$$c = \frac{C}{m_{\mathrm{r,sold}}}$$

in which $m_{\mathrm{r,sold}}$ is the resource mass sold at the customer location. The total cost C includes launch, development, manufacturing, operations and propellant costs. Whereas the previous Chapters focused on optimising the NPV, it is more appropriate here to compare the specific cost c. This is because the NPV compares all costs with those for Earth-launched resources, and the goal here is to compare a range of material sources with each other.

Missions starting at the Earth, mining at the source, and delivering the resources to various customer locations will be investigated. The following material source locations are proposed:

1. Earth surface;
2. Lunar surface;
3. Representative NEA;
4. Martian surface;
5. Representative MBA.

More specifically, the NEA 2000 SG344 (an Aten asteroid) and the MBA 2015 AE282 are considered, based on favourable orbital characteristics (i.e., close proximity to the Earth's orbit and in the inner belt, respectively, as well as a low inclination) and brightness (relating to their size). However, in Section 7.3.3 a search of other asteroids is conducted to assess the importance of specific target asteroid selection. In absence of a known spectral type for these asteroids, it is assumed that these asteroids are water-bearing C-type asteroids.

Note that for all combinations with the Earth surface as the material source, no mining takes place, meaning that the cargo spacecraft delivers resources directly to the customer, as visualised on the left in Fig. 4.4.

Customer locations to be considered are:

1. Earth surface;
2. LEO, 400 km, similar to the International Space Station;
3. GEO;
4. Sun-Earth L_1-point (SE-L_1);
5. Sun-Earth L_2-point (SE-L_2);
6. Lunar surface;
7. LLO, 100 km circular orbit;
8. Lunar Gateway;
9. Martian surface;
10. Mars Base Camp, elliptical orbit, 1 sol period, 400 km periapsis [230];
11. Sun-Mars L_1-point (SM-L_1);
12. 16 Psyche, a metallic MBA.

These destinations are considered because of the need for water and other volatiles, either for human consumption or as propellant [29, 30]. As briefly noted in Chapter 4, the Lunar Gateway is a proposed modular space station located in a stable orbit around an Earth-Moon Lagrange point, which will be used to test and verify technologies and procedures for crewed missions in deep space [237]. The Mars Base Camp is a proposed space station to be assembled in orbit around Mars [230]. Psyche is

considered as a possible destination since it is a large metallic M-type asteroid and in order to mine metals, water is required [118]. All possible combinations are investigated, leading to a total of 60 scenarios that have to be optimised. A schematic showing the wide spread of material source and customer locations is presented in Fig. 7.1 with labels corresponding to the two lists above.

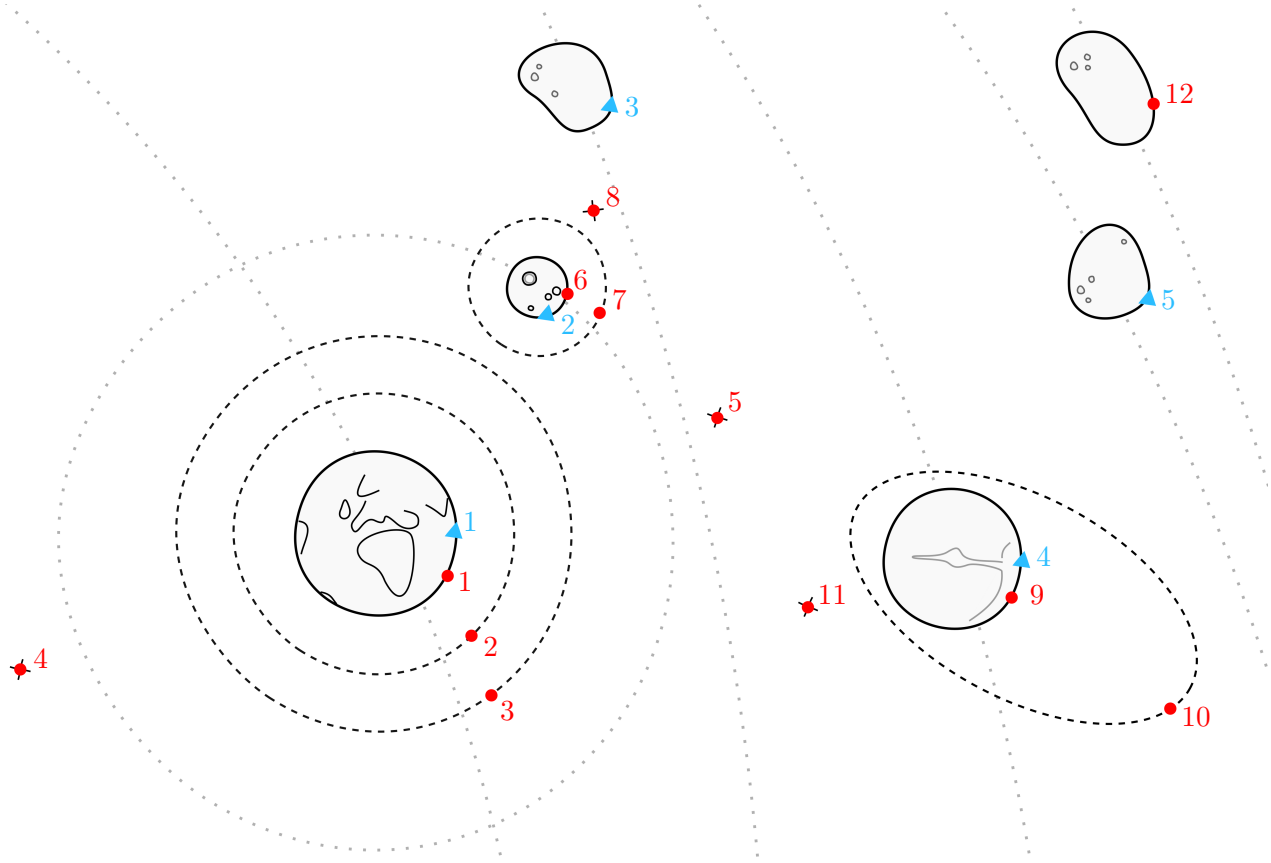

FIGURE 7.1: SCHEMATIC SHOWING THE SOURCE (BLUE TRIANGLES) AND CUSTOMER (RED CIRCLES) LOCATIONS. SOURCE LOCATIONS: 1) EARTH SURFACE, 2) LUNAR SURFACE, 3) NEA, 4) MARTIAN SURFACE AND 5) MBA. CUSTOMER LOCATIONS: 1) EARTH SURFACE, 2) LEO, 3) GEO, 4) SE-L_1, 5) SE-L_2, 6) LUNAR SURFACE, 7) LLO, 8) LUNAR GATEWAY, 9) MARTIAN SURFACE, 10) MARS BASE CAMP, 11) SM-L_1, AND 12) PSYCHE.

7.2 PRIMARY RESULTS

This Section presents the results obtained using the methodology in Section 7.1 and Chapter 4, for all material source and customer locations. Table 7.1 shows these primary results. For each scenario (i.e. combination of material source and customer location) for which the optimisation algorithm found a solution, the specific cost (c in \$/kg), total mission duration (t_{mis} in years), required velocity change from material source to customer location (ΔV^I in km/s) and delivered mass ($m_{\text{r,sold}}$ in tonnes) are presented. For each scenario for which the optimisation found no solution, meaning that the imposed non-linear constraints could not be satisfied, no information is given. For scenarios involving Earth-based resources (first column), ΔV^I is the ΔV from the parking orbit (at 185 km [164]) to the destination, because there is only a cargo spacecraft directly from LEO, without a mining phase, as discussed in Section 4.4.

Note that the results in Table 7.1 are optimised individually for each departure/target pair and cannot be directly combined to create new scenarios. For example, results for the "NEA → Lunar

Table 7.1: Primary results for all combinations of resource and customer locations. Legend in bottom-right corner. Specific-cost cells with the lowest value for each customer have been marked green.

Source → / Customer ↓	Earth surface		Lunar surface		NEA (2000 SG344)		Martian surface		MBA (2015 AE282)	
Earth surface	**1**	0 0 ∞	580	0.39 2.58 90.8	335	1.63 0.88 258.3	-	- - -	-	- - -
LEO (400 km)	**231**	∼0 0.01 118.6	967	0.47 5.81 55.0	411	1.46 3.33 204.4	-	- - -	3,603	5.01 7.38 20.6
GEO	658	∼0 3.94 41.7	485	0.47 3.70 109.6	**250**	1.46 1.54 336.6	-	- - -	2,750	5.04 6.79 27.1
SE-L_1	661	0.18 3.81 43.4	427	0.68 3.18 127.9	**212**	2.28 0.55 388.2	-	- - -	9,655	3.69 8.93 6.6
SE-L_2	661	0.18 3.81 43.4	427	0.66 3.18 127.7	**214**	1.49 1.00 397.6	-	- - -	4,090	3.69 7.79 15.7
Lunar surface	1,279	0.02 5.92 21.5	**177**[1]	0.45 0 299.9	362	1.48 2.88 232.8	-	- - -	6,326	5.11 8.33 11.8
LLO	665	0.02 3.96 41.4	291	0.45 1.91 182.2	**213**	1.48 0.92 396.4	19,387	3.22 7.74 4.3	2,289	3.77 6.42 27.5
Lunar Gateway	666	0.01 3.97 41.3	352	0.49 2.58 151.3	**216**	1.48 0.98 389.1	-	- - -	3,684	3.76 7.58 17.6
Martian surface	4,778	0.90 6.77 8.54	3,919	1.46 6.67 15.3	3,631	1.75 6.75 23.2	**336**[1]	1.09 0 148.9	1,987	4.07 4.42 34.1
Mars Base Camp	915	0.56 4.57 34.2	673	1.36 4.41 88.3	538	1.72 4.13 155.6	1,916	1.03 5.28 25.9	**511**	2.95 2.14 114.2
SM-L_1	1,563	0.56 6.11 20.0	1,104	1.36 5.87 53.8	1,085	3.33 5.91 86.9	2,455	1.36 5.70 21.2	**937**	4.04 3.92 72.0
16 Psyche	-	- - -	-	- - -	-	- - -	-	- - -	**916**	4.45 3.77 76.8

[1] Specific cost based on one full cargo spacecraft, mining equipment can potentially last longer.

Legend:	c	[$/kg]	t_{mis}	[years]
			ΔV^I	[km/s]
			$m_{\text{r,sold}}$	[tonnes]

Table 7.2: Details for example mission "NEA → Lunar Gateway".

Parameter	**Unit**	**Value**
Semi-major axis	AU	0.977
Eccentricity		0.067
Inclination	deg	0.112
Launch date		30-06-2055
Duration outbound transfer	days	218
Stay time at NEA	days	182
Duration inbound transfer	days	144
Total mission duration	years	1.490
ΔV^O	km/s	3.731
ΔV^I	km/s	0.982
m_{l}	tonnes	136.1
m^O_{prop}	tonnes	78.1
m_{cargo}	tonnes	55.7
m_{mpe}	tonnes	23.1
m_{r}	tonnes	501.1
m^I_{prop}	tonnes	111.9
$m_{\mathrm{r,sold}}$	tonnes	389.1
Launch cost	$	13,095,922
Development cost spacecraft	$	2,156,228
Manufacturing cost spacecraft	$	58,431,517
Propellant cost spacecraft	$	74,064
Operations cost	$	10,394,794
Total cost	$	84,152,525
Specific cost	$/kg	216.3

surface" scenario and "Lunar surface → Lunar Gateway" scenario cannot be combined for a "NEA → Lunar surface → Lunar Gateway" mission. Each scenario in Table 7.1 has been optimised for minimum specific cost. As part of this optimisation, the spacecraft is sized specific for that mission, as shown in Fig. 4.2, resulting in a range of different-sized cargo spacecraft. In addition, the cargo spacecraft will not be completely filled with propellant at the start of the next transfer as part of the propellant will already have been used.

A more detailed overview of one example mission scenario, "NEA → Lunar Gateway", is given in Table 7.2. Note that the launch date is in an arbitrarily-chosen time frame, as noted in Section 4.5, and could be moved by a (number of) synodic period(s).

To emphasise that the goal of this work is to compare different scenarios, rather than give absolute values, Table 7.3 presents the relative metrics for the Lunar Gateway and Mars Base Camp. The specific cost and delivered mass are normalised by the values for the scenarios involving a direct launch from the Earth's surface.

7.2.1 Discussion

There are a number of observations that stand out from Table 7.1. First, by far the lowest specific cost for LOX/LH_2 for customers on the Earth, Lunar and Martian surface is realised by material sourced in the same location, rather than mining and processing elsewhere. Mining elsewhere and subsequent

Table 7.3: Relative metrics for scenarios involving the Lunar Gateway or Mars Base Camp.

Material source location	Lunar Gateway		Mars Base Camp	
	c, normalised	**$m_{r,sold}$, normalised**	**c, normalised**	**$m_{r,sold}$, normalised**
Earth surface	1.000	1.000	1.000	1.000
Lunar surface	0.529	3.663	0.735	2.577
NEA (2000 SG344)	0.325	9.419	0.598	4.930
Martian surface	-	-	2.095	0.756
MBA (2015 AE282)	5.538	0.427	0.558	3.339

transport to surface locations means that a fraction of the propellant is used for this transfer, resulting in lower $m_{r,sold}$ than for the scenario where mining occurs on the same surface. The results in Table 7.1 are for only one full tank of propellant, but when mining occurs on the same surface, the equipment can last longer, which could drive down the costs with respect to the numbers presented in Table 7.1.

Furthermore, scenarios involving NEA 2000 SG344 show that this asteroid is in a strategic location, able to provide LOX/LH_2 to many destinations in the vicinity of Earth at the most competitive specific cost for one mission. Exceptions are customers at surface locations, as discussed before, and LEO, which is very close to the parking orbit after launch from the Earth surface. The reason for the competitive specific cost is the relatively low ΔV^O from Earth escape to the NEA, which allows for a large part of the payload capacity of the launch vehicle to be used for structural mass of the cargo spacecraft, which in turn allows for a relatively large quantity of propellant to be transported. The ΔV^O to other sources are higher because the spacecraft either has to perform a soft landing (for which $\Delta V = 1.963$ or 0.595 km/s, on the Moon and Mars, respectively, per Table 4.8), and/or transfer far from Earth to either Mars or the MBA, with a semi-major axis of 1.52 and 2.01 AU, respectively.

For customers further afield, in the vicinity of Mars and at the metallic MBA 16 Psyche, MBA 2015 AE282 is able to provide resources at the lowest specific cost for one mission. Resources from this MBA could possibly even be used to support deep space missions outward from the main belt. However, Table 7.1 also shows that it is in general cost-prohibitive or infeasible to transport resources from the MBA back to customers in vicinity of the Earth, even if the target asteroid is positioned in the inner main belt, as is the case for the MBA investigated in Table 7.1. Besides the high specific cost, long mission durations are associated with missions selling to customers in the vicinity of the Earth. Long mission durations are unattractive for investors [24].

Another observation is related to scenarios mining and processing on the Martian surface. Table 7.1 shows that many scenarios are infeasible. This is due to two reasons. First, there is a mass penalty on the structural mass of the spacecraft because it has to withstand atmospheric entry (as discussed in Section 4.5) and second, there is a large ΔV cost for ascent from the Martian surface (4.026 km/s [229]). Because of the increase in minimum structural coefficient ($\Delta\epsilon_{entry}$), the maximum ΔV decreases: $\Delta V_{max} = I_{sp} g_0 \log\left(1/\left(\epsilon_{min} + \Delta\epsilon_{entry}\right)\right)$. Combined with the high ΔV for ascent, this means that many scenarios are not feasible. Interestingly, scenarios mining and processing on the MBA perform better than those mining and processing on Mars, meaning that the larger semi-major axis of the MBA is outweighed by these two drawbacks for Mars. This is especially striking for customers at the Mars Base Camp: the specific cost is lower from all considered material sources other than the Martian

surface, when considering one single mission. Due to the proximity to the Martian surface, repeated missions would be possible and could drive down the cost, but $m_{\mathrm{r,sold}}$ of each mission is relatively small.

In addition, based on the results in Table 7.1, high-thrust missions to Psyche are shown to be only possible by refuelling at an intermediate MBA, for the mission architecture defined here: a single stage from the LEO parking orbit to the destination using a hyperbolic trajectory to escape from the Earth. Of course other mission scenarios can be envisaged, but if a fully reusable launch vehicle such as SpaceX's Starship system is to be used, a closed parking orbit is unavoidable. On Psyche, water would be needed to mine metals on the metal-rich asteroid [118]. In Table 7.1 only one NEA is investigated, but potentially other NEAs can be used as a refuelling location on the way to Psyche, which will be investigated in Section 7.3.3.

Finally, observations can be made regarding the total quantity of volatiles delivered to the customer. Because the missions delivering Earth-sourced volatiles are limited to the payload capacity of the launch vehicle, it is shown in Table 7.1 that $m_{\mathrm{r,sold}}$ is relatively low to customers beyond GEO, compared to other material sources. In contrast, scenarios mining and processing at NEA 2000 SG344 can deliver the largest quantity of volatiles to many destinations for one single mission. This is because ΔV^O is low, as discussed above, and therefore a significant fraction of the payload capacity of the launch vehicle is dedicated to the structural mass of a large cargo spacecraft. In addition, ΔV^I is also relatively low for the NEA-scenarios, meaning that less propellant is "wasted" on the transfer to the customer.

In 2016, the United Launch Alliance announced prices it is willing to pay for propellant in space at several locations. In a mid-term time frame, these prices are ∼1,000 $/kg at the Earth-Moon L_1-point and ∼500 $/kg on the Lunar surface [238]. Comparing these costs with Table 7.1, and assuming that propellant will not be sold at cost price but will include a mark-up, it is clear that delivery of propellant from the Earth will not meet these prices in the vicinity of the Moon, but mining on the Lunar surface or a NEA will be required. Whilst this study focuses on delivery to customers located at the final location in space, the commercial enterprise mining and processing these space-based resources can also choose to use these resources themselves, which would remove the need for a mark-up on the price.

It is worth noting that $m_{\mathrm{r,sold}}$ does not have to consist of the combination of LOX and LH_2 suitable for rocket propellant per se, but $m_{\mathrm{r,sold}}$ could consist of any other water-derived resource [239]. For example, instead of venting and therefore discarding oxygen, it can also be transported, such that customers only have to bring the (much lighter) LH_2 and can buy the (heavy) LOX in space. This way, less mined resources are wasted through venting and therefore the specific cost can be brought down. The potential value of this is confirmed in Ref. [236]. Also, pure water could be transported, which would also allow for a reduction in cost because less oxygen has to be vented and less water has to be electrolysed (note that the cargo spacecraft still requires LOX/LH_2). For any resource other than the combination of LOX/LH_2 used, the analysis would have to be carried out with slightly varied input values for the throughput rate, κ, and/or the mixture ratio, λ_{MR}. When transporting different resources than LOX/LH_2, care should be taken that there is sufficient propellant left in the spacecraft to transfer from the source to the final destination.

The results in Table 7.1 are optimised and obtained for one single mission, but the MPE can likely be reused for up to ∼10 years [236]. During these years, more propellant can be produced (for asteroids until $m_{\mathrm{r,available}}$ is used up) and transported to the customer. This can bring down

the specific costs with respect to the data presented in Table 7.1, depending on the material source location. For Earth-sourced propellant, the scenarios do not include mining of the resources, meaning that these specific costs cannot be brought down this way. For Lunar-sourced propellant, as pointed out in Ref. [236], the specific costs can decrease substantially because of the close proximity of the Moon to many customers investigated in Table 7.1, allowing for rapid turnaround times. This is less the case for asteroids, especially for MBAs, for which longer trip durations and a varying distance to the Earth complicate regular trips back and forth between the customer and the material source location. As noted in Ref. [236], when optimising more than one mission, it is likely that the optimiser favours utilising more of the payload capacity of the launch vehicle for MPE rather than the cargo spacecraft, such that propellant can be produced quicker and more (smaller) cargo spacecraft can be filled in the same timespan, which increases the total delivered resources for an equal total system mass.

It can be noted however, that the costs presented in this paper will have significant uncertainty and risks are likely weighted strongly towards the increased costs. Dependency on intermediate missions advancing technology readiness and planning for the mid- to far-term time frame adds to the inherent uncertainties of cost estimation. Nonetheless, the results presented here can be used to focus future research on potentially more profitable and feasible missions. More importantly, the relative metrics, such as those shown in Table 7.3 can be used to shape future research and mission design. Table 7.3 confirms the preferred selection of the material source for customers at the Lunar Gateway and Mars Base Camp, without relying on the absolute specific costs presented in Table 7.1, which have a higher uncertainty.

7.3 SENSITIVITY ANALYSIS

This Section presents a sensitivity analysis for a number of input parameters to the model. Because of the assumptions in the cost model and the inherent uncertainty of planning future missions, a sensitivity analysis is important. First, a range of Monte Carlo analyses investigates the sensitivity of the model to relevant input parameters. Next, the effect of some assumptions in the cost model are investigated. Also, the impact of asteroid selection is examined. Finally, the effects of incorporating aerocapture at Earth are investigated. Rather than producing a series of tables similar to Table 7.1, these sensitivity analyses are carried out for a smaller number of relevant scenarios, which depend on the input parameter under investigation.

7.3.1 Monte Carlo Analysis

Due to the highly non-linear nature of the optimisations in this thesis, a Monte Carlo simulation is considered appropriate to assess the uncertainty of the results based on uncertainty of the input parameters. For the Monte Carlo analysis, the following input parameters are regarded as relevant: specific impulse (I_{sp}), minimum allowed structural coefficient (ϵ_{min}) and the additional structural coefficient for atmospheric entry ($\Delta\epsilon_{\mathrm{entry}}$), cost elements for development, manufacturing, launch and operations (c_{dev}, c_{man}, C_{l}, c_{op}), throughput rate (κ) and launch vehicle payload capacity (m_{l}). For these input variables, the scenarios "NEA → Lunar Gateway" and "NEA → Mars Base Camp" are investigated. These two are considered due to their potential for human exploration and the corresponding need for propellant and other water-based resources. In addition, for the uncertainty in κ, "Lunar Surface → Lunar Gateway" and "Mars → Mars Base Camp" are considered, to investigate the sensitivity

to κ on other material source locations besides NEAs. For $\Delta\epsilon_{\text{entry}}$, "Mars → Mars Base Camp" is considered instead of "NEA → Lunar Gateway" and "NEA → Mars Base Camp", because $\Delta\epsilon_{\text{entry}}$ is not applicable in those scenarios due to the absence of atmospheric entry.

Note that Sections 5.3.4 and 6.4.4 have already shown the effect on NPV of various cost elements, but this Section shows the effect on the specific cost and adds a number of other parameters not considered earlier. The effect of these parameters can now be seen in relation to the parameters investigated earlier. In addition, different scenarios are investigated compared to previous Chapters.

The uncertainty on the input parameters is modelled using a Gaussian probability density function, with the mean value as described in Section 7.1, and a standard deviation σ is again chosen as 10% of this value to provide a means to assess the sensitivity of each parameter with respect to the others. The Monte Carlo simulations are performed for each input parameter separately by optimising the scenario using one changed input. For each scenario considered for each input parameter, a total of 500 pseudo-random samples of the input parameter are used to initialise the optimisation. The specific cost is subsequently optimised for each instance, following the optimisation procedure using a genetic algorithm described in Section 4.5. The resulting distributions of specific costs are visualised using boxplots in Figs. 7.2a–7.2d. Note that an explanation on the interpretation of boxplots can be found in Section 5.3.4. Due to how the uncertainties on the input parameters are modelled, the boxplots present clear indications of how sensitive the solution is to an equal relative change in the input parameters. The Monte Carlo simulations have been distributed over Figs. 7.2a–7.2d in a way that allows for meaningful comparison with other simulations. Note that within Fig. 7.2c and 7.2d the vertical axis spans an equal range, but centred around a different specific cost, to allow for comparison between the missions.

From Figs. 7.2a and 7.2b it is apparent that the minimum specific cost is most sensitive to uncertainties in the imposed minimum structural coefficient for the spacecraft and the manufacturing

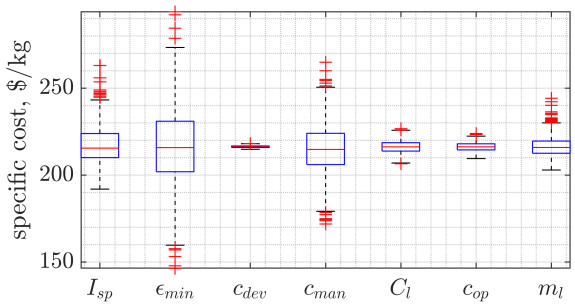

(a) For scenario NEA → Lunar Gateway.

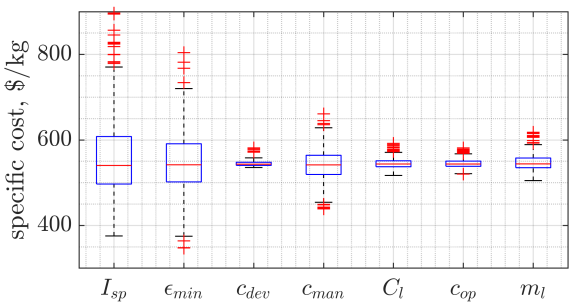

(b) For scenario NEA → Mars Base Camp.

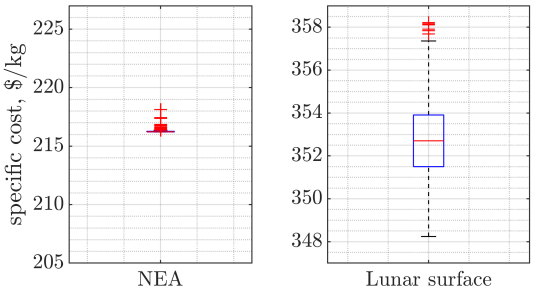

(c) For scenarios to Lunar Gateway, regarding κ.

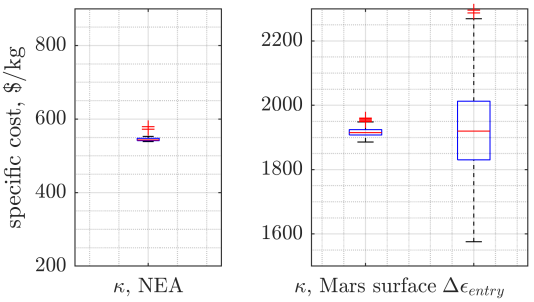

(d) For scenarios to Mars Base Camp, regarding κ and $\Delta\epsilon_{\text{entry}}$.

Figure 7.2: Resulting boxplots of Monte Carlo simulations.

cost. Also, uncertainties in the development cost have a relatively small effect on the specific cost of the mined resources. The observations are the same for both the Lunar Gateway and Mars Base Camp scenarios. From Figs. 7.2c and 7.2d it is evident that the throughput rate also has a relatively minor effect, especially when comparing the vertical axis range with Figs. 7.2a and 7.2b. It is shown that the sensitivity to the throughput rate differs slightly depending on the mining location, but the sensitivity is still minimal. In addition to this Monte Carlo simulation, which assumes a 10% standard deviation for the throughput rate, Table 7.4 shows the impact of smaller throughput rates for the "NEA → Lunar Gateway" and "NEA → Mars Base Camp" scenarios, beyond the 10% standard deviation. While Table 7.4 shows that the specific cost to produce LOX/LH_2 increases, as expected, it also shows that the impact is rather limited, even for dramatically lower throughput rates. These optimised missions with a lower throughput rate κ all show very similar trends: that to offset the decrease in throughput rate, the stay time at the source is increased, which has an impact on the operational costs as per Eq. (4.1). This is preferred over increasing m_{mpe}, as this would mean that the cargo spacecraft is smaller and therefore that less resources can be transported.

Table 7.4: Effect on specific cost (in $/kg) of lower throughput rates, for the primary mission from a NEA.

Multiplier	Lunar Gateway	Mars Base Camp
1	216	538
0.5	224	562
0.2	245	594
0.1	262	624
0.05	296	689

Where Figs. 7.2a and 7.2b show a relatively large sensitivity to the minimum structural coefficient, Fig. 7.2d shows that the specific cost is also relatively sensitive to the imposed additional structural coefficient for atmospheric entry. Because the spacecraft on which $\Delta\epsilon_{\text{entry}}$ is based have not yet flown, and could experience mass growth, this sensitivity is especially important. Future research should take this sensitivity into account. These observations are consistent with those in Chapter 6.

7.3.2 Cost Model Assumptions

The methodology described in Chapter 4 assumes aviation-like costs for development and manufacturing costs elements. It is assumed that technology has matured sufficiently through intermediate missions, because of the mid- to far-term time frame considered for the missions described in this thesis. Since there is significant uncertainty on when this time frame will occur, a sensitivity analysis has been carried out with higher development and manufacturing costs. To achieve this, the production volume has been varied, which, as described in Chapter 4, directly influences the development and manufacturing costs. The total development cost is spread evenly over all units in the production volume, while the manufacturing cost experiences the learning curve effect, following Eq. (4.3).

Table 7.5 shows the effect of changing the production volume for two scenarios: "NEA → Lunar Gateway" and "NEA → Mars Base Camp". In the baseline methodology, a production volume of 2,033 units is used, based on the production volume of the Boeing 777[1]. This sensitivity analysis investigates the effect of using from 1 to 10,000 units in various steps, by optimising the missions

[1] `http://www.boeing.com/commercial/#/orders-deliveries`, accessed May 31st, 2019

Table 7.5: Effect on specific cost (in $/kg) of changing the production volumes for the primary mission from a NEA.

Production volume	$\mathbf{c_{dev}}$	$\mathbf{c_{man}}$	**Lunar Gateway**	**Mars Base Camp**
1	75,600	2,875	10,917	27,663
10	7,560	2,094	1,456	3,590
100	756	1,525	400	987
500	151	1,222	265	664
1,000	76	1,111	238	593
2,033	37	1,007	**216**	**538**
5,000	15	890	195	490
10,000	7	809	182	458

again with the different development and manufacturing costs resulting from the production volume. Table 7.5 shows that, for the two investigated scenarios, in order to have specific costs under 1,000 $/kg, the production volume has to be at least 100 units, when assuming the cost model adopted in this paper. Note that these units do not necessarily have to be for the exact same mission, but that development/manufacturing costs can also be brought down when similar large deep-space cargo spacecraft are designed and built. In more general terms, the specific costs for the two investigated scenarios are under 1,000 $/kg when development costs are able to reach the level of ∼750 $/kg and manufacturing cost of ∼1,500 $/kg as a maximum, regardless of the cost estimation technique that is used. In even more general terms, this is possible when the sum of development and manufacturing costs are under ∼2250 $/kg.

The next sensitivity analysis is aimed at the development and manufacturing cost for the MPE. While industry has significant experience designing and building spacecraft, this is not necessarily the case yet for designing and manufacturing MPE. To this extent, the impact of higher development/manufacturing costs for MPE is investigated. Table 7.6 shows the resulting specific cost for two scenarios: "NEA → Lunar Gateway" and "NEA → Mars Base Camp", considering that development/manufacturing cost for MPE are n times the baseline, which is still used for the spacecraft in the re-optimised scenarios. As shown in Table 7.6, even when the development and manufacturing costs for MPE are 10 times as high, the specific cost per delivered kg of propellant to the Lunar Gateway and Mars Base Camp only changes by 18% and 15%, respectively.

Table 7.6: Effect on specific cost (in $/kg) of higher specific development and manufacturing cost for MPE, for the primary mission from a NEA.

Multiplier	**Lunar Gateway**	**Mars Base Camp**
1	216	538
1.25	218	545
1.50	219	550
2	222	554
2.50	225	561
3	228	565
4	233	575
5	238	601
10	257	620

7.3.3 Different asteroids

To investigate the influence of target selection for the asteroids, a sensitivity analysis is carried out. At the time of writing, there are 23,390 NEAs, 19,661 MCAs, and 977,006 MBAs catalogued in the JPL SBDB.[2] The NEA targeted in the primary scenario, 2000 SG344, has Earth-like orbital elements: semi-major axis $a = 0.977$ AU, eccentricity $e = 0.067$ and inclination $i = 0.011$ deg. This allows for low ΔVs to and from the Earth, but not necessarily to Mars, for example. To this extent, the algorithm is executed using NEAs and MCAs in the database, to assess the effect of asteroid selection. The NEAs and MCAs with the lowest specific cost to the Martian surface, Mars Base Camp, SM-L_1 and Psyche are given in Table 7.7. Upon comparison with Table 7.1, it is clear that asteroid selection is very important for the separate destinations. Specific costs for customers at the Martian surface, Mars Base Camp, and SM-L_1 are all much lower if an asteroid is selected which is appropriate for this scenario, with orbital elements similar to those of Mars. This ensures a low ΔV^I which in turn ensures that only a small fraction of mined resources is used for transportation to the customer. This shows that it is more important to minimise ΔV^I than it is to minimise ΔV^O, if the goal is to achieve minimum specific cost. The inclusion of $\Delta\epsilon_{\text{entry}}$ can explain why the NEA with the lowest specific cost is not the same for the Martian surface and the Mars Base Camp for the Martian surface scenario, as this affects the mission.

While Table 7.1 shows that for NEA 2000 SG344, Psyche is out of reach, Table 7.7 shows that appropriate asteroid selection for this customer allows for a specific cost as low as 674 \$/kg using the adopted cost model. The selected asteroid has a rather eccentric orbit, which brings its perihelion relatively close to the Earth (1.62 AU) and, more importantly, its aphelion close to Psyche's orbit (2.928 AU for the MCA and a semi-major axis of 2.921 AU for Psyche), again aiming to especially minimise ΔV^I to reduce the consumption of propellant for transportation.

Similarly, the MBA targeted in the primary scenario is positioned in the inner main belt, at $a = 2.015$ AU, $e = 0.173$ and $i = 0.477$ deg. The inner main belt stretches between $2.0 < a < 2.5$ AU and the middle main belt between $2.5 < a < 2.82$ AU. This asteroid was selected due to its relative proximity to the Earth. However, again, this does not necessarily imply that it is the optimal asteroid for destinations further afield. Due to the sheer number of MBAs, 938,938 at the time of writing, it

[2] `https://ssd.jpl.nasa.gov/tools/sbdb_query.html`, accessed on August 20th, 2020.

Table 7.7: NEA and MCA with lowest specific cost for destinations at Mars and beyond.

	Parameter	Unit	Martian surface	Mars Base Camp	SM-L1	16 Psyche
NEAs	Specific cost	\$/kg	592	260	295	951
	Asteroid name		2005 UK5	2017 QN17	2001 FC7	2017 HK49
	Semi-major axis	AU	1.420	1.391	1.436	2.011
	Eccentricity		0.087	0.095	0.115	0.384
	Inclination	deg	2.609	2.540	2.621	2.138
MCAs	Specific cost	\$/kg	822	302	403	674
	Asteroid name		1999 XO141	1999 XO141	2016 SA47	2009 UP96
	Semi-major axis	AU	1.670	1.670	1.687	2.282
	Eccentricity		0.175	0.175	0.151	0.283
	Inclination	deg	0.051	0.051	0.042	0.036

is computationally unrealistic to run the algorithm on all MBAs. Instead, 20,000 MBAs are selected at random and results are extrapolated to the entire set. Because of this approach, a table similar to Table 7.7 cannot be produced. However, other meaningful conclusions can still be drawn. Table 7.8 shows the quantity of NEAs and MBAs available for mining for customers at the various locations, for a range of minimum specific costs. In addition, Figs. 7.3a and 7.3b show the distribution of these specific costs as histograms for the Lunar Gateway and Mars Base Camp, respectively.

Table 7.8 shows that for most customers, transferring to the main-belt and back is not beneficial, compared to transferring to a NEA or MCA. This is especially evident in the column $c < 2,000$ \$/kg, where it can be seen that there are no MBAs available to deliver propellant under 2,000 \$/kg to customers in the vicinity of the Earth, including the nearby collinear Lagrange points and customers on or near the Moon. For customers on or near Mars and Psyche, there is a a wider range of asteroids to choose from for affordable propellant. Even though there are many MBAs to select with $c < 1,000$ \$/kg, for the Mars-customers (on the surface, in the Mars Base Camp and in SM-L1) it is still cheaper to select a NEA or some MCAs. Only once these NEAs and MCAs have been depleted, will it be more cost efficient to use MBAs. It is important to note that Lunar resources can be delivered to the Lunar Gateway and Mars Base Camp for 352 and 673 \$/kg, respectively, according to Table 7.1. While these resources are finite and may need to be reserved for use *on* the Moon, asteroid resources may still have to compete with them. There are 72 NEAs that can deliver resources to the Lunar Gateway under 352 \$/kg, and no MCAs or MBAs. For the Mars Base Camp, there are 2105 NEAs, 960 MCAs, and ∼2000 MBAs that can deliver resources under 673 \$/kg. This means that if Lunar resources are used

TABLE 7.8: NUMBER OF AVAILABLE ASTEROIDS FOR A CERTAIN SPECIFIC COST, c, \$/KG.

Customer	**c < 500**			**c < 1,000**			**c < 2,000**			**c < 5,000**		
location	**NEA**	**MCA**	**MBA**	**NEA**	**MCA**	**MBA**	**NEA**	**MCA**	**MBA**	**NEA**	**MCA**	**MBA**
Earth surface	28	0	0	341	0	0	1.3k	0	0	3.1k	14	0
LEO (400 km)	13	0	0	1.4k	0	0	5.2k	27	0	11.7k	2.4k	2.3k
GEO	371	0	0	2.3k	3	0	5.7k	69	0	11.7k	3.3k	113k
SE-L1	173	0	0	1.1k	0	0	2.7k	5	0	5.5k	69	0
SE-L2	262	0	0	1.5k	0	0	3.7k	31	0	7.8k	383	0
Lunar surface	35	0	0	868	0	0	2.8k	8	0	6.5k	127	0
LLO	696	0	0	2.9k	7	0	6.5k	138	0	12.3k	4.7k	33.1k
Lunar Gateway	346	0	0	1.8k	1	0	4.2k	38	0	8.9k	631	0
Martian surface	0	0	0	55	11	0	799	243	47	3.4k	3.1k	12.4k
Mars Base Camp	757	91	0	5.3k	4.9k	92.6k	11.5k	9.2k	310k	15.3k	10.5k	391k
SM-L1	72	9	0	1.2k	319	188	4.3k	5.0k	114k	10.0k	8.9k	300k
16 Psyche	0	0	0	8	712	100k	2.0k	6.4k	318k	7.8k	9.6k	378k

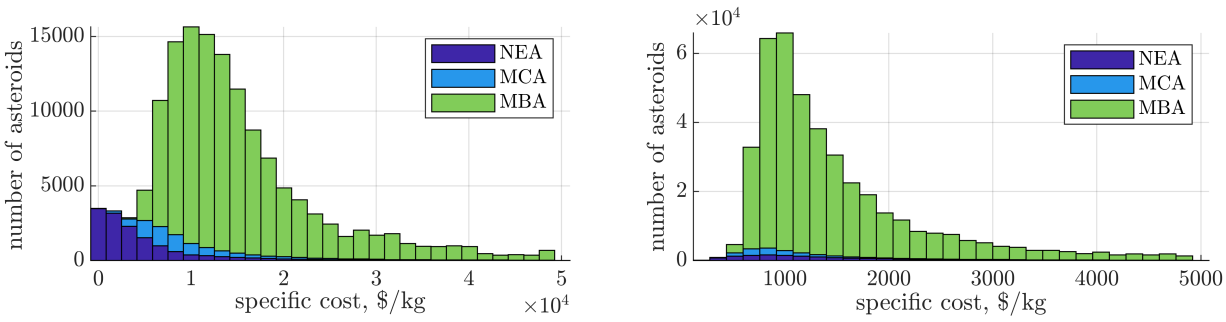

(A) FOR SCENARIOS TO LUNAR GATEWAY. (B) FOR SCENARIOS TO MARS BASE CAMP.

FIGURE 7.3: HISTOGRAMS OF AVAILABLE ASTEROIDS.

off the Moon, asteroids are unlikely to be used as a sole source for resources delivered to the Lunar Gateway, but plenty of them should be considered for use on the Mars Base Camp.

Figures 7.3a and 7.3b show more detail for the scenarios to the Lunar Gateway and Mars Base Camp, to illustrate the trends visible in Table 7.8 for customers near the Earth/Moon and customers near Mars, respectively. Note that the histograms are stacked to reflect the total number of available asteroids and that the scale on the horizontal and vertical axes are not the same for the two figures. In order to show meaningful results, the range for specific costs is ten times higher for the Lunar Gateway compared to the Mars Base Camp, indicating that the specific cost is much higher for many available asteroids. Also, the horizontal axis, the number of asteroids per bin, is three times as high for the Mars Base Camp, revealing that there are more asteroids available for customers there. These figures highlight that mining on NEAs in general results in cheaper resources, but that there are many more MBAs available. This conclusion can be drawn regardless the uncertainty on inputs for the cost model. This has implications for long-term SRU where extraction of asteroid resources changes the large-scale distribution of resources in the inner solar system.

Note that it is assumed that all asteroids are water-bearing C-type asteroids. As noted in Section 2.1.1, after applying bias-correction factors to the observed NEA population, there are relatively equal proportions of C- and S-type objects, for any given size. The main belt is dominated by C-type asteroids by as much as $5:1$ [49]. Assuming that these proportions are spread evenly throughout the bins in Figs. 7.3a and 7.3b, the bins for the NEAs would be reduced by approximately 50% and for the MBAs by approximately 17%. In that case, the difference in available NEAs and MBAs becomes even starker.

7.3.4 Aerocapture at Earth

The application of aerocapture to decrease the required ΔV for certain mission phases should be explored. To avoid having to make additional assumptions on, for example, perigee height and ballistic coefficient of the spacecraft, this investigation is performed parametrically, in line with the baseline mission and other sensitivity analyses.

Two changes are necessary to incorporate aerocapture in the mission scenarios:

1. A mass penalty is added to the dry mass for a heat shield, consistent with $\Delta\epsilon_{\text{entry}}$, meaning that on both the outbound and the inbound transfer, the spacecraft has to comply with:

$$\frac{m_{\text{sc,dry}}}{m_{\text{sc,wet}}} \geq \epsilon_{\text{min}} + \Delta\epsilon_{\text{entry}} \tag{7.1}$$

2. A decrease in the final impulsive burn (which contributes to ΔV^I) due to aerocapture, which affects $m_{\text{r,sold}}$.

Due to the significant increase in dry mass of the spacecraft because of the heat shield, less dry mass can be allocated to the actual cargo spacecraft, thereby decreasing the mass that can be transported: $m_{\text{r,transportable}}$. However, the ΔV reductions can be significant, which means that m^I_{prop} decreases, which in turn means that more of m_{r} can be sold to the customer.

Aerocapture is applied here to the mission scenarios to LEO. The mission from the Earth surface to LEO cannot include aerobraking, and the mission from the Mars surface to LEO is unlikely to be cost effective, given that the primary result for that scenario in Table 7.1 is infeasible, just as is

the case for many other missions mining on the Martian surface. The only three scenarios that are therefore investigated are from the Lunar surface, the NEA and MBA.

For these three scenarios, the mission is optimised including the heat shield and then a ΔV reduction is applied to ΔV^I of this mission. The maximum ΔV reduction applied is equal to the magnitude of the second burn of ΔV^I, which is different for each mission. How much ΔV^I can decrease during aerocapture depends on the perigee height, approach velocity, ballistic coefficient and the aerocapture strategy. Note that it is never possible to eliminate the complete ΔV^I, not only because of the first impulse that has to be delivered at or near the material source location, but also because a circularisation impulse is required to raise perigee out of the Earth's atmosphere and arrive in the customer's LEO at 400 km altitude.

The results are shown in Fig. 7.4, including reference points for the corresponding missions without aerobraking.

Figure 7.4 shows that when a heat shield is added to the spacecraft, initially the specific cost increases significantly, because the payload capacity of the cargo spacecraft decreases significantly. The total costs of the mission is then amortised over less sold resources. However, when the ΔV^I requirement decreases due to aerocapture, it can be seen that the specific cost decreases. Table 7.9 shows the minimum ΔV reduction necessary for each mission in order to achieve the same c and $m_{\text{r,sold}}$. Any decrease in ΔV above this minimum will result in a lower specific cost and/or higher delivered mass. These reductions in c and $m_{\text{r,sold}}$ come at the price of increased mission risk, through the inclusion of a risky mission event.

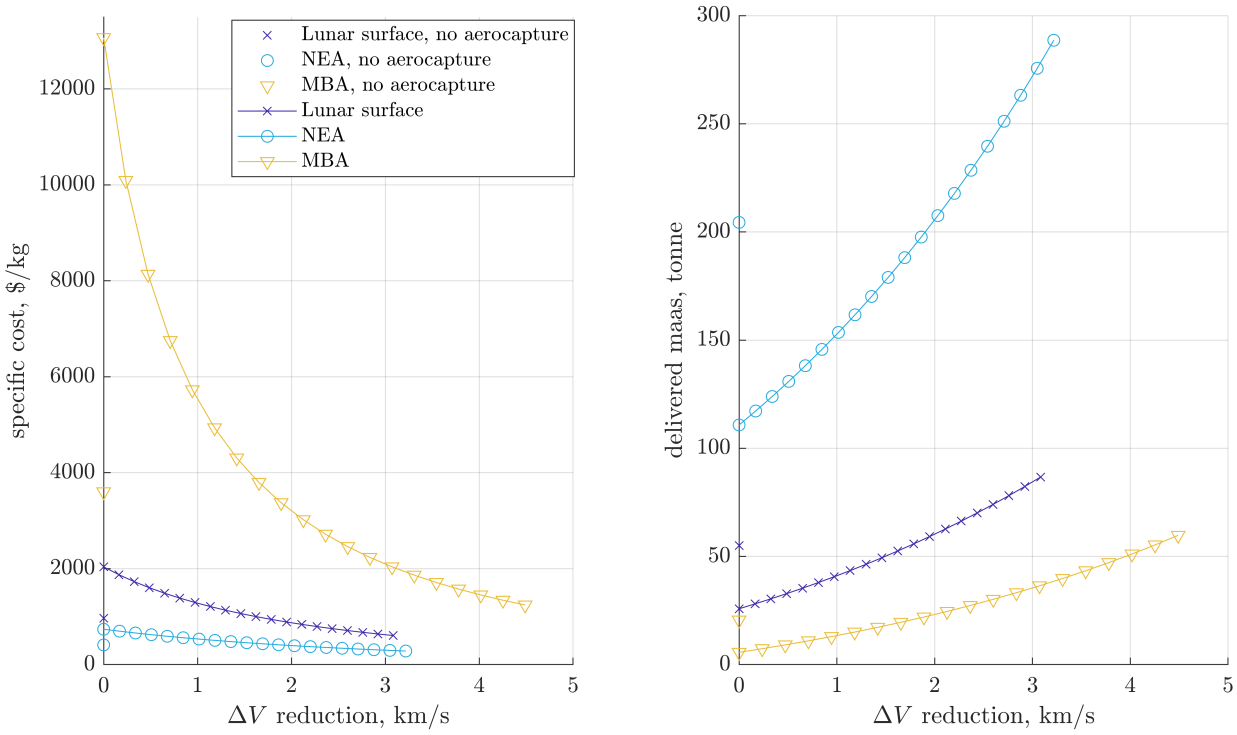

(A) SPECIFIC COST. (B) DELIVERED MASS.

FIGURE 7.4: PARAMETRIC INVESTIGATION OF AEROCAPTURE AT EARTH ON SCENARIOS TO LEO (400 KM).

While this sensitivity analysis shows that the specific costs of a mission can decrease when aerocapture is considered, it is important to note that to date, no spacecraft has used aerocapture yet to be captured into a closed orbit from an interplanetary trajectory [240]. Aerobraking, which uses many

Table 7.9: Minimum ΔV decrease due to aerobraking to achieve same performance of mission without aerobraking. Missions to LEO (400 km).

Material source	**ΔV reduction, km/s to achieve same c**	**ΔV reduction, km/s to achieve same $m_{r,sold}$**
Lunar surface	1.72	1.77
NEA (2000 SG344)	1.88	1.98
MBA (2015 AE282)	1.76	1.75

revolutions through the atmosphere to successively reduce the apoapsis of a spacecraft already in orbit, has been used. There are important differences between aerobraking and aerocapture through: the duration is weeks to months instead of one pass through the atmosphere and no heat shield is required because the spacecraft only dips into the sparse outer atmosphere instead of the dense mid-atmosphere [241].

7.4 KEY FINDINGS

For customers on the Earth, Moon and Mars, the minimum specific cost is found when mining and processing of water in LOX/LH_2 occurs on the same surface. For any customer beyond LEO, SRU is cheaper than directly launching the resources from the Earth and the total mass delivered using one spacecraft can be leveraged several times. The NEA considered, 2000 SG344, is in a strategic location for most customers in the vicinity of the Earth, except those on the surface of the Earth and Moon and in LEO, as noted earlier, due to a low ΔV^O to the asteroid. For other mining locations, ΔV^O is higher due to soft landing on the Moon or Mars and/or a transfer to a location far from Earth. For customers near Mars or beyond, mining and processing on MBA 2015 AE282 is most cost effective among the primary material sources considered. Mining and processing on the Martian surface and transporting these resources to a customer in the vicinity of the Earth is generally infeasible due to the high ΔV for ascent from Mars and imposed mass penalty, to cope with atmospheric entry. Note that these results are obtained for only one mission and no equipment is reused. When reusing equipment, the proximity of the material source location to the customer is important, which could cause a shift in which material source locations become cheaper to a customer.

Monte Carlo simulations show that the resulting specific cost is most sensitive to the manufacturing costs of the spacecraft and the imposed minimum structural coefficient, and least sensitive to uncertainties on the development costs and throughput rate. Also, in order for specific costs to be acceptable, the sum of development and manufacturing costs has to be lower than ∼2,250 $/kg. Furthermore, for all customers considered, except Psyche, there are NEAs and MCAs which are cheaper than the cheapest MBA. Only in the long term when these asteroids have been depleted, is it financially worth transferring to an MBA and back. Finally, it is shown that through aerocapture at Earth, the specific cost can decrease and delivered mass can increase if the decrease in ΔV^I is sufficient, at the expense of having to carry out a significantly riskier mission.

Concluding, for customers beyond LEO, SRU can and should be used rather than lifting water-derived resources from the Earth's surface to reduce cost, mass and risk for future human and robotic space exploration. The extension of the work performed in Ref. [236] confirms this and concludes that even customers in LEO can benefit from off-Earth mining when considering the close proximity of the Moon.

Chapter 8

LONG-TERM IMPLICATIONS OF A GROWING SPACE ECONOMY

While asteroids are often seen as able to provide a limitless supply of resources for use in space and on Earth, they are in fact a limited resource. Most analyses, including those in this thesis, often name specific asteroids to show how feasible or economical a certain architecture or mission is, and more often than not, these asteroids are small and easily reachable from Earth. This means that they will be used during the first few commercial missions and can quickly be depleted of usable resources, after which the architecture or mission discussed is increasingly more expensive in terms of duration and money. Moreover, when using asteroid resources for life support, most of the resources could be recycled, but every resource extracted from asteroids to use as propellant, can only serve a purpose once.

Many asteroids exist, most of which have not even been discovered [50, 242]. However, out of the one million asteroids considered in this thesis, the far majority are in the main belt: 95.8% (Fig. 2.3). Expansive sources for raw asteroid material exist, but not all resources can be retrieved in an economical way. The results obtained in Section 7.3.3 and in particular Figs. 7.3a and 7.3b and Table 7.8 show that only a limited number of asteroids can be retrieved at low specific cost, after which many resources are still available, but at a far higher specific cost.

This Chapter investigates trends occurring over time, after the most affordable resources have been retrieved and used up. Reuse of spacecraft and MPE is considered, which can bring down costs when considering multiple missions to the same asteroid and/or from the same depot. A demand model for the space economy is hypothesised, which is expected to grow each year. Customers are envisioned at the Lunar Gateway and Mars Base Camp, which have both been investigated in Chapter 7. The projected costs for a number of mission types (with and without spacecraft and/or MPE reuse) to all[1] asteroids are calculated. These estimated costs can subsequently be used to determine which asteroid and type of mission should be carried out. The most affordable resources are then incrementally removed from the available resources, meaning that more expensive asteroids must be used next. Cheaper resources are also associated with a low ΔV^I, meaning that in time, increasingly more resources are used for transport to the depots and therefore essentially wasted.

The goal of this Chapter is to determine what happens to the cost of asteroid mining over time, assuming that only asteroids are used to satisfy the demand of customers in the Lunar Gateway and Mars Base Camp. The increase in cost is investigated, due to both an increase in demand and the

[1] Similar to the approach in Section 7.3, a representative sample of MBAs is investigated and results are extrapolated.

increase in mission cost because cheaper resources have been used up.

The structure of this Chapter is as follows. First, Section 8.1 elaborates on the methodology used in this Chapter. Following this, Section 8.2 presents the dataset created and analysis thereof. Next, the results of a simulation of demand growth are presented in Section 8.3, followed by a sensitivity analysis in Section 8.4. Finally, conclusions are drawn in Section 8.5.

8.1 METHODOLOGY

This Section discusses the demand model, necessary changes to the baseline mission when considering reuse, clustering of asteroids, a year-by-year simulation utilising the cheapest resources at any time, and creating the dataset required. Finally, the limitations of the proposed model are discussed.

Elvis and Milligan [243] hypothesise that we should leave most of the asteroids untouched. Since the solar system is vast, it seems absurd and counter-intuitive to think that resources will be depleted. However, if a true space (propellant) economy emerges, this economy is likely to grow similar to the terrestrial economy, which grows exponentially. After one century of a modest 3% annual growth, an economy will be nearly 20 times as large. To avoid super-exploitation, a situation where resources are depleted faster than new resources can be made accessible, a limit should be set on what quantity of resources can be used. Reference [243] proposes a limit of $1/8^{\text{th}}$ of the resources, as three doubling times later (to 1/4, 1/2 and all resources) exhaustion would occur, assuming exponential growth. At 3% annual growth, the doubling time is just under 25 years, meaning that the $1/8^{\text{th}}$-limit would give a 75 year warning until potential exhaustion. While unimpeded and complete exploitation of all asteroids is unlikely not in the least because of increasing prices, enforcing this limit gives time to focus on reducing growth rates, recycling of resources and other mitigation efforts, by bringing it to everyone's attention in time. Reference [243] does not specify how the $1/8^{\text{th}}$-limit should be enforced: based on number, surface area, mass, or other parameters. This Chapter will impose the $1/8^{\text{th}}$-limit using the number of asteroids.

To this extent, this Chapter will investigate what the $1/8^{\text{th}}$-limit would mean for the year-by-year analysis of using the cheapest asteroid resources. Also, clustering of asteroids is considered to ensure that the left-over $7/8^{\text{th}}$ of the asteroids also include desirable asteroids (e.g. close to Earth) rather than the $7/8^{\text{th}}$ least desirable asteroids (e.g. all NEAs are depleted and future generations have to retrieve all required resources from the main belt).

8.1.1 Demand Model

The water contained in asteroids can be used for many purposes, as introduced in Section 2.3.1, such as life support and propellant. There is expected to be an insatiable demand for water, once the in-space propellant market is established [119]. The market for life support will be more constrained due to recycling of water of up to 95% [119]. The demand model in this Chapter is therefore solely based on the expected demand for propellant, but is considered sufficiently flexible to also cover the (much smaller) demand of water for life support.

As stated in the introduction of this Chapter, customer depots are envisioned at the Lunar Gateway (LG) and Mars Base Camp (MBC). Figure 8.1 depicts all considered segments used to calculate the demand at depots at the LG and MBC.

Two types of demand are distinguished in this work: customer demand and internal demand. The customer demand can be calculated a-priori and the internal demand follows from the missions that

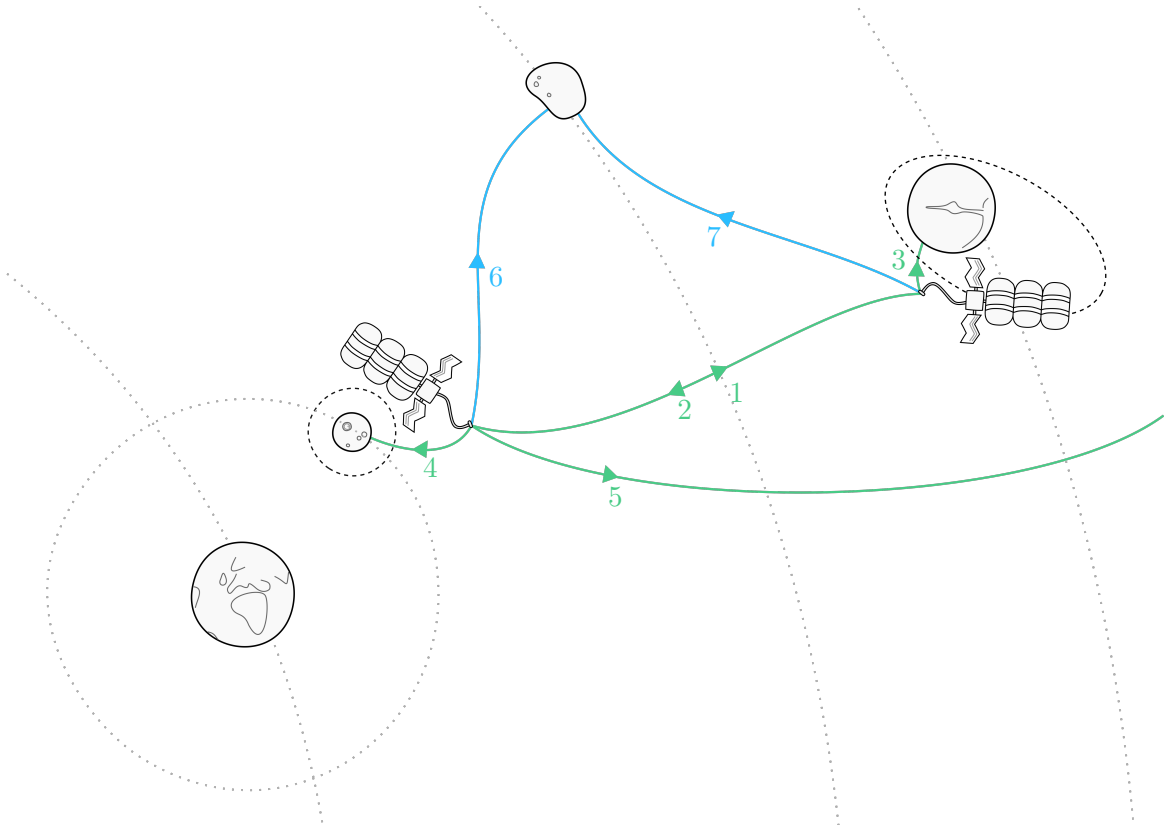

Figure 8.1: Demand model for a space propellant economy with depots at Lunar Gateway and Mars Base Camp.

are used in each year. Segments 1–5 in Fig. 8.1 are used to calculate the annual customer demand and segments 6 and 7 are the internal demand. The internal demand encompasses the propellant required for missions departing from the depots, when cargo spacecraft are reused.

Segments included for the initial customer demand are shown in Table 8.1. Interplanetary exploration missions are included in the demand model through a number of Juno-type missions. The Juno spacecraft was launched on a trajectory to Jupiter, where it entered a polar orbit [244]. As the LG is envisioned to be a staging ground for space explorations [237], the Juno-type missions depart from the LG.

In the demand model it is implicitly assumed that propellant used to transfer from the Lunar surface to the LG and from the Martian surface to the MBC are obtained on the surfaces themselves, following the conclusion in Chapter 7 that propellant needed on the surfaces of these bodies is best to be mined on the surface itself. These segments to calculate the in-space propellant demand are also named in Ref. [29]. Note that Ref. [29] also considers LEO to GEO and LEO to LG, but these are not considered here because they do not originate in the depots considered, and it follows from Chapter 7 that LEO is not a great location to deliver asteroids resources to.

For all segments included in the calculation of the initial customer demand, the following parameters are required:

1. The ΔV for the transfer;
2. The number of spacecraft transferring along the segment each year, i.e. the annual frequency;
3. The dry mass of spacecraft.

Table 8.1: Inputs for initial demand in demand model.

Segment		ΔV, km/s	Annual frequency	Rationale
1	LG to MBC	6.312	1000	Minimum ΔV Lambert arc for 115 days [96]. Frequency based on SpaceX plans [247].
2	MBC to LG	6.238	1000	Minimum ΔV Lambert arc for 115 days [96]. Frequency based on SpaceX plans [247].
3	MBC to Mars surface	0.615	1000	Periapsis lowering and ΔV for retro-propulsion from Table 4.8. Frequency based on SpaceX plans [247].
4	LG to Lunar surface	2.582	80	ΔV calculated following Section 4.4. High-demand case of Ref. [29] for frequency.
5	LG to a Juno-type mission	6.695	5	ΔV based on $C_3 = 30$ km^2/s^2 after Earth escape and 2.05 km/s additional ΔV [244].

Values for these parameters are largely based on SpaceX Mars colonisation plans. SpaceX envisions a self-sustaining Mars civilisation of a million people [245], to ensure human survival [246]. With 100 passengers per flight, this would take 10,000 flights and many more for equipment and supplies, in the order of 10 cargo trips per passenger trip.[2] The fully reusable Starship will be used to transport both crew and cargo to Mars after an in-orbit refuel ahead of the transfer to Mars [246]. SpaceX's design goal is an average of 1000 flights per year [247].

For each of the five customer segments, the first two parameters to calculate the initial demand are presented in Table 8.1 and the dry mass of the Starship is used for the third parameter: estimated at 85 tonnes [231]. It is important to note that the initial annual frequency for segment 1/2/3 is based on SpaceX's Mars colonisation plans, but starting from the Lunar Gateway as opposed to starting from LEO.

The required demand for each segment i, m_{demand_i}, can then be calculated using:

$$m_{\text{demand}_i} = (1+M) n_{\text{trips}} m_{\text{sc,dry}} \left(e^{\frac{\Delta V_i}{I_{\text{sp}} g_0}} - 1 \right); \tag{8.1}$$

where M is the margin applied for uncertainty in the calculation of the propellant requirement due to the speculative nature of the research, n_{trips} is the annual number of trips for that segment, $m_{\text{sc,dry}}$ is the dry mass of the spacecraft and ΔV_i is the ΔV requirement of the segment. The margin M is taken as 5%.

The total initial demand for each depot is then:

$$m_{\text{demand}_{\text{LG}}} = m_{\text{demand}_1} + m_{\text{demand}_4} + m_{\text{demand}_5} \tag{8.2}$$

$$m_{\text{demand}_{\text{MBC}}} = m_{\text{demand}_2} + m_{\text{demand}_3} \tag{8.3}$$

The initial demand is presented in Table 8.2 using the inputs from Table 8.1 and Eqs. (8.1)–(8.3).

This demand model assumes that SpaceX's ambitious Mars colonisations plans materialise and is therefore optimistic. A sensitivity analysis will be carried out to investigate what changes to the

[2] `https://www.huffingtonpost.co.uk/2014/10/01/elon-musk-mars-colony-million_n_5911758.html`, accessed on April 16th, 2022.

Table 8.2: Outputs for initial demand in demand model.

Segment		m_{demand} per trip, tonnes	Total annual m_{demand}, tonnes
1	LG to MBC	288.6	288,612
2	MBC to LG	282.3	282,269
3	MBC to Mars surface	13.5	13,474
4	LG to Lunar surface	71.8	5,744
5	LG to a Juno-type mission	323.2	1,616
	Total LG	-	295,972
	Total MBC	-	295,743

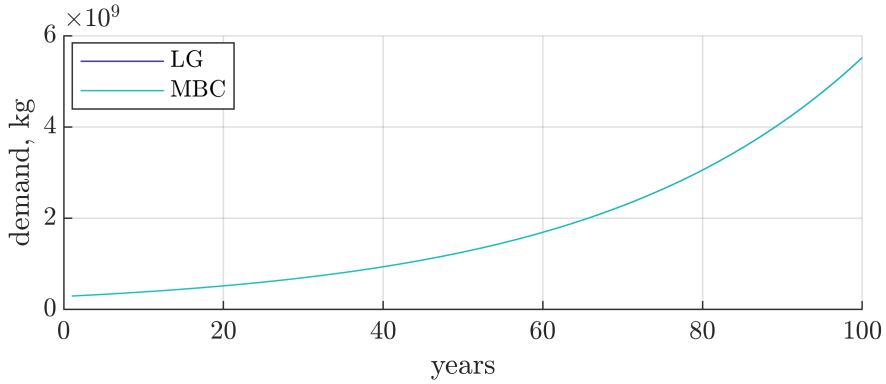

Figure 8.2: Annual demand for space propellant economy with 3% annual growth and initial demand from Table 8.2.

results are seen for a smaller annual demand. The process of populating Mars is predicted to evolve rapidly after the first settlers arrive [33].

The customer demand given in Table 8.2 is the initial yearly demand. As noted before, Elvis and Milligan [243] foresee an annual growth rate similar to that of a terrestrial market: 3%. Even this modest annual growth can quickly become significant. Applying a 3% annual growth rate results in the demand curve as shown in Fig. 8.2 for 100 years with the initial demand given in Table 8.2 (note that the LG and MBC demand curves overlap on the scale shown in this figure). The initial time frame in the demand model and Fig. 8.2 is not strictly defined, but is based on when SpaceX's colonisation plans are initiated and commercial asteroid mining is a reality. Note that all costs are given in FY2020 values and are thereby not influenced by inflation.

8.1.2 Changes to Baseline Mission

A number of changes are necessary to the baseline mission described in Chapter 4, due to the reuse of MPE and a cargo spacecraft:

- It is possible to start a mission at a depot instead of at the Earth. This does then of course no longer include a launch to LEO using the Starship system.
- When reusing MPE or a cargo spacecraft, no development and manufacturing costs shall be included for that system, and no launch costs in the case of a reused cargo spacecraft.
- Maintenance costs are added to missions that include reuse, as discussed in Section 4.2.1. Note that the maintenance costs for MPE and cargo spacecraft are different.

- Due to reuse, both the cargo spacecraft and MPE have to be a standardised size. The specific cost for a mission has to be calculated before running the year-by-year simulation and in the baseline mission these masses are optimised for each mission specifically, which would cause discrepancies when reusing these systems in other missions. To reach as many asteroids as possible, the cargo spacecraft is therefore sized such that ΔV^O and thereby m_{prop} is maximum, meaning that:

$$m_{\text{cargo}} = m_{\text{l}} \epsilon_{\text{min}} \tag{8.4}$$

  The standardised mass of the MPE will be determined in Section 8.1.5. These standardised masses have consequences:

  - λ_{mpe} is no longer an optimisation parameter;
  - Inequality constraints must ensure that $\Delta V < \Delta V_{\text{max}}$ instead of Eq. (4.28), where ΔV_{max} is:

$$\Delta V_{max} = \begin{cases} I_{\text{sp}} g_0 \log\left(\frac{m_{\text{l}}}{m_{\text{cargo}}}\right) & \text{if no MPE is onboard} \\ I_{\text{sp}} g_0 \log\left(\frac{m_{\text{l}}}{m_{\text{cargo}} + m_{\text{mpe}}}\right) & \text{if MPE is onboard} \end{cases} \tag{8.5}$$

While the changes discussed above are significant, there are still many similarities compared to the baseline mission in Chapter 4. The only changes to the mass budget are to Eqs. (4.10)–(4.12c) due to the standardised masses. The propellant mass requirement for the outbound transfer is now calculated as:

$$m^O_{\text{prop}} = m_{\text{sc,dry}} \left(e^{\frac{\Delta V^O}{I_{\text{sp}} g_0}} - 1 \right) \tag{8.6}$$

This means that not the complete m_{l} is utilised when ΔV^O is lower than ΔV_{max}.

For each asteroid, a number of missions have to be optimised using the built-in genetic algorithm in MATLAB®, such that during the year-by-year simulation the optimal mission scenario can be used. These missions are summarised in Table 8.3.

Table 8.3: Missions that need to be optimised to each asteroid.

Type	Departure location	Reused cargo spacecraft	Reused MPE	Depot location
1	Earth	No	No	LG
2	Earth	No	No	MBC
3	Earth	No	Yes	LG
4	Earth	No	Yes	MBC
5	LG	Yes	Yes	LG
6	LG	Yes	Yes	MBC
7	MBC	Yes	Yes	LG
8	MBC	Yes	Yes	MBC

Trajectories are calculated and optimised the same way as for the baseline mission. Costs are calculated using the same cost elements, but following the list of changes above, it depends on the scenario which costs are included:

$$C = \begin{cases} C_{\text{l}} + (c_{\text{dev}} + c_{\text{man}}) m_{\text{s/c,dry}} + c_{\text{op}} t_{\text{mis}} + c_{\text{prop}} m^O_{\text{prop}} & \text{if from Earth, no reuse} \\ C_{\text{l}} + (c_{\text{dev}} + c_{\text{man}}) m_{\text{cargo}} + c_{\text{main}_{\text{mpe}}} m_{\text{mpe}} + c_{\text{op}} t_{\text{mis}} + c_{\text{prop}} m^O_{\text{prop}} & \text{if from Earth, MPE reuse} \\ c_{\text{main}_{\text{cargo}}} m_{\text{cargo}} + c_{\text{main}_{\text{mpe}}} m_{\text{mpe}} + c_{\text{op}} t_{\text{mis}} & \text{if from depot, full reuse} \end{cases} \tag{8.7}$$

in which "full reuse" refers to the reuse of both MPE and the cargo spacecraft. Note that when departing from a depot, there will always be full reuse.

The last case in Eq. (8.7) (for "if from depot, full reuse") shows that there will be an issue when optimising for the specific cost c. Because the spacecraft departs from a depot, c_{prop} cannot be used to calculate the cost of the propellant, as this is the cost for Earth-sourced LOX/LH_2. The premise of this Chapter is that the cost of the propellant in the depot changes over time, which means that the total cost C cannot be determined a-priori, before running the year-by-year simulation. Therefore, an alternative optimisation objective is used:

$$J = -c_{\Delta\text{mass}} = -\frac{C}{m_{\text{r,sold}} - m^{O}_{\text{prop}}} \tag{8.8}$$

in which $c_{\Delta\text{mass}}$ is the adjusted specific cost which effectively amortises the mission cost over only the added mass, the difference between the mass delivered to the depot and the mass required from a depot. If $J = -c$ was used, the optimiser has no incentive to minimise the outbound propellant mass requirement, even though this is very important: if the mission required more mass from a depot than it returns, it should not be carried out.

DETERMINING STANDARDISED MPE

To determine the standardised m_{mpe}, the optimisation is performed for all asteroids for the initial missions (types 1 and 2), using a variable m_{mpe}. Note that the spacecraft mass is already standardised, following Eq. (8.4).

The results obtained for the sample of MBAs (20,000) are extrapolated to the size of the entire MBA population (977,007). The optimal missions to all NEAs, MCAs, and multiplicated MBA samples are subsequently sorted for the specific cost c and the median m_{mpe} of the top 1/8th of accessible asteroids is taken. An asteroid for which a mission can be optimised that satisfies the imposed constraints is considered an accessible asteroid. Figure 8.3 shows the distribution of all considered m_{mpe}.

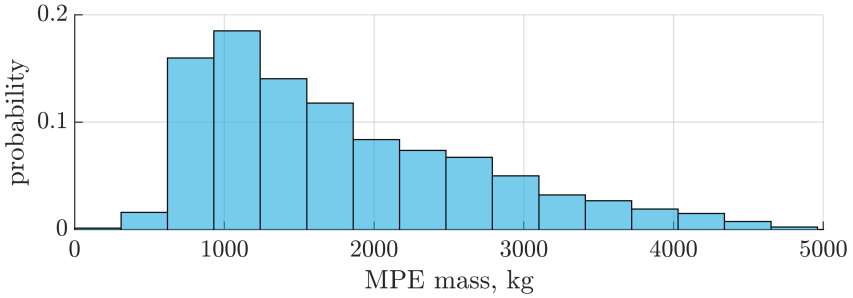

FIGURE 8.3: HISTOGRAM OF m_{MPE} FOR THE TOP 1/8TH CHEAPEST MISSIONS.

The resulting m_{mpe} is 1536 kg. The MBAs make up the bulk of the asteroids and therefore weigh more heavily in the calculation of the median. However, the median value of m_{mpe} is 1027 and 1594 kg for the NEA and MCA sets, respectively, meaning that the resulting 1536 kg can still be properly used for missions to those asteroids.

To fill up the complete standardised cargo spacecraft with this standardised MPE, Eqs. (4.19), (4.13) and (4.17) can be used to calculate how long this takes. Figure 8.4 shows the time required to fill the cargo spacecraft with 122.5 metric tonnes of propellant, based on the semi-major axis of the asteroid (which affects the throughput rate κ, see Section 4.3.2). The figure shows that for an asteroid

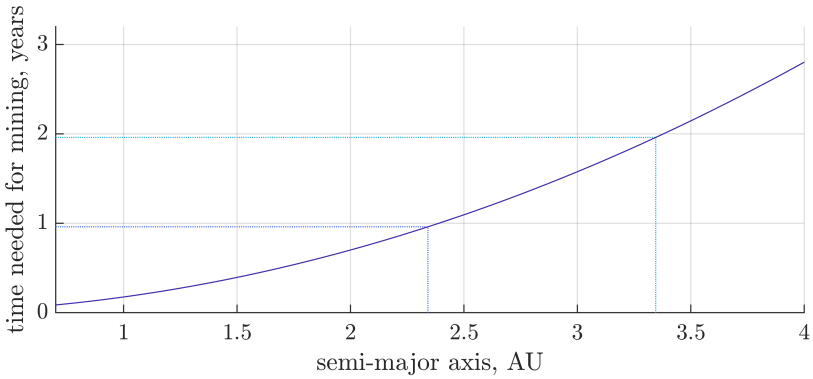

Figure 8.4: Time required to fill standardised cargo spacecraft with standardised MPE.

with $a < 2.341$ AU, the MPE can be reused ever year, once every two years for $2.341 \leq a < 3.345$ AU, and once every three years for the remaining asteroids (the sample of MBAs has only two asteroids with a semi-major axis just above 4.1 AU). This takes into account the 14 day allocated to proximity operations, installing the MPE and the completion of the transport of the resources to the cargo spacecraft at the end of the mining phase.

8.1.3 Clustering of Asteroids

To be able to enact the $1/8^{\text{th}}$-limit, the asteroids are clustered. Instead of posing the limit on $1/8^{\text{th}}$of all asteroids, which would see all desirable asteroids used right away, the limit can then be enforced within each cluster.

Clustering of the asteroids is performed using a k-means algorithm [248], frequently used in data science [249]. A k-means algorithm aims to iteratively partition n data points into k clusters, which are defined using centroids of the cluster. The number of clusters k is determined a-priori. The result is a partitioning of the data into Voronoi cells [249].

The algorithm is initialised using k randomly-chosen cluster centroids. The Euclidean distance from each point to each centroid is computed, after which the data points are assigned to the closest centroid. The average of the data points in each cluster is calculated to obtain new cluster centroids, after which the next iteration can start. This is repeated until cluster assignments do not change or when the maximum number of iterations is reached. The k-means algorithm is implemented in MATLAB®.[3]

Features used for the clustering of the asteroids are the semi-major axis, eccentricity, inclination and magnitude (which relates to the size of the asteroid). This is to ensure that asteroids are used evenly throughout the solar system and not just near Earth, and that asteroids of all sizes can remain. Only the accessible asteroids are clustered, all asteroids to which no feasible missions could be optimised are excluded from the clustering.

Before clustering, the features used for the clustering need to be scaled, in particular because of the different units for the features to be used for clustering. Robust scaling is used to perform the scaling, because this performs well in the case of outliers.[4] After scaling, the features have a zero mean and median, and a standard deviation of 1, not skewed by outliers. Robust scaling is performed

[3] `https://uk.mathworks.com/help/stats/kmeans.html`, accessed on March 2nd, 2022.

[4] `https://scikit-learn.org/stable/modules/generated/sklearn.preprocessing.RobustScaler.html`, accessed on April 1st, 2022

on features as:

$$x_{\text{scaled}} = \frac{x - Q_2}{Q_3 - Q_1} \tag{8.9}$$

where x is the feature that needs to be scaled and Q_1, Q_2 and Q_3 the first quartile (25%), second quartile (50%), and third quartile (75%) of all variables of that feature.

8.1.4 Year-By-Year Model of a Growing Space Economy

This Section describes the steps undertaken to create a year-by-year model of the growing space propellant economy. Using the asteroid dataset that will be described in Section 8.1.5, supply will meet the demand calculated in Section 8.1.1, by delivering the cheapest resources available at any time to the required depots.

At any point in time, the database can return what the best mission is to supply a specific depot. Each mission to each asteroid has an associated "sorting objective", used to determine what the best mission is to supply a specific depot. For the missions departing from the Earth (1–4) the sorting objective is c and for the missions departing from a depot (5–8) the sorting objective is $c_{\Delta\text{mass}}$ (the specific cost of the added mass, from Eq. (8.8)). The mission to an asteroid that has the lowest sorting objective is considered best and is returned by the database.

A maximum number of missions to an asteroid is enforced, to ensure that reuse of MPE can occur. If no limit is enforced, the asteroid will continue to be the most affordable at that time, meaning that it will be returned by the database until the asteroid has been used completely and the MPE cannot be reused in future years. The maximum number of missions per year per asteroid, $n_{\max}$, depends on the size of the asteroid through $m_{\text{r,available}}$ and the mass mined during one mission $m_{\text{r,mined}}$:

$$n_{\max} = \left\lceil \texttt{min}\left(\frac{m_{\text{r,available}}}{10 m_{\text{r,mined}}}, 100\right)\right\rceil \tag{8.10}$$

where $\lceil \square \rceil$ refers to ceiling rounding. Since the lifespan of the MPE is set at ten years [236], an asteroid will be used for ten years successively if the asteroid is large enough, allowing for optimal reuse of the MPE. An arbitrary maximum number of missions is set at 100 missions per year in case the asteroid is very large.

The database needs to be updated regularly when changes occur:

- At the start of the year, the available number of MPE on the asteroids and parked spacecraft at each depot limit the number of missions that can be carried out that year. Any mission not possible that year cannot be returned by the database.
- After an asteroid is used, certain missions might no longer be feasible due to changes in the available number of MPE or the remaining resource mass. Only complete missions can be carried out, so a small amount of resources can be left over on the asteroid. Any mission no longer feasible cannot be returned by the database.
- When there are no more parked spacecraft at a depot, no more missions can depart from that depot that year. Any mission departing from that depot cannot be returned by the database.
- When $1/8^{\text{th}}$ of the number of asteroids in a cluster are used, the remaining asteroids are considered 'off-limits' and preserved for future generations, meaning that they can no longer be returned by the database.

- When the maximum number of missions per year to that asteroid has been reached, no more missions to this asteroid can be returned by the database this year.

Using this up-to-date database, one-by-one missions are selected for both depots, until the selected missions return enough resources to satisfy the customer demand of each depot. Then, the total internal demand is calculated for each depot, as the sum of the outbound propellant mass requirement of all missions (both to supply the LG and MBC) departing from the LG and MBC. To satisfy the increase in demand, additional missions are returned by the database, until once more the supply satisfies the demand. This loop is carried out until convergence.

One of the depots selects the asteroids and missions to be used that year first, removing the resources from the database before the other depot can select the cheapest missions. As the LG is expected to have higher costs, this depot can claim asteroids first. In a sensitivity analysis it will be explored what the effect is on the simulation.

When sufficient missions have been selected to satisfy the total demand (customer and internal), several elements have to be calculated:

- The total cost for each depot, which takes into account the propellant used for the internal demand. The costs for the internal demand have to be spread according to which depots benefited from the missions.
- What quantity of resources are stored in the depot for the next year. Note that only complete missions are carried out, meaning that a portion of the last mission will be saved for next year.
- When the spacecraft used can be reused again. Spacecraft arriving at a depot can be reused in the future. Depending on the mission duration, spacecraft can be reused after an integer number of years.
- When the MPE used can be reused again. How often the MPE can be reused is detailed in Section 8.1.2. It is assumed that MPE can be reused for ten years [236].

An important point to note is that the simulation described above is a serial process by design and cannot be parallelised. The state of the database depends on all previous states.

8.1.5 Creating the Dataset

Considering the number of asteroids and eight different missions that need to be optimised to each asteroid, the dataset that will be used in the year-by-year simulation is large. This Section will detail the necessary steps to create the dataset.

For each asteroid, first, the initial missions are optimised (i.e. mission type 1 and 2). For each asteroid where at least one of these initial missions is feasible, the follow-up missions are calculated. Note that the follow-up missions departing from a depot are optimised using Eq. (8.8) using the increase in propellant mass. Only the missions that add mass are included in the final dataset, any mission that requires more propellant from a depot than it returns to a depot is excluded.

The input dataset contains the following information for each asteroid:

- Identifier: unique SPK-ID as used in JPL SBDB;
- Type: NEA, MCA or MBA;
- Cluster number the asteroid belongs to;

- Mission data for all eight missions;
- Maximum available mass: $m_{\text{r,available}}$, calculated using Eq. (4.15) and a maximum excavation depth of 10 m.

For each optimised mission, the following data needs to be recorded:

- Sorting objective, as treated in Section 8.1.4;
- Mission cost (total): C;
- Mission duration: t_{mis};
- Mined mass: $m_{\text{r,mined}}$;
- Delivered mass: $m_{\text{r,sold}}$;
- Propellant mass required from LG for outbound transfer;
- Propellant mass required from MBC for outbound transfer;
- Requires MPE to be present on asteroid and available for reuse: yes/no;
- Requires cargo spacecraft to be available at LG: yes/no;
- Requires cargo spacecraft to be available at MBC: yes/no.

Additional data fields must be created for asteroids during the simulation, to track what happens over time, such as the number of MPE present and which year they can be used.

Note that for MBAs, a subset of 20,000 asteroids is taken and the results are multiplicated to form a complete dataset. It is assumed that this is representative of optimising missions to all MBAs separately.

As noted in Section 2.3, the spectral type of most asteroids is unknown. However, the baseline mission described in Chapter 4 assumes that the asteroid is a C-type, affecting the albedo, density and the recovery ratio of volatiles. While this assumption is legitimate when optimising missions to separate asteroids, assuming that *all* asteroids are C-type in this simulation is not acceptable. As noted in Section 2.3, approximately half of the NEAs and approximately $5/6^{\text{th}}$ of MBAs are expected to be C-type asteroids. It is assumed that the average of these two ratios ($2/3^{\text{rd}}$) holds for the MCAs, which are also between NEAs and MBAs in regards of spatial distribution and size of asteroids. Therefore, random distributions following these ratios are applied to the separate asteroid sets, resulting in a new dataset assumed to represent the C-type asteroids.

8.1.6 Limitations of Model

The model discussed above has a number of limitations:

1. It is assumed that technology does not change over time. Because all data pertaining to the missions is generated a-priori using the same input parameters, a decrease in any cost due to improved technologies cannot be taken into account.

2. All missions are optimised individually, resulting in a specific timing of the transfers. The timing of these transfers is not taken into account in the year-by-year model. Note that the timing can be repeated every synodic period, meaning that for asteroids which are not close to Earth and/or Mars, this effect can be limited. For asteroids closer to Earth and/or Mars, small changes to the required ΔV would be necessary to account for non-optimal phasing, but this is not taken into

account. For single missions this approach would not be accurate enough, but when considering and averaging many asteroids and only drawing conclusions from the average trend, it is assumed that this limitation is acceptable.

3. Only two depots are taken into account, even though a growing space propellant economy could mean the addition of more depots over time.

4. All spacecraft and MPE are standardised to the same size. In reality, it could be beneficial to design a number of different spacecraft that can be used for different missions. For example, asteroids that can be reached using a low ΔV^O can fit a larger m_{cargo} into the Starship payload capacity and therefore have a larger payload capacity. With a larger payload capacity, the costs not related to mass (i.e. the launch and operations cost) can be amortised over more resources, thereby reducing the specific cost. The standardised spacecraft, sized to reach most asteroids, is therefore a bigger disadvantage to asteroids reachable with low ΔV^O.

5. The internal demand each year is calculated based on the missions of the same year, while these missions have actually departed a few years ago. This means that the internal demand is assumed to arrive at the depots instantaneously. If the missions supplying resources to satisfy the internal demand would depart a number of years before the resources are needed, the internal demand of previous years could be changed, which would affect the dataset containing available resources for all years to follow. This would severely complicate the analysis and affect the computational time significantly through the application of looping until convergence. The impact of this limitation will be more pronounced during the first years of the simulation, but especially as the number of missions per year grows, the internal demand is relatively constant each year.

6. It is assumed that the demand grows exponentially. While there is no reason to assume that this is inaccurate in a mid-term time frame, demand growth could level off in the future, when faced by the scarcity of affordable resources; the precise phenomenon this Chapter investigates. However, it is still very useful to assess the situation if the growth remains exponential.

Most of the above limitations arise from having to generate the dataset prior to running the year-by-year simulation using a fixed set of inputs. If this were not done though, the size of the problem would increase significantly, because each time a new asteroid and scenario has to be selected, all possibilities would have to be optimised again.

Similarly, each added depot, spacecraft or MPE of a different size, or different cost due to technology improvements means that additional scenarios have to be optimised, stored, and distinguished between in the code. This greatly increases the size of the problem at hand and therefore the computational time.

The dataset and simulation described above will therefore only be an approximation of how the actual growing economy could evolve, but it will be sufficient to draw initial conclusions. Care should be taken not too read too much into the individual numerical results, but the analysis should focus on the trends occurring over time. Additionally, the simulation should not run for multiple centuries, as the accuracy of the dataset and model will degrade over time, when new technologies are available.

8.2 ANALYSIS OF DATASET

The dataset generated using the methodology above is analysed before it is used in the year-by-year simulation. This Section addresses the clustering of the asteroids, the impact of fixed cargo spacecraft

and MPE masses and the feasibility of missions departing from the depots instead of Earth.

8.2.1 Clustering of Asteroids

Figure 8.5 shows the result of clustering using $k = 10$ clusters. The size of the markers is scaled according to the relative size of the asteroids. This shows that by far the most massive asteroids are in the main belt, and that most NEAs with orbital elements similar to Earth are very small. The latter are more accessible and therefore likely cheaper to mine, but will also be depleted much faster due to their size.

Table 8.4 presents information on the clusters, with the centroid of the cluster and the number of asteroids in each cluster. Note that both here and in Fig. 8.5 the ratio of C-type asteroids as introduced in Section 8.1.5 has already been applied.

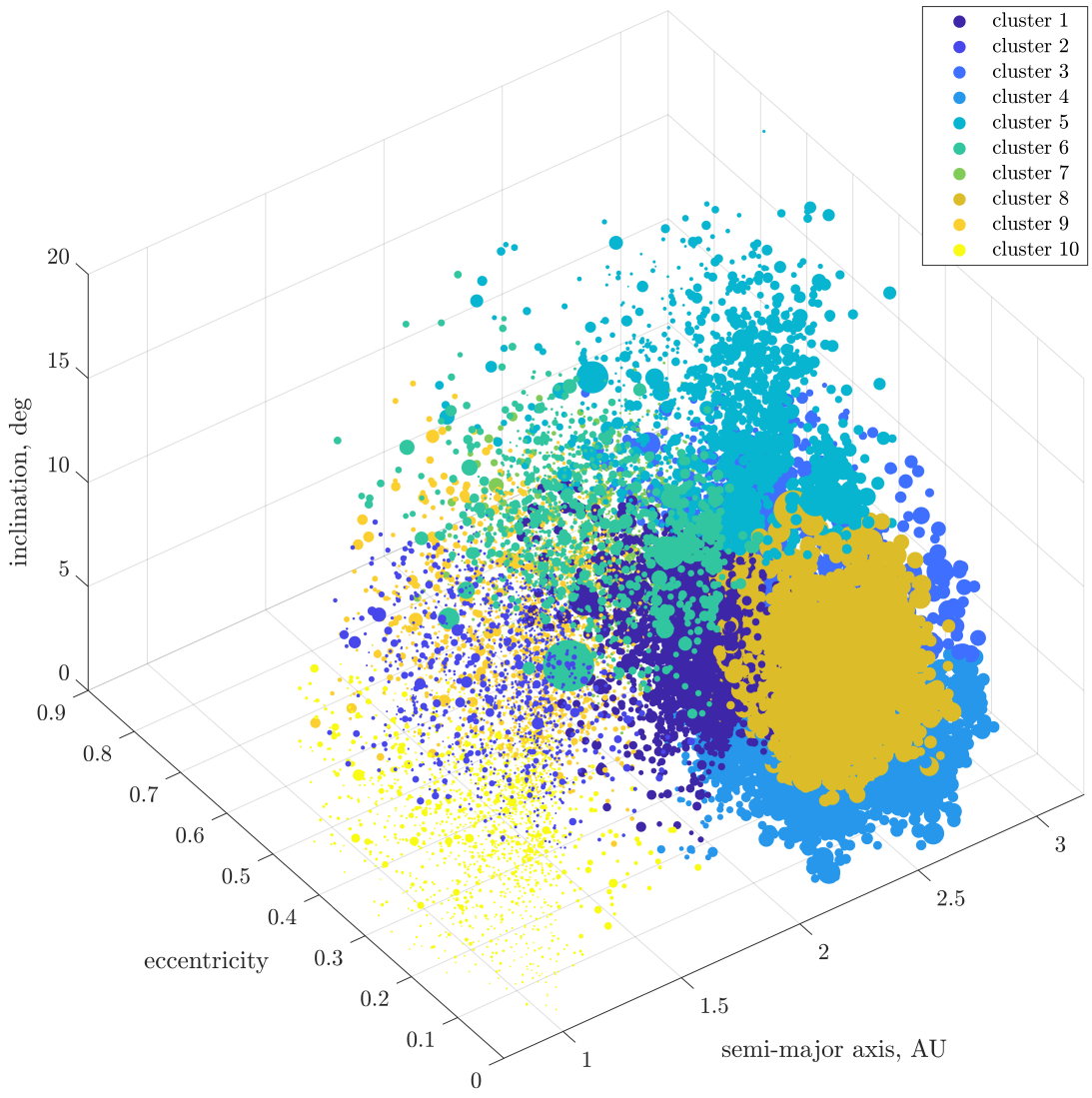

Figure 8.5: Distribution of clusters, size of markers corresponding to the relative volume of each asteroid.

It can be seen that the clusters that are mainly composed of NEAs and MCAs (2, 6, 7, 9 and 10) have a higher average magnitude, meaning that the asteroids are far smaller and therefore contain less volatiles. Out of these clusters, clusters 9 and 10 have more desirable orbital elements and are therefore likely to be used first, but these unfortunately also have the highest magnitude. To ensure that some of these accessible asteroids remain available for future generations, using these clusters in combination with the $1/8^{\text{th}}$ limit are beneficial. Without the clusters, the imposed $1/8^{\text{th}}$ limit would be enforced after $1/8^{\text{th}}$ of all asteroids are used, leaving likely only MBAs which are relatively hard to reach from the Earth.

Table 8.4: Result of k-means clustering algorithm.

Group	**Centroid of cluster**				**Number of asteroids**			
	Semi-major axis, AU	**Eccentricity**	**Inclination, deg**	**Magnitude**	**NEA**	**MCA**	**MBA (sample)**	**MBA total**
1	2.26	0.25	6.11	18.80	397	3,789	(269)	13,141
2	1.24	0.25	10.93	24.06	1,176	16	(0)	0
3	2.76	0.29	6.84	17.44	175	990	(395)	19,296
4	2.44	0.17	2.77	17.54	0	734	(3,926)	191,786
5	2.59	0.27	13.00	17.69	424	753	(209)	10,210
6	1.75	0.22	15.84	20.17	705	308	(10)	489
7	2.37	0.59	4.12	23.81	1,563	62	(0)	0
8	2.40	0.14	6.61	17.04	0	83	(2,944)	143,815
9	1.82	0.49	5.30	24.14	2,013	18	(0)	0
10	1.21	0.27	3.73	25.46	1,541	13	(0)	0

8.2.2 Impact of Fixed Cargo Spacecraft and MPE Mass

Two significant changes to the baseline mission scenario as noted in Section 8.1.2 are standardising both the cargo spacecraft mass and the MPE mass. These changes are necessary to allow reuse in combination with a pre-calculated dataset. Figure 8.6 shows the change to the specific cost due to these changes for the missions departing from the Earth with new MPE. First, the specific cost as optimised in Chapter 7, where both m_{cargo} and m_{mpe} can be optimised, is shown as a reference value. Second, the specific cost resulting from fixing m_{cargo}, but leaving m_{mpe} free, i.e. the dataset used to determine the standardised m_{mpe}. Last, the specific cost resulting from fixing both m_{cargo} and m_{mpe}, i.e. the dataset that will be used in the simulation. Note that all missions have been optimised for minimum specific cost.

The results in Fig. 8.6 show that the effect of standardising m_{cargo} is bigger than the effect of subsequently standardising m_{mpe}. When fixing m_{cargo} to a mass that allows for most asteroids to be reached ($m_{\text{cargo}} = \epsilon_{min} m_{\text{l}}$), the missions to asteroids with lower ΔV^O are penalised the most. These missions could previously benefit from a large payload capacity by leveraging the large m_{cargo}, allowing some of them to bring multiples of m_{l} to the customer. The cost could then be amortised over more resources, allowing for a low specific cost. However, note that a greater m_{cargo} also comes with increased development and manufacturing costs. This explains the shift in specific cost apparent in Fig. 8.6. Subsequently fixing m_{mpe} means that missions might have to stay longer at the asteroid, resulting in higher operational costs, or that m_{mpe} is larger than necessary in the case of the optimised m_{mpe}, leading to higher development and manufacturing costs.

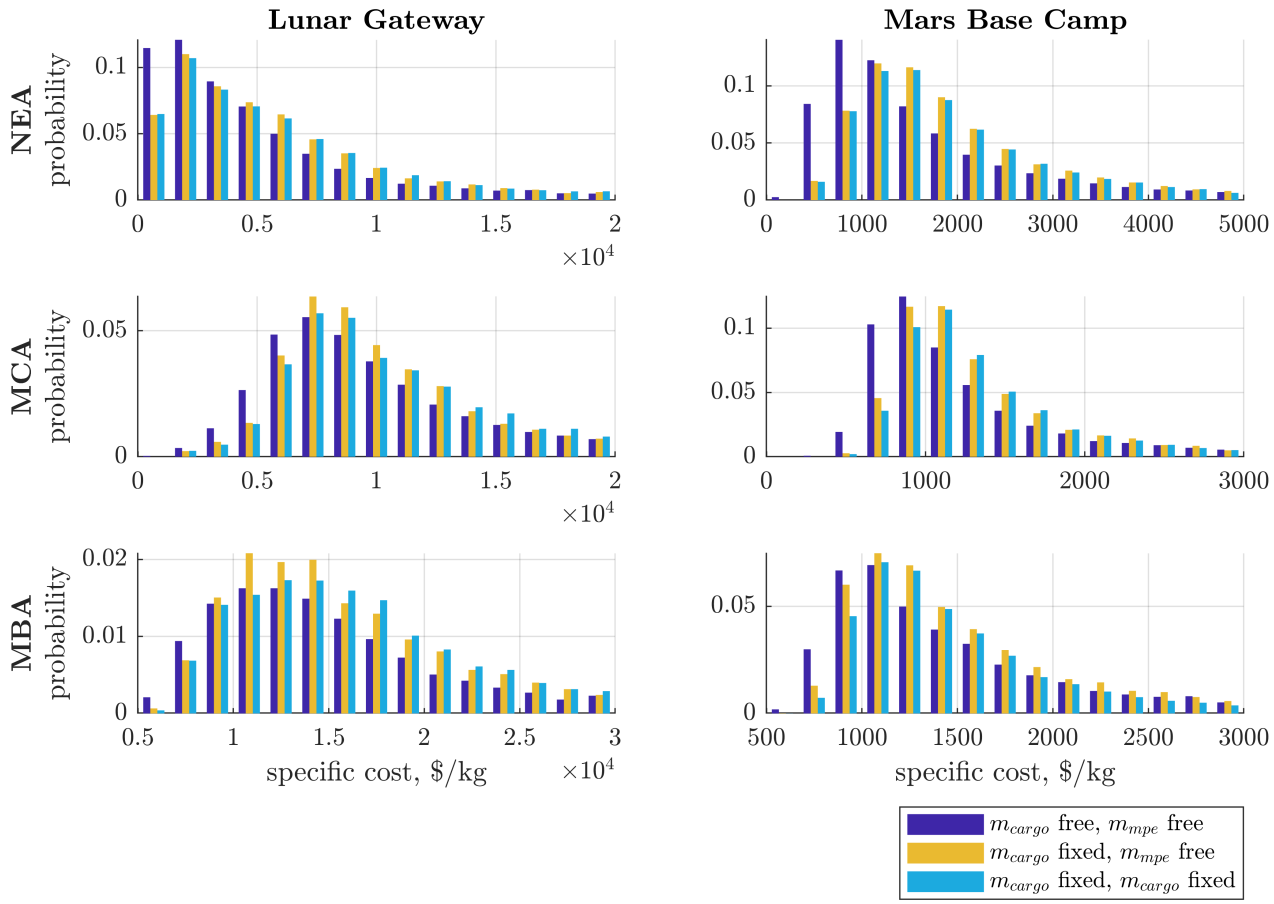

Figure 8.6: Comparison of the specific cost of missions with an optimisable and standardised cargo spacecraft and MPE mass.

8.2.3 Feasibility of Missions from Depots

Another major change with respect to the baseline mission scenario is the possibility of departing from a depot, reusing the cargo spacecraft parked at the depot and the MPE still stationed on the asteroid. As noted in Section 8.1.2, these missions cannot be optimised for minimum specific cost c. First of all, the actual cost of propellant is unknown, as this depends on the year-by-year simulation and the missions that will supply the depot at that time. Therefore, the propellant cost cannot be taken into account, and there is no incentive for the optimiser to minimise the propellant mass that is required from the depot for the outbound transfer. Instead, optimised missions would aim to minimise the outbound transfer time to limit operational costs, which would lead to $\Delta V^O = \Delta V_{\max}$, thereby requiring large quantities of propellant from the depot. Therefore, these missions are optimised using Eq. (8.8), amortising the total cost over the difference between the required and delivered mass. Note that this assumes that $m_{\text{r,sold}}$ and m^O_{prop} have an equal value per kg. Also note that upon delivering the resources to the depot, they will still be sold using c and not $c_{\Delta\text{mass}}$, dividing the total cost by all delivered resources. Only missions with $m_{\text{r,sold}} > m^O_{\text{prop}}$ are considered, all other missions discarded.

Figure 8.7 compares the follow-up missions (i.e. those reusing MPE) with the initial missions from Earth (i.e. the mission without any reuse) in terms of the delivered mass. Scatter plots relating the delivered mass are shown separately for the different sets of asteroids (NEA, MCA and MBA), the different departure locations for the follow-up missions (Earth, LG and MBC) and the different delivery depots (LG and MBC). Any combination that did not result in any possible mission (for example:

depart from LG to MCA, deliver to LG), no graph is shown. Note that each data point in the graphs is for one asteroid. Also, note that the random C-type distribution discussed in Section 8.1.5 has already been applied to the data. Table 8.5 shows the number of missions that are shown in each graph, which can be used to interpret the results in the figures.

Several conclusions can be drawn from Fig. 8.7. First, the delivered mass of the initial and follow-up missions are largely similar, with a smaller portion of the missions deviating slightly from the diagonal of the plot, which can be attributed to the random behaviour of the genetic algorithm used. This is expected, because ΔV^I determines $m_{\mathrm{r,sold}}$ and can be the same for the initial and follow-up missions. Next, returning from a MCA or MBA to the LG instead of the MBC requires in general a much higher ΔV^I, meaning that the delivered mass is low. The MBC is in a more strategic location. Also, it can be seen that departure from the depots to non-NEAs is not always possible, especially when departing from the LG.

The next figure, Fig. 8.8 gives even more insights into these follow-up missions by comparing the specific cost of the initial mission with the specific cost of any follow-up missions, for the same combinations as Fig. 8.7. First, it can be seen that the follow-up missions departing from the Earth result in broadly the same specific cost, but are slightly cheaper because the maintenance cost for the MPE is lower than the sum of development and manufacturing cost for the MPE. For the follow-up missions departing from a depot, this is however not the case. It can be seen that while a number of missions to asteroids can result in a $c_{\Delta\mathrm{mass}}$ less than the c of the initial mission, for the majority, $c_{\Delta\mathrm{mass}} > c$ of the initial mission (i.e. the data point is above the diagonal). This means that even though the mission can deliver more resources than it requires from a depot, it cannot do so more economically than launching a new spacecraft from Earth. Also, the number of missions that can depart from a depot to deliver resources to the LG is small, shown by the lower number of data points in the rows "LG to LG" and "MBC to LG".

Summarising, these figures therefore show that reuse of spacecraft could be rather limited, especially to and from the LG. For a number of asteroids, missions of type 5–8 are possible, but not more economically than launching a new spacecraft, meaning that they will not be selected in the simulation.

Table 8.5: Overview of possible missions for each asteroid set and mission type.

		NEA	**MCA**	**MBA**	
				(sample)	**total**
	number of asteroids	23,484	19,661	(20,000)	977,007
	after applying C-type ratio	11,742	13,107	N/A	814,173
Initial mission	to LG	7,273	5,214	(3,627)	147,650
	to MBC	7,967	6,735	(7,716)	314,108
	at least one initial mission possible	7,994	6,766	(7,753)	315,613
Follow-up missions	Earth to LG	7,234	5,285	(4,022)	163,730
	LG to LG	1,010	0	(0)	0
	MBC to LG	1,731	277	(0)	0
	Earth to MBC	7,994	6,766	(7,753)	315,613
	LG to MBC	1,753	282	(0)	0
	MBC to MBC	3,876	5,967	(7,208)	293,428

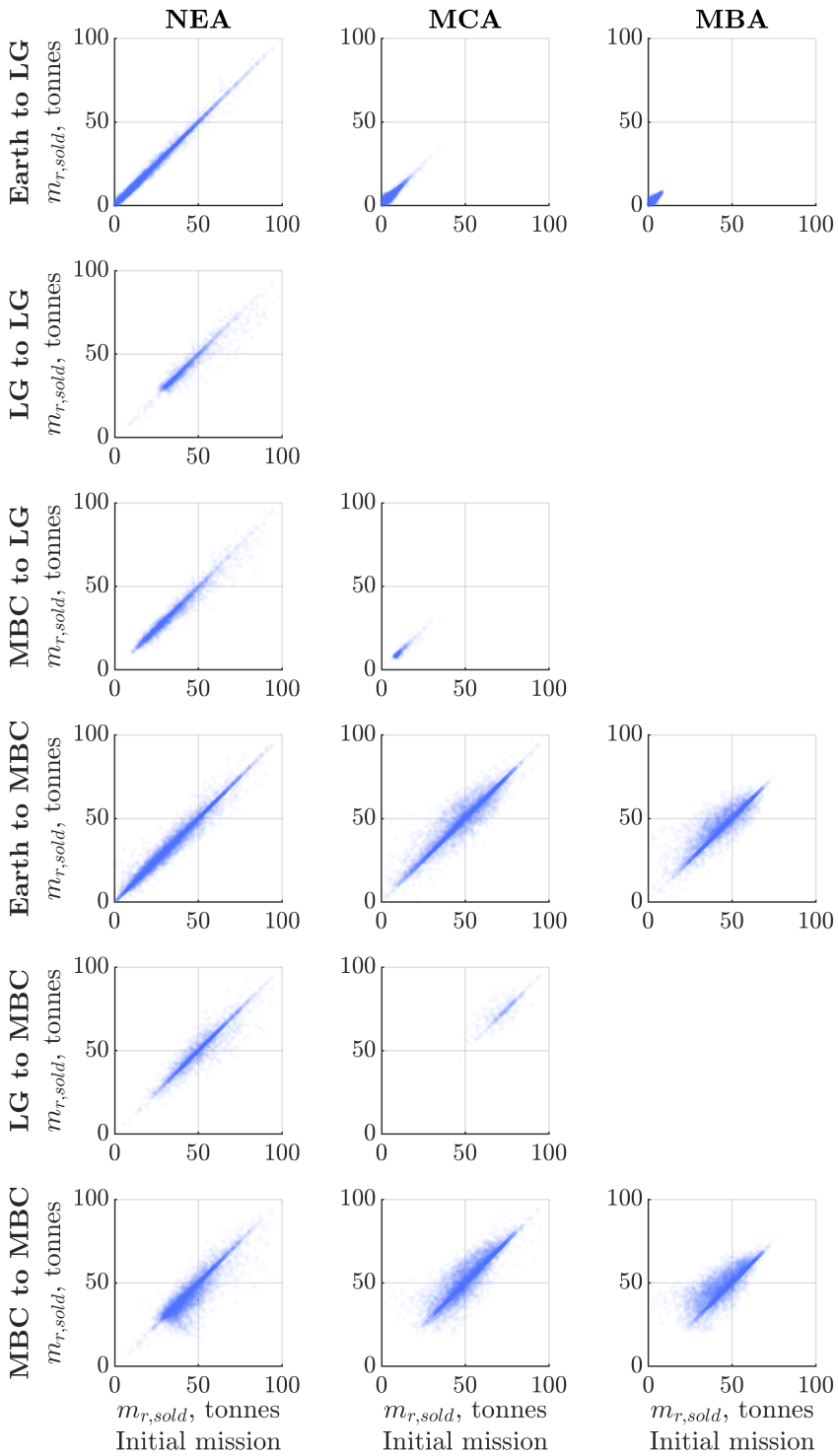

Figure 8.7: Comparison of the delivered mass of initial missions (no reuse) with the delivered mass of follow-up missions. Note that vertical and horizontal axis labels are used for all graphs in the rows and columns, respectively.

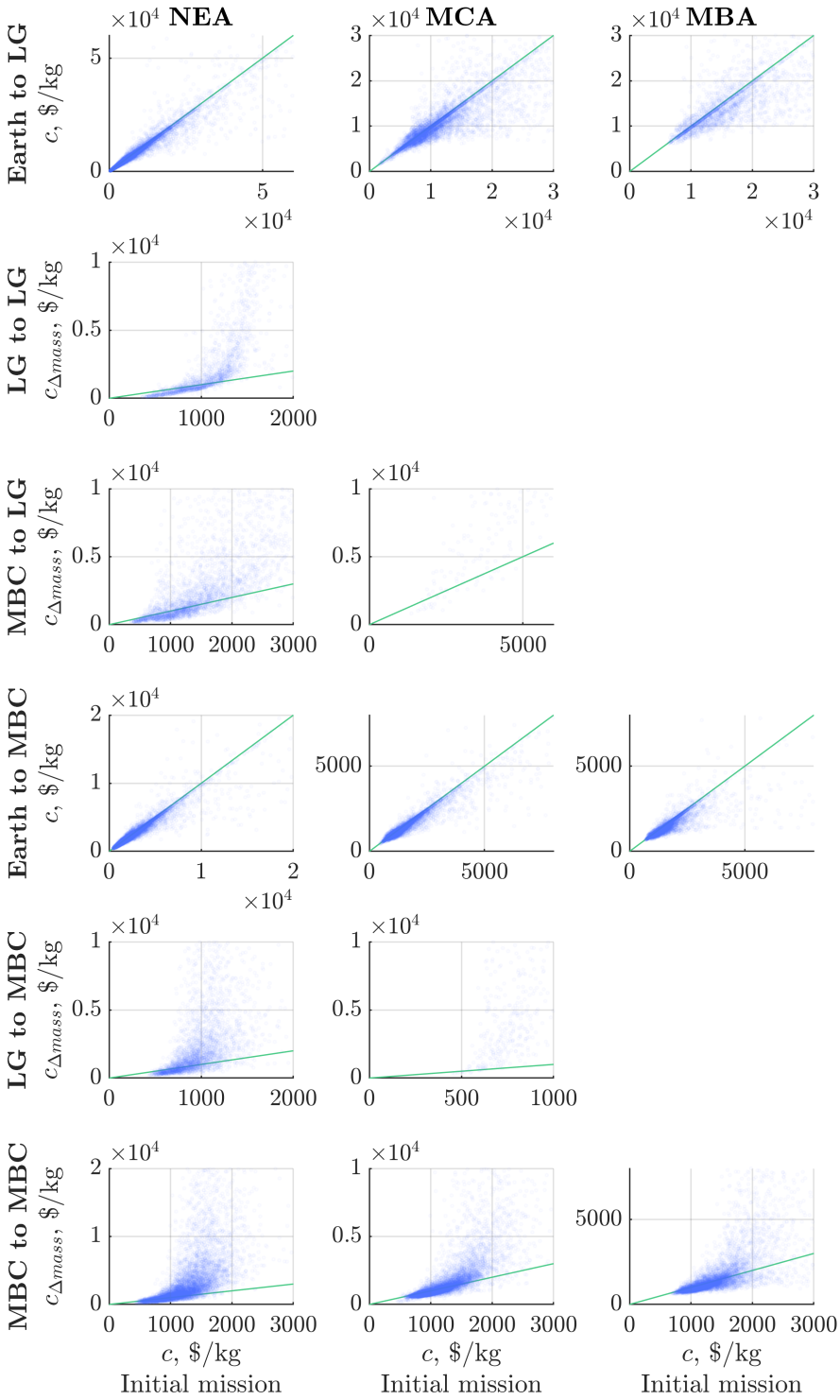

Figure 8.8: Comparison of the specific cost of initial missions (no reuse) with the (adjusted) specific cost of follow-up missions. Adjusted specific cost is shown for missions departing from a depot, following Eq. (8.8). Diagonal line added for easier interpretation of results. Note that vertical and horizontal axis labels are used for all graphs in the rows and columns, respectively.

8.3 MODEL SIMULATION

This Section presents the results obtained by running the simulation described in Section 8.1.4 using the dataset created using Section 8.1.5. As noted above, due to the limitations of both the model and dataset, it is important to interpret the trends, not the absolute values of the results.

Figure 8.9 presents the development of the specific cost to supply the required resources to both depots. Figure 8.10 shows the annual growth rate for the customer cost and demand.

Figure 8.11 presents the evolution of the total demand over time. Where the customer demand is given by the demand model as described in Section 8.1.1 and therefore determined a-priori, the internal demand follows from the simulation. For each executed mission that departs from a depot, the required propellant for the outbound mission is recorded, which as an approximation is added to that year's demand, for reasons explained in Section 8.1.6.

Figures 8.12–8.14 present a breakdown of the missions used to satisfy the demand at each of the two depots. The relative proportions of the missions are given rather than the absolute number, otherwise the breakdown of the first few decades would be imperceptible due to the exponential growth. Also, trends are more important than absolute values. Figure 8.12 shows the annual share of the mission types used for each depot, where mission type refers to those in Table 8.3. Figure 8.13 shows the annual share of missions to the different asteroid sets: NEA, MCA or MBA. Finally, Fig. 8.14 shows the annual share of mission to specific clusters following from the clustering in Section 8.1.3, as presented in Fig. 8.5 and Table 8.4. Note that the LG has priority each year for selecting the asteroids and missions, the impact of which will be explored in Section 8.4.2.

To explain the more rapid growth rate of customer cost with respect to the growth rate of the demand as seen in Fig. 8.10, Fig. 8.15 shows the normalised number of missions required to satisfy the demand each year for both depots, compared with the normalised demand of each depot.

Figure 8.16 presents for each asteroid cluster the annual percentage of asteroids in that cluster that have been used or are in use. Note that after $1/8^{\text{th}}$ of the resources have been used, the remainder of the cluster is marked off-limits. Figure 8.16 shows how quickly this moment is reached for the individual cluster. Note that after the remainder of the cluster has been marked off-limits, the asteroids that are already in use can still be used, sometimes for a number of decades, until depletion.

Figure 8.17 shows a scatter plot of the asteroid distribution, with asteroids coloured by the year each asteroid is used first. The size of each displayed asteroid is representative of the relative size of the asteroid, as calculated using Eq. (2.1). Any asteroid not used during the considered period of 100 years in the simulation is coloured grey, which can be either because the cluster the asteroid belongs to has been marked off-limits, or because the missions to the asteroid were not yet desirable due to higher specific cost than other missions. Note that asteroids can be used for a number of years or even decades, depending on its size. Figure 8.18 presents the top view of Fig. 8.17, to aid with the interpretation of the 3D figure.

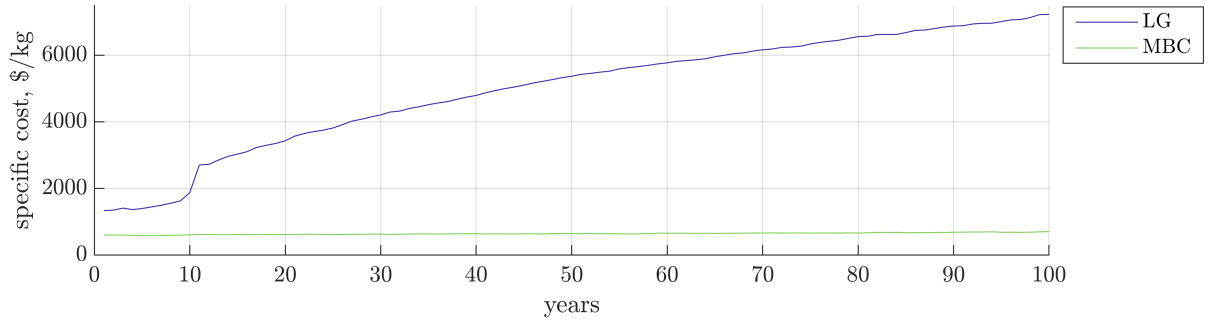

FIGURE 8.9: ANNUAL SPECIFIC COST TO SUPPLY TO EACH DEPOT.

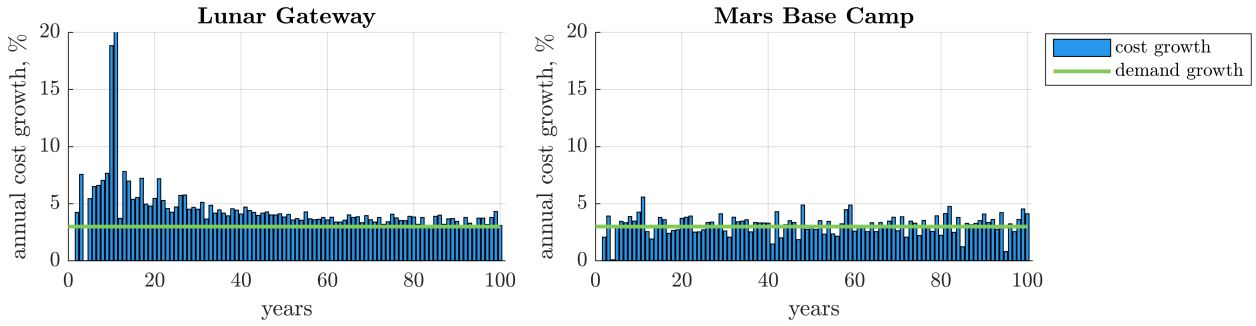

FIGURE 8.10: CUSTOMER COST AND DEMAND ANNUAL GROWTH.

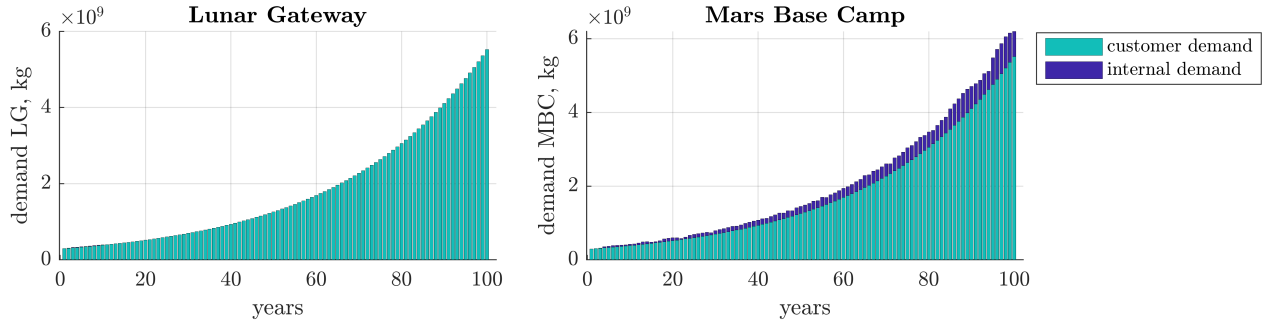

FIGURE 8.11: ANNUAL DEMAND, BOTH CUSTOMER DEMAND (FOLLOWING FROM DEMAND MODEL) AND INTERNAL DEMAND (FOR MISSIONS DEPARTING FROM DEPOT).

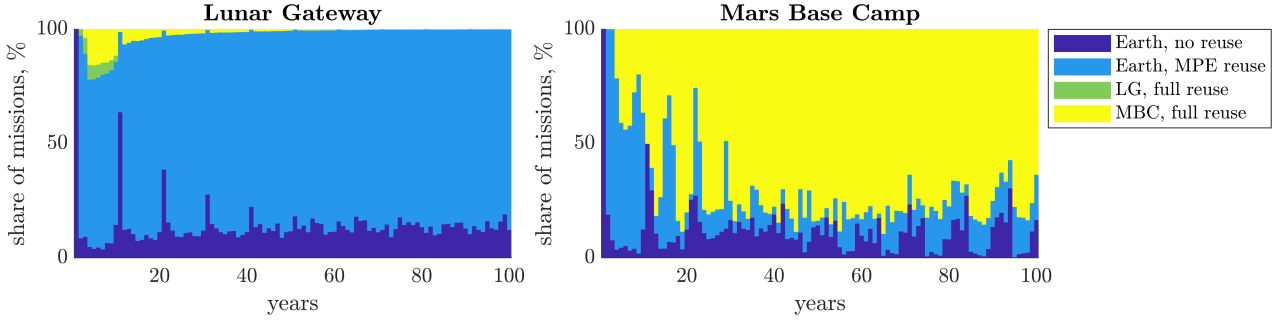

FIGURE 8.12: ANNUAL SHARE OF MISSION TYPES FOR EACH DEPOT.

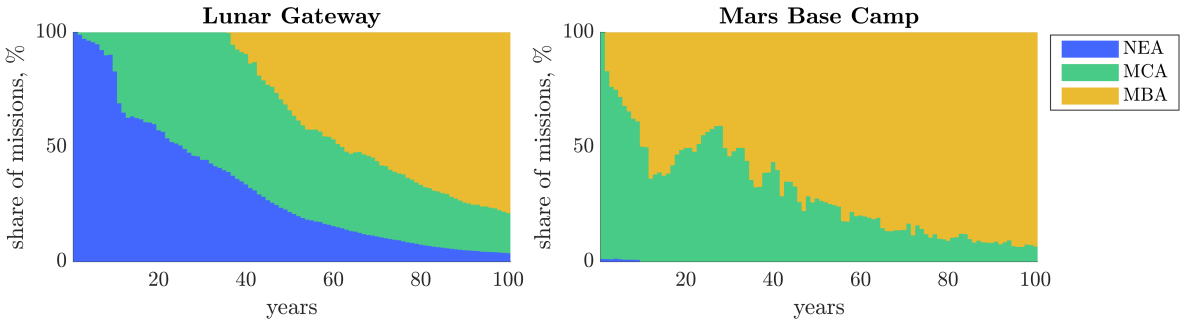

Figure 8.13: Annual share of set (NEA, MCA or MBA) used for missions to each depot.

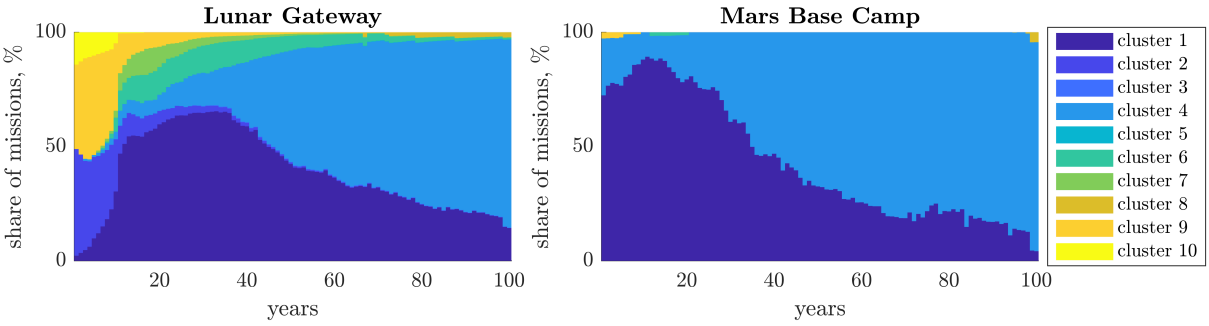

Figure 8.14: Annual share of missions to specific clusters (from Fig. 8.5) for each depot.

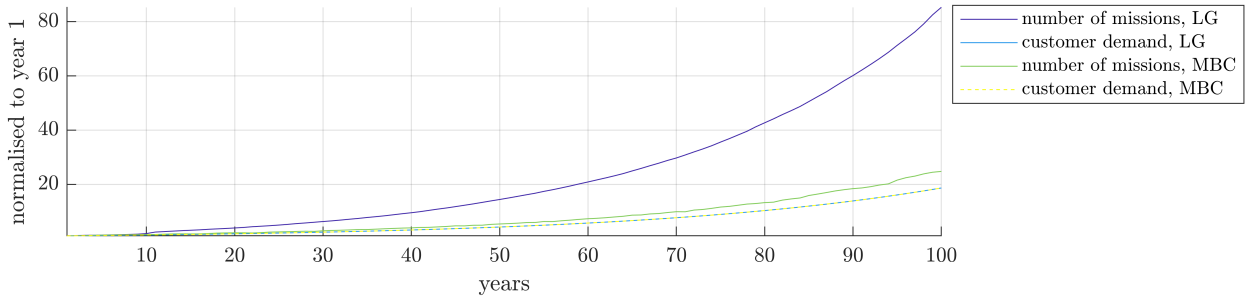

Figure 8.15: Annual customer demand and number of missions required to satisfy total demand of each depot, normalised values.

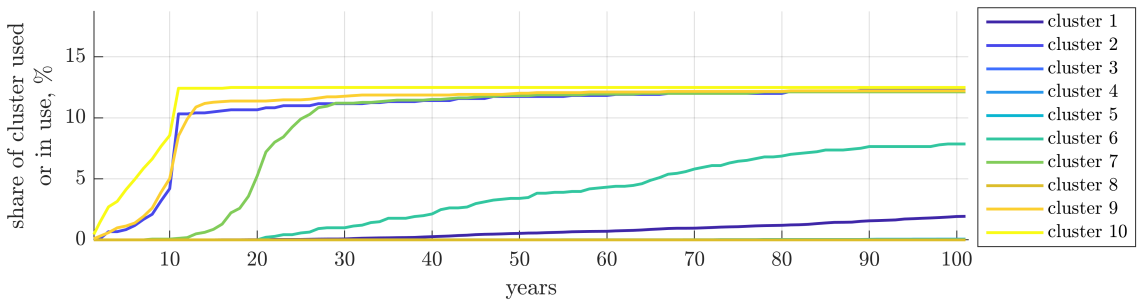

Figure 8.16: Annual percentage of asteroid cluster used or in use.

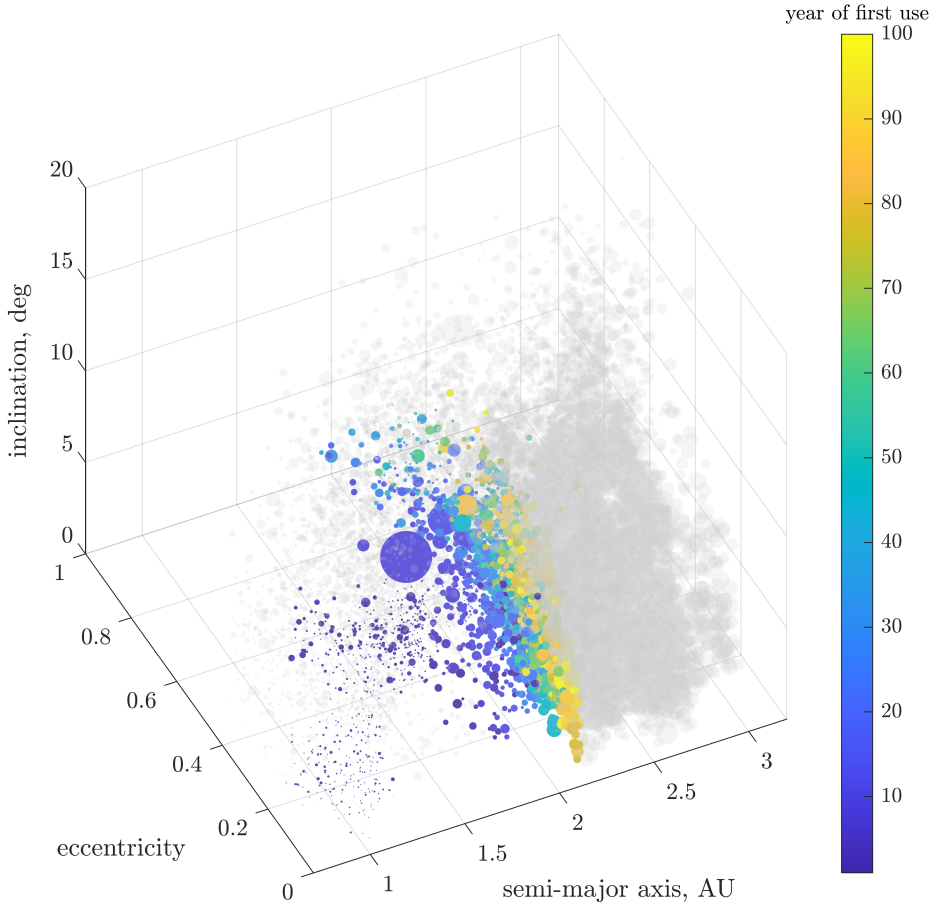

Figure 8.17: Asteroid distribution coloured by the year each asteroid is used first. Grey asteroids are unused during the considered period of 100 years.

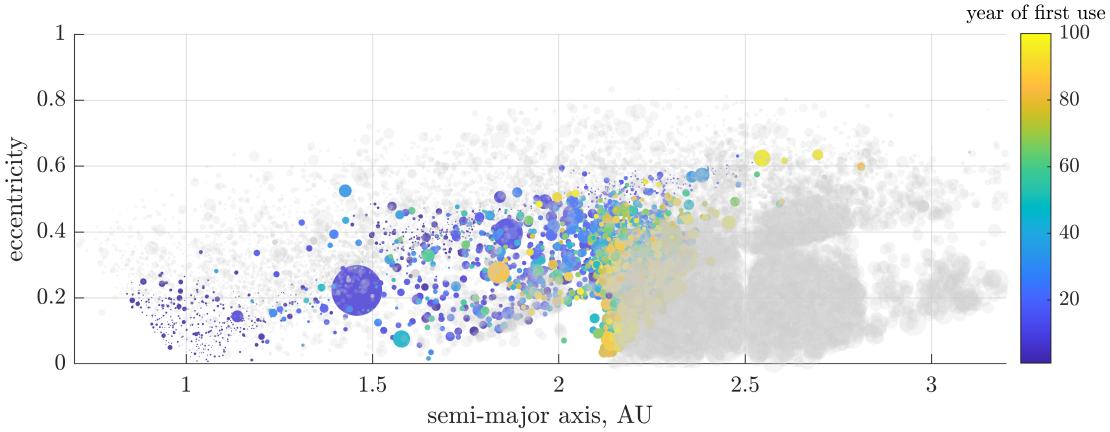

Figure 8.18: Top view of Fig. 8.17. Asteroid distribution coloured by the year each asteroid is used first. Grey asteroids are unused during the considered period of 100 years.

8.3.1 Discussion

This Section will discuss the trends that can be deduced from Figs. 8.11–8.17, supported by insights from earlier data, figures and tables in this Chapter.

Conclusions that can be drawn are as follows:

- **Increase in specific cost for customers, especially those in LG.**
  First and foremost, Fig. 8.9 shows a significant increase in specific cost for the LG. Fig. 8.10 shows that while the demand experiences the exponential growth rate of 3% per year, the cost to supply the LG grows significantly faster, especially as the target asteroids are no longer primarily NEAs. This is because the specific costs in \$/kg increase as the more affordable resources have been depleted. Figure 8.9 shows a marked increase in specific cost after approximately 10-11 years, which is around the same time as a number of clusters with NEAs reaching the $1/8^{\text{th}}$-limit, as shown in Fig. 8.16. It can be seen that this effect is significantly stronger for the LG than it is for the MBC. This is mainly due to the significant annual cost growth of the first number of years, as can be seen in Fig. 8.10. After the first two decades in the simulation, during which the year-on-year growth is significant as small yet very desirable asteroids are depleted in rapid succession, the growth levels off, but is still more than 3%. For the MBC, the annual growth in customer cost remains around the 3%, where any cost growth under 3% can be explained by asteroids being 'unlocked' by an initial mission with MPE, after which more affordable follow-up missions (which employ reuse of the MPE or all systems) can be used.

- **First NEA, then MCA and then MBA.**
  Where Fig. 8.13 already shows that the order of preference is NEA, MCA and only then MBA, as expected, Figs. 8.17 and 8.18 show more detail about which asteroids have preference. First the asteroids closest to Earth are used, after which targets asteroids have increasingly larger semi-major axis, eccentricity and/or inclination.

  Comparing Fig. 8.17 with Fig. 8.5, it can be seen that, perhaps unsurprisingly, the $1/8^{\text{th}}$ of the clusters closest to the Earth are used first, after which the remainder of the asteroids in that cluster is marked off-limits. A sensitivity analysis in Section 8.4 will show what changes when no clustering is used, which allows the simulation to use up all near-Earth resources before being directed to asteroids further away.

- **Over time less resources are delivered per executed mission.**
  Figure 8.15 shows that as the more affordable missions have been completed and these resources are depleted, the cargo spacecraft can deliver a smaller portion of the asteroid resources during each mission, as shown by the increase in n_{mis} per year which outpaces the increase in demand. This is due to the increase in ΔV^I for the transfer to return from the asteroid, as the asteroids that allow for a low ΔV^I are depleted first. As shown in Fig. 8.13, first the NEAs are used, followed by the MCAs and then finally the MBAs. Figure 8.7 then shows that, especially for the LG, this means that the delivered mass per executed mission, $m_{\text{r,sold}}$, will therefore decline over time. This is a major factor causing the increase in cost for the customers, especially those in the LG.

- **Limited number of missions departing from LG depot.**
  Figure 8.12 shows that only a very small share of the executed missions depart from the LG. Also, Fig. 8.11 shows that the internal demand for the Lunar Gateway is very limited. This is

consistent with the conclusions in Section 8.2.3, where it was concluded that missions departing from the Lunar Gateway are often not possible, with the exception of a number of NEAs. However, NEAs are relatively small and therefore reuse is limited: asteroids are likely to be depleted after a small number of missions, thereby limiting reuse of MPE. Missions departing from depots need to use resources from that depot, meaning that the subsequent mission needs a favourable ratio of ΔV^O versus ΔV^I in order to deliver more resources than it uses. The simulation shows that this is often not the case for the LG. Missions departing from the MBC are more common, as shown in Fig. 8.12, due to the proximity to many asteroids.

This means that there will be many unused empty spacecraft at the LG. While the simulation shows that it is not cost effective to use these for further mining missions, the spacecraft can be used for other purposes. For example, they can be converted to transport crew or payload from the LG, for example to the MBC. A smaller (i.e. less comfortable) spacecraft can be used to launch a crew to the LG, where they can split up in a number of spacecraft for a more comfortable trip to Mars.

- **It will take a long time to run out of asteroid resources.**
  Even in a very prosperous space (propellant) economy, it will take a very long time to run out of resources, but this is mainly due to the resources available in MBAs. The accessible resources (NEAs and MCAs) could be depleted surprisingly quickly, but the sheer number and size of MBAs means that there will be resources for centuries to come. Figure 8.14 shows that at the end of the simulation, mainly asteroids in cluster 4 are used. Table 8.4 then shows that this cluster consists of a very large set of MBAs (∼191k) and a number of MCAs (∼700). Finally, Fig. 8.16 shows that, even though cluster 4 has been used for a large portion of the simulation, barely a dent has been made in the resources of cluster 4. Table 8.4 also shows that the mean magnitude of this cluster is 17.54, meaning that the asteroids in this cluster are large and it will take a long time to deplete the asteroids, even with 100 missions per year (following Eq. (8.10)). From this it can be concluded that these resources will last for a long time, even when considering exponential growth of the space economy.

  This result also provides a justification for not running the simulation for a longer time, besides the reasons listed in Section 8.1.6. The asteroids in use at the end of the simulation can still be used for a number of years or even decades, after which cluster 4 contains many more MBAs that can be used. It is very likely that these will be used for the years beyond the current simulation.

- **Using asteroid resources at the LG is expensive and alternatives should be explored.**
  From the above conclusions it can be concluded that the LG is not an ideal location for a propellant depot supplied with asteroid resources. Costs quickly rise as it is necessary to move to less accessible asteroids. A significant portion of the harvested propellant has to be used to transport resources to the depot, resulting in a high number of missions necessary to supply the required propellant.

  It is recommended that alternative locations for a propellant depot are investigated or that alternative sources to supply the volatiles, such as the Lunar surface, are explored.

Due to the optimistic demand model, results are likely exaggerated, but still provide very valuable information regarding which asteroids are desirable, the order in which asteroid resources are utilised,

the suitability of the depot locations and what causes asteroid resources to be more expensive over time. Whether these conclusions hold for a smaller demand will be investigated in Section 8.4.3.

8.4 SENSITIVITY ANALYSIS

A number of sensitivity analyses are carried out on the simulation. First, Section 8.4.1 investigates the impact of not applying clustering, which in practice means that no asteroids are marked off-limits during the 100-year simulation. Second, the order of propellant depots is changed in the simulation in Section 8.4.2, which means that the MBC gets to select which asteroids to use first each year. Then, Section 8.4.3 investigates the effect of a significantly smaller annual customer demand. Finally, Section 8.4.4 addresses the impact of new asteroid discoveries on the obtained results.

8.4.1 No Clustering of Asteroids

When asteroids are not clustered, asteroids will only be marked off-limits after $1/8^{\text{th}}$ of all asteroids have been used, which as concluded in Section 8.3 will take a very long time. During this 100-year simulation, no asteroids are marked off-limits, which in practice means that more of the relatively affordable NEAs and MCAs can be used to supply the propellant depots. A number of figures from Section 8.3 have been reproduced for this changed simulation: Figs. 8.19 and 8.20 show the asteroid distribution coloured by the year each asteroid is used first, Fig. 8.21 shows the share of mission types each year and Fig. 8.22 the share of asteroid sets (NEA, MCA or MBA) used each year. Finally, Fig. 8.23 shows the ratio of customer costs of the new simulation (no clustering) with respect to the primary results of Fig. 8.9.

Changes in the results with respect to the primary simulation are that the NEAs and MCAs are used for longer, as these are the most attractive targets. This delays the need to use MBAs, which are expensive, especially for the LG. More missions will depart from the LG than in the primary simulation, but this is simply due to the use of NEAs.

These results show that it would be beneficial to allocate space resources through an international regulatory organisation. To preserve asteroids for future generations, not just to use as propellant, but also for other applications such as habitats or for scientific research, a number of asteroids should remain undisturbed. If these asteroids are not actively preserved, they are very attractive targets for commercial companies mining volatiles to sell, meaning that they will be devoid of volatiles and their surface material processed. This could affect the usability of these asteroids for future generations.

8.4.2 Change Priority Order of Depots

The methodology as described in Section 8.1.4 gives the LG first priority in selecting asteroids each year. As there is an imposed limit on how many missions can be executed to each asteroid each year following Eq. (8.10), this means that a number of asteroids are inaccessible to the MBC due to the design of the simulation. This Section reverses the priority order of the depots to investigate what the effect is on the annual customer cost and the allocation of asteroids clusters, sets and mission types to the depots.

Figure 8.24 presents the annual share of missions to each set, Fig. 8.25 the annual share of missions to specific asteroid clusters and Fig. 8.26 the annual share of each mission type. Finally, Fig. 8.27 shows the ratio of customer costs of the new simulation (MBC as the priority depot) with respect to the primary results of Fig. 8.9.

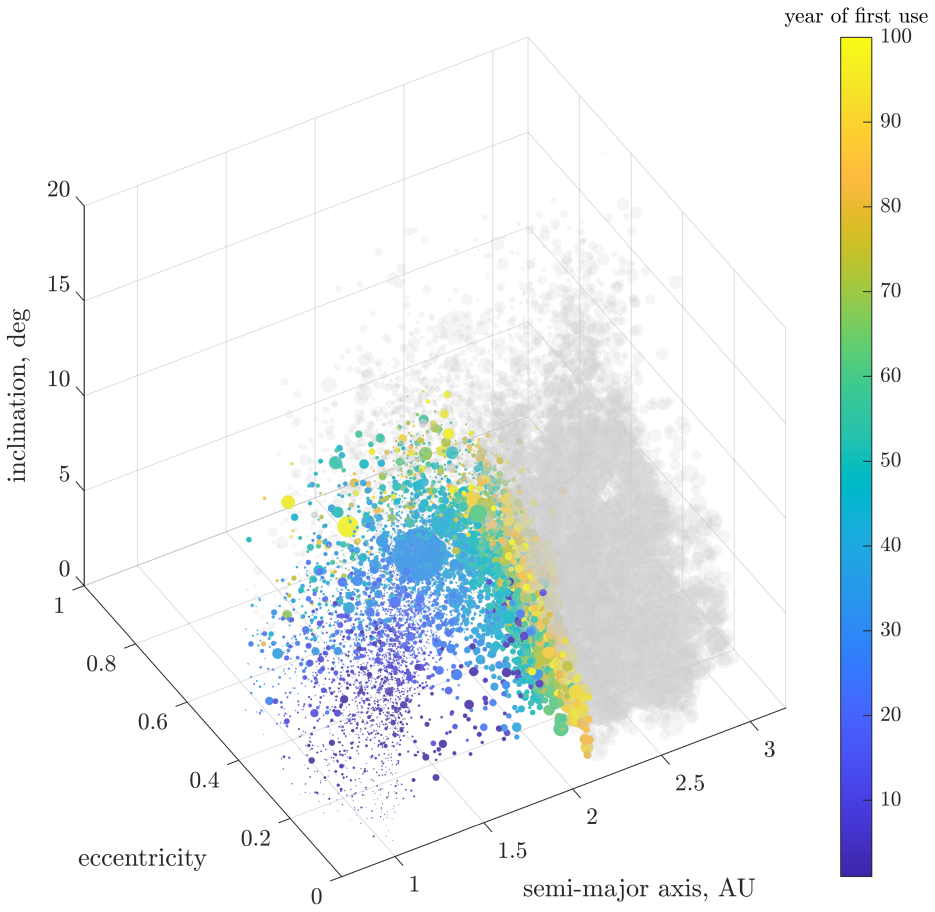

Figure 8.19: Asteroid distribution coloured by the year each asteroid is used first if no clustering is applied to asteroid dataset. Grey asteroids are unused during the considered period of 100 years.

This simulation shows that the priority order has an influence on the cost to fill each depot: LG is now more expensive and MBC is now more affordable. Especially during the first decade in the simulation, when the majority of used asteroids for the LG were NEAs in the primary simulation, this influence is most pronounced in Fig. 8.27. A portion of these NEAs are now used for the MBC instead and are therefore no longer available to supply the LG, as seen in Figs. 8.24 and 8.25. Over time, the difference in cost compared with the primary simulation is less, which can be due to either less competition in resources or because there are more asteroids available at that cost point and therefore the difference in cost due to diverting to a different asteroid is not as apparent.

As the cost to supply the LG in the primary simulation is already significantly higher, it is beneficial to give the LG priority in selecting target asteroids. Other propellant depots in the vicinity of Earth are likely to suffer the same fate as the LG in terms of rising costs, and the same will hold for these depots. Figures 8.9 and 8.27 show that the MBC is not significantly impacted by the move from predominantly using NEA/MCA to using MBA, meaning that it could be very helpful to give the LG even more priority than just within each year in the simulation, but by barring the MBC from using asteroids that can supply the LG at a favourable specific cost.

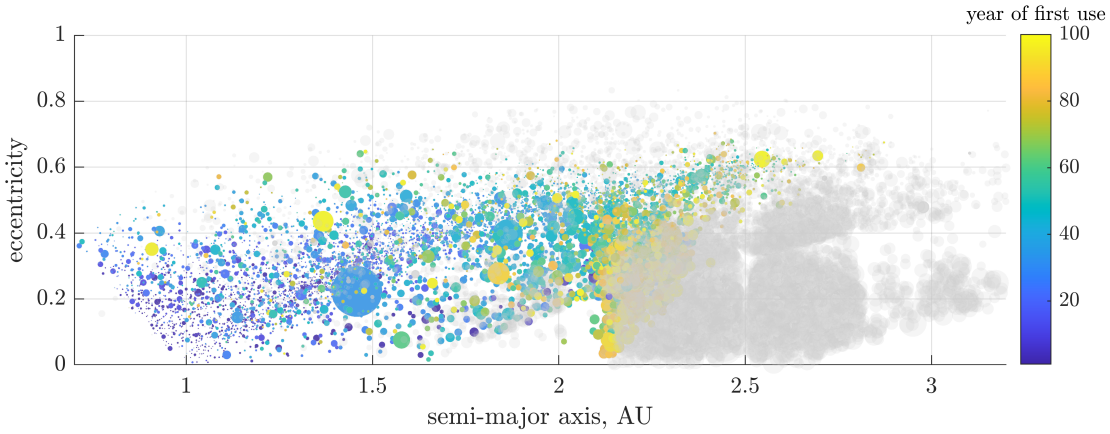

Figure 8.20: Top view of Fig. 8.19. Asteroid distribution coloured by the year each asteroid is used first if no clustering is applied to asteroid dataset. Grey asteroids are unused during the considered period of 100 years.

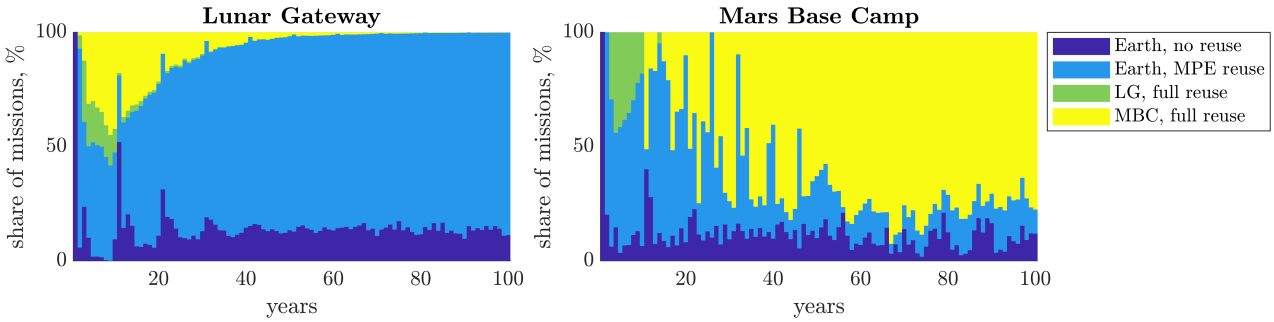

Figure 8.21: Annual share of mission types for each depot if no clustering is applied.

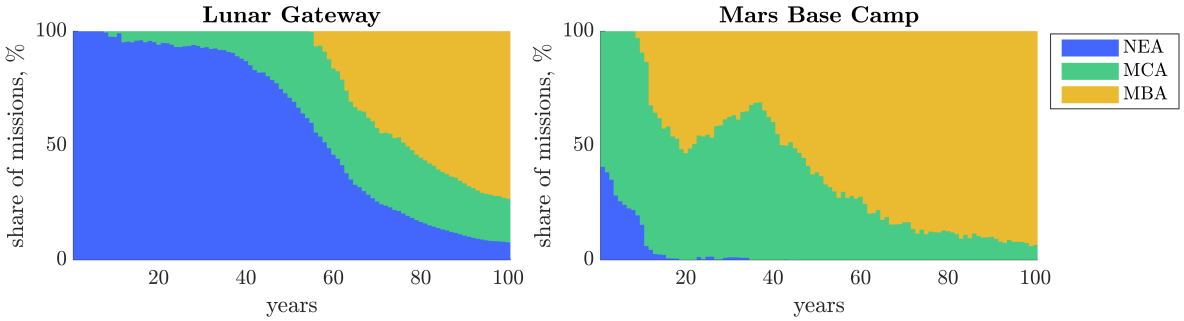

Figure 8.22: Annual share of set (NEA, MCA or MBA) used for missions to each depot if no clustering is applied.

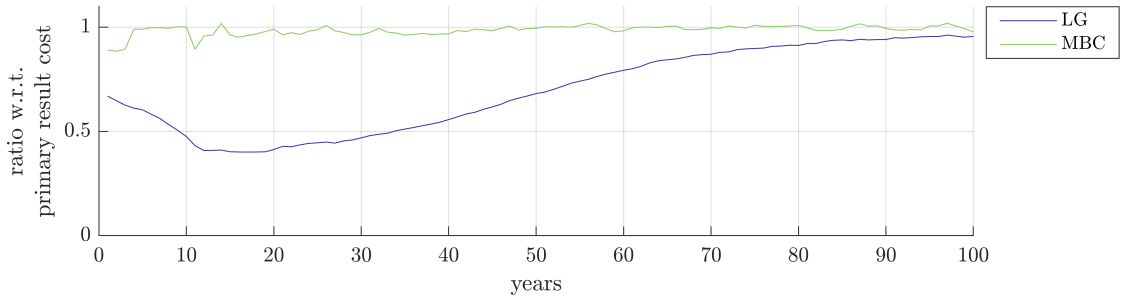

Figure 8.23: Ratio of customer cost compared with the primary results from Fig. 8.9.

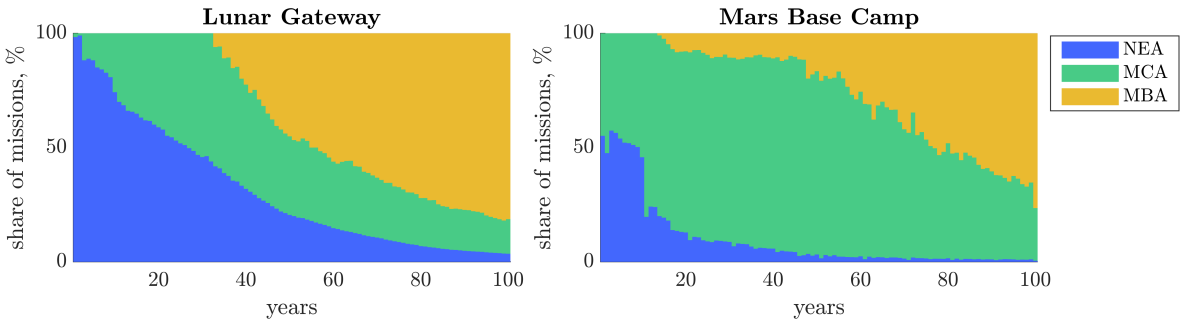

Figure 8.24: Annual share of set (NEA, MCA or MBA) used for missions to each depot in simulation where MBC has priority.

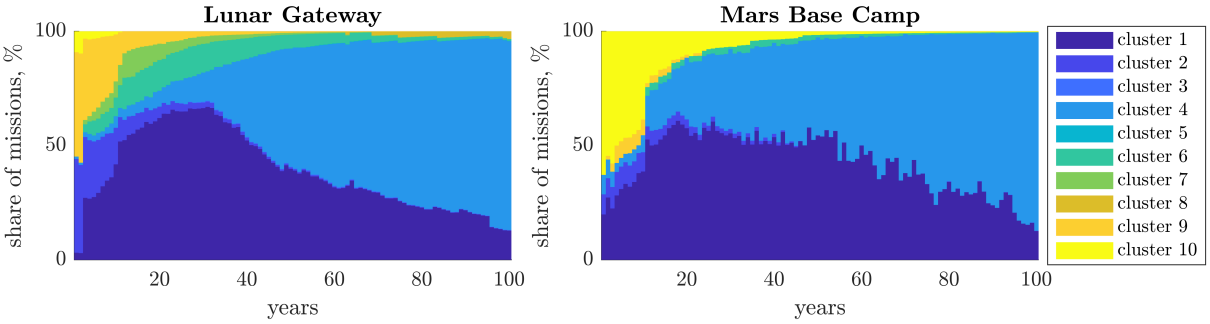

Figure 8.25: Annual share of mission to specific clusters for each depot in simulation where MBC has priority.

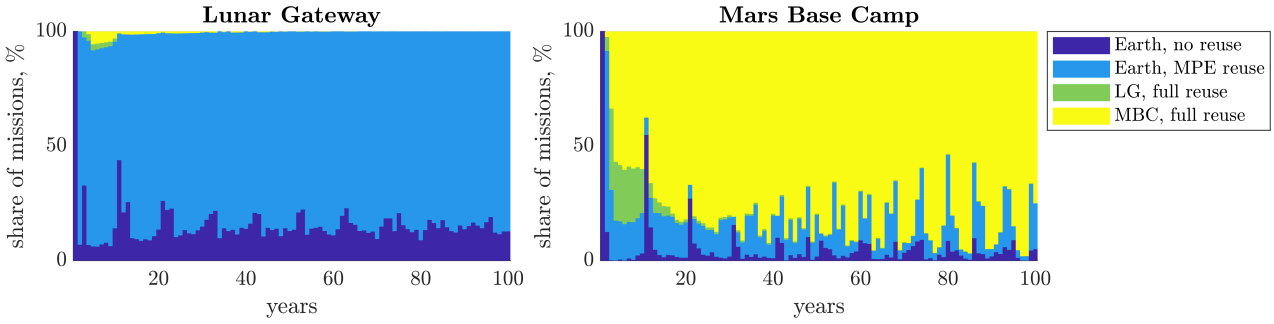

Figure 8.26: Annual share of mission types for each depot in simulation where MBC has priority.

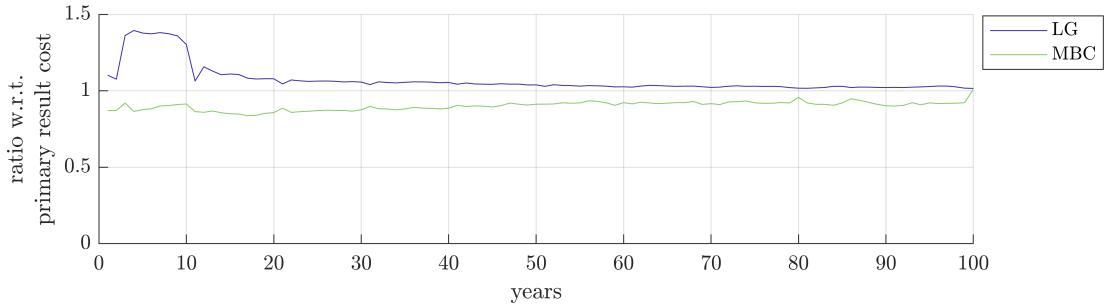

Figure 8.27: Ratio of customer cost compared with the primary results from Fig. 8.9.

8.4.3 Conservative Demand Model

The demand model discussed in Section 8.1.1 is optimistic as it assumes that SpaceX colonisation plans materialise and that only asteroid resources are used to supply propellant. To this extent, the simulation is now carried out using a significantly lower initial demand: only 1% of the initial demand in Table 8.2. With an annual demand growth rate of 3%, it takes 156 years to reach a demand that is equal to the initial demand in Table 8.2. Also, the sum of the first 46 years is equal to the demand in the first year of the simulation in Section 8.3. Rather than carrying the simulation out for 100 years, it is therefore carried out for 250 years.

Figure 8.28 presents the annual share of missions to each set, Fig. 8.29 the annual usage of each asteroid cluster and Fig. 8.30 the annual share of each mission type.

At a first glance, it appears that Figs. 8.28–8.30 are quite different from their counterpart figures in the primary simulation. For example, Fig. 8.30 shows that spacecraft depart from the LG significantly more often than in the primary simulation in Section 8.3. However, these first decades have a

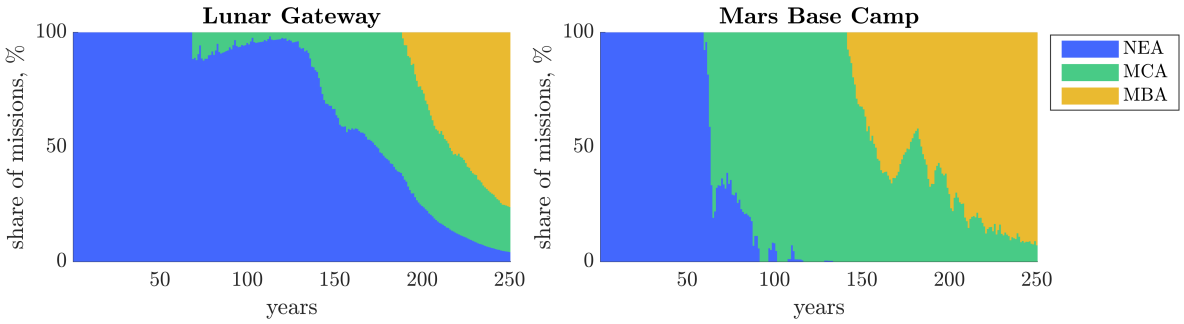

Figure 8.28: Annual share of set (NEA, MCA or MBA) used for missions to each depot with $1/100^{\text{th}}$ of the demand.

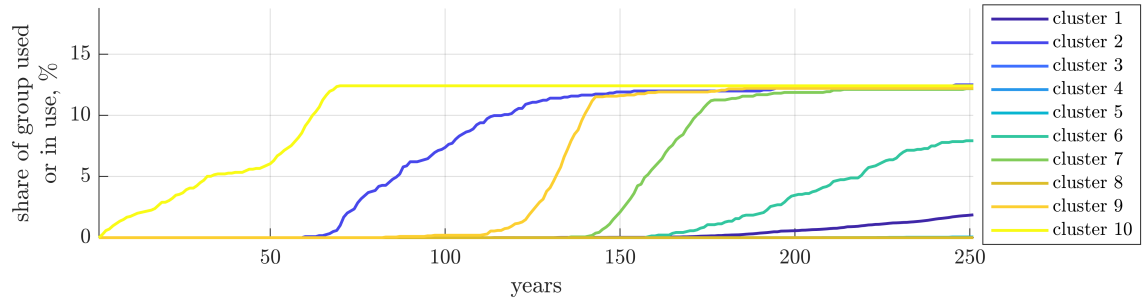

Figure 8.29: Annual percentage of asteroid cluster used or in use with $1/100^{\text{th}}$ of the demand.

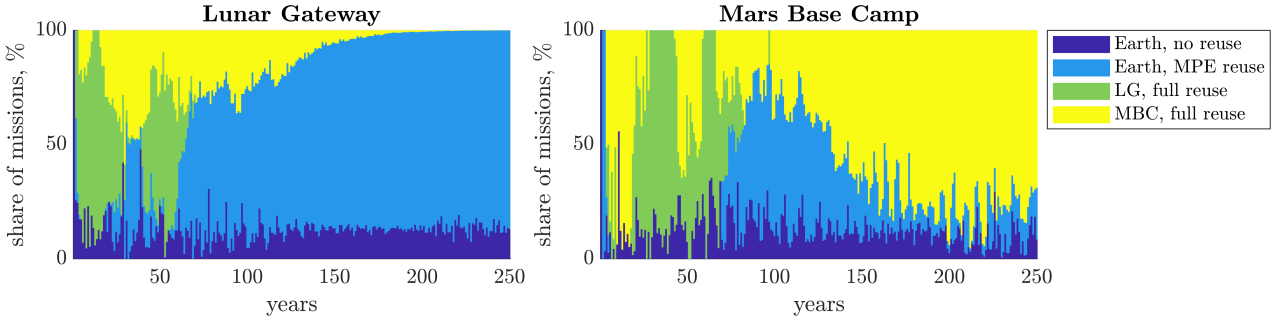

Figure 8.30: Annual share of mission types for each depot with $1/100^{\text{th}}$ of the demand.

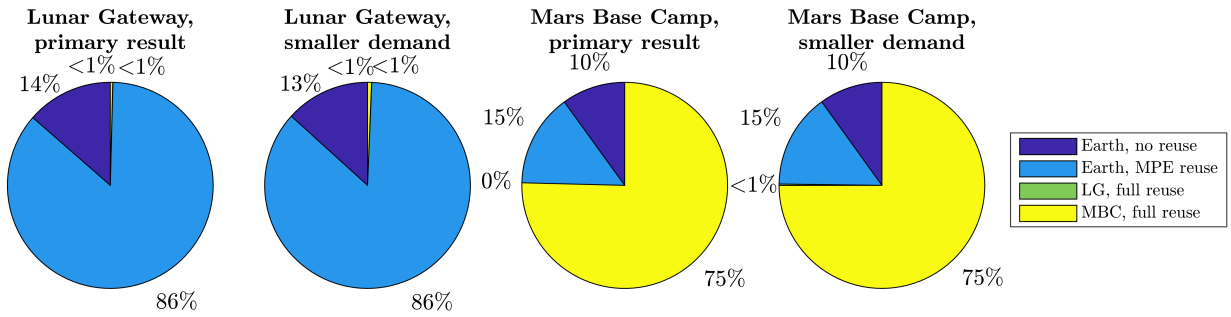

Figure 8.31: Compare the total share of mission types for each depot between the primary simulation and the simulation with $1/100^{\text{th}}$ of the demand.

significantly lower demand, meaning that even though a large share of the missions departs from the LG, in absolute numbers this is still negligible. This is visualised in Fig. 8.31, where the total share of each mission type is compared between the primary simulation and the simulation with $1/100^{\text{th}}$ of the demand. Note that the primary simulation runs for 100 years and the simulation in this Section for 250 year.

As Fig. 8.29 shows, the clusters are used similar to those in Fig. 8.16, but stretched out over a longer timeline. This means that the conclusions in Section 8.3.1 will hold even for more conservative demand models, but the timescales will change.

8.4.4 New Asteroid Discoveries

The asteroids used in this thesis are based on the JPL SBDB obtained on August 20^{th}, 2020. Since then, new asteroids have been discovered, but these have not been included in the analysis. Between August 21^{st}, 2020 and March 20^{th}, 2022, 26,696 asteroids have been added to the JPL SBDB. Out of these asteroids, 18.2% are NEAs, 5.8% are MCAs and 76.0% are MBAs. This means that, compared to Fig. 2.3, there is a relatively higher proportion of NEAs and MCAs compared to the MBAs in the set of new asteroids. Figure 8.32 shows the relative distribution of four important characteristics of the new asteroids, compared to the asteroids from the dataset until August 20^{th}, 2020: magnitude, semi-major axis, eccentricity and inclination.

Figure 8.32 also shows that the new asteroids are in general smaller, as they have a higher absolute magnitude H. This is confirmed in Fig. 8.33, which displays the magnitude of discovered asteroids over time, which shows that the discovered asteroids are increasingly small. Also, the spatial distribution of the asteroids is broadly similar to the current dataset, noting that the relatively lower semi-major axes in the new asteroid set is due to the higher proportion of NEAs.

Therefore, it is not expected that newly-discovered asteroids will have a major impact on the observed findings in this Chapter. Asteroids in a suitable location can lengthen the timescales at which trends occur, such as the increase in specific cost because more affordable resources have been used, but are not expected to radically change the observed behaviour, especially because the new asteroids are in general small.

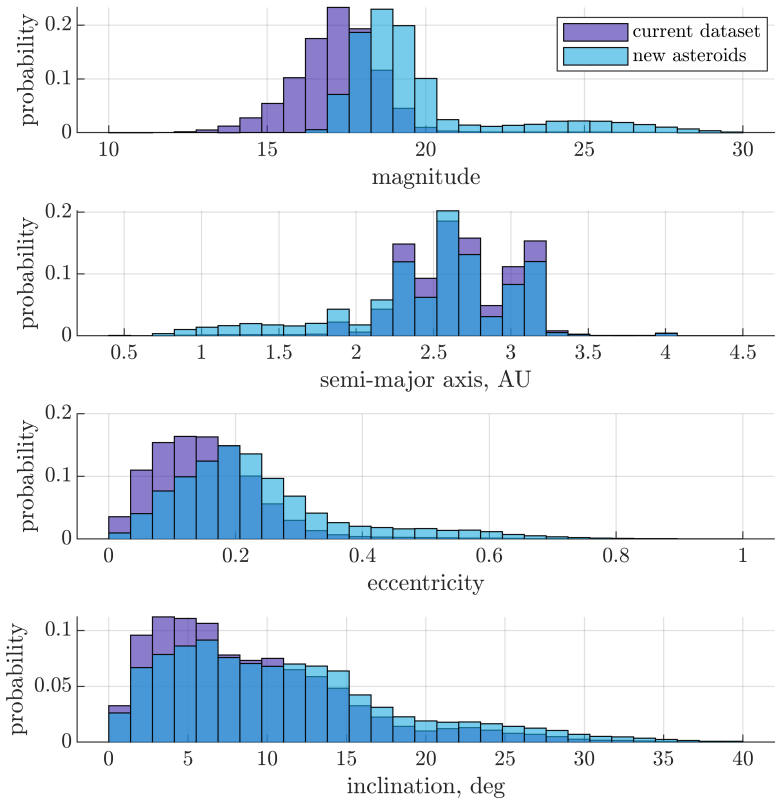

FIGURE 8.32: COMPARISON OF NEWLY DISCOVERED ASTEROIDS IN JPL SBDB WITH CURRENT DATASET.

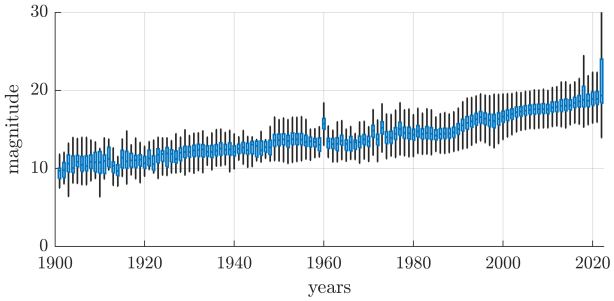

FIGURE 8.33: BOX CHART OF MAGNITUDE OF DISCOVERED ASTEROIDS PER YEAR FROM JPL SBDB.

8.5 KEY FINDINGS

NEAs are likely to be the first target asteroids due to the low ΔV to and from the asteroids. As NEAs are depleted, MCAs will be the next targets, finally followed by the MBAs. Due to the increase in ΔV^I, more resources are used on transport and less of the mined resources can reach the depots, causing an increase in specific cost. This is especially significant for the LG, which sees significant growth of the cost, outpacing the growth in demand. Specific costs for the MBC are more constant, as the MBC is in a more strategic position in relation to many asteroids. Not only are the costs more constant, they are also significantly lower.

Spacecraft can be reused by departing from the propellant depots to asteroids after the previous mission if MPE is already present at the asteroid, ready to be reused. As these spacecraft require

propellant from the depot for the outbound transfer, this is not always favourable, even though the total mission costs are lower through the reuse of equipment. Results show that often it is not desirable to reuse spacecraft at the LG, as the difference in propellant (delivered propellant minus required propellant for the outbound transfer) is often too low or even negative. The simulation shows that only to a small number of NEAs it will be beneficial to depart from the LG. For the MBC, this is different. Results show that departing from the MBC is useful to NEAs, MCAs and even MBAs.

In addition, results show that it would be helpful to have an international regulatory organisation allocate space resources to commercial entities. Unregulated, many asteroids in attractive orbits (NEAs and MCAs) will be devoid of volatiles and/or other useful materials, forcing future generations to move out to the main belt. This can happen relatively quickly, as most of these asteroids are significantly smaller than the asteroids in the main belt. Future generations may need these asteroids, not just for propellant, but also possibly for habitats or undisturbed asteroids for scientific research. Also, the international organisation could preserve certain asteroids for use near Earth (e.g. at the LG), forcing propellant depots further away to source their resources elsewhere. Sourcing elsewhere could only come at a minor cost penalty for these depots, but could be very expensive for use near Earth.

Chapter 9

CONCLUSIONS

This thesis presented a methodology for the economic modelling of asteroid mining ventures, investigations regarding the mission architecture of these asteroid mining missions and the implications of long-term asteroid resource utilisation. This final Chapter will present answers to the Research Questions posed in Chapter 1. Known limitations to the work are discussed and potential directions for future work are presented.

The research questions have been answered using a baseline mission scenario, which starts with a launch from Earth to LEO using the reusable SpaceX Starship system. The complete payload capacity of the launch vehicle is utilised, either for the cargo spacecraft, the MPE or the propellant required for the transfer to the mining location. The mining location can be an asteroid but also the Lunar or Martian surface for comparison. The MPE is deployed at the mining location and mining and processing takes place until shortly before the cargo spacecraft departs on the transfer to the customer location. The baseline mission architecture employs chemical propulsion for the transfers and therefore a portion of the recovered resources are used to transfer to the customer. At the customer location, the remaining resources are sold at a price competitive with resources launched directly from the Earth. Transfers are designed using a patched-conic approach, combining hyperbolic escape and capture where necessary, Hohmann transfers between two closed orbits around the same body, and time-dependent Lambert arcs for interplanetary transfers. The only aspects of this baseline mission that need to be optimised using a genetic algorithm are the timing of the transfers (and therefore duration of mining) and a parameter relating to how much MPE is brought to the mining location. With these optimised parameters, the architecture, mass budget and economic model are fully defined. Other parameters that are not optimised but given are the asteroid orbit and size, cost estimations (per kg of spacecraft, per year, or per launch).

1. **How can economic modelling and trajectory optimisation be integrated to produce economically viable missions?**
   The answer to this question is treated in Chapter 4.

   When basing a parametric economic model on actual trajectories (and their corresponding ΔV and duration), the trajectory optimisation can focus on optimising economic objectives that result from the economic model. In the economic model, cost elements such as development, manufacturing and propellant must be reliant on the mass of the system that follows from a parametric mass budget, and cost elements such as the operational costs must be dependent on

the actual mission duration. That way, the mission duration and ΔV can be balanced, or the the time spent on mining versus the MPE mass, or the transported mass on a solar sail versus the resulting decrease in sail performance, rather than focussing on one optimising one of these elements. Where the merits of asteroid mining are determined in relation to Earth-launched resources, the calculation of NPV which incorporates the time-cost of money, can be used to gauge the economic viability of a mission. In other cases, when asteroid mining missions need to be compared with Lunar and Martian mining, the specific cost (in \$/kg) is relevant. The optimisation of each mission can focus on minimising or maximising these economic objectives to assess the profitability or economic viability of asteroid mining.

2. **Can the propellantless nature of solar sailing be leveraged to transport low value-to-mass asteroid resources to GEO in a more economical way than chemical propulsion?**
As concluded in Chapter 5, using solar sails to transport low value-to-mass asteroid resources, such as volatiles, is likely only more economical for a small subset of NEAs. For most asteroids, a chemical propulsion mission outperforms a solar-sail mission. Using chemical propulsion, target asteroids with orbits farther away from Earth and/or higher inclinations can be reached and resources returned profitably. For the small subsets of NEAs, those very close to Earth, solar sails can return a significantly larger resource mass than the chemical spacecraft, which allows the NPV to be positive despite much longer mission durations.

   While the solar sails do not require any of the asteroid-derived propellant to transfer to GEO, which is a great advantage, transfer durations are very long, especially during the return transfer when the sail is loaded with resources. The resulting long mission duration has a profound negative effect on the NPV that can be generated with the mission. Due to the long mission duration, the IRR of the solar-sail missions is also lower than for the chemical mission, making them less attractive for investors.

3. **What happens to the profitability of selling asteroid volatiles when specific launch costs from Earth (in \$/kg) decrease?**
The conclusions from Chapter 6 are used to answer this question. Specific launch costs can decrease when the total launch costs decrease, when the payload capacity of the launch vehicle increases, or a combination of these changes. Recent advances, for example due to reusability, have caused a marked decrease in specific launch costs. For example, the Arianespace Ariane V ES launch vehicle launches 21.5 metric tonnes at a cost of 195 M\$ (9,065 \$/kg) but the SpaceX Starship system is envisioned to launch 136 metric tonnes at an estimated cost of 13.1 M\$ (96 \$/kg).

   When comparing these two launch vehicles, the NPV is a valuable tool. To calculate the NPV, the revenue has to be calculated, which is based on a price that must be competitive with launching the same resources from Earth. This means that not only the cost of the asteroid mining mission depends on the specific launch cost, but also the revenue. Using the methodology in Chapter 4, for the Ariane V ES the selling price is 29,947 \$/kg and for the Starship 658 \$/kg. This significant difference in price results in a NPV that is far higher for the Ariane V ES than for the Starship: 1,111 M\$ versus 102.2 M\$ to asteroid 2000 SG344. This shows that the profitability of asteroid volatiles is significantly lower with the Starship, whose costs are far more likely to be the norm in the future. Using a launch vehicle more expensive than the cheapest one available results in even lower NPV values, as the resource price should still be based on

this cheaper launch vehicle.

In more general terms, all other things equal, decreasing launch costs result in a net decrease in NPV, as the decrease in mission cost cannot make up for the decrease in revenue. However, all other things equal, an increase in payload capacity results in a slight increase in NPV, because the quantity of delivered resources increases correspondingly, allowing for fixed costs to be amortised over more sold resources. Therefore, what happens to the profitability of selling asteroid volatiles when specific launch costs from Earth (in \$/kg) decrease, depends on what the cause for the decrease in specific launch costs is. The resulting effect of a combination of these two factors will depend on the relative decrease in launch cost and increase in payload capacity, but is more likely to be a decrease of NPV.

Finally, it can be concluded that the specific launch costs have a significant impact on the profitability of an asteroid mining mission. In order not to overestimate the profitability of asteroid mining, realistic specific launch costs should be used in an analysis.

4. **In which customer locations can asteroid volatiles compete financially with volatiles obtained from the Earth, Moon and Mars?**
The results obtained in Chapter 7 are used for this answer.

   On the surface of these bodies, asteroid volatiles cannot compete with resources mined and processed on the same surface. This is the case even when comparing the specific cost for producing only one cargo spacecraft filled with resources, even though the MPE can be reused on the surface for multiple years to drive down costs.

   Customers in LEO benefit from the lowest ΔV from the Earth surface compared to the other sources, and therefore also a relatively high ΔV when returning from asteroids. This means that for customers in LEO, asteroid volatiles are not competitive with resources from the Earth's surface.

   For the other customer locations, such as GEO, in Sun-Earth or Sun-Mars Lagrange points, in orbit around or near the Moon or Mars, or in the main asteroid belt, asteroids can compete financially with volatiles from the Earth, Lunar and Martian surface. It should however be noted that this is for one full cargo spacecraft and when a customer is in close proximity to for example the Moon, it could benefit from this proximity by reusing the MPE for a number of years. Due to the moderate ΔV for descent and ascent, the Moon would allow for these repeated trips, but for Mars, this would be impractical due to the relatively high ΔVs and the heat shield needed for atmospheric entry. Even though the cost of Lunar resources can be brought down by repeated trips, Lunar volatiles are finite and found at lower concentrations than on asteroids and the argument could be made that these resources need to be reserved for future Lunar colonies.

5. **What happens to the affordability of asteroid volatiles after the lowest-cost resources have been used up?**
The simulation in Chapter 8 is used for this answer. NEAs are likely the first targets of commercial asteroid mining companies, as they are easily accessible from Earth and also have low ΔV^I to a depot near Earth or Mars, allowing for relatively low specific cost for the delivered resources. However, NEAs only make up a small portion of asteroids and they are generally small. This means that NEAs can be depleted of volatiles surprisingly quickly in a thriving space propellant market. When the attractive targets with low specific cost volatiles have been

used up, asteroids with orbits further away from the Earth will be targeted. After the NEAs, commercial companies will turn to MCAs and finally to MBAs. This means that the ΔV^I increases and more propellant is used on the transfer, which in turn means that both the specific cost will increase and that more missions are required to satisfy an equal demand. This makes asteroid volatiles less affordable.

How much less affordable depends on the location of the customer. For example, the specific cost of resources delivered to the Lunar Gateway is more dependent on whether NEAs are still available than the specific cost of resources delivered to the Mars Base Camp. The Mars Base Camp is in closer proximity to more asteroids: NEAs, MCAs and MBAs. This causes the specific cost for volatiles to be more resistant to unavailability of NEA resources.

There is a risk of disadvantaging future generations by using up the most affordable resources. After these resources have been used for propellant, they are gone forever. As commercial companies are likely to target the asteroids with the most affordable resources, a need for regulation arises to ensure an equitable distribution of asteroid resources for multiple generations, all countries, and different in-space depots.

6. **Is reusing spacecraft for successive asteroid mining missions for propellant more profitable than single-use spacecraft?**
Sections 5.3.3, 6.4.1, and 8.2.3, as well as insights from the simulation in Chapter 8 are used to answer this question.

Reusing spacecraft means a reduction in cost as no new launch has to be paid for and no additional development and manufacturing costs are applicable, only maintenance costs. Therefore, profits can increase when spacecraft are reused, depending on the situation. However, a number of drawbacks make reusing spacecraft less attractive for asteroid mining missions.

First, the spacecraft cannot deliver the full load of propellant to the customer at the end of the trip, as a portion of propellant will need to be reserved for the outbound transfer of the next trip. This decreases the revenue of the first mission, possibly significantly.

Second, on top of the decreased revenue of the first trip, the revenue of the successive trips will suffer from a high discount in the calculation of the NPV, due to the long total mission duration. Missions to even the closest NEAs are likely to last upwards of a year or two. For example, for a two year mission duration and 10% annual discount rate, revenues of the first trip are decreased by 21%, a second trip by 46%, third trip by 77% and a fourth trip 114%. For the return trips to MBAs, which have much longer mission durations, this effect is even more pronounced. The discount rate is applied because investors could have invested the same capital in other projects, meaning that the time-cost of money needs to be taken into account. Note that each successive trip decreases the revenue of the previous trip by requiring propellant for the outbound transfer, which would have been discounted less than any propellant returned during the successive trip.

Third, while any trip can be optimised for optimal ΔV, phasing of successive trips is likely to cause an increase in ΔV. Repeated trips within the Earth-Moon system for Lunar mining, for example, would not suffer from this drawback, but it should be taken into account for repeated trips to asteroids.

Concluding, it is shown that whether reuse results in net lower costs and increased profitability depends on the location where the resources are needed. For example, a successive trip departing

from a propellant depot near the Moon is likely only cost effective for a small number of NEAs. Reusing spacecraft from a propellant depot in Martian orbit, which is energetically closer to a larger number of asteroids (NEAs, MCAs but also MBAs) is more likely to be cost effective.

Note that these results are based on simplifying assumptions and should be treated with caution. However, they provide some important indications for where, how and under which conditions asteroid mining can be profitable.

9.1 LIMITATIONS

The research presented in this thesis has been able to answer the Research Questions outlined in Chapter 1, by developing a generic parametric approach. While initial conclusions have been drawn, the proposed methodology has included a number of simplifications and approximations, to allow for the development of the analysis. Known limitations of the current methodology and results are described here:

- **Lack of heritage data**, as no asteroid mining mission, large-scale in-space commercial cargo transport, high-performance solar sails, or long-term storage of LOX/LH_2 has taken place yet. This has implications on the TRL levels and therefore risk and cost, and so complicates accurate cost estimations.
- **Cost estimations** had to be made for the mid- to far-term. Where cost estimations for the short term are already subject to significant uncertainties in the case of novel technologies, this is exacerbated for cost estimations further in the future. Even if heritage data analogous to asteroid mining missions would exist, the data often suffers from a temporal, cultural, and technological gap due to time delay.
- **Generic approach** used means that advantageous trajectory manoeuvres specific to the combination of mining and customer locations are not incorporated, which could bring down the ΔV of individual cases.
- **Only one mission** is considered in the baseline scenario. If multiple follow-up missions would be considered, the proximity between the mining and customer locations would have a larger influence on the obtained results, especially in the case of long synodic periods. However, if the NPV is used to assess the profitability of these follow-up missions, they would suffer from a very high discount, making these far less attractive. This was also concluded in Ref. [126].
- **Asteroid compositions** are uncertain. The spectral type of only a small number of asteroids has been determined, meaning that for most asteroids, highly uncertain assumptions have to be made. Even if the spectral type is known, there are still many unknowns. This research has incorporated average values for albedo, density and volatile recovery ratio, but even those are uncertain in some way, as not many sample-return missions have taken place and a myriad of spectral types exists.
- **Simplifying dynamical models** have been used, such as the two-body model. In an initial investigation to assess the feasibility of an architecture, this is appropriate, but for any follow-up analysis, more complex dynamical models may be required.

In future research work, these uncertainties and limitations can be addressed to further investigate the profitability of asteroid mining. However, the lack of heritage data and uncertain asteroid compositions depend on expensive space missions and these could therefore not easily be mitigated with low-cost (academic) research projects.

9.2 FUTURE RECOMMENDATIONS

Considering the current limitations of this thesis, as well as promising avenues for future research identified in this thesis, a number of recommendations for future research are presented.

- **A dedicated comparison of Lunar and asteroid mining**, especially for multiple missions, can provide insights into the benefits of close proximity of the source and customer location and the resulting rapid turn-around time for repeated missions. As the asteroids from which we can use resources most affordably in the Earth-Moon system, are located near the Earth, the synodic periods are long, which can become an issue for repeated missions to the same asteroid.

  A similar comparison for Martian and asteroid mining does not have the same urgency. This is because it follows from this thesis that customers on the surface of Mars would be better off using Martian resources and not asteroid resources, and any customer off the surface of Mars would not benefit from Martian resources due to the high costs of lifting these resources off the Martian surface.

- **Prevent the need for long-term LOX/LH_2 storage**, possibly by comparing different water-based propulsion techniques or investigating the possibility of electrolysing the water into LOX/LH_2 shortly before it is required. Long-term storage of LOX/LH_2 suffers from boil-off and/or requires significant cooling, meaning that long-term storage has not yet been applied for space missions. Other options for water-based propulsion techniques include nuclear-thermal propulsion with hydrogen (which could be an issue due to the nuclear aspect), solar-thermal steam propulsion (which has a significantly lower I_{sp}), or water electrolysis propulsion (which has a very low TRL, especially for large spacecraft). A thorough analysis of these options and a quantification of the issues with long-term storage of LOX/LH_2 would be a very useful avenue of future research.

- **Incorporate specific methods to bring down individual ΔV** for specific combinations of mining location and customer locations. Examples are low-energy transfers, gravity assists or aerobraking. Even though these concepts could impose additional requirements on the structure of the spacecraft or the complexity of mission operations, as well as add to the mission duration significantly, the potential ΔV reduction merits further investigation into their effect on the NPV or specific cost.

- **Cost estimations for commercial space entities** instead of space agencies are highly uncertain currently, in part because of commercial proprietary information. The consensus is that cost estimations for commercial parties are lower than for the more traditional governmental space agencies as NASA and ESA. However, how much lower is not known. Since asteroid mining will (eventually) be undertaken by commercial parties, for which cost is a very important factor, proper cost estimation is essential.

- **Include risk in the economic model**, for example by including insurance costs or a probability of mission success. This is especially interesting when considering a larger space infrastructure, where any commercial space company would have a larger number of spacecraft operating simultaneously. Depending on how much risk is covered by insurance, the costs for insurance can be significant. This could change when the number of missions increases, as economic returns are not as dependent on one single successful mission. However, it would be useful to investigate how these costs change over time and how much they impact the profitability of asteroid mining missions.

- **High value-to-mass resources**, such as PGMs, have not been researched in this thesis, which focuses on LOX/LH_2 propellant. Even though the TRL for mining PGMs is low, it will be interesting to perform the same analyses for these resources, as PGMs are needed on Earth for technology development. Especially the investigation of different propulsion methods should be repeated for these resources, as propellant for both the outbound and inbound might have to be brought from Earth, as using asteroid resources might not be possible. For solar sails, a smaller total mass of resources will have to be transported for similar revenues, resulting in a higher sail performance on the transfer from the mining location to the customer location. High value-to-mass resources could therefore change the propulsion technique trade-off results which was carried out for low value-to-mass resources. Mining, processing and transporting other resources, such as semi-conductors or other valuable metals, either for use in space or on Earth, would also be interesting.

- **A more detailed mining model**, not only a throughput rate, would be beneficial for the mass budget, estimated cost and a more accurate representation of the mining phase and the time needed. This more detailed model can also indicate the technology maturity needed to initiate a commercial venture, as the required technologies could be too expensive for only one commercial entity to bear the R&D costs.

APPENDIX A

SUMMARIES OF EXISTING COST MODELS FOR ASTEROID MINING

Note that any symbol in this appendix are used directly from the source treated in that Section and may differ from the rest of the thesis. This will be indicated clearly where necessary.

A.1 SONTER

Sonter presented one of the first economic models for asteroid mining in Ref. [21], based on the NPV introduced by Ref. [27], from a terrestrial mining background. The NPV model is still used and referenced to this day, due to its flexibility and parametric and multi-disciplinary approach. It recognises that just optimising physical parameters such as ΔV or I_{sp} does in general *not* lead to the most economical system. Also, Ref. [21] notes that that up till then (1997) no quantitative comparison had been possible between different cost estimations from different researchers. Each study calculates costs differently and with different scenarios, without isolating the effects of separate system components. The proposed model aims to quantitatively assess the merit of a large number of combinations of destinations, processes, and products. The classic NPV from Eq. (3.4) is expanded for astrodynamics and rocket equation variables [21]:

$$NPV = \$/kg_{\text{orbit}} \times M_{\text{mpe}} \times f \times t \times \%\text{recov} \times e^{\frac{-\Delta V}{v_e}} \times (1+I)^{-a^{(3/2)}} - (M_{\text{mpe}} + M_{\text{ps}} + M_{\text{i\&c}}) \times \$/kg_{\text{manuf}} + \text{budget} \times n \tag{A.1}$$

where $\$/kg_{\text{orbit}}$ is the price of the mined products per kg in the destination orbit of the products, M_{mpe} the mass of the MPE, f the throughout rate (kg of processed resources per kg of equipment per unit of time), t the time allocated to mining and processing, %recov is the percentage of the asteroid that can be recovered as a volatile, v_e the exhaust velocity of the propulsion system, a the semi-major axis of the transfer orbit, M_{ps} the mass of the power source, $M_{\text{i\&c}}$ mass of the instrumentation and controls, $\$/kg_{\text{manuf}}$ the specific cost of manufacturing, 'budget' the annual budget in \$, and n the number of years from capital-raising until product return [126]. Unless defined elsewhere in this thesis, these symbols will not be reused.

Equation (A.1) means that the time spent on mining is not taken into account for the discount, which is only based on the period of the transfer orbit through $a^{3/2}$. Other elements not taken into account in the NPV calculation, which are treated elsewhere in Ref. [126], are the mass and associated cost of the payload container/bag, propellant, and of the spacecraft itself (except for $M_{\text{i\&c}}$). Only

manufacturing costs are considered, meaning that development costs, are ignored. Calculations for trajectories are based on simple Hohmann transfers and therefore likely optimistic, although they do include plane changes, which are not insignificant for some asteroids.

The MPBR for the same scenario is simply given by [21]:

$$MPBR = \frac{M_{\text{mpe}} \times f \times t \times \%\text{recov} \times e^{\frac{-\Delta V}{v_e}}}{M_{\text{mpe}} + M_{\text{ps}} + M_{\text{i\&c}}} \tag{A.2}$$

meaning that variables related to time ($a^{3/2}$) and money (\$/kg-values, I, and budget) are not included. Both time and money related to asteroid mining ventures are significant, so including them in the economic decision making process is key.

A.2 ROBOTIC ASTEROID PROSPECTOR (NASA INNOVATIVE AND ADVANCED CONCEPTS)

In a nine-month NASA-funded study (Refs. [31, 119, 250]), a team of industry experts investigated the feasibility of mining asteroids, including an infrastructure framework, identification of potentially feasible resources and a spacecraft design. With respect to economics, the team was unable to find sufficient economic data, models and expertise to produce a verifiable economic model, or the expertise to perform the demand model study. Predicting costs for PGM extraction on Earth is extremely difficult, let alone in space. Therefore, the team focused focusing on water as the main resource, "since extracting water is much easier than extracting PGMs or other metals", to create a parametric analysis. The parametric model examines the market price and sales over time to recoup an initial investment, to begin making a profit. The model utilises NPV and risk-adjusted ROI as decision variables to determine feasibility. The team stresses that many factors that cannot be well established at this time are part of the calculation for the total system cost. Also, the asteroid mining project would be a commercial venture and likely not mirror the costs for a traditional NASA project, rendering conventional cost estimation methodologies inaccurate.

The investigation includes a preliminary ΔV budget: 3.50 km/s for Earth departure from LEO, 1.25 km/s for asteroid arrival, 1.35 km/s for asteroid departure and 2.50 km/s for Earth arrival.

The goals of the parametric analysis is to determine whether or not asteroid mining can deliver resources to the Earth-Moon L_1-point (EM-L_1) at a lower cost than the competition, which at present is the delivery of resources from Earth. To estimate the cost for these resources, it is assumed that a Falcon Heavy is used to lift ~ 50 tons of payload to LEO (at a cost of \$125 million), with a LOX/LH_2 kickstage and the water as the payload. This payload consists of: the payload of water for EM-L_1, a carrier to hold that water and a LOX/LH_2-stage. The payload carrier is simply a tank to hold the water and has a structural fraction of 10%, well within the state-of-the-art, allowing for mass margin for rendezvous, proximity operations and berthing aids to dock the spacecraft at the destination. The same structural fraction is used for the LOX/LH_2 stage, also within the state-of-the-art. With this methodology, it is calculated that of the 50 ton payload in the Falcon Heavy, $16,267$ kg of water can be delivered. For the cost of the carrier and LOX/LH_2 stage, \$75 million is estimated. This results in a specific cost of 12,295 \$/kg of resource from Earth to EM-L_1, which is the threshold for asteroid mining to become an economic success.

The cost of the spacecraft is based on previous interplanetary spacecraft. Development and production costs are estimated at \$500 million and \$300 million, based on the fact that a number of inter-

planetary spacecraft have been designed, built and flown for that cost. Other included cost elements are for refurbishment (10% of procurement costs) and annual operations ($40 million), all estimated by experts but not verified through a cost estimating technique. The team assumed a development cost of $500 million, since a number of interplanetary spacecraft have been designed, built and flown for that cost. They assume that the subsystems can mostly be derived from existing systems. Production cost have been estimated at $300 million per spacecraft, based on the estimated mass. Refurbishment costs are estimated at 10% of the procurement costs. The solar-thermal propulsion unit is expected to incur another $1 billion in development cost, and $300 million of production cost. For the mining equipment, the team ran into great uncertainty and estimated $1 billion in development costs for the system and $300 million for production costs. The annual operation budget depends on the number of spacecraft, starting at $40 million per year, adding $2.5 million for each additional spacecraft after the first. Note that these values are not verified by any other cost estimation technique, nor does the report provide references. They are however senior members of industry of well-respected companies, operating under a NASA contract.

The model requires 11 years of building the infrastructure and performing the first mission, after which the first revenue can be created. Each of the envisioned four mining spacecraft is expected to return 150 metric tons of water to EM-L_1. Selling this at 8,000 $/kg, comfortably below the 12,000 $/kg from terrestrial water, means that they can compete with terrestrial competition. When running the model, the first revenue would be created after 11 years of building up the in-space infrastructure and completing the first mission. Over the course of 25 years, 2 spacecraft will have completed 4 missions and 2 spacecraft will have completed 3 missions. At the end of year 25, the specific cost of water mined from asteroids and delivered to EM-L_1 would reduce to 5,205 $/kg, which is enough to compete with terrestrial water. The report shows that after 19 years, the accumulated expenses and income reach break-even and only improve from there on. From year 19, the project operates with a net profit. In this model, a constant price of 8,000 $/kg is used, rather than basing the price each year to break-even that year, which would result in very high prices at the start and very low prices later.

The above results are a first-order estimate for an economic model, but they are sufficient to draw initial conclusions. The team determined that the only feasible path to long-term asteroid mining profitability is not through an Earth-based market (i.e. for PGM and other high-value products) but through the space-based market [31].

A.3 UNIVERSITY OF WASHINGTON

Research performed at the University of Washington [25] focuses on creating an asteroid mining architecture for both PGMs for use on Earth and water for use in Earth orbit. The planning horizon of the project is 25 years, starting in 2015. Their goal was to reach a discounted ROI over 20% in order to attract investors. All key technologies are either at TRL6 or higher, or have included a backup technology demonstration program in the non-recurring costs.

For launch, a newly-developed single stage to orbit (SSTO) is expected to pay for itself, by offering major savings in launch costs in return for development costs. The operating costs for the SSTO are estimated at approximately $9.5 million per flight based on 50 flights each year. Costs for a dedicated and newly-built launch site are included. Nuclear-electric spacecraft are used to transport resources and nuclear power plants are used for surface operations. The architecture includes operations centres in high LEO, which double as a research centre and tourist destination to generate revenue, and as a waypoint for spacecraft deliveries (critical metals for use on Earth, water and other materials for

space industrialisation). The research centre is expected to lease out experiment lockers for $100,000 per month, and a two-week tourist stay costs $4 million, therefore ensuring a yearly income of $360 million and $1.66 billion, respectively. Without the use of in-situ propellant (water), the business case was determined to be unviable. In absence of the new SSTO, water sold at the operations centre is priced at $1,500 and is competitive with Earth-launched water. Assuming existence of the new SSTO, water has to be priced at 500 $/kg to be competitive.

Little detail is given about the information feeding into the model, except that commercial costing data is used, which runs at 30% to 40% of NASA's costing guidelines. A year-on-year overview of all elements of the architecture is presented. All non-recurring (development) costs invested before the initial base year are not included in the NPV calculation, even though these costs are significant. The first revenue is generated in year 8, although it takes until year 11 until the net cash flow is no longer negative but positive (i.e. more revenue than costs in that year). By that time, production has been ramped up significantly and the entire venture is returning a profit as of year 12. Beyond year 12, the cumulative net cash flow is growing rapidly, eventually resulting in a NPV of $14.364 billion at 20 years after "go-ahead", a discounted ROI of 34.67% and a non-discounted ROI of 227%. Therefore, the study concludes that for a reasonable investment (comparable with the US North Slope Oil Field in terms of time and money) and using existing and near-term technologies, it is possible to construct an asteroid mining architecture to significantly impact the world's PGM supply and kickstart in-space industrialisation [25].

A.4 TRANSASTRA CORPORATION

TransAstra Corporation, introduced in Table 2.3, performed an economic analysis for resources obtained from near-Earth objects (NEOs) [93]. The study builds on architectures and designs from previous publications by the company. The architecture includes a crewed propellant depot in orbit around or near the moon, which processes propellant, and a reusable spacecraft functioning as both a cargo vehicle and ascent/descent vehicle. A cost analysis for a roadmap stretching beyond 20 years is presented, to calculate and compare the costs of the NEO approach to current approaches.

The cost analysis includes an estimation of costs for: initial design, development, test and evaluation (DDT&E), recurring units, replacement and launch. Variations are given for four different scenarios, combinations of: "supplied from Earth" vs "asteroid resources", and "NASA business as usual" vs "best commercial practices". The costs associated with best commercial practices are lower than NASA's estimates, as demonstrated by SpaceX and Blue Origin, which are producing spacecraft at a fraction of the costs traditionally associated with NASA projects.

Cost estimations for un-crewed elements are done through the NASA QuickCost Model, which uses historical data for robotic missions. First units are based on the QuickCost costs, with subsequent units costed at 20% of these DDT&E costs. The CER of the QuickCost model estimates the total first-unit cost Y as follows:

$$\begin{aligned} Y &= 2.718^{-0.260} \times \text{DryMass}^{0.585} \times 2.718^{2.6\times\text{BusNew}} \times 2.718^{0.231\times\text{Destination}} \\ &\quad +2.718^{-1.46} \times \text{InstDryMass}^{0.475} \times \text{InstAvgWatts}^{0.223} \times \text{InstDesLife}^{0.386} \times 2.718^{1.44\times\text{InstNew}} \end{aligned} \tag{A.3}$$

where DryMass is the spacecraft bus dry mass in kg, BusNew is the percentage of bus mass considered new development, Destination is zero for an Earth orbit and 1 otherwise, InstDryMass is the dry mass of the instrumentation, InstAvgWatts is the average power usage of instruments in W, InstDesLife is

the design life of the instrument in months, and InstNew is the percentage of instrument dry mass considered new development. This notation will not be used elsewhere in the thesis, unless introduced again. As TransAstra Corporation has been designing the spacecraft referenced in this paper for a number of years, the input values for this CER are available to them.

Revenue is generated by providing services for operations, launch, LEO to GEO transport, astronaut and cargo transport, and a space hotel. Propellant for these services is obtained through asteroid mining. Profit margins for these services are set at 20%.

For the first four years, the project receives financing to cover the DDT&E, recurring and operations costs. All loans are paid back with interest (10%) when sufficient revenue can be generated. The study concludes that asteroid resources, in combination with costs associated with best commercial practices, allows for the creation of a self-sustaining business in space resources with an estimated ROI of 23% within 20 years [93].

A.5 INTERNATIONAL SPACE UNIVERSITY

Where the previous sections have employed large spacecraft, Ref. [30] explores using small spacecraft for asteroid mining and its economic feasibility. The spacecraft under investigation are under 500 kg and deliver 100 kg of water per trip. In-situ propellant (water) is used and each spacecraft can repeat mining trips several times. The spacecraft can only target a small subset of NEAs within ~ 0.03 AU of the Earth.

For the economic model, traditional CERs are employed. The calculated first-unit cost ($113.6 million per spacecraft) is therefore based on heritage and similarity, although the CERs are based on remote-sensing and communication spacecraft, of which the studied spacecraft is neither. The learning curve effect is applied for subsequent units. Launch costs are based on SpaceX's Falcon Heavy rocket ($90 million). Other cost contributions are based on the cost of the payload and bus. Annual operations are estimated at $5.7 million (based on Ref. [132]).

Revenue is estimated based on a price per kg that is pre-determined for each market: 3,000 $/kg to LEO (average value), 7,500 $/kg to GEO (based on Falcon-9), 21,500 $/kg to geosynchronous orbit (based on Proton-M) and 35,000 $/kg to cislunar space (unclear what this is based on). The total revenue is based on the price per kg of the resources and the total mass of resources delivered to the destination, as a separate demand model is not included in the analysis. Results indicate that approximately 200 spacecraft, each operating successfully for five years, are needed to reach break-even financially. The results identify cislunar space as the use case most likely to be economically feasible for water mined on asteroids [30].

A.6 SCIENCE AND TECHNOLOGY POLICY INSTITUTE

Reference [29] assesses the economic viability of using asteroid-based resources to support space missions between 2031 and 2050. In this period of interest, water used for propellant is the only resource found to be economical. The spacecraft and infrastructure described in Ref. [110] is used. The study investigates the demand from NASA and other governmental agencies, as well as the private space sector. The cost of delivering the same resources from Earth is also estimated, which is used to assess the feasibility of asteroid mining.

Demand is estimated based on five transfers, namely: 1) Lunar Gateway to Lunar surface, 2) LEO to Lunar Gateway (and return), 3) Lunar Gateway to Mars orbit (and return), 4) Mars orbit to Mars

surface, and 5) LEO to GEO. For each transfer, the expected frequency and propellant mass needed are estimated for a low- and high-demand scenario. Two versions of the demand model are presented, one for a low demand and one for a high demand. In the low-demand (i.e. conservative) demand model, one crewed Lunar landing and one supporting un-crewed Lunar landing are envisioned each year, thus totalling 20 complete missions over the course of 20 years. In the high-demand model, this increases to two of each, each year, totalling 80 missions from LEO to the Lunar Gateway and down to the Lunar surface. The other demands are the same for both models: 13 return trips to Mars, 12 down to the Martian surface and 400 between LEO and GEO. Costs are estimated for development and construction of systems, as well as costs for operations and maintenance. Where possible, actual and estimated costs of various missions from NASA and JAXA are used, as are the launch costs advertised by SpaceX.

The specific cost of delivering the same resources from Earth, is based on the payload capacity and cost of SpaceX's Falcon-9 and Falcon Heavy, with the Falcon Heavy resulting in lower costs due to the larger payload capacity: 2,000 $/kg to LEO and 6,700 $/kg to the Lunar Gateway. Using asteroid mining, the total specific costs to deliver resources are 2,700 $/kg using the low-demand scenario (for both destinations) and 2,300 $/kg using the high-demand scenario. This means that according to this analysis, asteroid mining is not viable for the LEO market, but could be used for delivery of LOX/LH_2 to the Lunar Gateway. Deprived of the LEO market however, the architecture will have to be reworked to account for the loss of demand, causing the price to the Lunar Gateway to increase to 3,600 $/kg, because non-recurring costs can be amortised over less delivered resources.

A.7 INITIATIVE FOR INTERSTELLAR STUDIES

The last example of an existing economic model is from Ref. [23], which employs a technique similar to that of Sonter in Refs. [21, 126] as described above. The study remarks that while Sonter's NPV analysis is currently the most detailed analysis linking technology and economic parameters, it has a number of shortcomings. These are: 1) only one mission is considered, 2) development costs are not considered, 3) costs to return resources to Earth are not considered, and 4) impulsive, chemical transfers are used.

The study in Ref. [23] states that it includes multiple missions, development costs, costs of return to Earth and includes transfer time. It appears that the authors of Ref. [23] did not consider the inclusion of $a^{3/2}$ and n in Section A.1, which already do include the transfer and mission time in the NPV calculation in Ref. [21]. Regardless, Ref. [23] shows how much analysis can be done using variations on the classic NPV calculation, with its final version of the NPV equation as:

$$\begin{aligned} NPV &= \sum_{i=1}^{T} n_i \sum_{j} \left[m_{\mathrm{SC}} c_{\mathrm{price_{mat}}} \left(\frac{f t M_{\mathrm{p}}}{(1+I)^{t_j}} \right.\right. \\ &\quad \left.\left. - \left\lceil \frac{n_i}{s_i+1} \right\rceil \frac{c_{\mathrm{prod_1}} \left[p \left\lceil \frac{n_i}{s_i+1} \right\rceil \right]^a + c_{\mathrm{transport}}}{c_{\mathrm{price_{mat}}} (1+r)^{t_j - t_m}} \right) - \frac{C_{\mathrm{ops}}}{(1+r)^{t_j}} \right] - c_{\mathrm{dev}} \frac{m_{\mathrm{SC}}}{p} \end{aligned} \tag{A.4}$$

which includes the learning curve effect (through a, the learning factor), multiple missions (through a summation over mission indices j), reuse of spacecraft (through s, the number of times the spacecraft is reused), and a summation over the years i until the final year T. Variables are as follows: m_{SC} is the spacecraft dry mass, $c_{\mathrm{price_{mat}}}$ the material price, f the throughput rate, t the mining phase duration, M_{p} the fraction of extracted resources from the total material processed, c_{prod} the mass-

specific production cost, p the number of spacecraft per mission, $c_{\text{transport}}$ the mass-specific cost of transportation service providers (e.g. the cost for launch into LEO), C_{ops} cost of operations, and c_{dev} the mass-specific development cost. Some missions incur costs at different points in time (e.g. for production and launch), so the variable t_m is included as the mission duration, and t_j denotes the moment in time after the initial time t_0 when a cash flow occurs. Once again, note that none of these symbols will not be reused in this thesis, unless introduced elsewhere.

Input values for the NPV equation are given for a conservative and optimistic scenario, both of which are subject to large uncertainties and assumptions. Conclusions drawn using this economic model are as follows. The profitability model shows that the economic viability of an asteroid mining venture greatly depends on the throughput rate. It is also shown that using multiple smaller spacecraft instead of a larger spacecraft results in lower development costs and, through the learning curve effect, lower maintenance cost. Reusing spacecraft allows reaching profitability sooner, but not too much, as that means that the mission sequence cannot be compressed more by using multiple spacecraft in parallel instead of sequential.

References

[1] G. B. Sanders, K. A. Romig, W. E. Larson, R. Johnson, D. Rapp, K. R. Johnson, K. Sacksteder, D. Linne, P. Curren, M. Duke, B. R. Blair, L. Gertsch, D. Boucher, E. Rice, L. Clark, E. McCullough, R. Zubrin, Results from the NASA Capability Roadmap Team for In-Situ Resource Utilization (ISRU), in: International Lunar Conference 2005, Toronto, Canada, 2005, pp. 1–49.

[2] J. S. Lewis, Mining the Sky, Addison-Wesley Publishing Company, Inc., 1996.

[3] C. L. Gerlach, Profitably Exploiting Near-Earth Object Resources, in: 2005 International Space Development Conference, National Space Society, Washington, DC, 2005, pp. 1–56.

[4] V. Badescu (Ed.), Asteroids: Prospective Energy and Material Resources, Springer, Heidelberg, New York, 2013.

[5] International Space Exploration Coordination Group, Global Exploration Roadmap, Tech. rep. (Feb. 2018).
URL `https://go.nasa.gov/2nCkbFV`

[6] I. Christensen, I. Lange, G. Sowers, A. Abbud-Madrid, M. Bazilian, New Policies Needed to Advance Space Mining, Issues in Science and Technology 35 (2) (2019) 26–30.

[7] J.-M. Salotti, R. Heidmann, Roadmap to a human Mars mission, Acta Astronautica 104 (2) (2014) 558–564. `doi:10.1016/j.actaastro.2014.06.038`.

[8] A. B. Chmielewski, C. H. M. Jenkins, Gossamer spacecraft, in: Compliant Structures in Nature and Engineering, WIT Press, 2005, pp. 203–243. `doi:10.2495/978-1-85312-941-4/10`.

[9] J. C. Mankins, New directions for space solar power, Acta Astronautica 65 (1-2) (2009) 146–156. `doi:10.1016/j.actaastro.2009.01.032`.

[10] J. B. Pezent, R. Sood, A. Heaton, Contingency target assessment, trajectory design, and analysis for NASA's NEA scout solar sail mission, Advances in Space Research 67 (9) (2021) 2890–2898. `doi:10.1016/j.asr.2020.02.004`.

[11] D. Y. Oh, S. Collins, T. Drain, W. Hart, T. Imken, K. Larson, D. Marsh, D. Muthulingam, J. S. Snyder, D. Trofimov, L. T. Elkins-Tanton, I. Johnson, P. Lord, Z. Pirkl, Development of the Psyche Mission for NASA's Discovery Program, in: 36th International Electric Propulsion Conference, Vienna, Austria, 2019, pp. IEPC–2019–192.

[12] X. Zhang, J. Huang, T. Wang, Z. Huo, ZhengHe - A mission to a near-Earth asteroid and a main-belt comet, in: 50th Lunar and Planetary Science Conference, Houston, Texas, 2019, p. No. 2132.

[13] M. Yoshikawa, J. Kawaguchi, A. Fujiwara, A. Tsuchiyama, Hayabusa Sample Return Mission, in: P. Michel, F. E. DeMeo, W. F. Bottke (Eds.), Asteroids IV, University of Arizona Press, 2015, pp. 397–418. doi:10.2458/azu_uapress_9780816532131-ch021.

[14] L. Riu, R. Brunetto, J. Carter, B. Gondet, V. Hamm, K. Hatakeda, Y. Langevin, C. Lantz, T. Le Pivert-Jolivet, D. Loizeau, A. Nakatoh, T. Okada, C. Pilorget, F. Poulet, T. Usui, T. Yada, K. Yogata, A. Moussi-Soffys, J.-P. Bibring, Hayabusa2 Returned Samples: First Results From the MicrOmega Investigation Within the ISAS Curation Facility, in: Europlanet Science Congress 2021, Virtual Meeting, 2021. doi:10.5194/epsc2021-564.

[15] P. Michel, F. E. DeMeo, W. F. Bottke (Eds.), Asteroids IV, The University of Arizona Space Science Series, The University of Arizona Press, Lunar and Planetary Institute, Tucson, Houston, USA, 2015.

[16] R. E. March, OSIRIS-REx: A NASA Asteroid Space Mission, International Journal of Mass Spectrometry (2021) 1–3doi:10.1016/j.ijms.2021.116677.

[17] R. Shishko, R. Fradet, S. Do, S. Saydam, C. Tapia-Cortez, A. G. Dempster, J. Coulton, Mars Colony in situ resource utilization: An integrated architecture and economics model, Acta Astronautica 138 (2017) 53–67. doi:10.1016/j.actaastro.2017.05.024.

[18] A. Meurisse, J. Carpenter, Past, present and future rationale for space resource utilisation, Planetary and Space Science 182 (2020) 104853. doi:10.1016/j.pss.2020.104853.

[19] R. S. Jakhu, J. N. Pelton, Y. O. M. Nyampong, Private Sector Space Mining Initiatives and Policies in the United States, Springer Cham, 2017, pp. 59–71.

[20] E. Kulu, In-Space Economy in 2021 - Statistical Overview and Classification of Commercial Entities, in: 72nd International Astronautical Congress (IAC 2021), Dubai, UAE, 2021, pp. 1–23.

[21] M. J. Sonter, The technical and economic feasibility of mining the near-Earth asteroids, Acta Astronautica 41 (4-10) (1997) 637–647. doi:10.1016/S0094-5765(98)00087-3.

[22] S. D. Ross, Near-Earth Asteroid Mining, Space Industry Report, Control and Dynamical Systems, Caltech 107-81, Pasadena, CA 91125 (Dec. 2001).

[23] A. M. Hein, R. Matheson, D. Fries, A techno-economic analysis of asteroid mining, Acta Astronautica 168 (2020) 104–115. doi:10.1016/j.actaastro.2019.05.009.

[24] R. Gertsch, L. Gertsch, Economic Analysis Tools for Mineral Projects in Space, Space Resources Roundtable (2005).

[25] D. G. Andrews, K. D. Bonner, A. W. Butterworth, H. R. Calvert, B. R. H. Dagang, K. J. Dimond, L. G. Eckenroth, J. M. Erickson, B. A. Gilbertson, N. R. Gompertz, O. J. Igbinosun, T. J. Ip, B. H. Khan, S. L. Marquez, N. M. Neilson, C. O. Parker, E. H. Ransom, B. W. Reeve, T. L. Robinson, M. Rogers, P. M. Schuh, C. J. Tom, S. E. Wall, N. Watanabe, C. J. Yoo, Defining a successful commercial asteroid mining program, Acta Astronautica 108 (2015) 106–118. doi:10.1016/j.actaastro.2014.10.034.

[26] M. C. F. Bazzocchi, M. R. Emami, Asteroid Redirection Mission Evaluation Using Multiple Landers, The Journal of the Astronautical Sciences 65 (2) (2018) 183–204. doi:10.1007/s40295-017-0125-5.

[27] K. I. Oxnevad, An Investment Analysis Model for Space Mining Ventures, International Transactions of the American Association of Cost Engineers (Jan. 1991).

[28] S. Dorrington, The trajectory optimization and space logistics of asteroid mining missions, Ph.D. thesis, School of Mechanical and Manufacturing Engineering Faculty of Engineering University of New South Wales, Sydney, Sydney, Australia (Jun. 2019).
URL http://unsworks.unsw.edu.au/fapi/datastream/unsworks:64731/SOURCE02?view=true

[29] T. J. Colvin, K. Crane, B. Lal, Assessing the economics of asteroid-derived water for propellant, Acta Astronautica 176 (2020) 298–305. doi:10.1016/j.actaastro.2020.05.029.

[30] P. Calla, D. Fries, C. Welch, Asteroid mining with small spacecraft and its economic feasibility, arXiv:1808.05099 [astro-ph] (Jun. 2019). arXiv:1808.05099.

[31] M. M. Cohen, Robotic Asteroid Prospector (RAP) Staged from L-1: Start of the Deep Space Economy, Tech. Rep. NNX12AR04G, NASA Space Technology Mission Directorate (Jul. 2013).
URL https://www.nasa.gov/sites/default/files/files/Cohen_2012_PhI_RAP.pdf

[32] European Space Agency, ESA Space Resources Strategy, Tech. rep. (May 2019).
URL https://sci.esa.int/documents/34161/35992/1567260390250-ESA_Space_Resources_Strategy.pdf

[33] SpaceResources.lu, Opportunities for Space Resources Utilization: Future Markets & Value Chains, Tech. rep., Luxembourg Space Agency (Dec. 2018).
URL https://space-agency.public.lu/dam-assets/publications/2018/Study-Summary-of-the-Space-Resources-Value-Chain-Study.pdf

[34] M. H. Ryan, I. Kutschera, The Case for Asteroids: Commercial Concerns and Considerations, in: V. Badescu (Ed.), Asteroids: Prospective Energy and Material Resources, Springer, Berlin, Heidelberg, 2013, pp. 645–657. doi:10.1007/978-3-642-39244-3_28.

[35] M. Vergaaij, C. R. McInnes, M. Ceriotti, Influence of Launcher Cost and Payload Capacity on Asteroid Mining Profitability, Journal of the British Interplanetary Society 72 (12) (2019) 435–444.

[36] M. Vergaaij, C. R. McInnes, M. Ceriotti, Economic assessment of high-thrust and solar-sail propulsion for near-Earth asteroid mining, Advances in Space Research 67 (9) (2021) 3045–3058. doi:10.1016/j.asr.2020.06.012.

[37] M. Vergaaij, C. R. McInnes, M. Ceriotti, Comparison of material sources and customer locations for commercial space resource utilization, Acta Astronautica 184 (2021) 23–34. doi:10.1016/j.actaastro.2021.03.010.

[38] M. Vergaaij, C. R. McInnes, M. Ceriotti, Economic assessment of high-thrust and solar-sail propulsion for near-Earth asteroid mining, in: 5th International Symposium on Solar Sailing, Aachen, Germany, 2019.

[39] M. Vergaaij, C. R. McInnes, M. Ceriotti, Influence of Launcher Cost and Payload Capacity on Asteroid Mining Profitability, in: 17th Reinventing Space Conference 2019, , 12-14 November 2019, no. BIS-RS-2019-04, Belfast, UK, 2019.

[40] J. J. Lissauer, I. de Pater, Fundamental Planetary Science: Physics, Chemistry and Habitability, Cambridge University Press, USA, 2013.

[41] W. F. Bottke (Ed.), Asteroids III, University of Arizona Space Science Series, University of Arizona Press, Lunar and Planetary Institute, Tucson, Houston, 2002.

[42] C. Lewicki, P. Diamandis, E. Anderson, C. Voorhees, F. Mycroft, Planetary Resources—The Asteroid Mining Company, New Space 1 (2) (2013) 105–108. doi:10.1089/space.2013.0013.

[43] S. Biktimirov, A. Ivanov, R. Lipkis, A. Toporkov, P. Skobelev, A. Tsarev, A. Kharlan, Near-Earth Asteroids Utilization as a Base for Building of Earth-Mars-Moon Economy, in: 69th International Astronautical Congress (IAC), Bremen, Germany, 2018.

[44] J. S. Lewis, Logistical implications of water extraction from near-Earth asteroids, in: Princeton Conference on Space Manufacturing, Space Studies Institute, 1993.

[45] S. Bus, R. P. Binzel, Small Main-belt Asteroid Spectroscopic Survey, Phase II, Tech. rep., Planetary Science Institute (2003).

[46] D. Takir, K. Howard, H. Yabuta, M. McAdam, C. Hibbitts, J. Emery, Linking Water-Rich Asteroids and Meteorites, in: Primitive Meteorites and Asteroids, Elsevier, 2018, pp. 371–408. doi:10.1016/B978-0-12-813325-5.00006-9.

[47] D. J. Tholen, Asteroid Taxonomic Classifications, in: R. P. Binzel, T. Gehrels, M. Shapley Matthews (Eds.), Asteroids II, University of Arizona Press, 1989, pp. 1139–1150.

[48] B. E. Clark, S. J. Bus, A. S. Rivkin, M. K. Shepard, S. Shah, Spectroscopy of X-Type Asteroids, The Astronomical Journal 128 (6) (2004) 3070–3081. doi:10.1086/424856.

[49] R. P. Binzel, D. Lupishko, M. Di Martino, R. Whiteley, G. Hahn, Physical Properties of Near-Earth Objects, in: Asteroids III, Space Science Series, University of Arizona Press, Lunar and Planetary Institute, 2002.

[50] M. Elvis, How many ore-bearing asteroids?, Planetary and Space Science 91 (2014) 20–26. doi:10.1016/j.pss.2013.11.008.

[51] A. W. Harris, A. W. Harris, On the Revision of Radiometric Albedos and Diameters of Asteroids, Icarus 126 (2) (1997) 450–454. doi:10.1006/icar.1996.5664.

[52] B. Carry, Density of Asteroids, Planetary and Space Science 73 (1) (2012) 98–118. doi:10.1016/j.pss.2012.03.009.

[53] P. Beyer, R. O'Connor, D. Mudgway, Galileo Early Cruise, Including Venus, First Earth, and Gaspra Encounters, Tech. Rep. Telecommunications and Data Acquisition Progress Report 42-109, NASA (May 1992).

[54] M. J. Belton, C. R. Chapman, K. P. Klaasen, A. P. Harch, P. C. Thomas, J. Veverka, A. S. McEwen, R. T. Pappalardo, Galileo's Encounter with 243 Ida: An Overview of the Imaging Experiment, Icarus 120 (1) (1996) 1–19. doi:10.1006/icar.1996.0032.

[55] L. Prockter, S. Murchie, A. Cheng, S. Krimigis, R. Farquhar, A. Santo, J. Trombka, The NEAR shoemaker mission to asteroid 433 eros, Acta Astronautica 51 (1-9) (2002) 491–500. doi:10.1016/S0094-5765(02)00098-X.

[56] D. Doody, Cassini - Huygens: Heavily instrumented flight systems approaching Saturn and Titan, in: 2003 IEEE Aerospace Conference, Big Sky, Montana, USA, 2003.

[57] J. Oberst, A Model for Rotation and Shape of Asteroid 9969 Braille from Ground-Based Observations and Images Obtained during the Deep Space 1 (DS1) Flyby, Icarus 153 (1) (2001) 16–23. doi:10.1006/icar.2001.6648.

[58] T. C. Duxbury, R. L. Newburn, C. H. Acton, E. Carranza, T. P. McElrath, R. E. Ryan, S. P. Synnott, T. H. You, D. E. Brownlee, A. R. Cheuvront, W. R. Adams, S. L. Toro-Allen, S. Freund, K. V. Gilliland, K. J. Irish, C. R. Love, J. G. McAllister, S. J. Mumaw, T. H. Oliver, D. E. Perkins, Asteroid 5535 Annefrank size, shape, and orientation: Stardust first results: BRIEF REPORT, Journal of Geophysical Research: Planets 109 (E2) (Feb. 2004). doi:10.1029/2003JE002108.

[59] A. Fujiwara, J. Kawaguchi, D. K. Yeomans, M. Abe, T. Mukai, T. Okada, J. Saito, H. Yano, M. Yoshikawa, D. J. Scheeres, O. Barnouin-Jha, A. F. Cheng, H. Demura, R. W. Gaskell, N. Hirata, H. Ikeda, T. Kominato, H. Miyamoto, A. M. Nakamura, R. Nakamura, S. Sasaki, K. Uesugi, The Rubble-Pile Asteroid Itokawa as Observed by Hayabusa, Science 312 (5778) (2006) 1330–1334. doi:10.1126/science.1125841.

[60] S.-i. Watanabe, Y. Tsuda, M. Yoshikawa, S. Tanaka, T. Saiki, S. Nakazawa, Hayabusa2 Mission Overview, Space Science Reviews 208 (1-4) (2017) 3–16. doi:10.1007/s11214-017-0377-1.

[61] M. Hirabayashi, Y. Mimasu, N. Sakatani, S. Watanabe, Y. Tsuda, T. Saiki, S. Kikuchi, T. Kouyama, M. Yoshikawa, S. Tanaka, S. Nakazawa, Y. Takei, F. Terui, H. Takeuchi, A. Fujii, T. Iwata, K. Tsumura, S. Matsuura, Y. Shimaki, S. Urakawa, Y. Ishibashi, S. Hasegawa, M. Ishiguro, D. Kuroda, S. Okumura, S. Sugita, T. Okada, S. Kameda, S. Kamata, A. Higuchi, H. Senshu, H. Noda, K. Matsumoto, R. Suetsugu, T. Hirai, K. Kitazato, D. Farnocchia, S. Naidu, D. Tholen, C. Hergenrother, R. Whiteley, N. Moskovitz, P. Abell, Hayabusa2 extended mission: New voyage to rendezvous with a small asteroid rotating with a short period, Advances in Space Research 68 (3) (2021) 1533–1555. doi:10.1016/j.asr.2021.03.030.

[62] H. F. Levison, S. Marchi, K. Noll, C. Olkin, T. S. Statler, NASA's Lucy Mission to the Trojan Asteroids, in: 2021 IEEE Aerospace Conference (50100), IEEE, Big Sky, MT, USA, 2021, pp. 1–10. doi:10.1109/AERO50100.2021.9438453.

[63] A. F. Cheng, A. S. Rivkin, P. Michel, J. Atchison, O. Barnouin, L. Benner, N. L. Chabot, C. Ernst, E. G. Fahnestock, M. Kueppers, P. Pravec, E. Rainey, D. C. Richardson, A. M. Stickle, C. Thomas, AIDA DART asteroid deflection test: Planetary defense and science objectives, Planetary and Space Science 157 (2018) 104–115. doi:10.1016/j.pss.2018.02.015.

[64] P. Michel, M. Küppers, A. Fitzsimmons, S. F. Green, M. Lazzarin, S. Ulamec, I. Carnelli, P. Martini, The ESA Hera mission to the near-Earth asteroid binary Didymos: Planetary defense and science return, in: Global Space Exploration Conference 2021 (GLEX 2021), virtual, 2021.

[65] O. Çelik, D. A. Dei Tos, T. Yamamoto, N. Ozaki, Y. Kawakatsu, C. H. Yam, Multiple-Target Low-Thrust Interplanetary Trajectory of DESTINY+, Journal of Spacecraft and Rockets 58 (3) (2021) 830–847. doi:10.2514/1.A34804.

[66] G. Sanders, W. Larson, K. Sacksteder, C. Mclemore, NASA In-Situ Resource Utilization (ISRU) Project: Development and Implementation, in: AIAA SPACE 2008 Conference & Exposition, American Institute of Aeronautics and Astronautics, San Diego, California, 2008. doi:10.2514/6.2008-7853.

[67] G. Sanders, In Situ Resource Utilization on Mars - Update from DRA 5.0 Study, in: 48th AIAA Aerospace Sciences Meeting Including the New Horizons Forum and Aerospace Exposition, American Institute of Aeronautics and Astronautics, Orlando, Florida, 2010. doi:10.2514/6.2010-799.

[68] K. Hadler, D. Martin, J. Carpenter, J. Cilliers, A. Morse, S. Starr, J. Rasera, K. Seweryn, P. Reiss, A. Meurisse, A universal framework for Space Resource Utilisation (SRU), Planetary and Space Science 182 (2020) 104811. doi:10.1016/j.pss.2019.104811.

[69] I. A. Crawford, Lunar resources: A review, Progress in Physical Geography: Earth and Environment 39 (2) (2015) 137–167. doi:10.1177/0309133314567585.

[70] M. Anand, Lunar Water: A Brief Review, Earth, Moon, and Planets 107 (1) (2010) 65–73. doi:10.1007/s11038-010-9377-9.

[71] D. Rapp, Use of Extraterrestrial Resources for Human Space Missions to Moon or Mars, Springer Science & Business Media, 2018.

[72] S. O. Starr, A. C. Muscatello, Mars in situ resource utilization: A review, Planetary and Space Science 182 (2020) 104824. doi:10.1016/j.pss.2019.104824.

[73] J. E. Kleinhenz, A. Paz, An ISRU propellant production system for a fully fueled Mars Ascent Vehicle, in: 10th Symposium on Space Resource Utilization, American Institute of Aeronautics and Astronautics, Grapevine, Texas, 2017. doi:10.2514/6.2017-0423.

[74] A. S. Rivkin, H. Campins, J. P. Emery, E. S. Howell, J. Licandro, D. Takir, F. Vilas, Astronomical Observations of Volatiles on Asteroids, in: P. Michel, F. E. DeMeo, W. F. Bottke (Eds.), Asteroids IV, University of Arizona Press, 2015.

[75] L. Karr, M. S. Paley, M. Marone, W. Kaukler, P. A. Curreri, Metals and Oxygen Mining from Meteorites, Asteroids and Planets using Reusable Ionic Liquids, in: Pioneering Planetary Surface Systems Technologies and Capabilities, 2012.

[76] R. Burgher, T. DeTora, H. Fisher, M. Stein, Red Mars - green Mars? Mars Regolith as a growing Medium, in: Human Exploration and Development of Space-University Partners (HEDS-UP), Houston, Texas, 2000.

[77] M. Horan, R. Walker, J. Morgan, High Precision Measurements of Pt and OS in Chondrites, in: Lunar and Planetary Science Conference, Vol. 30 of Lunar and Planetary Science Conference, 1999.

[78] T. Simko, M. Gray, Lunar Helium-3 Fuel for Nuclear Fusion: Technology, Economics, and Resources, World Futures Review 6 (2) (2014) 158–171. doi:10.1177/1946756714536142.

[79] G. W. W. Wamelink, J. Y. Frissel, W. H. J. Krijnen, M. R. Verwoert, P. W. Goedhart, Can Plants Grow on Mars and the Moon: A Growth Experiment on Mars and Moon Soil Simulants, PLoS ONE 9 (8) (2014) 1–9. doi:10.1371/journal.pone.0103138.

[80] D. Bienhoff, From Importing to Exporting: The Impact of ISRU on Space Logistics, in: AIAA SPACE 2011 Conference & Exposition, American Institute of Aeronautics and Astronautics, Long Beach, California, 2011. doi:10.2514/6.2011-7112.

[81] E. Musk, Making Humans a Multi-Planetary Species, New Space 5 (2) (2017) 46–61. doi:10.1089/space.2017.29009.emu.

[82] T. Sarton du Jonchay, H. Chen, A. Wieger, Z. Szajnfarber, K. Ho, Space architecture design for commercial suitability: A case study in in-situ resource utilization systems, Acta Astronautica (2020) 45–50doi:10.1016/j.actaastro.2020.05.012.

[83] M. B. Duke, B. R. Blair, J. Diaz, Lunar resource utilization: Implications for commerce and exploration, Advances in Space Research 31 (11) (2003) 2413–2419. doi:10.1016/S0273-1177(03)00550-7.

[84] R. Mitchell, Into the Final Frontier: The Expanse of Space Commercialization, Missouri Law Review 83 (2) (2018) 429–454.

[85] Orbit Fab, J. Bultitude, Z. Burkhardt, J. Schiel, D. Faber, G. Kendall-Bell, J. McIntyre, A. O'Leary, Business Case for Innovative Commercial In-Orbit Satellite/Debris Removal, White Paper, Orbit Fab (2021).

[86] C. Geiman, D. Faber, J. Bultitude, Z. Burkhardt, A. O'leary, In-Situ Propellant Architecture for Near-Term Lunar Missions, in: Luxembourg Space Resources Week 2021, Luxembourg, Luxembourg, 2021. doi:10.13140/RG.2.2.11822.43843.

[87] K. MacWorther, Sustainable mining: Incentivizing asteroid mining in the name of environmentalism, William & Mary Environmental Law and Policy Review 40 (2) (2015) 645–676.

[88] K. Deplanche, A. Murray, C. Mennan, S. Taylor, L. Macaskie, Biorecycling of precious metals and rare earth elements, in: Nanomaterials, 2011, pp. 279–314.

[89] M. Saidani, Monitoring and advancing the circular economy transition - Circularity indicators and tools applied to the heavy vehicle industry, Ph.D. thesis, Paris-Saclay University, CentraleSupélec, Paris, France (Oct. 2018).

[90] A. Clark, Electromagnetic launching as a major contribution to space flight, Journal of the British Interplanetary Society 9 (6) (1950) 261–267.

[91] K. Chang, Florida Company Gets Approval to Put Robotic Lander on Moon, New York Times (Aug. 2016).

[92] E. Tepper, Structuring the Discourse on the Exploitation of Space Resources: Between Economic and Legal Commons, Space Policy 49 (2019) 101290. doi:10.1016/j.spacepol.2018.06.004.

[93] J. C. Sercel, C. E. Peterson, J. R. French, A. Longman, S. G. Love, R. Shishko, Stepping stones: Economic analysis of space transportation supplied from NEO resources, in: 2018 IEEE Aerospace Conference, IEEE, Big Sky, MT, 2018, pp. 1–21. doi:10.1109/AERO.2018.8396702.

[94] OffWorld, OffWorld's Master Plan (Jul. 2019).
URL https://www.offworld.ai/masterplan

[95] C. Lewicki, A. Graps, M. Elvis, P. Metzger, A. Rivkin, Furthering Asteroid Resource Utilization in the Next Decade through Technology Leadership, arXiv:2103.02435 [astro-ph] (Mar. 2021). arXiv:2103.02435.

[96] E. Musk, Making Humans a Multiplanetary Species (Sep. 2016).
URL https://web.archive.org/web/20160928040332/http://www.spacex.com/sites/spacex/files/mars_presentation.pdf

[97] F. G. von der Dunk, Asteroid Mining: International and National Legal Aspects, Michigan State International Law Review 26 (1) (2017) 83–102.

[98] United Nations, United Nations Treaties and Principles on Outer Space, United Nations, New York, 2002.

[99] R.-J. Bartunek, Luxembourg sets aside 200 million euros to fund space mining ventures, Reuters (Jun. 2016).
URL https://www.reuters.com/article/us-luxembourg-space-mining-idUSKCN0YP22H

[100] The Government of the Grand Duchy of Luxembourg, Luxembourg is the first European nation to offer a legal framework for space resources utilization, Press Release (Jul. 2017).
URL https://space-agency.public.lu/dam-assets/press-release/2017/2017_07_13%20PressRelease_Law_Space_Resources_EN.pdf

[101] J. A. P. Ramos, F. R. R. de Luis, Resources in space and asteroid mining: Where we are and which challenges should be expected, International Journal of Technology Management 82 (3/4) (2020) 197. doi:10.1504/IJTM.2020.108980.

[102] R. Kelso, Lunar/NEO Commercial Initiatives, in: AIAA SPACE 2011 Conference & Exposition, American Institute of Aeronautics and Astronautics, Long Beach, California, 2011. doi:10.2514/6.2011-7111.

[103] J. Edwards, Goldman Sachs: Space-mining for platinum is 'more realistic than perceived', Business Insider (Apr. 2017).

[104] ESA ESTEC, Outcome ISRU Workshop - Towards the Use of Lunar Resources, Tech. rep., ESA, Noordwijk, The Netherlands (Jul. 2018).
URL https://sci.esa.int/documents/34161/35992/1567260361376-Outcome_ISRU_Workshop_2018.pdf

[105] A. Meurisse, J. Flahaut, P. Reiss, J. D. Carpenter, Preface to the special issue on "Space resources", Planetary and Space Science 185 (2020) 1–2. doi:10.1016/j.pss.2020.104894.

[106] M. Hecht, J. Hoffman, D. Rapp, J. McClean, J. SooHoo, R. Schaefer, A. Aboobaker, J. Mellstrom, J. Hartvigsen, F. Meyen, E. Hinterman, G. Voecks, A. Liu, M. Nasr, J. Lewis, J. Johnson, C. Guernsey, J. Swoboda, C. Eckert, C. Alcalde, M. Poirier, P. Khopkar, S. Elangovan, M. Madsen, P. Smith, C. Graves, G. Sanders, K. Araghi, M. de la Torre Juarez, D. Larsen, J. Agui, A. Burns, K. Lackner, R. Nielsen, T. Pike, B. Tata, K. Wilson, T. Brown, T. Disarro, R. Morris, R. Schaefer, R. Steinkraus, R. Surampudi, T. Werne, A. Ponce, Mars Oxygen ISRU Experiment (MOXIE), Space Science Reviews 217 (1) (2021) 9. doi:10.1007/s11214-020-00782-8.

[107] K. Fox, A. Johnson, C. Skelly, A. Good, NASA's Perseverance Mars Rover Extracts First Oxygen from Red Planet, Press Release (Apr. 2021).

[108] R. Campa, K. Szocik, M. Braddock, Why space colonization will be fully automated, Technological Forecasting and Social Change 143 (2019) 162–171. doi:10.1016/j.techfore.2019.03.021.

[109] C. Culbert, D. Linne, F. Chandler, L. Alexander, S. Jefferies, K. J. Kennedy, M. Lupisella, P. Metzger, N. Moore, K. Taminger, NASA Technology Roadmaps - TA7: Human Exploration Destination Systems, Tech. rep., National Aeronautics and Space Administration (May 2015).

[110] J. C. Sercel, C. E. Peterson, D. T. Britt, C. Dreyer, R. Jedicke, S. G. Love, O. Walton, Practical Applications of Asteroidal ISRU in Support of Human Exploration, in: Primitive Meteorites and Asteroids, Elsevier, 2018, pp. 477–524.

[111] J. P. Sanchez, C. R. McInnes, Asteroid Resource Map for Near-Earth Space, Journal of Spacecraft and Rockets 48 (1) (January - February 2011) 153–165. doi:10.2514/1.49851.

[112] M. Sonter, Near earth objects as resources for space industrialization, Solar System Development Journal 1 (1) (2001) 1–31.

[113] C. R. McInnes, Harvesting Near Earth Asteroid Resources Using Solar Sail Technology, in: 4th International Symposium on Solar Sailing, Kyoto, Japan, 2017.

[114] J. P. Sanchez, C. R. McInnes, Assessment on the feasibility of future shepherding of asteroid resources, Acta Astronautica 73 (2012) 49–66. doi:10.1016/j.actaastro.2011.12.010.

[115] A. M. Hein, R. Matheson, D. Fries, A Techno-Economic Analysis of Asteroid Mining, in: 69th International Astronautical Congress (IAC), Bremen, Germany, 2018.

[116] J. S. Kargel, Semiconductor and precious-metal resources of metallic asteroids, in: Princeton Conference on Space Manufacturing, Space Studies Institute, 1997.

[117] M. Elvis, T. Esty, How many assay probes to find one ore-bearing asteroid?, Acta Astronautica 96 (2014) 227–231. doi:10.1016/j.actaastro.2013.11.027.

[118] V. Hessel, N. N. Tran, S. Orandi, M. R. Asrami, M. E. Goodsite, H. Nguyen, Continuous-Flow Extraction of Adjacent Metals - a Disruptive Economic Window for In-Situ Resource Utilization of Asteroids?, Angewandte Chemie International Edition (Jan. 2020). doi:10.1002/anie.201912205.

[119] K. Zacny, M. M. Cohen, W. W. James, B. Hilscher, Asteroid Mining, in: AIAA Space 2013 Conference and Explosition, AIAA Space Forum, AIAA 2013-5304, 2013. doi:10.2514/6.2013-5304.

[120] N. Anthony, M. R. Emami, Asteroid engineering: The state-of-the-art of Near-Earth Asteroids science and technology, Progress in Aerospace Sciences 100 (2018) 1–17. doi:10.1016/j.paerosci.2018.05.001.

[121] A. Smith, An Inquiry into the Nature and Causes of the Wealth of Nations, Oxford, England, 1776.

[122] M. Elvis, Prospecting Asteroid Resources, in: V. Badescu (Ed.), Asteroids, Springer Berlin Heidelberg, Berlin, Heidelberg, 2013, pp. 81–129. doi:10.1007/978-3-642-39244-3_4.

[123] N. Stacey, S. D'Amico, Autonomous Swarming for Simultaneous Navigation and Asteroid Characterization, in: AAS/AIAA Astrodynamics Specialist Conference, Snowbird, UT, 2018, pp. AAS 18–448.

[124] M. Elvis, A. Stark, B. Stalder, C. Desira, Astronomical Prospecting of Asteroid Resources, in: European Planetary Science Congress 2017, EPSC2017-94-1, Riga, Latvia, 2017.

[125] A. Peloni, A. V. Rao, M. Ceriotti, Automated Trajectory Optimizer for Solar Sailing (ATOSS), Aerospace Science and Technology 72 (2018) 465–475. doi:10.1016/j.ast.2017.11.025.

[126] M. Sonter, The Technical and Economic Feasibility of Mining the Near-Earth Asteroids, Thesis Master of Science, Department of Physics and Department of Civil and Mining Engineering, University of Wollongong, Wollongong (1996).
URL https://space.nss.org/wp-content/uploads/Mining-Near-Earth-Asteroids-Sonter.pdf

[127] A. Sommariva, Rationale, Strategies, and Economics for Exploration and Mining of Asteroids, Astropolitics 13 (1) (2015) 25–42. doi:10.1080/14777622.2015.1014244.

[128] T. Cichan, S. A. Bailey, A. Burch, N. Kirby, Concept for a Crewed Lunar Lander Operating from the Lunar Orbiting Platform-Gateway, in: 69th International Astronautical Congress (IAC), Bremen, Germany, 2018.

[129] T. C. Taylor, W. Grandl, M. Pinni, H. Benaroya, M. S. El-Genk, Space Colony from a Commercial Asteroid Mining Company Town, in: AIP Conference Proceedings, Vol. 969, Albuquerque, New Mexico, United States, 2008, pp. 934–941. doi:10.1063/1.2845060.

[130] K. R. Erickson, Optimal Architecture for an Asteroid Mining Mission: System Components and Project Execution, in: AIP Conference Proceedings, Vol. 880, AIP, Albuquerque, New Mexico (USA), 2007, pp. 896–903. doi:10.1063/1.2437531.

[131] M. Busch, Profitable Asteroid Mining, Journal of the British Interplanetary Society 57 (2004) 301–305.

[132] J. R. Wertz, D. F. Everett, J. J. Puschell, Space Mission Engineering: The New SMAD, Microcosm Press, Hawthorne, CA, 2011.

[133] S. Rabade, N. Barba, G. Liu, L. A. Garvie, J. Thangavelauthamb, The Case for Solar Thermal Steam Propulsion System for Interplanetary Travel: Enabling Simplified ISRU Utilizing NEOs and Small Bodies, in: 67th International Astronautical Congress (IAC), D4, 5, 7 (34659), Guadalajara, Mexico, 2016.

[134] S. K. Borowski, D. R. McCurdy, T. W. Packard, Nuclear Thermal Propulsion (NTP): A proven growth technology for human NEO/Mars exploration missions, in: 2012 IEEE Aerospace Conference, IEEE, Big Sky, MT, 2012, pp. 1–20. doi:10.1109/AERO.2012.6187301.

[135] R. Pothamsetti, J. Thangavelauthamb, Photovoltaic electrolysis propulsion system for interplanetary CubeSats, in: 2016 IEEE Aerospace Conference, IEEE, Big Sky, MT, USA, 2016. doi:10.1109/AERO.2016.7500829.

[136] K. P. Doyle, M. A. Peck, Water Electrolysis Propulsion as a Case Study in Resource-Based Spacecraft Architecture (February 2020), IEEE Aerospace and Electronic Systems Magazine 34 (9) (2019) 4–19. doi:10.1109/MAES.2019.2923312.

[137] K. P. Doyle, M. A. Peck, Water Electrolysis for Propulsion of a Crewed Mars Mission, Journal of Spacecraft and Rockets 57 (6) (2020) 1103–1117. doi:10.2514/1.A34632.

[138] A. Schwertheim, A. Knoll, Experimental investigation of a water electrolysis Hall effect thruster, Acta Astronautica 193 (2022) 607–618. doi:10.1016/j.actaastro.2021.11.002.
URL https://linkinghub.elsevier.com/retrieve/pii/S0094576521005890

[139] C. R. McInnes, Solar Sailing: Technology, Dynamics and Mission Applications., Springer-Praxis series in space science and technology, Berlin, 1999. doi:10.1007/978-1-4471-3992-8_1.

[140] D. G. Andrews, R. M. Zubrin, Magnetic Sails and Interstellar Travel, Journal of the British Interplanetary Society 43 (1990) 265–272.

[141] C. D. Hunt, M. O. van Pelt, Comparing NASA and ESA Cost Estimating Methods for Human Missions to Mars, in: 26th International Society of Parametric Analysts, Frascati, Italy, 2004.

[142] M. Mealing, Think like an investor. Think like a customer, in: Presented at Space Resources Week 2021, Luxembourg, Luxembourg, 2021.

[143] S. Dorrington, J. Olsen, Logistics Problems in the Design of an Asteroid Mining Industry, in: 69th International Astronautical Congress (IAC), Bremen, Germany, 2018.

[144] F. Tronchetti, Private property rights on asteroid resources: Assessing the legality of the ASTEROIDS Act, Space Policy 30 (4) (2014) 193–196. doi:10.1016/j.spacepol.2014.07.005.

[145] J. Dallas, S. Raval, S. Saydam, Off-Earth mining in the context of sustainable development, in: 9th International Conference on Sustainable Development in the Minerals Industry, Sydney, Australia, 2019.

[146] B. O'Leary, Asteroid mining and the moons of Mars, Acta Astronautica 17 (4) (1988) 457–462. doi:10.1016/0094-5765(88)90059-8.

[147] M. Simpson, Welcome from Dr. Michael Simpson (2019).
URL https://iisc.im/

[148] G. Craig, S. Saydam, A. Dempster, Mining off-earth minerals: A long-term play?, Journal of the Southern African Institute of Mining and Metallurgy 114 (12) (2014) 1039–1047. URL https://www.saimm.co.za/Journal/v114n12p1039.pdf

[149] M. Zacharias, L. Gertsch, A. Abbud-Madrid, B. Blair, K. Zacny, Real-World Mining Feasibility Studies Applied to Asteroids, the Moon and Mars, in: AIAA SPACE 2011 Conference & Exposition, American Institute of Aeronautics and Astronautics, Long Beach, California, 2011. doi:10.2514/6.2011-7115.

[150] H. R. Hertzfeld, J. S. Greenberg, Space Economics, 1st Edition, Vol. 144 of Progress in Astronautics and Aeronautics, Americn Institute of Aeronautics and Astronautics, 370 L'Enfant Promenade, SW, Washington, DC, 1992. doi:10.2514/4.866166.

[151] M. R. Jude, Risk Assessment Of Space Mining Ventures Using Decision Modeling And Monte Carlo Simulation, MSc Thesis, University of North Dakota, Grand Forks, ND, USA (May 2018).

[152] F.-W. Wellmer, Statistical Evaluations in Exploration for Mineral Deposits, Springer Berlin Heidelberg, Berlin, Heidelberg, 1998. doi:10.1007/978-3-642-60262-7.

[153] A. Probst, C. Nitzl, F. Kraus, R. Förstner, Cost estimation of an asteroid mining mission using partial least squares structural equation modelling (PLS-SEM), Acta Astronautica 167 (2020) 440–454. doi:10.1016/j.actaastro.2019.07.032.

[154] G. T. Friedlob, F. J. Plewa, Understanding Return on Investment, Wiley, New York, 1996.

[155] O. Trivailo, M. Sippel, Y. A. Sekercioğlu, Review of hardware cost estimation methods, models and tools applied to early phases of space mission planning, Progress in Aerospace Sciences 53 (2012) 1–17. doi:10.1016/j.paerosci.2012.02.001.

[156] F. A. Prince, Weight and the Future of Space Flight Hardware Cost Modeling, in: International Society of Parametric Analysis/Society of Cost Estimating and Analysis 2003 International Conference, Orlando, Florida, USA, 2003.

[157] F. A. Prince, Why NASA's Management Doesn't Believe the Cost Estimate, Engineering Management Journal 14 (1) (2015) 7–12. doi:10.1080/10429247.2002.11415143.

[158] N. T. Drenthe, B. T. Zandbergen, M. O. van Pelt, Cost Estimating of Commercial Smallsat Launch Vehicles, in: EUCASS 2017, Milan, Italy, 2017.

[159] C. F. Lillie, B. E. Thompson, Parametric cost estimation for space science missions, in: E. Atad-Ettedgui, D. Lemke (Eds.), SPIE Astronomical Telescopes + Instrumentation, Marseille, France, 2008, pp. 701827–1–12. doi:10.1117/12.789615.

[160] S. Keller, P. Collopy, P. Componation, What is wrong with space system cost models? A survey and assessment of cost estimating approaches, Acta Astronautica 93 (2014) 345–351. doi:10.1016/j.actaastro.2013.07.014.

[161] J. Markish, Valuation Techniques for Commercial Aircraft Program Design, Ph.D. thesis, Massachusetts Institute of Technology (Jun. 2002).

[162] X. Wang, S. Zhang, Cost Analysis for Mass Customized Production of Satellites Based on Modularity, IEEE Access 9 (2021) 13754–13760. doi:10.1109/ACCESS.2020.3048845.

[163] D. D. Mazanek, R. G. Merrill, J. R. Brophy, R. P. Mueller, Asteroid Redirect Mission concept: A bold approach for utilizing space resources, Acta Astronautica 117 (2015) 163–171. doi:10.1016/j.actaastro.2015.06.018.

[164] G. Gargioni, D. Alexandre, M. Peterson, K. Schroeder, Multiple Asteroid Retrieval Mission from Lunar Orbital Platform-Gateway Using Reusable Spacecrafts, in: 2019 IEEE Aerospace Conference, IEEE, Big Sky, MT, USA, 2019. doi:10.1109/aero.2019.8741985.

[165] J. R. Brophy, S. Oleson, Spacecraft Conceptual Design for Returning Entire Near-Earth asteroids, in: 48th AIAA/ASME/SAE/ASEE Joint Propulsion Conference & Exhibit, Atlanta, GA, USA, 2012. doi:10.2514/6.2012-4067.

[166] R. Xie, N. J. Bennett, A. G. Dempster, Target evaluation for near earth asteroid long-term mining missions, Acta Astronautica 181 (2021) 249–270. doi:10.1016/j.actaastro.2021.01.011.

[167] D. Landau, J. Dankanich, N. Strange, J. Bellerose, P. Llanos, M. Tantardini, Trajectories to Nab a NEA (Near-Earth Asteroid), in: AAS/AIAA Spaceflight Mechanics Meeting, Kauai, Hawaii, USA, 2013.

[168] C. A. Jones, J. Klovstad, E. Judd, D. Komar, Cost Breakeven Analysis of Cis-lunar ISRU for Propellant, in: AIAA Scitech 2019 Forum, American Institute of Aeronautics and Astronautics, San Diego, California, 2019. doi:10.2514/6.2019-1372.

[169] N. J. Bennett, D. Ellender, A. G. Dempster, Commercial viability of lunar In-Situ Resource Utilization (ISRU), Planetary and Space Science 182 (2020) 104842. doi:10.1016/j.pss.2020.104842.

[170] T. M. Pelech, G. Roesler, S. Saydam, Technical evaluation of Off-Earth ice mining scenarios through an opportunity cost approach, Acta Astronautica 162 (2019) 388–404. doi:10.1016/j.actaastro.2019.06.030.

[171] B. Barbee, T. Esposito, E. Piñon, S. Hur-Diaz, R. Mink, D. Adamo, A Comprehensive Ongoing Survey of the Near-Earth Asteroid Population for Human Mission Accessibility, in: AIAA/AAS Astrodynamics Specialist Conference, American Institute of Aeronautics and Astronautics, Toronto, Ontario, Canada, 2010. doi:10.2514/6.2010-8368.

[172] J. Karsten, T. Moser, A. Conley, J. Slostad, R. Hoyt, Performance Characterization of the HYDROS Water Electrolysis Thruster, in: 29th Annual AIAA/USU Conference on Small Satellites, Logan, UT, USA, 2015.

[173] B. A. Conway, Spacecraft Trajectory Optimization, Cambridge Aerospace Series, American Institute of Aeronautics and Astronautics, Cambridge, 2010. doi:10.1017/cbo9780511778025.

[174] A. Rao, A Survey of Numerical Methods for Optimal Control, Advances in the Austronautical Sciences 135 (1) (2009) 4. doi:10.1.1.661.6337.

[175] M. Vergaaij, J. Heiligers, Time-optimal solar sail heteroclinic-like connections for an Earth-Mars cycler, Acta Astronautica 152 (2018) 474–485. doi:10.1016/j.actaastro.2018.08.008.

[176] R. H. Battin, An Introduction to the Mathematics and Methods of Astrodynamics, Revised Edition, AIAA Education Series, American Institute of Aeronautics & Astronautics, Reston, VA, 1999. doi:10.2514/4.861543.

[177] J. F. Jordan, The Application of Lambert's Theorem to the Solution of Interplanetary Transfer Problems, Technical Report 32-521, Jet Propulsion Laboratory, Pasadena,CA, USA (Feb. 1964).

[178] R. Blanchard, E. Lancaster, A unified form of Lambert's theorem, Technical Note D-5368, Goddard Space Flight Center, Greenbelt, MD, USA (Sep. 1969).

[179] R. Gooding, A procedure for the solution of Lambert's orbital boundary-value problem, Celestial Mechanics and Dynamical Astronomy 48 (1990) 145–165.

[180] D. Izzo, Revisiting Lambert's problem, Celestial Mechanics and Dynamical Astronomy 121 (1) (2015) 1–15. doi:10.1007/s10569-014-9587-y.

[181] D. de la Torre Sangra, E. Fantino, Review of Lambert's Problem, in: 25th International Symposium on Space Flight Dynamics ISSFD, Munich, Germany, October 19 – 23, 2015.

[182] R. Kemble, Interplanetary Mission Analysis and Design, Springer-Praxis books in Astronautical Engineering, Berlin, 2006.

[183] M. Benayas Penas, A Rapid Grid-Search Technique for KBO Exploration Trajectories, MSc Thesis, Delft University of Technology, Delft, The Netherlands (Jan. 2020).

[184] S. Wagner, B. Wie, B. Kaplinger, Computational Solutions to Lambert's Problem on Modern Graphics Processing Units, Journal of Guidance, Control, and Dynamics 38 (7) (2015) 1305–1311. doi:10.2514/1.G000840.

[185] S. Hernandez, D. R. Jones, M. Jesick, One Class of Io-Europa-Ganymede Triple Cyclers, in: AAS/AIAA Astrodynamics Specialist Conference, Stevenson, WA, USA, 2017.

[186] M. Pontani, B. A. Conway, Particle swarm optimization applied to impulsive orbital transfers, Acta Astronautica 74 (2012) 141–155. doi:10.1016/j.actaastro.2011.09.007.

[187] P. Khushboo, Optimal Landing Trajectories on the Moon using Lambert Targeting and Particle Swarn Optimization, MSc Thesis, Pennsylvania State University, State College, PA, USA (Jul. 2019).

[188] K. Soyinka Olukunle, N. Nwanze, E. C. A. Akoma Henry, Time Dependent Fuel Optimal Satellite Formation Reconfiguration Using Quantum Particle Swarm Optimization, in: L. Rutkowski, R. Scherer, M. Korytkowski, W. Pedrycz, R. Tadeusiewicz, J. M. Zurada (Eds.), Artificial Intelligence and Soft Computing, Vol. 12855, Springer International Publishing, Cham, 2021, pp. 379–389. doi:10.1007/978-3-030-87897-9_34.

[189] A. D. Olds, C. A. Kluever, M. L. Cupples, Interplanetary Mission Design Using Differential Evolution, Journal of Spacecraft and Rockets 44 (5) (2007) 1060–1070. doi:10.2514/1.27242.

[190] Z. Renyong, L. Jianjun, C. Yu, T. Geshi, C. Jing, S. Erlong, F. Jinglang, The Global Optimization of Space Exploration Trajectory Design based on Differential Evolution Algorithm, Chinese Journal of Theoretical and Applied Mechanics 44 (6) (2012) 1079–1083.

[191] B. Addis, A. Cassioli, M. Locatelli, F. Schoen, A global optimization method for the design of space trajectories, Computational Optimization and Applications 48 (3) (2011) 635–652. doi:10.1007/s10589-009-9261-6.

[192] P. Cage, I. Kroo, R. Braun, Interplanetary trajectory optimization using a genetic algorithm, in: Astrodynamics Conference, American Institute of Aeronautics and Astronautics, 1994. doi:10.2514/6.1994-3773.

[193] M. Vasile, E. Minisci, M. Locatelli, Analysis of Some Global Optimization Algorithms for Space Trajectory Design, Journal of Spacecraft and Rockets 47 (2) (2010) 334–344. doi:10.2514/1.45742.

[194] D. Zhang, S. Song, G. Duan, Fuel and time optimal transfer of spacecrafts rendezvous using Lambert's theorem and improved genetic algorithm, in: 2008 2nd International Symposium on Systems and Control in Aerospace and Astronautics, IEEE, Shenzhen, China, 2008, pp. 1–6. doi:10.1109/ISSCAA.2008.4776390.

[195] O. Abdelkhalik, D. Mortari, N-Impulse Orbit Transfer Using Genetic Algorithms, Journal of Spacecraft and Rockets 44 (2) (2007) 456–460. doi:10.2514/1.24701.

[196] F. Cacciatore, C. Toglia, Optimization of orbital trajectories using genetic algorithms, Journal of Aerospace Engineering, Sciences and Applications 1 (1) (2008) 58–69. doi:10.7446/jaesa.0101.06.

[197] I. Moore, M. Ceriotti, Solar sails for perturbation relief: Application to asteroids, Advances in Space Research 67 (9) (2021) 3027–3044. doi:10.1016/j.asr.2020.08.014.

[198] D. E. Goldberg, Genetic Algorithms in Search, Optimization, and Machine Learning, Addison-Wesley Publishing Company, Inc., 1989.

[199] J. Heiligers, S. Hiddink, R. Noomen, C. R. McInnes, Solar sail Lyapunov and Halo orbits in the Earth–Moon three-body problem, Acta Astronautica 116 (2015) 25–35. doi:10.1016/j.actaastro.2015.05.034.

[200] J. P. Sánchez, D. G. Yárnoz, Asteroid retrieval missions enabled by invariant manifold dynamics, Acta Astronautica 127 (2016) 667–677. doi:10.1016/j.actaastro.2016.05.034.

[201] A. Peloni, M. Ceriotti, B. Dachwald, Solar sail trajectory design for a multiple near-Earth asteroid rendezvous mission, Journal of Guidance, Control, and Dynamics, 39 (12) (2016) 2712–2724. doi:10.2514/1.G000470.

[202] M. A. Patterson, A. V. Rao, GPOPS-II: A MATLAB Software for Solving Multiple-Phase Optimal Control Problems Using hp-Adaptive Gaussian Quadrature Collocation Methods and Sparse Nonlinear Programming, ACM Transactions on Mathematical Software (TOMS) 41 (1) (2014) 1:1–1:37. doi:10.1145/2558904.

[203] V. M. Becerra, Solving complex optimal control problem at no cost with PSOPT, in: IEEE International Symposium on Computer-Aided Control System Design, Yokohama, Japan, 2010. doi:10.1109/CACSD.2010.5612676.

[204] G. Mengali, A. A. Quarta, Solar sail trajectories with piecewise-constant steering laws, Aerospace Science and Technology 13 (8) (2009) 431–441. doi:10.1016/j.ast.2009.06.007.

[205] I. Goodfellow, Y. Bengio, A. Courville, Deep Learning, Adaptive Computation and Machine Learning, The MIT Press, Cambridge, Massachusetts, 2016.

[206] B. Dachwald, Evolutionary neurocontrol: A smart method for global optimization of low-thrust trajectories, in: Collection of Technical Papers - AIAA/AAS Astrodynamics Specialist Conference, Vol. 3, AIAA, Reston, Virginia, USA, 2004, pp. 1705–1720. doi:10.2514/6.2004-5405.

[207] G. Viavattene, M. Ceriotti, Artificial Neural Networks for Tours of Multiple Asteroids, in: E. A. de la Cal, J. R. Villar Flecha, H. Quintián, E. Corchado (Eds.), Hybrid Artificial Intelligent Systems, Vol. 12344, Springer International Publishing, Cham, 2020, pp. 751–762. doi:10.1007/978-3-030-61705-9_63.

[208] A. Peloni, Solar-sail mission design for multiple near-Earth asteroid rendezvous, Ph.D. thesis, University of Glasgow, Glasgow, UK (Mar. 2018).

[209] E. Musk, Making life multi-planetary, New Space 6 (1) (2018) 2–11. doi:10.1089/space.2018.29013.

[210] C. Hunt, 2018 NASA New Start Inflation Index, Tech. rep. (2018).
URL http://nasa.gov/sites/default/files/atoms/files/2018_nasa_new_start_inflation_index_for_fy19_use_final_dist.xlsx

[211] S. M. Pekkanen, Governing the New Space Race, American Journal of International Law 113 (2019) 92–97. doi:10.1017/aju.2019.16.

[212] K. Hartley, Aerospace: The Political Economy of an Industry, in: H. W. Jong, W. G. Shepherd, H. W. Jong (Eds.), The Structure of European Industry, Vol. 18, Springer Netherlands, Dordrecht, 1993, pp. 307–335. doi:10.1007/978-94-011-1733-3_11.

[213] S. F. Imam, J. Raza, R. M. C. Ratnayake, World Class Maintenance (WCM): Measurable indicators creating opportunities for the Norwegian Oil and Gas industry, in: 2013 IEEE International Conference on Industrial Engineering and Engineering Management, IEEE, Bangkok, Thailand, 2013, pp. 1479–1483. doi:10.1109/IEEM.2013.6962656.

[214] R. Gulati, R. Smith, Maintenance and Reliability Best Practices, Industrial Press, New York, NY, 2009.

[215] M. Ben-Daya, U. Kumar, D. N. P. Murthy, Introduction to Maintenance Engineering: Modelling, Optimization and Management, John Wiley & Sons, Inc, Hoboken, New Jersey, USA, 2016.

[216] T. R. Boone, D. P. Miller, Capability and Cost-Effectiveness of Launch Vehicles, New Space 4 (3) (2016) 168–189. doi:10.1089/space.2016.0011.

[217] S. R. Chesley, P. W. Chodas, A. Milani, G. B. Valsecchi, D. K. Yeomans, Quantifying the Risk Posed by Potential Earth Impacts, Icarus 159 (2) (2002) 423–432. doi:10.1006/icar.2002.6910.

[218] M. Burchell, Human spaceflight and an asteroid redirect mission: Why?, Space Policy 30 (3) (2014) 163–169. doi:10.1016/j.spacepol.2014.07.003.

[219] B. R. Blair, J. Diaz, M. B. Duke, E. Lamassoure, R. Easter, M. Oderman, M. Vaucher, Space Resource Economic Analysis Toolkit: The Case for Commercial Lunar Ice Mining, Final Report to the NASA Exploration Team (Dec. 2002).

[220] G. P. Sutton, O. Biblarz, Rocket Propulsion Elements, eighth Edition, John Wiley & Sons, 2010.

[221] G. Just, K. Smith, K. Joy, M. Roy, Parametric review of existing regolith excavation techniques for lunar In Situ Resource Utilisation (ISRU) and recommendations for future excavation experiments, Planetary and Space Science 180 (2020) 104746. doi:10.1016/j.pss.2019.104746.

[222] R. Surampudi, J. Blosiu, P. Stella, J. Elliott, J. Castillo, T. Yi, J. Lyons, M. Piszczor, J. McNatt, C. Taylor, E. Gaddy, S. Liu, E. Plichta, C. Iannello, P. M. Beauchamp, J. A. Cutts, Solar Power Technologies for Future Planetary Science Missions, Technical Report JPL D-101316, Jet Propulsion Laboratory (Dec. 2017).
URL https://solarsystem.nasa.gov/system/downloadable_items/715_Solar_Power_Tech_Report_FINAL.PDF

[223] W. M. Haynes, D. R. Lide, T. J. Bruno, CRC Handbook of Chemistry and Physics: A Ready-Reference Book of Chemical and Physical Data., ninety-seventh Edition, CRC Press, Boca Raton, Florida, 2016.

[224] K. R. Erickson, Optimal Architecture for an Asteroid Mining Mission: Equipment Details and Integration, in: Space 2006, AIAA, San Jose, California, USA, 2006. doi:10.2514/6.2006-7504.

[225] Wooster, Keynote talk: SpaceX's Plans for Sending Humans to Mars, in: 22nd Annual Mars Society Convention, University of Southern California, CA, USA, 2019.
URL https://www.youtube.com/watch?v=Z3mVGBiiI

[226] SpaceX, Vehicle Landing (Oct. 2017).
URL https://www.youtube.com/watch?v=5seefpjMQJI

[227] B. G. Drake, K. D. Watts, Human Exploration of Mars Design Reference Architecture 5.0, Addendum #2, Tech. Rep. NASA/SP–2009-566-ADD2 (Mar. 2014).

[228] B. Donahue, G. Caplin, D. Smith, Lunar Lander Concept Design for the 2019 NASA Outpost Mission, in: AIAA SPACE 2007 Conference & Exposition, American Institute of Aeronautics and Astronautics, Long Beach, California, 2007. doi:10.2514/6.2007-6175.

[229] J. V. Bowles, L. C. Huynh, V. M. Hawke, X. J. Jiang, Mars Sample Return: Mars Ascent Vehicle Mission and Technology Requirements, Technical Report NASA/TM-2013-216620, ARC-E-DAA-TN12232, NASA Ames Research Center; Moffett Field, CA, United States (Nov. 2013).

[230] T. Cichan, S. A. Bailey, S. D. Norris, R. P. Chambers, S. D. Jolly, J. W. Ehrlich, Mars Base Camp: An architecture for sending humans to Mars by 2028, in: 2017 IEEE Aerospace Conference, IEEE, Big Sky, MT, USA, 2017, pp. 1–18. doi:10.1109/AERO.2017.7943981.

[231] M. Sippel, S. Stappert, A. Koch, Assessment of multiple mission reusable launch vehicles, Journal of Space Safety Engineering 6 (3) (2019) 165–180. doi:10.1016/j.jsse.2019.09.001.

[232] B. L. Benedict, Rationale for Need of In-Orbit Servicing Capabilities for GEO Spacecraft, in: AIAA SPACE 2013 Conference and Exposition, American Institute of Aeronautics and Astronautics, San Diego, CA, 2013. doi:10.2514/6.2013-5444.

[233] B. Dachwald, Optimal solar sail trajectories for missions to the outer Solar System, Journal of Guidance, Control, and Dynamics 28 (6) (2005) 1187–1193.

[234] M. Vergaaij, J. Heiligers, Solar-Sail Trajectory Design to Planetary Pole Sitters, Journal of Guidance, Control, and Dynamics 42 (6) (2019) 1402–1412. doi:10.2514/1.G003952.

[235] J. Heiligers, J. M. Fernandez, O. R. Stohlman, W. K. Wilkie, Trajectory design for a solar-sail mission to asteroid 2016 HO3, Astrodynamics 3 (3) (2019) 231–246. doi:10.1007/s42064-019-0061-1.

[236] N. J. Bennett, R. Xie, A. G. Dempster, The Moon and NEAs as sources of cislunar propellant; removing some constraints from a recent paper drives down lunar sourced propellant cost, Acta Astronautica 190 (2022) 409–412. doi:10.1016/j.actaastro.2021.10.038.

[237] T. D. Haws, J. S. Zimmerman, M. E. Fuller, SLS, the Gateway, and a Lunar Outpost in the Early 2030s, in: 2019 IEEE Aerospace Conference, IEEE, Big Sky, MT, USA, 2019, pp. 1–15. doi:10.1109/AERO.2019.8741598.

[238] L. David, Inside ULA's Plan to Have 1,000 People Working in Space by 2045, Space.com (Jun. 2016).
URL https://www.space.com/33297-satellite-refueling-business-proposal-ula.html

[239] S. Dorrington, J. Olsen, A location-routing problem for the design of an asteroid mining supply chain network, Acta Astronautica 157 (2019) 350–373. doi:10.1016/j.actaastro.2018.08.040.

[240] T. R. Spilker, M. Adler, N. Arora, P. M. Beauchamp, J. A. Cutts, M. M. Munk, R. W. Powell, R. D. Braun, P. F. Wercinski, Qualitative Assessment of Aerocapture and Applications to Future Missions, Journal of Spacecraft and Rockets 56 (2) (2019) 536–545. doi:10.2514/1.A34056.

[241] S. Hoffman, A comparison of aerobraking and aerocapture vehicles for interplanetary missions, in: Astrodynamics Conference, American Institute of Aeronautics and Astronautics, Seattle,WA,U.S.A., 1984. doi:10.2514/6.1984-2057.

[242] G. Krasinsky, Hidden Mass in the Asteroid Belt, Icarus 158 (1) (2002) 98–105. doi:10.1006/icar.2002.6837.

[243] M. Elvis, T. Milligan, How much of the Solar System should we leave as wilderness?, Acta Astronautica 162 (2019) 574–580. doi:10.1016/j.actaastro.2019.03.014.

[244] T. Kowalkowski, J. Johannesen, T. Lam, Launch Period Development for the Juno Mission to Jupiter, in: AIAA/AAS Astrodynamics Specialist Conference and Exhibit, American Institute of Aeronautics and Astronautics, Honolulu, Hawaii, 2008. doi:10.2514/6.2008-7369.

[245] K. Chang, Elon Musk's Plan: Get Humans to Mars, and Beyond, The New York Times (Sep. 2016).
URL https://www.nytimes.com/2016/09/28/science/elon-musk-spacex-mars-exploration.html

[246] C. Palmer, SpaceX Starship Lands on Earth, But Manned Missions to Mars Will Require More, Engineering 7 (10) (2021) 1345–1347. doi:10.1016/j.eng.2021.08.005.

[247] Elon Musk, @Erdayastronaut Starship design goal is 3 flights/day avg rate, so ~1000 flights/year at >100 tons/flight, so every 10 ships yield 1 megaton per year to orbit (Jan. 2020).
URL https://twitter.com/elonmusk/status/1217989066181898240

[248] S. Lloyd, Least squares quantization in PCM, IEEE Transactions on Information Theory 28 (2) (1982) 129–137. doi:10.1109/TIT.1982.1056489.

[249] V. Kotu, Data Science: Concepts and Practice, second edition Edition, Elsevier/Morgan Kaufmann Publishers, Cambridge, MA, 2019.

[250] M. M. Cohen, W. W. James, K. Zacny, P. Chu, J. Craft, Robotic Asteroid Prospector, in: AIAA 2014 SciTech Forum, National Harbor, MD, USA, 2014.